'ErbB activation and heterodimerisation is responsible for resistance upon PI3K-mTOR inhibition in metastatic prostate cancer'

A thesis submitted to University College London for the degree of Doctor of Philosophy

Myria Galazi

University College London

Departmenf of Molecular Oncology

2018

‘I, Myria Galazi confirm that the work presented in this thesis is my own. Where information has been derived from other sources, I confirm that this has been indicated in the thesis.’

This thesis is dedicated to my parents Dimitris and Androula for their unfailing love, support and reassurance, as well as my fiancé Dimitris for encouraging me to achieve my aspirations.

Acknowledgements:

This project was supported by a research grant from Cancer Research UK at University College London.

I wish to thank my supervisors, Professor Tony Ng and Dr Manuel Rodriguez-Justo, without whom this work would not have existed. I especially want to thank Professor Tony Ng for his immense inspiration, support and encouragement. He has allowed me to understand to origins of scientific advances and has shared his visions about the future of translational research in oncology. His contributions have helped shape the work described in this thesis and more importantly inspired me for the future.

In addition, thanks to Manuel I obtained histopathological training and I closely collaborated with his laboratory to optimise staining in mouse tissue for immunofluorescence and IHC. Our valuable collaborators, Professor Hardev Pandha, contributed intellectually and provided me with patient samples to perform important preliminary experiments. Professor Hing Leung kindly offered us the prostate cancer cell lines used in Chapter 4 of this work and has dedicated his valuable time to provide his scientific knowledge to guide further work. I would like to thank Dr James Monypenny for mentoring me during the first months of my laboratory time and provided supervision with various laboratory techniques, Dr Gregory Weitsman for introducing me to the imaging side of FRET/FLIM work and of course Dr Valenti Gomez for his extensive academic teaching throughout the project that has enhanced my scientific knowledge. Last but not least, I would like to thank all the members of Tony's lab, both past and present, who have helped me enjoy the work I did.

Abstract:

My hypothesis is that resistance to PI3K-AKT-mTOR targeting in metastatic prostate cancer involves ErbB activation and heterodimerisation. Better description of the mechanisms implicated will allow the identification of appropriate predictive biomarkers.

Current clinical trials are investigating the use of PI3K-AKT-mTOR inhibitors in metastatic castration-resistant prostate cancer (CRPC). 50-70% of metastatic CRPC patients have genomic aberrations of the PI3K pathway, mainly involving loss of PTEN, an important negative regulator of the PI3K-AKT pathway. Upregulation of HER3 was previously suggested to be an important resistance mechanism.

Within the context of this project I have applied biophysical techniques to quantify protein-protein interactions i.e fluorescence lifetime imaging microscopy (FLIM) which is the gold-standard technique for measuring Forster resonance energy transfer (FRET). This is an established technology in our laboratory and was used to evaluate HER3 heterodimerisation in prostate cancer cells and mouse xenograft tissue, alongside biochemical methods to demonstrate changes in ErbB expression in response to PI3K-AKT-mTOR inhibition. In addition, I optimised this technology for use in cell line and patient-derived exosomes.

Different ErbB subtypes are upregulated *in vitro* as part of a potential resistance mechanism in response to PI3K-mTOR inhibition, depending on the cell line PTEN status. Concomitant upregulation of either AR or PSMA is also observed.

In PTEN WT prostate cancer cells, the upregulation of PSMA is demonstrated to be HER2 dependent and can be inhibited by lapatinib.

The clinical implications of my results propose the use of PI3K-AKT-mTOR inhibitors in the metastatic hormone-sensitive setting as well. In addition, tissue and/or exosomal ErbB heterodimerisation, together with the use of clinically available PSMA imaging probes, might prove an additional biomarker in resistance detection and subgroup classification. Some initial PSMA PET imaging analyses upon PI3K-mTOR inhibition *in vivo* will be presented. Finally, this might allow the design of prospective clinical trials using PSMA-targeted therapies.

Impact statement:

The treatment landscape in metastatic prostate cancer is rapidly evolving with the approval of numerous novel agents for use both in hormone-sensitive and castrate-resistant settings. Clinicians however, are faced with numerous challenges due to the multitude of available treatment options but the lack of predictive biomarkers of response and resistance that would guide treatment decisions. Understanding mechanisms of resistance to targeted novel agents in metastatic prostate cancer is an area of current unmet need in order to transition to more personalised treatment approaches for our patients.

In this project, we wished to study resistance mechanisms to targeted inhibition of the PI3K-AKT-mTOR pathway in metastatic prostate cancer. Inhibitors of the pathway are currently being investigated with early phase as well as Phase III clinical trials. PTEN status, assessed by tumour IHC, is used as a predictive biomarker of response in these clinical trials. We were interested to see whether the resistance mechanisms demonstrated between PTEN WT and MT/null cell lines in vitro could guide any further pharmacological intervention at the time of resistance.

The results of this project demonstrate distinct patterns of resistance between PTEN WT and MT/null prostate cancer cell lines with differential overexpression of ErbB receptors and their heterodimerisation as well as upregulation of key oncogenic pathways. We propose that ErbB receptor overexpression and/or heterodimerisation could be used as predictive biomarkers of treatment resistance based on the baseline PTEN status of the patients. In addition, based on respective ErbB changes the overexpression of

specific pathways known to be important in disease proliferation and progression in metastatic prostate cancer, such as AR and PSMA, could be predicted and detected at the time of resistance to guide further targeted therapy. The use of PSMA-targeted therapeutics is now being investigated within clinical trials in metastatic castrate-resistant prostate cancer and could be relevant in a subgroup of PTEN WT patients that progress upon PI3K-AKT-mTOR targeted inhibition. Finally, within this project we presented preliminary work using patient serum-derived exosomes in prostate cancer and the ability to use our FRET-FLIM assay to detect exosomal ErbB heterodimerisation as valuable liquid biopsies that could be evaluated further within prospective clinical trials in the future.

The completion of this project was the result of contributions of members of Professor Ng's laboratory, based both at UCL Cancer Institute and King's College London. Furthermore, our collaborators Professor Hardev Pandha at the University of Surrey and Professor Hing Leung at the University of Glasgow contributed intellectually at important times along the project. As an example, the exosomal samples I have prepared are going to be deployed as part 1 of a National Cancer Imaging Translational Accelerator (Cambridge/ICR/Imperial College London/KCL/Oxford/UCL) clinical programme funded by CRUK (£10 million. 2018-23) known as 'Evaluation of PSMA (68Ga) PET/CT as a tool to guide treatment choice in patients with high risk prostate cancer'. The latter is likely to transform prostate cancer management by an integrated imaging and liquid biopsy based technological approach.

Chapter 1: Introduction

Chapter 2: Materials and methods

List of figures

Chapter 1

Chapter 3

Chapter 4

Chapter 5

List of tables

Chapter 1

Chapter 2

Chapter 5

List of abbreviations:

4EBP1 – eukaryotic translation initiation factor 4E-binding protein 1

αα – amino acid

Ack1 – Acetate kinase

ADT – androgen deprivation therapy

AKT – protein kinase B

APS – ammonium persulfate

AR – androgen receptor

ATP – adenosine triphosphate

AUC - area under the curve

BSA – bovine serum albumin

CRPC – castrate-resistant prostate cancer

CTC – circulating tumour cell

CYP17A1 – Cytochrome P450 17A1 (also called 17α hydrolase)

DNA – Deoxyribonucleic acid

dNTP – deoxyribose nucleoside triphosphate

EGF – Epidermal growth factor

eIF4E – eukaryotic translation initiation factor 4E

ERG – ETS-related gene

ERK – extracellular signal-regulated kinases

ETS – E26 transformation specific

ETV1 – ETS translocation variant 1

FFPE – formalin-fixed paraffin embedded

FISH – fluorescence in situ hybridisation

FLIM – fluorescence lifetime imaging microscopy

Fol – folate

FOLH1 – folate hydrolase 1

FRET – fluorescence resonance energy transfer (or Forster resonance energy transfer)

$FRET_{eff}$ – FRET efficiency

Glu - glutamate

GPCR – G-protein coupled receptor

GRM1 – glutamate metabotropic receptor 1

HCL – hydrochloric acid

HRG – heregulin

HSP – heat shock protein

IHC – immunohistochemistry

IP3(R) – inositol 1,4,5-triphosphate (receptor)

KLK3 – kallikrein-3

LDS – lithium dodecyl sulphate

LHRH – luteinising hormone releasing hormone

MAPK or MEK – mitogen-activated protein kinases

mCRPC – metastatic castration-resistant prostate cancer

mGLUR – metabotropic glutamate receptor

mGLUR1 – metabotropic glutamate receptor 1

MRI – magnetic resonance imaging

mRNA – messenger RNA

mTOR – mammalian target of rapamycin

NGS - next-generation sequencing

NSCLC – non-small cell lung cancer

NRG-1 – Neuregulin-1

NTA – nanoparticle tracking analysis

OS – overall survival

PARP – poly(adenosine diphosphate [ADP]-ribose) polymerase

PDK1 – phosphoinositide-dependent kinase 1

PCA-3 – prostate cancer antigen 3

PCR – polymerase chain reaction

PET – Positron emission tomography

PFS – progression-free survival

PI3K – phosphatidylinositol-4,5-biphosphate 3-kinase

PIP2 – phosphatidylinositols (4,5) P_2

PIP3 – phosphatidylinositols (4,5) P_3

PLC – phospholipase C

PSA – prostate specific antigen

PSMA – prostate specific membrane antigen

PTEN – phosphatase and tensin homolog

qRT-PCR – quantitative reverse transcription polymerase chain reaction

RAC1 – Ras-related C3 botulinum toxin substrate 1

RACK1 – Receptor of activated protein C kinase 1

RNA –ribonucleic acid

RTK – receptor tyrosine kinaseSEM – standard error of the mean

SDS – Sodium dodecyl sulphate

siRNA – small interfering RNA

SPEDF – SAM pointed domain-containing Ets transcription factor

SPRY – Sprouty protein 2

Src – proto-oncogene tyrosine-protein kinase

STAT – signal transducer and activator of transcription

TDE – 2,2’ thiodiethanol

TKI – tyrosine kinase inhibitor

TMA - tissue microarray

TNM – Tumour Nodes Metastasis (for the classification of malignant tumours)

TRAMP – transgenic adenocarcinoma of the mouse prostate

TMPRSS2 – transmembrane protease serine 2

WT – wild-type

Chapter 1: Introduction

1.1 Prostate cancer

1.1.1 – Introduction

Prostate cancer is the commonest cancer in men in the UK and the second most common cause of cancer-related death in men in the UK (1). The disease exhibits remarkable heterogeneity in clinical behaviour and outcome ranging from years of indolence to lethal disease despite similar histological features (2).

The androgen dependency of prostate cancer was first established by Huggins and Hodges in the 1940s (3) and since then androgen deprivation therapy, with Luteinising-hormone releasing hormone or orchidectomy, is the first-line treatment for metastatic disease. Although initial response rates exceed 80%, these are transient and patients invariably progress to the more aggressive state of the disease termed castration-resistant prostate cancer or CRPC (4).

The advances in genomic and proteomic research have provided improved understanding of the molecular events underlying castration resistance and have shown that CRPC is a molecularly heterogeneous disease, even within a single patient. It is now established that CRPC remains dependent on persistent activation of the androgen receptor (AR) and its signaling pathway (5) despite reduced or absent androgen ligand levels. The phosphatidylinositol 3-kinase (PI3K) pathway also plays an important role in CRPC. To date, we

know that the PI3K-AKT-mTOR and AR signaling pathways can regulate each other through complex feedback mechanisms (6) . Understanding the critical events and complexities of AR signaling and its interaction with other oncogenic molecular pathways is essential in developing successful therapies for the future based on molecular stratification for individual patients' disease.

Recently, a multi-institutional clinical sequencing infrastructure conducted prospective whole exome and transcriptome sequencing of bone and soft tissue tumour biopsies from 150 mCRPC patients. It was notable from this study that 89% of patients had clinically actionable aberrations. Importantly, the PI3K pathway was found to be frequently altered, with somatic alterations in 49% of mCRPC patients, suggesting that understanding the complex interplay between this pathway and AR signaling is an important area to focus (7).

The detection and monitoring of genomic and molecular aberrations longitudinally requires a minimally invasive technique. As a result, the concept of liquid biopsies has become very appealing; offering the potential to capture the majority of the cancer burden (and not just the primary or metastatic tissue) and provide information about critical and therapeutically targetable aberrations. In addition, whole body imaging can detect tumour heterogeneity non-invasively and describe the existence of subpopulations of cancer cells with distinct genomic and proteomic variations. The advantage of combining the two is to harness the detection of treatment-resistance variants that evolve as a mechanism of acquired resistance along the time course of the disease (8).

1.1.2 - The management of metastatic prostate cancer

The synthesis of androgens is under the physiological regulation of the hypothalamic-pituitary-testicular axis, with contributions from the adrenal glands resulting from *de novo* steroidogenesis (9). ADT continues to be the first-line therapy for patients with metastatic prostate cancer. This is in the form of chemical castration through the use of gonadotrophin-releasing hormone agonists or antagonists which lower testosterone levels by suppression of androgen secretion from the testes. Combined androgen blockade includes the use of competitive AR inhibitor (anti-androgen) to further reduce AR signaling in prostate cancer cells (10). Despite effective, ADT is associated with toxicity, mainly decreased bone density, sexual dysfunction, hot flushes and cardiac morbidity (11). Although nearly all patients respond to ADT the duration of response varies for months to years, and inevitably the disease progresses and evolves to become resistant to further hormonal treatment. At this stage of the disease the patients are classified as castrate-refractory or hormone-resistant (**Figure 1.1**).

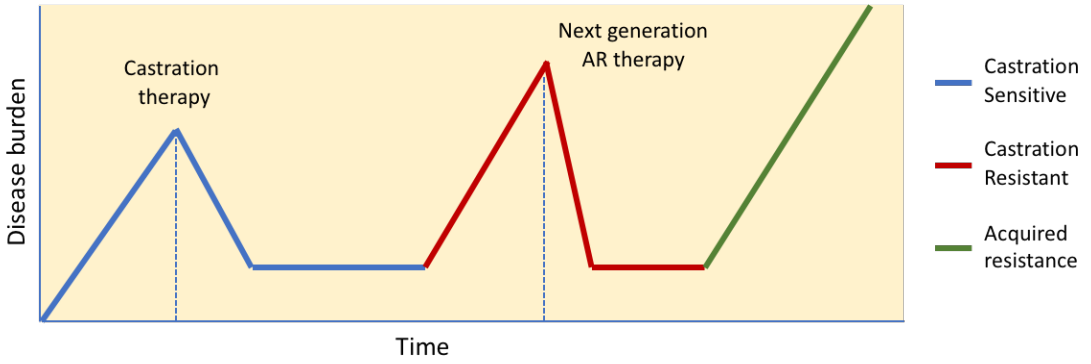

Figure 1.1 – Prostate cancer trajectory: Increasing disease burden following primary prostate cancer therapy is indicated by rising PSA levels and/or radiographic progression, and is treated with medical castration. The CRPC stage follows the failure of castration therapy. Treatment with next-generation AR inhibitors is initiated in CRPC, but acquired (or inherent) resistance mechanisms lead to disease recurrence and ultimately death.

Docetaxel chemotherapy also has an established role in metastatic CRPC, after results of the TAX-327 clinical trial that showed significantly improved survival in the docetaxel versus the mitoxantrone group (12) . In the last 8 years, large randomised Phase III clinical trials showed significant improvements in survival and outcomes leading to the approval of additional new therapies for CRPC such as abiraterone acetate (13), enzalutamide (14), cabazitaxel (15), Radium-223 (16), denosumab (17) and sipuleucel-T (18). These have significantly changed the treatment landscape of metastatic CRPC with overall survival (OS) increasing from approximately 9-18 months to >30 months (19).

Both abiraterone acetate and enzalutamide act on the androgen axis. Abiraterone acetate is a potent, selective and irreversible inhibitor of CYP17A1, an important enzyme in the steroidogenic pathway involved in the synthesis of androgens and other steroid hormones. Abiraterone acetate therefore, acts by

inhibiting androgen biosynthesis (20). Enzalutamide is a non-steroidal anti-androgen that competitively inhibits androgen binding to AR as well the nuclear translocation of AR, DNA binding and co-activator recruitment, therefore interfering with androgen receptor signalling (21). Both these agents, when used before and after treatment with docetaxel, they have showed decreases in disease progression and improvements in overall survival as well as in other secondary endpoints (13, 14, 22, 23). Cabazitaxel, like docetaxel, is another taxane chemotherapeutic agent that showed increased survival by 2.4 months when compared to mitoxantrone (15). Radium is an α-emitter particle that selectively binds and targets bone metastases. It prolonged median OS by 3.6 months and time to first skeletal-related event by 5.8 months compared to placebo (16). Denosumab on the other hand is a monoclonal antibody against the receptor activator of nuclear factor κ-B ligand and can promote osteoclast formation and propagation. When compared to zolendronic acid, denosumab delayed the first skeletal-related event by 3.6 months (17). Finally, sipuleucel-T is an autologous cellular immunotherapy that is thought to work through APCs to stimulate T-cell immune response targeted against prostatic acid phosphatase (PAP), an antigen that is highly expressed in most prostate cancer cells (24). Its use within the clinical trial setting it demonstrated increase in median survival by 4.1 months compared to placebo (18).

In addition to the above, the results of two Phase II clinical trials in metastatic CRPC treated with olaparib also produced important results. Olaparib is a PARP inhibitor and preclinical data showed that genomic aberrations in

tumours that interfere with DNA repair respond to PARP inhibition, by the exploitation of synthetic lethal interaction from these agents (25, 26). PARP inhibition showed durable anti-tumour activity in men with metastatic castration-resistant prostate cancer and deleterious germline BRCA2 mutations, a disease subgroup associated with poor prognosis (25, 27). TOPARP was a Phase II trial that investigated the activity of olaparib in metastatic CRPC and showed that 33% of patient had a response (objective response as per RECIST criteria or PSA reduction). In the 16 out of 49 patients who had aberrations in DNA repair genes by next-generation sequencing, 88% had response to olaparib (28).

In summary, the results of the recent clinical trials in metastatic CRPC show that metastatic CRPC responds to a variety of treatments ranging from potent anti-androgens to chemotherapy, immunotherapy, monoclonal antibodies and PARP inhibition. Unfortunately, despite these advances in the availability of systemic therapies, clinicians are still faced with several challenges regarding the best sequence for therapy use and the most effective combinations for each patient. Prospective clinical trials are needed with the inclusion of clinically relevant biomarkers to guide decisions and allow personalised treatment approaches.

In addition, there is a lot of interest in assessing the use of several of the above agents in the metastatic hormone-sensitive setting and recently the use of docetaxel was investigated in two randomized clinical trials in this context. In

the CHAARTED trial, docetaxel increased median survival in the docetaxel and ADT group compared to ADT alone (57.6 versus 44 months respectively - HR 0.61; 95% CI, 0.47-0.8) and delayed progression to 20.2 months versus 11.7 months (HR 0.61; 95% CI, 0.51-0.72). The benefit from the addition of docetaxel to ADT was observed to be greater in patients with high-volume disease (29). Similarly, the STAMPEDE trial showed that the addition of docetaxel to ADT increased the time to biochemical recurrence, progression or death from prostate cancer by 17 months (HR 0.61; 95% CI, 0.53-0.7) and overall survival by 10 months (HR 0.78; 95% CI, 0.66-0.93) (30).

Furthermore, the recent LATITUDE and STAMPEDE trials also showed substantial improvement in survival with the addition of abiraterone plus prednisolone to ADT in metastatic hormone-sensitive prostate cancer. The LATITUDE study recruited patients with newly diagnosed high risk hormone-sensitive prostate cancer, as defined by Gleason score 8 or higher, 3 or more bone metastases or the presence of measurable visceral metastases. The results showed significantly improved OS in the abiraterone and ADT group compared to the placebo and ADT group (not reached versus 34.7 months) (hazard ratio for death, 0.62; 95% CI, 0.51-0.76, $p<0.001$). in addition, the median radiographic PFS was 33.0 months in the abiraterone group compared to 14.8 months in the placebo group (31). The STAMPEDE trial also included an abiraterone and ADT arm alongside the standard of care ADT alone arm. In the patients with metastatic disease (88% of total) the majority (95%) were *de novo* metastatic. The results again showed that the abiraterone and ADT

combination improved median OS when compared to ADT alone (3-year OS 83% vs 76%, HR 0.63; 95% CI, 0.52-0.76; P<0.001) (32).

Undoubtedly, the results of these clinical trials demonstrate that docetaxel and ADT and abiraterone and ADT are standard-of-care treatment options for high-volume, high-risk metastatic hormone-sensitive prostate cancer. Decision about the preferred combination is now made based on clinician judgement and patient individual characteristics. Several ongoing clinical trials are continuing to investigate the role of secondary hormone therapy in the hormone-sensitive setting including the use of enzalutamide and other AR antagonists (33). Clearly, areas of future research should concentrate on combination strategies, treatment sequencing and biomarker development. Apart from anti-hormonal and chemotherapy treatments in metastatic hormone-sensitive prostate cancer, other targeted therapies are being investigated for their efficacy at this stage of the disease.

1.1.3 - Prognostic and predictive biomarkers

The management of prostate cancer commonly includes uncertainties due to the inability to accurately predict the natural history and aggressiveness of the tumour at individual level. The integration of preclinical and clinical information revealed the intricacies of inter- and intra-patient heterogeneity CRPC. Tissue, liquid and imaging-based biomarkers in prostate cancer hold great potential for response assessment, staging, early detection, biologic characterization and drug development (**Figure 1.2**). The translation of these in clinic requires

prospective validation within carefully designed clinical trials to demonstrate prognostication and prediction of response.

1.1.3.1 – The role of PSA in prostate cancer

Prostate specific antigen (PSA) is one of the few molecular markers routinely used for detection, risk stratification and monitoring in cancer. PSA belongs to the family of kallikrein-related peptidases and is under the regulation of androgen through androgen response elements (34). It strongly discriminates different prostate cancer stages; it is higher in men with localized disease than in cancer free individuals, and it is higher in men with metastatic disease than those with localized disease. In addition, the levels of PSA at diagnosis and the initiation of therapy are predictive of clinical outcomes. Furthermore, PSA doubling time is used to monitor disease progression in patients who have had initial surgery or radiotherapy and in patients under active surveillance (35).

PSA is also very useful in monitoring treatment response to ADT, and the decrease in PSA levels indicate prostate cancer growth arrest and tumour cytotoxicity. Progression to castrate-resistant disease after ADT is also defined by two consecutive increases in PSA after the post-ADT nadir, and PSA increase at this stage invariably indicates disease progression (36). At the stage of CRPC PSA levels are still used to monitor the effects of treatment, however this is not very accurate and the value of PSA as surrogate marker of disease response in clinical trials is generally questionable, making the development of novel biomarkers an unmet need (37).

1.1.3.2 – Prognostic biomarkers at diagnosis

Current classification systems at diagnosis include TNM staging, Gleason score grading, D'amico risk classification (38) and many others (39-41). Despite the importance of these tests in improving our ability to evaluate and predict aggressiveness in prostate cancer, their performance in many cases is still suboptimal (42). Part of the limitations with these systems stems from the fact that they rely on macro- and microscopic features of the tumour which are unfortunately misleading. It is no surprise that there is a need for genomic markers to complement these tools.

At prostate cancer diagnosis new molecular biomarkers, such as Decipher, Prolaris and Oncotype DX, that classify tumour aggressiveness have become available. The Decipher test uses the expression of 22 selected RNA markers in the radical prostatectomy specimen and can predict clinical likelihood of metastasis and cancer- specific mortality with high discrimination. It has also shown ability to independently predict clinical metastasis in patients with biochemical relapse after surgery (43). Prolaris cell cycle progression (CCP) test is also a genomic test that looks at a group of genes in the tumour that provide information on their proliferation and multiplication. It incorporates information on changes in 31 cell cycle progression genes and 15 housekeeping genes to generate a score on tumour aggressiveness and 10-year cancer mortality risk (44). Finally, Oncotype DX Prostate Cancer Assay is a multi-gene RT-PCR expression assay for use in paraffin-embedded diagnostic prostate needle biopsies. It measures the expression of 12 cancer-

related genes representing 4 biological pathways and other 5 reference genes that are then combined to calculate the Genomic Prostate Score (GPS). Data with its use so far demonstrates that the Oncotype DX GPS is a strong independent predictor of biochemical relapse and aggressive disease following initial surgery (45). These tests can therefore provide important additional information, especially in the case of intermediate risk prostate cancer aggressiveness based on Gleason score. For instance, patients with prostate cancer Gleason score 7 demonstrate a range of clinical outcomes and encompass a very heterogeneous group of prostate cancer patients. The availability of further prognostic biomarkers/tests of disease aggressiveness and patient outcome are imperative when managing patients at that stage of their disease.

1.1.3.3 – Biomarkers in metastatic disease

Primary prostate cancer is commonly multi-focal at diagnosis with a long natural history of 5 years or more until the detection of metastases and the development of castration resistance. Models of clonal evolution support the idea that a single tumour clone present within a multifocal primary is responsible for metastasis but the identification of dominant lesions at diagnosis is challenging as it might never represent the lesion with the highest Gleason grade (46). Further molecular changes can occur in the tumour with disease progression and treatment resistance. Recent evidence also supports polyclonal metastasis-to-metastasis seeding in metastatic hormone-deprived prostate cancer (47). This makes the use of archival primary tumour not

representative of the current molecular state of the disease when making decisions regarding targeted systemic therapies. Further, the use of metastatic tissue biopsy samples in prostate cancer are challenging due to the high frequency of sclerotic bone metastases that make molecular profiling difficult. In addition to that, the acquisition of single site metastatic biopsies does not represent the entire tumour burden because of intra-patient heterogeneity. The availability of blood-based approaches (i.e liquid biopsies) and molecular imaging are attractive to optimise as they add the advantage of performing them serially to track tumour evolution and treatment response longitudinally.

In the metastatic CRPC setting the results of preclinical and clinical work has provided important insights into the mechanisms of resistance, disease heterogeneity and potential novel therapeutic targets. As a result, several clinical studies focused on evaluating novel tissue, liquid and imaging biomarkers. Prospective biomarker evaluation within clinical trials is being performed more frequently. For example, next generation sequencing studies on fresh-frozen tumour biopsy samples obtained before treatment could identify mutations and deletions in DNA-repair genes in patients receiving olaparib in the TOPARP trial and the anti-tumour activity of olaparib was significantly higher in the patients with aberrations in DNA-repair genes, showing that prospective evaluation of DNA-repair gene aberrations could be used to stratify patients to treatment with olaparib in the future (28). A subsequent question that arises from this however, is whether DNA repair defects can be detected reliably by non-invasive means.

Non-invasive assays involving CTCs and/or plasma DNA can also be used to capture heterogeneity. CTC count and CTC conversion could be used as prognostic biomarkers of disease progression or predictive of response in clinical trials respectively (48). However, any available CTC assay still requires further validation within large Phase III clinical trials. Further, a targeted next-generation sequencing approach amenable to plasma DNA has been used retrospectively using patient blood samples previously treated with abiraterone to quantify AR copy number state as a biomarker of castration and treatment resistance. Patients with AR gain or mutations prior to abiraterone treatment were less likely to respond (as measured by PSA decline) and had significantly worse overall and progression-free survival suggesting that this could be used as a non-invasive biomarker to identify patients with primary resistance to abiraterone (49). Prospective evaluation of plasma AR gene aberrations in clinical trials with novel and standard AR targeting agents and chemotherapy are now being planned.

The evaluation of the detection of AR-V7 prospectively as a prognostic biomarker in CRPC has also been performed within clinical trials of patients on enzalutamide and abiraterone by IHC on bone marrow biopsy specimens (50) and mRNA level in CTCs (51). Specifically, AR-V7 in bone marrow was detected in the 57% of patient who developed resistance to enzalutamide (50). Similarly, AR-V7 in CTCs was associated with lower response rate, shorter PFS and shorter overall survival compared to patients without detectable circulating AR-V7 (51). The serial assessment of CTC samples along the course of the

treatment showed that it could identify patients that were negative at baseline but then converted to AR-V7 positive during the treatment. In conclusion, the data with AR-V7 show that this can be used as marker of treatment resistance in CRPC, however further prospective validation is needed before this is used in routine clinical practice to guide decisions.

Finally, PTEN-negative tumours as demonstrated by IHC in a cohort of CRPC patients are associated with shorter median OS and shorter median duration of abiraterone treatment (52), however the utility of PTEN as a biomarker in clinic is hugely limited by the need of metastatic tissue biopsies that are generally hard to obtain in the metastatic prostate cancer setting.

1.1.3.4 - Imaging biomarkers

Advances in imaging technology have the ability of not only assessing disease extent and distribution, but it can also identify biologic features of patients' imaged lesions. Accurate staging is important in patients with high risk localised disease and in those whose disease has biochemically relapsed following local therapy to allow clinical decision making as well as personalized treatment stratification and clinical trial enrolment when relevant.

Multiparametric MRI is a widely accepted imaging modality in the detection and localization of prostate cancer recurrence in patients with biochemical failure after radical prostatectomy. It is a powerful imaging modality as it combines biologic and anatomical information together, due to the combination of

morphological imaging (e.g T2-weighted imaging) and functional techniques, such as dynamic-contrast enhanced imaging (DCEI), diffusion-weighted imaging (DWI) and MR spectroscopic imaging (MRSI) (53). Biochemical relapse after radical prostatectomy, as defined by elevation of serum PSA, develops in 50% of high risk patients and in about 10% of low risk patients within 15 years from surgery (54). However, in clinical practice the detection of PSA origin as a local recurrence or distant, metastatic disease is not always easy to identify. This is crucial as the management of patients with local recurrence will differ in the absence of distant metastases and will involve salvage radiotherapy with the potential of cure, whereas in the case of metastatic disease androgen-deprivation therapy will be indicated to improve mortality outcomes (55). Furthermore, multiparametric MRI also has utility in patients undergoing active surveillance (56) by allowing reclassification of patient Gleason grade when biopsies were carried out at targets or regions of interest identified by multiparametric MRI. Therefore, there is a clear utility for molecular and imaging based biomarkers in prostate cancer and unsurprisingly, this is an area of active research.

Moreover, multiparametric MRI has been used for the local staging, detection and characterization of primary foci of prostate cancer within the gland at diagnosis. This has enabled for the improved assessment of the prostate to detect areas of malignancy for biopsy sampling (57). In addition, the quantitative evaluation of DWI with calculated apparent coefficients (ADC)

values correlates with Gleason score on tissue histology and therefore allows for the more confident risk stratification of patients (58).

As well as multiparametric MRI, numerous radiolabeled tracers have been approved for use to image PSMA in prostate cancer to identify sites of disease. PSMA is a transmembrane carboxypeptidase that is expressed in prostatic tissue, upregulated in prostate cancer (especially CRPC) and present regardless of disease site (more on PSMA is discussed in a separate chapter; see chapter 1.4). The most commonly used anti-PSMA small molecule ligand is Glu-NH-CO-NH-Lys-(Ahx)-[^{68}Ga(HBED-CC)](^{68}Ga-DKFZ-PSMA-11). In a retrospective analysis involving 319 patients with progressive disease across a variety of clinical states sensitivity and specificity were 76.6% and 100% respectively with the use of PSMA-PET (59). PSMA-PET also demonstrated ability to detect disease in biochemical relapse even when PSA level is very low (60). This suggests that PSMA imaging might be very useful to detect clinically relevant disease at very low PSA levels, especially at disease stages where decisions about salvage radiotherapy are highly relevant. When the outcome of studies with long follow-up becomes available more insight will be gained into the long-term outcome from salvage treatment in relationship to PSMA-PET guidance. The use of PSMA-PET restaging in biochemical recurrence also adds in the detection of oligometastatic disease, hence differentiating better the decision making regarding systemic or salvage therapies as well (61). Despite the available evidence regarding the utility of

PSMA-PET imaging, its role in personalised prostate cancer treatment is still not established and will be a subject of intense research in the years to come.

Even with the availability of these imaging modalities and the information generated with their use, there are limited prospective clinical studies to confirm the power of their true positive and negative findings. Further, clinical trials evaluating molecular imaging biomarkers with molecular and genomic aberrations in the same patients is also lacking. The correlation of these as well as their use to complement each other could allow for predictive biomarkers and treatment stratification based on global assessment of the patients' disease.

1.1.4 - The AR signaling pathway in prostate cancer

1.1.4.1 AR structure, function and regulation

The human androgen receptor gene is a nuclear transcription factor and a member of the steroid hormone receptor superfamily of genes. It is located on the X chromosome (q11-12) and consists of 8 exons. It encodes for a protein of 919 amino acids with a mass of 110kDa. The AR consists of four structurally and functionally distinct domains (**Figure 1**); the N-terminal domain (NTD), a highly conserved DNA-binding domain (DBD) and the ligand-binding domain (LBD). The 'hinge region' separates the DBD from the LBD and contains a ligand-dependent nuclear localisation signal for AR nuclear transport (62).

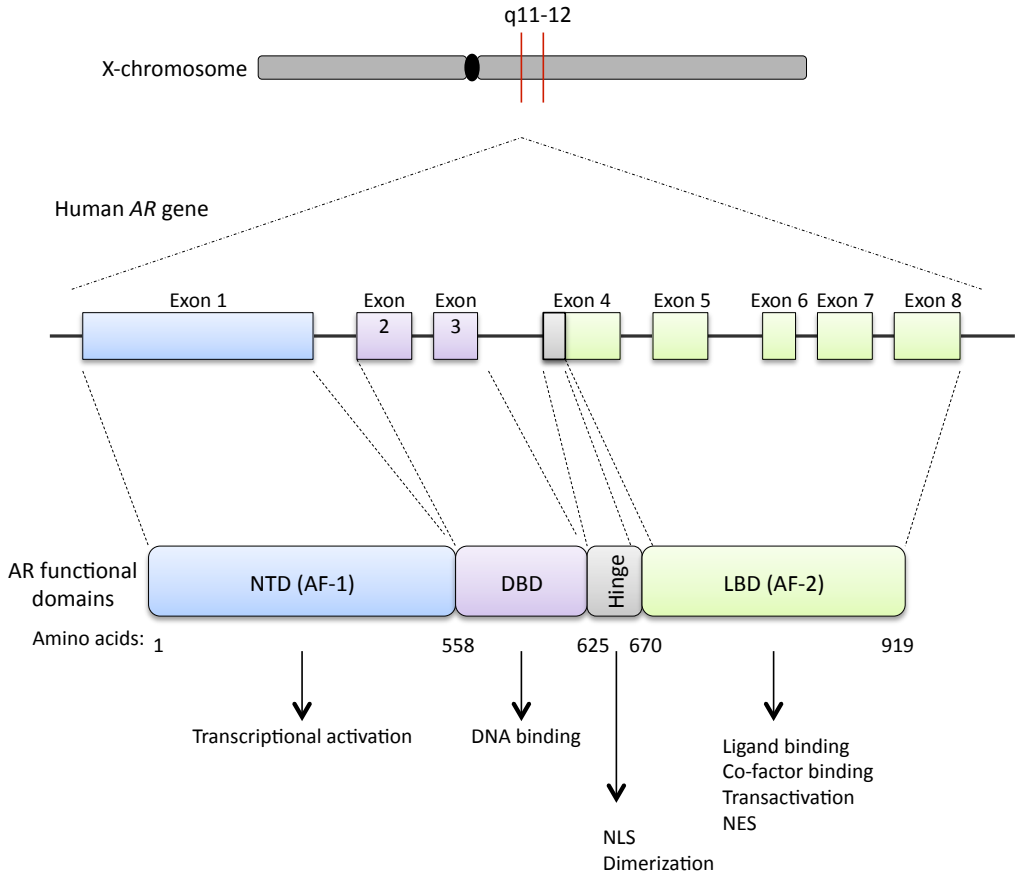

Figure 1.2 – Representative schematic of the Androgen Receptor (AR) gene and modular protein structure: The AR is encoded within the long arm of X-chromosome and is formed by eight exons. The AR is organized in a modular structure containing an amino terminal domain (NTD), a DNA binding domain (DBD), a hinge region and ligand binding domain (LBD). The AR contains two activation function domains (AF-1 and AF-2) responsible for the transcriptional activity of the receptor. Amino acid boundaries are indicated by amino acid residue numbers and known functions for each domain are listed below.

In the absence of ligand, the AR is primarily located in the cytoplasm where it associates with heat shock proteins (HSP)-90, -70, -56, cytoskeletal proteins and other chaperones. These maintain a conformation favourable of ligand binding and protect the AR from proteolysis (63). The NTD contains the activation function-1 (AF-1) domain which supports AR transcriptional activation in the presence of AR ligand and on the other hand is able to confer AR ligand-independent activation when the NTD is separated from the LBD

(64). In addition, AF-1 interaction with the LBD leads to AR stabilisation (65, 66). The AR NTD contains various phosphorylation and sumoylation regulatory sites and has been shown to be able to be phosphorylated by various kinases, playing an important role in AR transactivation (67).

The binding of ligand leads to HSP90 dissociation and induces a conformational change in AR whereby helices 3, 4 and 12 within the LBD form the AF-2 binding surface (68). AF-2 is the principal protein-protein interaction surface that stabilises the AR and is important to recruit FxxLL motifs/transcription coregulators in the NTD (65). As a result, this hydrophobic pocket within the LBD facilitates intra- and intermolecular interaction between the AR NTD and its carboxy-terminal domain (CTD) resulting in the dimerization of AR. This NTD-CTD interaction occurs predominantly when AR is not bound to DNA and allows the AR to interact with its co-activators facilitating AR homodimer formation and nuclear localisation (69). Once inside the nucleus, AR binds to specific recognition sequences known as androgen response elements (AREs) in the promoter and enhancer regions of target genes. Under these conditions, the AR recruits various coregulators resulting in the initiation of transcription of its target genes. In prostate cancer, it can drive the modulation of gene expression, especially that of oncogenes such as the ETS transcription factors (ERG and ETV1) (70). Evidence also suggests that AR can additionally activate transcription by binding to other transcription factors hence acting as a coactivator (71). The transcriptional activity of the AR depends on the ability to access cognate binding sites on chromatin, partly enabled by

histone-modifying enzymes (p300 and CREB-binding protein) as well as pioneer factors such as FOXA1 and GATA2 (4).

Regulation of the AR occurs under the influence of androgen at the mRNA (transcriptional and posttranscriptional level) and protein level. Androgens have been reported to modulate both stability and translation efficiency of the AR mRNA; AR mRNA downregulation is observed after 48hr treatment of LNCAP cells with androgen. However, the AR protein level is not downregulated under the stimulation of androgens but undergoes a process of receptor recycling with androgen withdrawal where it migrates back and forth between cytoplasm and nucleus (72).

Since AR does not undergo ligand-dependent downregulation of its protein level, the effect of the ubiquitin-proteasome pathway has been implicated in its degradation (73). Inhibition of the ubiquitin-proteasome pathway by MG132 in LNCAP cells has shown an increase in endogenous AR protein levels (74). Specifically, the Mdm2 E3 ubiquitin ligase has been found to interact with the AR NTD and DBD in a process dependent on AR phosphorylation at Ser^{213} and Ser^{719} by the PI3K-AKT pathway (75). CHIP (C-terminus of Hsp70-interacting protein), another ubiquitin ligase, was reported to degrade AR protein (76). However, whereas Mdm2 and CHIP promote AR degradation, RNF6, another ubiquitin E3 ligase that was identified within a proteomic screen, was found to promote AR transcriptional activity and cofactor recruitment by mediating ubiquitination of lysine 845 (K845) and K847 on the AR LBD. Furthermore,

RNF6 is overexpressed in hormone-refractory human prostate cancer tissues and is required for prostate cancer cell growth under androgen-depleted conditions (77). More recently, Siah2 was reported to have E3 ubiquitin ligase activity that contributes to CRPC by regulating AR transcriptional activity as well (78). In conclusion, the above studies reveal that various E3 ubiquitin ligases are playing differential roles on AR regulation in prostate cancer and at given oncogenic environments.

1.1.4.2 The role of androgen receptor in CRPC

The AR signalling axis plays a critical role in the development and progression of prostate cancer. Indeed, the AR is the most commonly altered gene in CRPC and there is a complex interplay of networks of signalling molecules attributed to aberrant AR signalling (79).

The main mechanisms broadly include (also summarised schematically in **Figure 1.4**):

- AR amplification/overexpression (80)
- Gain-of-function AR mutations; mostly of the ligand binding domain (81)
- AR mutations resulting in conformation changes of the AR (82)
- Autocrine androgen production (83)
- Overexpression of AR cofactors, sensitising cells to low levels of androgens (84)
- Ligand-independent AR activation by cytokines or growth factors, such as interleukins (IL-6 and IL-8) (85), EGF and IGF-1 (86)

- Constitutively active messenger ribonucleic acid (mRNA) splice variants of AR (87, 88)
- Intracellular kinase signalling, such as Src and AKT, through protein-protein interactions and phosphorylation events (85)

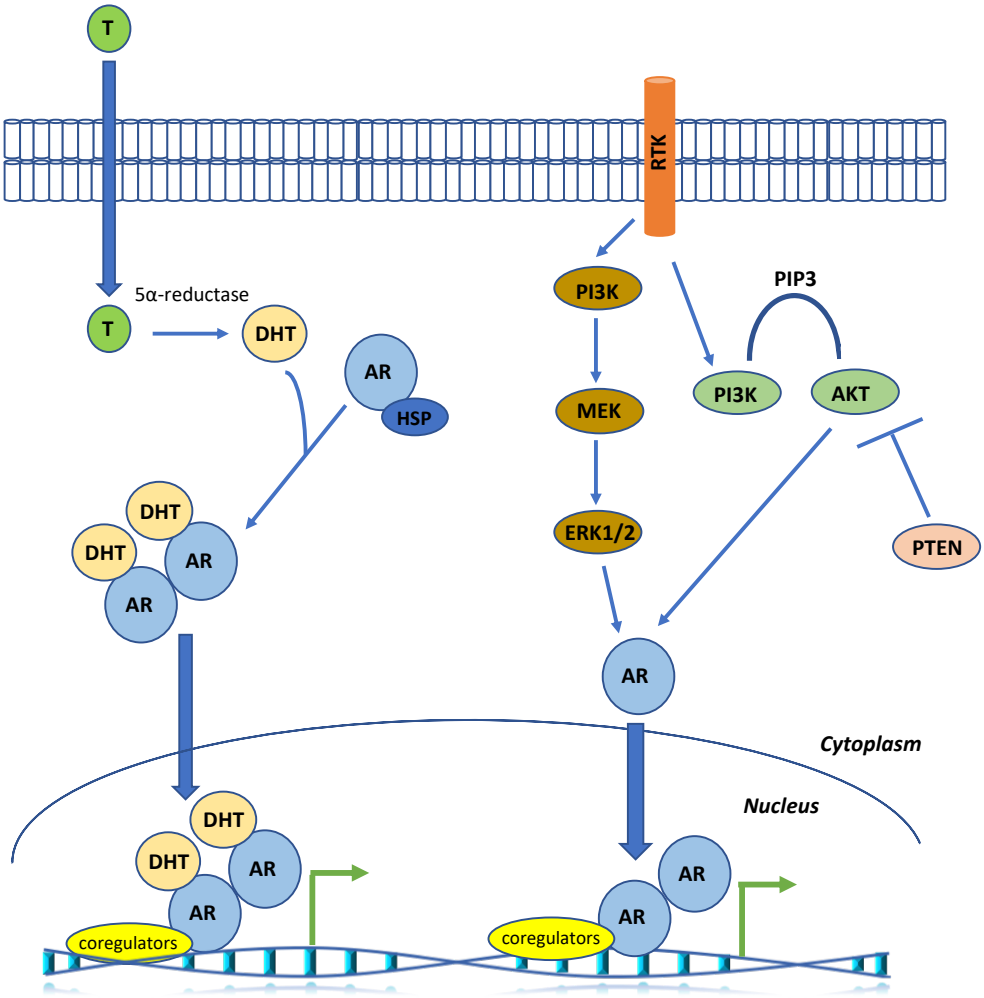

Figure 1.3 – Summary of the main androgen receptor signaling pathways in metastatic prostate cancer:

Upon binding to dihydrotestosterone (DHT), the androgen receptor translocates to the nucleus, binds to its target genes and regulates their expression. The AR can be activated in the absence, or in very low levels of DHT. Activating signals arise from several, non-mutually-exclusive mechanisms including extracellular growth factors such as EGF and intracellular signaling pathways (T=testosterone).

Since the discovery that CRPC commonly remains AR-driven novel AR-targeted therapies have been developed to overcome resistance by targeting steroidal hormone production through inhibition of CYP17A1 (Abiraterone acetate) or preventing hormone-mediated activation of AR by blocking the LBD (Enzalutamide) with a higher affinity than bicalutamide. These agents are being used routinely now to treat patients (89). ARN-509, or apalutamide, is another competitive inhibitor of the AR that has also shown improved outcomes in patients with CRPC (90). ODM-201 is a selective antagonist of the AR whose activity in CRPC is also been evaluated within a Phase III clinical trial (91). ODM-201 has activity against the F876L mutant AR where enzalutamide and ARN-509 have no potency against and preclinical models suggest that its anti-tumour activity is superior to enzalutamide (92).

1.2 – The ErbB receptor family

The ErbB receptors are a family of transmembrane receptor tyrosine kinases that are integral to cell signalling and proliferation (93). They are referred to as the human epidermal growth factor receptor, HER or ErbB, and comprise of EGFR (ErbB1), HER2, HER3 and HER4.

The receptors possess an extracellular N-terminal ligand-binding domain, a helical transmembrane domain and an intracellular C-terminal tail which contains the catalytic function of the tyrosine kinase domain (94). Receptor dimerisation is essential for their function and signalling and occurs upon ligand

binding to the extracellular domain (95, 96). Dimerisation can occur between two different ErbB receptors (heterodimerisation) or between two molecules of the same receptor (homodimerisation). Normally, they exist as inactive monomers folded in a conformation to prevent dimerisation (97).

Ligand binding to the extracellular domain encourages a change in the receptor conformation allowing the dimerisation domain to become exposed and to interact with another receptor (98). Following dimerisation, transphosphorylation of the receptors occurs that activates the tyrosine kinase portion to stimulate downstream intracellular signalling pathways such as the MAPK/ERK, PI3K/AKT/Mtor, Src kinases and STAT transcription factors (99).

Although all four ErbB receptors have the same essential domains, the functional activity of each domain varies. EGFR and HER4 have active tyrosine kinase domains and known ligands. The majority of ErbB complexes function as heterodimers despite the ability of EGFR and HER4 to signal autonomously via homodimerisation. The molecular structure and dynamics of EGFR have been studied more extensively and are used as a model to help our understanding of ErbB dimerisation. The baseline inactive state of the receptor is in a ‘closed’ conformation where the tyrosine kinase is hidden. Ligand binding induces conformational change in the structure of EGFR to expose the tyrosine kinase domain and allow it to become catalytically active (98). HER3 can bind to several ligands but has a weak intrinsic tyrosine kinase activity compared to the other ErbB receptors and is unable to bind ATP (95). Transphosphorylation

of HER3 however, with another ErbB receptor allows it to act as a potent activator of downstream signalling (100). Finally, HER2 possesses an active tyrosine kinase domain but does not bind to any of the ErbB ligands directly (95). It is instead found in a conformation that mimics the ligand-bound state ('open') and this allows it to form dimers (101).

The activating ligand involved and the heterodimer partner are the most important factors in determining which downstream adaptor protein is engaged and therefore which signalling pathway is finally activated. In addition, ErbB dimers have different signalling potencies, with homodimers being weaker than heterodimers in general (95). The HER2-HER3 heterodimer is considered the most potent ErbB pair in terms of tyrosine kinase phosphorylation and downstream signalling (102) and seems to preferentially recruit through the PI3K pathway (103). In fact, HER3 has six p85 binding phosphotyrosine containing motifs and in the presence of heterodimer formation it is a potent activator of PI3K, therefore driving the activation of the pro-oncogenic AKT-mTOR pathways (104, 105). Studies using HER3 siRNA knockdown in HER2-amplified breast cancer cells have shown anti-proliferative results with this strategy hence further supporting the importance of HER3 and its interaction with other RTKs in driving oncogenesis (106).

In addition to the ligand-dependent HER3 heterodimerisation in cells with very high HER2 expression but lacking HRG ligand, HER2-HER3 heterodimers can form spontaneously and enable downstream signalling in a ligand-independent

manner. The HER2-HER3 heterodimers formed in the presence of absence of HER3 ligand have been shown to be structurally distinct as demonstrated by studies investigating the mechanisms of the anti-HER2 monoclonal antibodies trastuzumab and pertuzumab. Pertuzumab disrupts ligand-dependent dimerisation, while trastuzumab blocks ligand-independent signalling (106).

Because of their oncogenic ability, targeting the ErbB receptors has become very attractive both in the form of monoclonal antibodies against the extracellular ligand-binding region of the receptor and also small molecule tyrosine kinase inhibitors that prevent signal transduction (107). These strategies have been developed against EGFR and HER2, however because of the emergence of resistance to these agents and the new apparent role of HER3 as a dimerisation partner a lot of effort is now focused on new therapies that target HER3. HER3-specific monoclonal antibodies are now under evaluation (108).

1.2.1 - HER3 upregulation in cancer

HER3 plays an important role in cell proliferation and survival (99). Neuregulin binding to HER3 induces HER3 heterodimerisation with other ErbB receptor members, especially HER2, leading to the phosphorylation of the tyrosine residues of the C-terminal tail of HER3 (109). HER3 was also detected within the context of acquired resistance to other ErbB family members targeted therapeutics. For example, resistance to EGFR tyrosine kinase inhibitor gefinitib was originated due to activation of HER3 phosphorylation in lung

cancer (110). HER3 activation is also associated with resistance to HER2 targeted TKIs in breast cancer (111). Furthermore, HER3 and PI3K signalling pathway can escape inhibition of ErbB members by TKIs, both *in vitro* and *in vivo*, via an AKT mediated negative feedback mechanism that affects the HER3 phosphorylation-dephosphorylation equilibrium. Increased membrane HER3 drives phosphorylation therefore dephosphorylation is prevented by decreased phosphatase activity. Small interference RNA to knockdown HER3 experimentally showed that the pro-apoptotic activity of ErbB TKIs is re-established suggesting that the transphosphorylation of HER3 could be used as a marker of anti-ErbB targeted TKIs instead (111). Besides its implication in tumour resistance to ErbB receptor-targeted drugs, HER3 has also been shown to be a mechanism of resistance to other inhibitors of downstream kinases (112-114).

Furthermore, studies have shown that 50-70% of human breast cancers have detectable HER3 levels as evaluated by IHC and that this correlates with HER2 overexpression (115). In addition, oncogenic gain of function mutations in the HER3 gene were also detected in human colorectal and gastric cancers (116). Studies also report the increase in HER3 mRNA levels in numerous tumour types and its correlation with cell proliferation, invasion and disease progression (117, 118). MicroRNAs, including miR-205, miR-125a and miR-125b, that are known to regulate gene expression (either acting as oncogenes or tumour suppressor) have been found to regulate HER3 expression in several studies in cancer (119, 120).

In conclusion, HER3 expression promotes tumour growth directly but allows cancer cells to escape the effects of targeted, cytotoxic and anti-endocrine therapies and potentially contributes to the clinical progression of patients. This capacity of HER3 makes it an attractive target for therapeutic intervention (**table 1**).

Name	Drug company	Mechanism of action	Development stage	Biomarker
U3-1287	Daiichi Sankyo	Human monoclonal antibody against HER3	1. Phase III in EGFR WT with advanced NSCLC (NCT02134015). 2. Phase II in squamous Head and Neck cancer (NCT02633800).	HRG mRNA by qRT-PCR from tumour tissue
MM-121	Merrimack	Fully-human monoclonal antibody against HER3	1. Phase II in heregulin positive NSCLC (NCT02387216). 2. Phase II in heregulin positive, HER2 negative metastatic breast cancer (NCT03241810).	HRG by RNA in situ hybridization assay on biopsy tissue
MM-111	Merrimack	Bispecific antibody that inhibits ligand-induced phosphorylation of HER3	1. Phase II in HER2 positive gastrointestinal cancers (NCT01774851). 2. Phase I in HER2 amplified, advanced and refractory solid cancers (NCT00911898).	HRG mRNA from tumour tissue
MEDH7945A	Genentech	Dual humanised IgG1 that blocks ligand-binding to EGFR and HER3	1. Phase II in squamous Head and Neck cancer (NCT01577173).	HRG mRNA from tissue by both qRT-PCR and in situ hybridisation
LJM716	Novartis	Human monoclonal antibody against HER3	1. Phase I in HER2 positive breast or head and neck cancer (NCT01602406). 2. Phase I in squamous head and neck cancer or HER2 positive breast and gastric cancer (NCT01598077).	N/A
AV-203	AVEO	IgG1k humanized monoclonal antibody with high affinity for HER3	1. Phase I in solid tumours (NCT01603979).	N/A
MM-141	Merrimack	Bispecific monoclonal antibody against HER3 and IGF-1	1. Phase I in advanced solid tumours (NCT01733004).	N/A
KTN-3379	Celldex therapeutics	Fully human monoclonal antibody against HER3	1. Phase I in advanced solid tumours (NCT02014909).	N/A
GSK2849330	GlaxoSmithKline	Anti-HER3 monoclonal antibody	1. Phase I in HER3 positive advanced solid tumours (NCT01966445).	N/A

Table 1.1 – HER3 targeted therapeutics currently in clinical trials.

1.2.2 - ErbB in prostate cancer

ErbB receptor members have been shown to be expressed in the recurrent prostate cancer model CWR-R1 and that heregulin signalling through HER2 and HER3 increases AR transactivation and alters prostate cancer cell line growth in vitro (121). The EGFR ligand EGF is also known to be able to activate the AR in a ligand-independent manner, however the mechanistic details of this are not described (122).

The use of the EGFR-selective TKI gefitinib in mouse xenograft models of both androgen-dependent and androgen-independent prostate cancer demonstrated promisingly strong anti-tumour activity and markedly enhanced the anti-proliferative action of the anti-androgen bicalutamide, suggesting that targeting ErbB concomitantly with existing anti-androgen therapies could improve clinical outcomes (123).

HER2 is overexpressed in prostate cancer cell lines as the disease progresses from the androgen sensitive to the castrate resistant setting and can activate the androgen receptor pathway in the absence of ligand to contribute to disease progression, suggesting that there is a cross-talk between HER2 and AR pathways (124). Evidence suggests that HER2 is able to activate the AR with minimal or absent ligand, via heterodimerisation with HER3, and to promote DNA binding and AR stability through the MAPK and AKT pathways (125). Various studies using archival clinical prostatectomy samples also report the overexpression of HER2 (by IHC) and amplification at DNA level in a subset of

prostate cancer patients (126) and has been associated with disease recurrence following radical prostatectomy (127) and worse prognosis (128). The use of anti-HER2 monoclonal antibodies have shown ability to decrease proliferation of the 22Rv1 prostate cancer cell line (129) as well as of the CWR22 human prostate cancer xenograft (130). In addition, HER2-HER3 heterodimerisation was suggested in the past as a mechanism of aberrant AR signalling in metastatic castrate resistant prostate cancer. EBP1, a HER3 binding protein and AR co-repressor, was also found to be depressed in castrate resistant disease (131).

Despite the available preclinical evidence suggesting the ErbB targeting could be an important strategy in metastatic castration-resistant disease, Phase II clinical trials using gefitinib, erlotinib (both EGFR TKIs) and trastuzumab failed to demonstrate any objective responses in CRPC when used as single agents (132-134). A Phase II study of lapatinib (an inhibitor of both EGFR and HER2) showed PSA response in only a small number of patients (135). Pertuzumab, acting as a HER2 dimerisation inhibitor was thought to be a more exciting therapeutic intervention in this setting. Unfortunately, the use of pertuzumab within two Phase II clinical trials in CRPC (pre- and post-chemotherapy respectively) also failed to demonstrate significant clinical activity (136, 137). The modulation of ErbB receptor and autocrine ligand expression by androgen independent prostate cancer cells can support the sustained growth of cancer cells despite EGFR blockade, and HER3 was found to have an important role in mediating such resistance to EGFR inhibition (138, 139).

Studies in clinical samples of human prostate cancer has shown that the overexpression of heregulin and HER3 is associated with worse prognosis (140). *In vitro* work has shown that HER3 is required for and promotes invasive capacity of prostate cancer cells upon growth factor stimulation (141). HER3 nuclear localisation in prostate cancer cells *in vitro* and in tissues, however, showed inconsistent results with its association with the hormone-refractory phenotype (142) but HER3 immunohistochemistry (IHC) studies in prostate cancer tissue samples showed that HER3 overexpression is associated with worse prognosis (143). In addition, IHC shows that 90% of human prostate cancers have significant HER3 staining demonstrating the importance of this oncogenic signalling in the disease (144). Similarly, a study using microarray analysis has shown increased expression of HER3 in human prostate cancer compared to the normal prostate (142). Due to the potency of HER3 heterodimerisation to preferentially activate the PI3K-AKT pathway as described previously, phosphorylation of AKT is pronounced in CRPC and acts as a mechanism of cell proliferation and ligand-independent AR activation (145). HER3 is one of the implicated oncogenic changes responsible for this increase in AKT phosphorylation making it a likely cause for the sustained cell proliferation seen despite anti-androgen treatment (143).

In addition, HER3 has been shown to be negatively regulated by AR in androgen sensitive cells, however with androgen targeting treatments a simultaneous increase in HER3 has been observed together with the emergence of castration-resistance cells. This has suggested that HER3 plays

an important role in the transformation pathways that drive prostate cancer to a castration resistant phenotype (143) and might also indicate that anti-HER3 agents are best used early in the disease (in combination with anti-androgens) to prevent progression to castration resistant phenotype. HER3 overexpression or heterodimerisation might also prove to be a biomarker to predict CRPC or the development of treatment resistance.

1.3 The PI3K signalling pathway

1.3.1 – Introduction

The phosphoinositide 3-kinases (PI3Ks) are a large family of lipid enzymes that phosphorylate the 3'-OH group of phosphatidylinositols on the plasma membrane and have an established role in different cellular processes including metabolism, inflammation, cell survival, motility and cancer progression (146). There are three classes of PI3Ks described in mammals: class I, class II and class III. Class I PI3Ks are further subcategorised in class IA and IB and are the ones best characterised to have a role in cancer (147).

The class I PI3Ks are heterodimeric enzymes that consist of a regulatory and a catalytic subunit (p110). p110 has four different isoforms (α, β, γ, δ) and several regulatory subnits. p85 is the regulatory subunit for p110α, p110β and p110δ (147). Class I PI3Ks form dimers in cells and can transduce signals from activated RTKs, G-protein coupled receptors and from activated RAS (148).

Upon stimulation, the regulatory unit may interact with the intracellular portion of the activated receptor and this allows subsequent activation of the catalytic unit which will then associate with the lipid membranes to phosphorylate phosphatidylinositol (4,5) P_2 to phosphatidylinositol (3,4,5) P_3. Phosphatidylinositol (3,4,5) P_3 is the principal mediator of Class I PI3K activity and constitutes a docking site for proteins that contain pleckstin homology (PH) domain, controlling their localization and activation (148). Signaling is then mediated mainly via proteins such as phosphoinositide-3-kinase-protein kinase B/AKT.

AKT is one of the major downstream effectors of PI3K. Upon PI3K activation, AKT is translocated via its PH domain to the inner membrane where it is phosphorylated by PDK1 on its activation loop (T308) (149). This subsequently activates mTORC1 which results in increased protein synthesis and cell survival by direct phosphorylation of its effectors, such as the ribosomal S6 kinase and 4E-BPs. Furthermore, the mTORC2 complex also contributes to full activation of AKT by phosphorylating its serine 473. Complete AKT activation leads to additional substrate phosphorylation events both in the cell cytoplasm and nucleus, including phosphorylation of the pro-apoptotic FOXO proteins (150) (**Figure 1.6**).

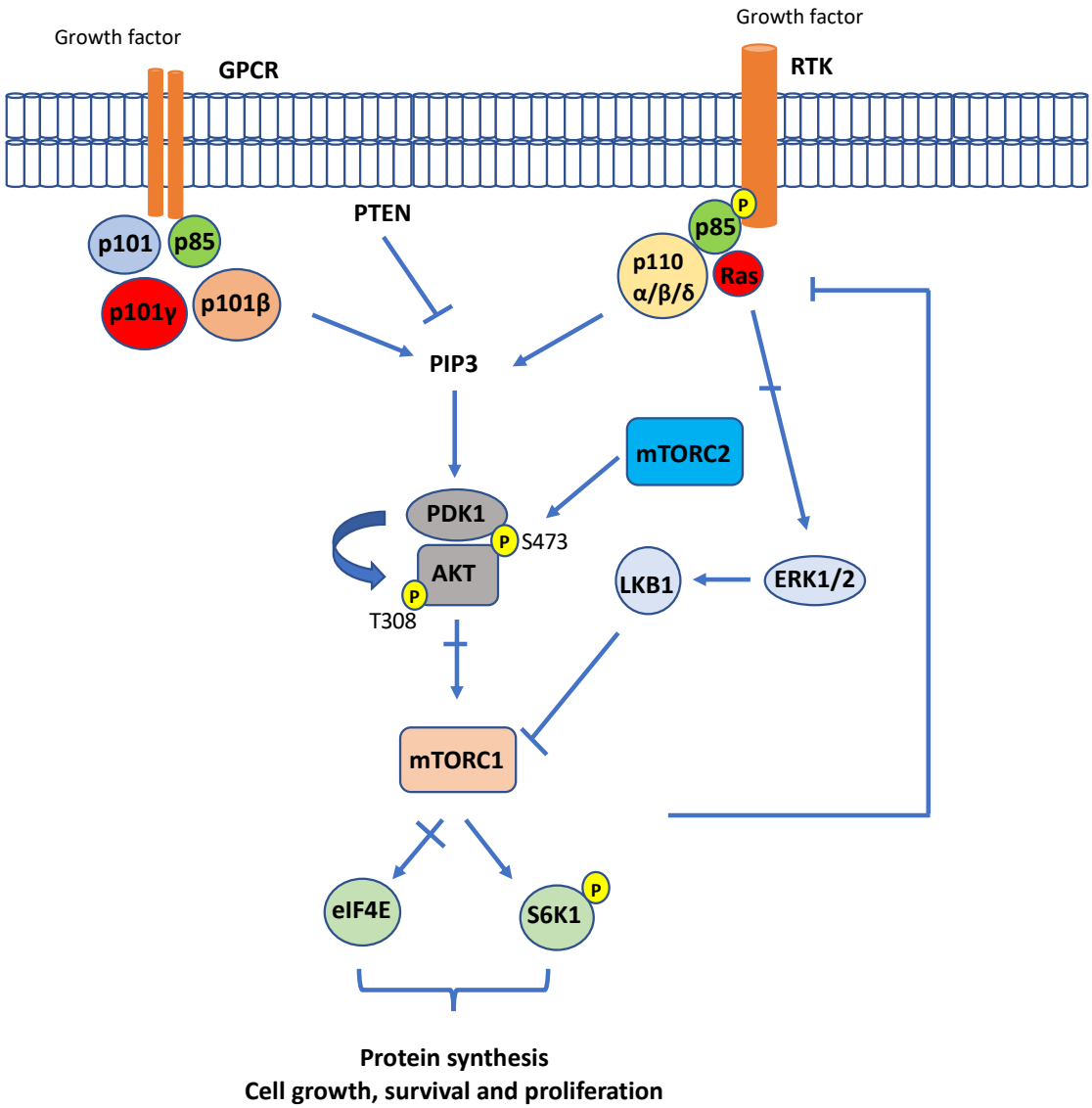

Figure 1.4 – Overview of PI3K-AKT-mTOR signalling pathway:
Class I PI3Ks are activated by growth factors through GPCR or RTK receptors. PI3K activation results in the conversion of PIP2 to PIP3, a process that is negatively regulated by PTEN. PIP3 constitutes a docking site for PH-containing proteins (PDK1 and AKT) recruitment and activation. Subsequently AKT removes the inhibition on the mTOR/Raptor complex (also known as mTORC1), thus leading to mTORC1 activation.

PI3K signalling is antagonised by the PTEN tumour suppressor. The PTEN gene is frequently mutated in many cancers especially brain, breast and prostate (151). PTEN has a strong phosphatase activity for PIP3 which is

important for its tumour suppressor action (152). It is therefore not surprising that mutations or loss of the PTEN gene lead to tumour development.

1.3.2 – The PI3K pathway in prostate cancer

PI3K-AKT-mTOR pathway aberrations have been identified in about 40% of early prostate cancer and up to 70-100% in advanced disease (153). Loss of PTEN, the negative regulator of the PI3K pathway, is documented in approximately 30% of primary and 60% of castrate-resistant prostate cancers (154). Activation of the PI3K pathway is associated with resistance to ADT, disease progression and poor outcomes (155, 156). PTEN loss, being responsible for activation of the pathway, has been shown to be associated with prostate cancer initiation and progression to the castrate-resistant phenotype (157). Increase of p-AKT expression has been shown to correlate with higher Gleason score and to act as a strong predictor of poor clinical outcome in patients and it could be used as a predictive biomarker of disease progression (158, 159). Even the more downstream effectors of the pathway are predictive of disease progression, such as high phospho-4EBP1 and eIF4E levels that have been shown to be associated with increased mortality from prostate cancer (160).

PI3K and AKT are constitutively expressed in human prostate carcinoma and a study has shown that their overexpression is involved in enhancing tissue invasiveness (161). In addition, increased AKT activity facilitates prostate

cancer progression through down-regulation of the cyclin-dependent kinase inhibitor, p27/Kip1 (162). Also, AKT/PKB activation correlates with increase in angiogenesis and metastasis through hypoxia-inducible factor-1α (163). In general, the PI3K-AKT pathway seems to act in conjunction with other proteins implicated in prostate cancer growth. For example, the recruitment of Ack1 by upstream receptors activates AKT and enables the progression of prostate cancer (164). Deficiency of SPRY2 interacts with EGFR in the setting of PTEN loss in prostate cancer to enhance activation of the PI3K-AKT pathway via enhancing RTK trafficking (165). The development of castration resistance in patients that received long-term ADT was shown to be associated with activation of PI3K-AKT pathway (166).

Other preclinical studies also demonstrated another fundamental relationship between the PI3K pathway and AR in the development of CRPC. Specifically, the loss of PTEN in prostate epithelial cells leads to decrease in transcription of AR target genes through release of repression of negative regulators of AR activity (167). This deregulation in the PI3K-AKT-mTOR pathway has therefore the ability to rewire the AR signalling pathway, decrease the requirements of cancer cell for androgen-dependent growth and allow the development of castration resistance. Furthermore, genetic and pharmacologic studies have demonstrated that inhibition of either PI3K-AKT-mTOR or AR signalling can allow reciprocal activation of the other. For example, genetic loss of AR or treatment with enzalutamide in *in vivo* models of prostate cancer driven by PTEN loss enhanced AKT signalling though downregulation of FKBP5 (167).

On the other hand, Carver et al have shown that increased AR protein and target gene expression were associated with a mechanism dependent on HER3 upon mTOR inhibition in prostate cancer models with background of PTEN loss (6). Also AR and PI3K cross-talk may occur through interactions of the AR/Src and the p85α subunit of PI3K to promote cell survival in androgen-deplete conditions (168).

The clinical implication of all findings that demonstrate the interplay between these two signalling pathways is that these can compensate each other in the setting of therapeutic inhibition of the other pathway alone. Finally, there is limited data to date to demonstrate the relationship of the AR and PI3K-AKT-mTOR pathways in models with wild-type PTEN and earlier disease stage where this interplay between the two pathways might function in different ways.

1.3.3 – PI3K targeting in prostate cancer

Undoubtedly, there is strong evidence about the involvement of PI3K pathway in the evolution of prostate cancer and especially castration-resistant disease. Several drugs have been developed targeting PI3K signalling and its downstream targets, however initial results have been negative unfortunately. Preclinical evidence supporting combined pathway inhibition, as well as the negative results by the use of single-agent inhibitors of PI3K-AKT-mTOR pathway have led to the design of clinical trials using small molecule inhibitors in combination with anti-androgens or chemotherapy. A summarised table showing all clinical trials using inhibitors of the PI3K-AKT-mTOR pathway is

shown below (**Table 1.2**). It is noticeable that two clinical trials are investigating the use of AKT and PI3K inhibitors in the hormone-sensitive setting post biochemical relapse (NCT01251861) and neoadjuvant setting prior to radical prostatectomy (NCT01695473) respectively. There is suggestion that earlier treatment with these agents might be an important strategy to prevent the development of castration resistance (169).

Results so far from the Phase II study using the pan-AKT inhibitor GDC-0068 and abiraterone (versus abiraterone alone) in metastatic CRPC have been encouraging showing improved radiological PFS and OS with potentially increased benefit in patients with decreased PTEN expression (170).

In addition to evaluating the optimal timing, combinations and sequence of these treatments, many of the clinical trials listed below are also investigating the role of predictive biomarkers. These involve mainly evaluation of PTEN status on tumour samples, however it would be important to incorporate further exploratory biomarkers within future clinical trials that will allow the non-invasive, longitudinal evaluation of disease response and resistance to treatment along the time-course of therapy. The development, therefore, of robust assays to use in liquid biopsies would make it more straightforward to assess.

Trial number	Drugs	Mode of action	Phase	Previous treatments	Primary outcome measures	Biomarker	Results
NCT01485861	Abiraterone acetate +/- GDC-0068	Pan AKT inhibitor	Ib/II	Docetaxel	- Radiographic PFS (rPFS) - OS	- PTEN expression (IHC) and genomic loss (FISH/NGS)	- Improved rPFS and OS - Effects superior in pts with PTEN loss
NCT01884285	AZD8186 +/- Abiraterone acetate	Selective PI3Kβ and PI3Kδ inhibitor	I	Anti-androgens	- Pharmacokinetics/ Pharmacodynamics - Safety and tolerability	N/A	Recruiting
NCT02215096	GSK2636771 + Enzalutamide	Selective PI3Kβ inhibitor	I	Enzalutamide	- Pharmacokinetics/ Pharmacokodynamics - Safety and tolerability	- PTEN status	Recruiting
NCT02407054	Enzalutamide +/- LY3023414	Pan class I PI3K-mTOR	II	Abiraterone	- PFS (PSA level)	N/A	Recruiting
NCT02525068	Enzalutamide +/- AZD5363	Pan AKT inhibitor	II	N/A	- Best overall tumour response (PSA level, RECIST, CTC enumeration)	- PTEN status	Recruiting
NCT02121639	Docetaxel +/- AZD5363	Pan AKT inhibitor	I/II	Chemo-naive	- PFS (PSA level)	N/A	Recruiting
NCT01251861	Bicalutamide +/- MK2206	Pan AKT inhibitor	II	Hormone-sensitive Pca at biochemical relapse	- PSA levels	N/A	Accrued, results awaited
NCT01695473	BKM120	PI3K inhibitor	II	Neoadjuvant, pre-radical prostatectomy	- PI3K inhibition in tumour measured by IHC	- IHC for pS6, pAKT, pEBP1	Accrued, results awaited

Table 1.2 – Current clinical trials investigating the use of inhibitors of the PI3K-AKT-mTOR pathway in prostate cancer.

1.4 - PSMA in prostate cancer

1.4.1 – PSMA structure, function, expression and regulation

PSMA is considered the most well established target antigen in prostate cancer, since it is highly and specifically expressed at all tumour stages on the surface of prostate tumour cells (171). PSMA is also known as glutamate carboxypeptidase II (GCPII) or N-acetyl-α-linked acidic dipeptidase I (NAALADase) or folate hydrolase and is a type II transmembrane protein expressed on the cell membrane of prostate epithelial cells (172). It is encoded by the FOLH1 gene which resides on chromosome 11p11-p12 and encodes for a 750 αα protein of approximately 100kDa (173). The extracellular domain makes the biggest part of the protein (707 αα) while it has small intracellular and transmembrane domains. Crystallisation data has allowed detailed characterisation of the PSMA extracellular domain. This, forms three well-defined structural and functional entities; the protease domain, the apical domain and the C-terminal domain. In addition, PSMA exists as a highly glycosylated homodimer (174).

The PSMA protein has two unique enzymatic functions. It contains a binuclear zinc site that has glutamate carboxypeptidase or folate hydrolase activity allowing it to catalyse the cleavage of terminal glutamates from poly-γ-glutamated folates (coming from the diet) on the brush border surface of the small intestine enabling folate uptake. PSMA probably has a role in folate metabolism in the prostate as well (175). It also has NAALADase activity that

allows the cleavage of terminal glutamate from the neurotransmitter N-acetyl-aspartyl-glutamate (NAAG) in neuronal synapses.

PSMA is not secreted into the circulation but undergoes constitutive internalisation. This is increased 3-fold in a dose-dependent manner after antibody binding by the PSMA specific monoclonal antibody J591 (176). Once inside the cell PSMA undergoes clathrin-mediated endocytosis ending up in lysosomes. This could represent either protein recycling or ligand binding (similar to ErbB). Therefore, this internalisation property of PSMA allows us to speculate that there is a natural ligand for PSMA (177). PSMA has also been shown to undergo macropinocytosis and clathrin-, caveola-independent endocytosis (176, 178). Furthermore, the expression of PSMA is shown to be inversely modulated by androgen levels (179). At the transcriptional level, activation of PSME, the PSMA enhancer that is located in the third intron of the FOLH1, is prostate specific and negatively regulated by the AR (180). It is believed that this occurs via tissue specific proteins that interact with the AR DBD to cause PSME repression (177). Finally, PSMA is known to undergo extensive glycosylation and this post-translation modification of the protein is thought to play an important role in its enzymatic activity and protein folding. It is reported that the glycosylation profile of PSMA in difference prostate cancer cell lines varies, suggesting that the distribution of sugar epitopes on PSMA might have a role in prostate cancer disease progression. Evidence also suggests that the de-glycosylation of PSMA reduces its enzymatic activity (175).

PSMA is upregulated many-fold in prostate cancers, metastatic disease and castrate-refractory disease. IHC studies on prostate cancer tissue have allowed us to define PSMA expression in the prostate, showing that the percentage of PSMA positive stained cells increases as the disease stages increases as well, from benign (69.5%) to adenocarcinoma (80.2%). Furthermore, the expression of PSMA in tumour stroma, urothelium and normal vasculature is negative (181). PSMA expression is highly organ-specific. There is now known expression in the salivary glands (179), the cryptic cells of the duodenum (182), the proximal renal tubules (182) and in the brain (183). Remarkably, PSMA expression is also detected in the neovasculature of various cancers (bladder, kidneys, breast, pancreas, lung) but is not found in normal established vasculature, making it an interesting tumour angiogenesis marker (182, 184). Conway et al, report that PSMA regulates cell invasion and tumour angiogenesis via integrin signal transduction modulation in endothelial cells (185).

1.4.2 PSMA as a prognostic and diagnostic biomarker

PSMA expression and enzymatic activity is increased in prostate cancer cells compared to normal and benign prostatic tissue and has therefore gained a lot of interest about its utility as a prognostic biomarker of the disease (186, 187).

Various studies are now available that report the correlation between PSMA expression and increased Gleason score (187, 188). In addition to Gleason

score, it was found that PSMA expression significantly correlates with other prognostic factors of adverse outcome, including tumour grade, pathological stage, aneuploidy and biochemical recurrence (189). Recently, a splice variant of PSMA was identified (PSM-E) and it also correlates with Gleason score (190). Interestingly, this is found in the cytoplasm of prostate cancer cells (191).

Furthermore, PSMA appears to have an enzymatic role in activating intracellular signaling pathways to allow further cell proliferation. It has been described that PSMA activates the small GTPases RAS and RAC1 leading to downstream MAPK pathway activation in LNCAP prostate cancer cells. This leads to further induction of NF-κβ activity, increased expression of IL-6 and CCL5 genes and finally enhanced survival and proliferation of prostate cancer cells. Consequently, it appears that PSMA expression and its enzymatic activity in aggressive tumours play an important role in disease progression (192).

To conclude, the expression of PSMA levels in patient tumours can serve to compliment other established biomarkers and provide more robust indications of treatment response, especially when evaluating the activity of specific targeted therapies.

1.4.3 The link with PIK3 pathway

The function of PSMA in prostate cancer has been elusive for years, however recent data shows that it plays an important role in modulating cellular signaling

pathways implicated in the pathogenesis of prostate cancer, such as the PI3K-AKT-mTOR pathway.

Guo et al have shown that PSMA knockdown by siRNA transfection led to abrogation of pAKT (s473) levels in LNCaP cells and that the use of a PI3K inhibitor was also able to reduce pAKT levels in both PSMA WT and knockdown groups. Decrease in cell proliferation, migration and survival was also observed with PSMA knockdown and PI3K inhibition. These observations led to the conclusion that PSMA regulates cellular signaling via the PI3K-AKT pathway, a mechanism for PSMA that was largerly undescribed (193).

In addition, the study of PSMA-negative tumours, generated by crossing PSMA-deficient mice with transgenic prostate cancer TRAMP models confirmed the observation that PSMA has an important pro-angiogenic role as demonstrated by more apoptotic and less vascular tumour production. Moreover, and compared to PSMA-positive tumours, PSMA-negative tumours had less activity of the PI3K-AKT pathway. The interaction of PSMA with the scaffolding protein RACK1 was identified as a mechanism of AKT signalling activation in this model (194).

Furthermore, more recent work done demonstrated that PSMA in prostate cancer can initiate signalling upstream of PI3K through mGLUR (**Figure 1.7**). The enzymatic activity of PSMA is capable of releasing glutamate from glutamated substrates leading to the activation of mGLUR1 and this can

subsequently induce the activation of PI3K pathway through the phosphorylation of p110β. This effect is independent of PTEN status and was noted in *in vitro*, *in vivo* and clinical experiments. Inhibition of PSMA in preclinical experiments demonstrated decrease in PI3K signalling and tumour regression and this was interrogated by PET imaging. This oncogenic axis between PSMA-PI3K can therefore be exploited further therapeutically (195).

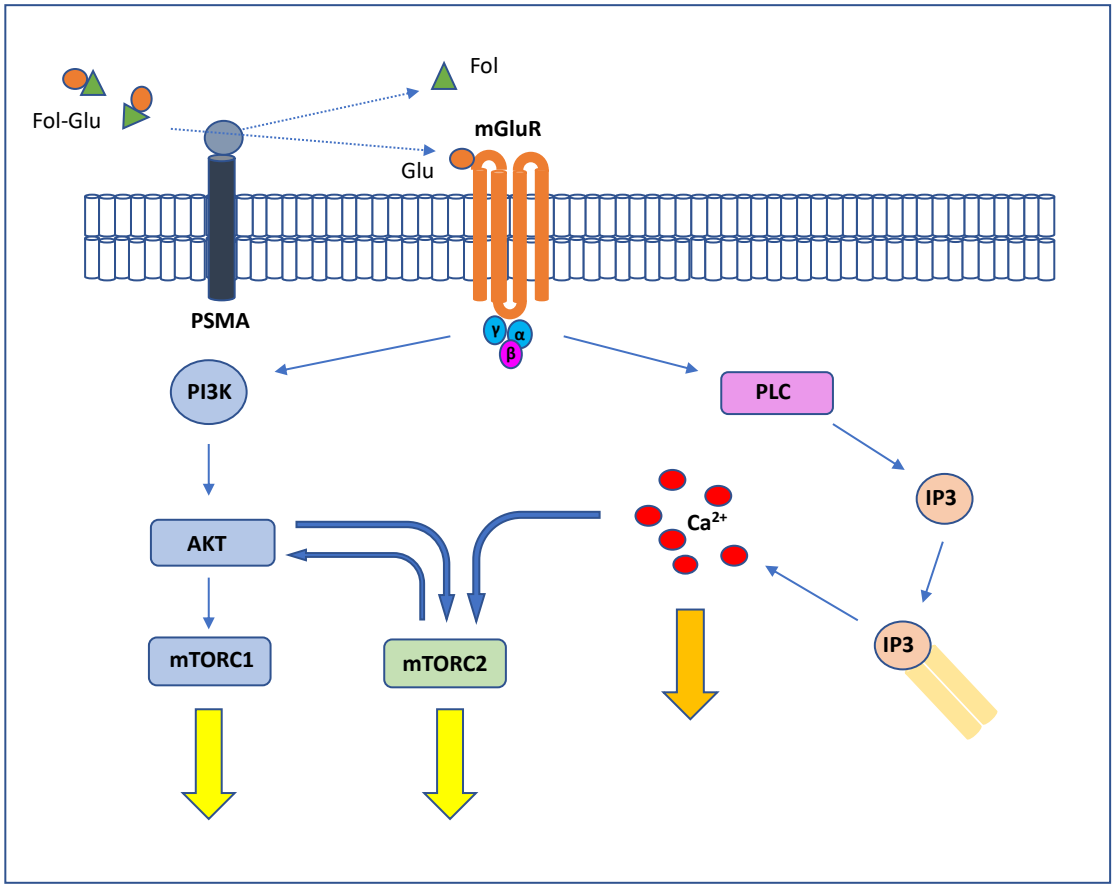

Figure 1.5 – The schematic representation of the overall pathway involving PSMA and induction of PI3K-AKT signalling:

Free glutamate released from PSMA after processing of glutamate-containing substrates activates mGLUR1 receptors on the plasma membrane of prostate cancer cells. Activation of the glutamatergic pathway induces calcium signalling and activation of the PI3K cascade supporting tumour growth.

1.4.4 PSMA as a therapeutic target

The high expression of PSMA on the cell surface, its large extracellular target and high organ specific allow its use as a target antigen for the treatment of prostate cancer as well as a target of imaging agents. Furthermore, its internalization upon ligand binding enable the use for targeted delivery of intracellular acting drugs. As a result, many preclinical and clinical studies were done using PSMA as a target antigen.

Small molecule binding to PSMA can be linked by a chelator to a therapeutic isotope to treat cancer lesions in a theranostic approach. ^{177}Lutetium-PSMA-617 radioligand therapy is the commonest reported therapy. Phase 1 and 2 clinical trials using radiolabeled (using ^{177}Lu) PSMA mAb J591, that targets the extracellular domain of PSMA, have shown promising results. These early phase clinical trials have demonstrated the safety and tolerability of 177Lu-PSMA treatment in metastatic CRPC (196-200). In addition, outcomes of PSA response and clinical OS survival also showed positive results in patients with metastatic CRPC (201, 202). Furthermore, the use of 177Lu-PSMA-617 also showed better outcomes when compared to cabazitaxel and also caused less grade 3 and 4 toxicities (203). Phase 3 trial results would be really important to determine whether this therapy can become standard of care in metastatic CRPC (204).

Antibody-based therapies utilizing PSMA can also be employed. For example, MLN2704 is an antibody-drug conjugate (ADC) in which the antibody

component of the drug is huJ591. The use of this agent was unfortunately limited by its dose-limiting toxicity profile (205). Further interest in the development of other PSMA-targeted cytotoxic agents is still high.

1.5 The FRET-FLIM technology

Fluorescence resonance energy transfer (FRET) has become widely used in medical diagnostics, DNA analysis and optical imaging. FRET and fluorescence lifetime imaging microscopy (FLIM) assays are suitable for use in cell line models of cancer, fresh human tissues and formalin-fixed paraffin embedded tissue (FFPE) to quantify the interaction between signalling proteins by measuring the energy transfer between fluorophores attached to specific proteins (206). The analysis of FRET assays performed on FFPE tissue can be correlated with clinical outcomes of disease in individual patients. Furthermore, response to therapy at a molecular level can be monitored using FRET assays while the patient receives treatment by utilising re-biopsy tumour tissue sample or by examining surrogate tissues. Such technologies can provide both prognostic and predictive biomarker information and have great potential for translation into real-life monitoring of cancer patients (206).

FRET is an electrodynamic phenomenon that can be explained using classical physics. A fluorophore is a molecule that contains a fluorescent group. The fluorescent group absorbs energy at a specific wavelength, is excited, and then emits energy at a longer wavelength as it reverts to the ground state. The

fluorescent lifetime, τ, is the average lifetime that a fluorophore remains in the excited state. FRET occurs between a donor (D) fluorophore in the excited state and an acceptor (A) fluorophore in the ground state. Fluorophores are attached to the proteins of interest by direct conjugation of antibodies (207).

FRET is the process of non-radiative energy transfer from one fluorophore (donor) to another (acceptor) when in close proximity. The donor molecules typically emit at shorter wavelengths that overlap with the absorption spectrum of the acceptor. The rate of energy transfer depends on the extent of spectral overlap between the emission spectrum of the donor and absorbance spectrum of the acceptor, the relative orientation of the donor and acceptor transition dipoles and the distance between the donor and acceptor molecules (nanometer proximity). The FRET efficiency is relative to the inverse sixth power of the distance, R, between the two molecules. The Forster radius, R_0, (typically 1-10nm) is the distance at which $FRET_{eff}$ is half its maximal value and depends on the spectral characteristics of the fluorophore. In order for $FRET_{eff}$ to be significant, the distance between the fluorophores must be within nanometres. Within experimental conditions, therefore, FRET is only likely to occur when two fluorophores, and their attached proteins are directly interacting.

$$FRET_{eff} = 1/ [1+(R/R_0)^6]$$

For example, the absorption spectrum of Cy5 is 590-650 nm and the emission spectrum of Alexa546 is 573-648 nm, making Alexa546-Cy5 an appropriate

FRET pair and this has been used by our laboratory previously but also in this project to quantify protein-to-protein interactions by FLIM. Alexa546 is excited by the laser source and the fluorescence signal is measured as a function of time. The fluorescence lifetime can then be calculated by fitting an exponential model to the decay of the signal.

The study of HER2-HER3 heterodimerisation in this project in models of metastatic hormone-sensitive and castrate-refractory prostate cancer has the ability to provide important information to complement HER2 and/or HER3 protein upregulation observed by biochemical assays upon treatment pressure with PI3K-mTOR inhibitors. In support of preclinical data showing changes in ErbB heterodimerisation, the quantification of HER2-HER3 heterodimer in patient tissue samples and circulating exosomes could be utilised as predictive biomarker for response and resistance to treatment. The quantification of HER2-HER3 heterodimer in FFPE breast cancer tissue samples was shown to be prognostic for metastatic recurrence for up to 10 years, independent of routine clinic-pathological biomarkers, including HER2 overexpression (208) and similar information regarding HER2-HER3 heterodimerisation in prostate cancer especially with targeted treatments might provide important information for predictive biomarkers in this disease.

1.6 Exosomes as liquid biopsies

Currently available diagnostic and prognostic tools for monitoring molecular changes in cancer consist of invasive methods requiring tumour tissue. Of particular interest in this context are exosomes that are secreted by a variety of cell types and tissues in the body, including cancer cells. They have gained enormous attention lately due to their ability to reflect tumourigenesis and the proteome and RNAome of the cells of origin (209). In addition, exosome analysis is ideally suited for monitoring the evolving tumour longitudinally, in terms of its whole transcriptome, miRome and proteome profiles (210) and can be used to monitor tumour progression in response to cancer therapy (211).

Exosomes are vesicles with a size of 30-120 nm that are shed extracellularly. They are defined as small extracellular vesicles with a multivesicular endosomal origin (212) that are released from various cells, such as epithelial, immune and inflammatory cells, as well as body fluids including saliva, urine and blood. Exosomes are highly heterogeneous and likely reflect the phenotypic state of the cell that generated them (213). They are composed of a lipid bilayer and their cargo contains proteins, mRNA, microRNA, DNA and lipids that can be exchanged between donor and recipient cells (214, 215). The number of identified proteins, mRNA and lipids in exosomes is growing comprehensively comprised in the ExoCarta database (216). Exosomes are characterised by canonical proteins, such as CD63, TSG101 and CD9, but also of cell specific content reflecting their origin.

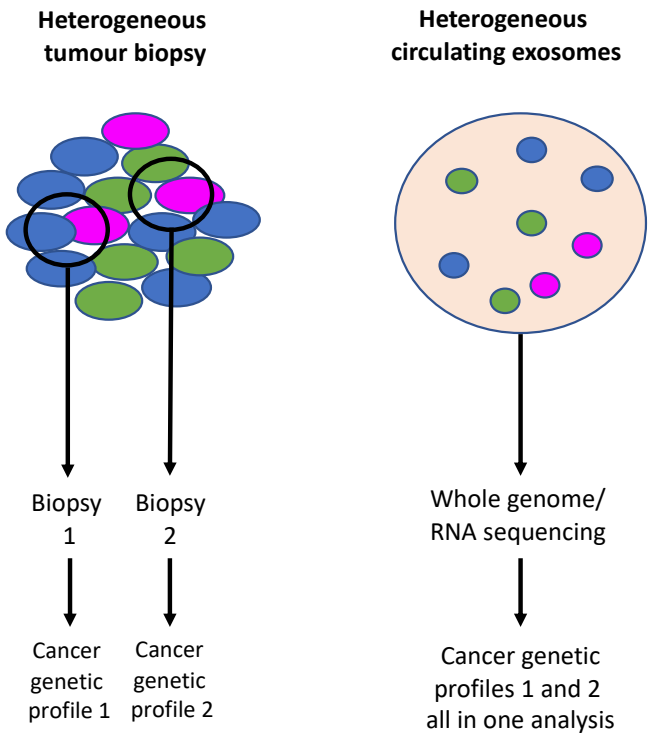

Figure 1.6 – Sequencing of exosomal RNA and DNA can identify driver and passenger mutations and deletions providing information on actionable genetic defects associated with cancer: Tumours contain a heterogeneous population of cancer cells. Clonal heterogeneity emerges when different sets of mutations and deletions drive different cancer cell clones, generating zones within tumours that contain unique sets of cancer cells with defined genetics. Therefore, tumour biopsies or portions cannot provide a view of the entire landscape of cancer-associated genetic defects. Analysis of cancer exosomes from the patient's blood can potentially overcome this limitation and offer genetic information reflecting the status of all the cancer cells in the tumour in order to account for tumour heterogeneity.

Exosomes are released from cells under both physiological and pathological conditions, therefore their biogenesis might represent a response to different biological processes such as ligand stimulation (217) or cell stress (218) as well as a particular pathological phenotype. Exosomes and their contents in cancer have emerged as potential source of information to detect cancer and provide information on regulatory drivers of tumour progression and metastasis.

Furthermore, exosome biogenesis in cancer might reflect changes in the microenvironment, hypoxia or malignant transformation.

The functions of exosomes in cancer are summarised below from the research evidence available to date:

- Liquid biopsy to aid in the diagnosis of malignancies: both their elevated concentration and enrichment of specific markers and detection of nucleic acids. In prostate cancer, the presence of PCA-3 and TMPRSS2:ERG in exosomes isolated from urine of patients demonstrated the potential to aid in diagnosis and monitoring (219). Furthermore, exosomal miR-141 levels in the serum of patients with prostate cancer discriminates those with metastatic disease from those with localised disease (220).
- Regulation of tumour microenvironment: by participating in the generation of protumourigenic or antitumourigenic setting by manipulating host stromal responses (221).
- Regulation of tumour immunity: the immunological activities of exosomes in tumours are likely complex and dynamic, ranging from modulation of tumour antigen presentation to polarisation of tumour immunity. While the reported immune activities of exosomes support their role in promoting anti-tumour immune responses, they may also aid in immune evasion and better understanding of their functions is needed (222).

- Regulation of tumour angiogenesis: by modulation of hypoxia-induced cell signalling (223).
- Tumour growth and metastasis: through reciprocal signalling, the remodelling of extracellular matrix to promote cancer cell invasion (224), the induction of invasive phenotypes in recipient cells and the modulation of the metastatic site to enhance metastatic disease.

Of course, future studies need to focus on the potential heterogeneity of cancer exosomes and how this enables further understanding of the clonal expansion of cancer cells and changes in response to therapies. In addition, RNA and DNA sequencing of serum-derived exosomes will likely aid in the early diagnosis of cancer and this coupled with exosomal proteomic analysis could provide predictive biomarker information during the evolution of malignant disease during its time course and in response to therapies. The research in exosomes is still in its early days from the clinical perspective, but the importance of exosome for monitoring the response to anticancer treatments is increasing.

Chapter 2: Materials and methods

2.1 Reagents

2.1.1 Mammalian cell lines

LNCaP, DU145 and PC3 prostate cancer cells were obtained from Dr Claire Wells' laboratory in King's College London.

CWR22 and 22Rv1 prostate cancer cells were a kind gift from Professor Hing Leung's laboratory (Beatson Institute).

2.1.2 Reagents for cell culture

RPMI-1640 media without glutamine (Sigma-Aldrich, Gillingham, UK)

Phenol red-free RPMI-1640 media without glutamine (Lonza, Basel, Switzerland).

For cell culture, media were supplemented with 10% heat-inactivated fetal bovine serum (Gibco, Thermo Fisher Scientific, USA) or 10% charcoal-stripped fetal bovine serum (Gibco, Thermo Fisher Scientific, USA) 1% Penicillin/Streptomycin (50 units Penicillin and 50µg/ml Streptomycin) (Sigma-Aldrich, Gillingham, UK) and 1% L-Glutamine (2mM) (Sigma-Aldrich, UK).

For exosome extraction, RPMI media with 1% Penicillin/Streptomycin and 1% L-Glutamine (as above) supplemented with 10% exo-free fetal bovine serum (Cambridge Bioscience, Cambridge, UK).

Trypsin/EDTA (Sigma-Aldrich, Gillingham, UK).

2.1.3 Transfection reagents

Opti-MEM media (Gibco, UK)

Fugene 6 (Promega, USA)

2.1.4 Reagents for molecular biology

293T cells (kind donation from Dr James Monypenny of Pitmilly, KCL)

LB agar and broth (Sigma-Aldrich, UK)

Ampicillin at 100 µg/ml (Sigma-Aldrich, UK)

Plasmid plus Maxi Kit (Qiagen, Germany)

Nuclease free H_20 (Invitrogen, USA)

dNTP set (Thermo Scientific, USA)

OligoDT primer (Invitrogen, USA)

5x first-strand buffer (Invitrogen, USA)

DTT at 100mM (Invitrogen, USA)

RNAase out (Thermo Scientific, USA)

Super script III reverse transcriptase 2000 units at 200U/µL (Invitrogen, USA)

Power SYBR Green Master mix (Applied Biosystems, USA)

PSA (KLK3 gene) primers: Fw CTTAGGTGTGAGGTCCAGGG, Rev TGTCCAGCACATGTCACTCT

QIAGEN Plasmid Midi kit

2.1.5 Cell stimulation

NRG-1: Neuregulin/recombinant human heregulin-β1, 50ng/ml (PeproTech, USA)

EGF: recombinant human epidermal growth factor, 100ng/ml (PeproTech, USA)

Mibolerone: synthetic anabolic steroid with high affinity for androgen receptor, 1nM (Sigma-Aldrich, Gillingham, UK)

2.1.6 Cell inhibitors

- DS7423: small molecule inhibitor against PI3K and mTOR (mTORC1/2); used at 1000nM in DMSO (Daiichi-Sankyo Company Ltd, Tokyo, Japan)

- Patritumab (U3-1287): fully human monoclonal antibody against HER3; used at 10μg/ml in sterile water (Daiichi-Sankyo Company Ltd, Tokyo, Japan)

- GDC0068 (Ipatasertib): highly-selective pan-AKT inhibitor; used at 100nM in DMSO, was a kind gift from Professor Bart Vanhaesebroeck's group (UCL Cancer Institute)

- GDC0941 (Pictilisib): potent inhibitor of PI3Kα/δ; used at 1000nM in DMSO, was a kind gift from Professor Bart Vanhaesebroeck's group (UCL Cancer Institute)

- Everolimus: mTOR pathway inhibitor (both mTORC1 and mTORC2 complexes) (Stemcell technologies, USA)

- Lapatinib: anti-EGFR and HER2 TKI; used at 10 μM in DMSO, (LC Labs, USA)

- Enzalutamide (MDV3100): androgen receptor antagonist; used at 10 μM in DMSO, (APExBIO, Houston, USA)

Cell inhibitors	
DS7423	small molecule inhibitor against PI3K and mTOR (mTORC1/2)
Patritumab (U3-1287)	fully human monoclonal antibody against HER3
GDC0068 (Ipatasertib)	highly-selective pan-AKT inhibitor
GDC0941 (Pictilisib)	potent inhibitor of PI3Kα/δ
Everolimus	mTOR pathway inhibitor (both mTORC1 and mTORC2 complexes)
Lapatinib	anti-EGFR and HER2 TKI
Enzalutamide (MDV3100)	androgen receptor antagonist

Table 2.1 – Table of cell inhibitors used in *in vitro* experiments

2.1.7 Reagents for cell and tumour lysis

Lysis buffer for western blotting:

100mM Tris/HCL (pH 6.8), 300mM NaCl, 0.5% NP40, H_2O. Adjust to pH 7.4 and filter.

On the day of use, supplement with protease (Roche, Switzerland) and phosphatase inhibitors (Roche, Switzerland), 1 tablet per 10 mls.

2.1.8 Reagents for Western blotting

4x Sample buffer: NuPAGE^{TM} LDS sample buffer (Invitrogen, USA)

Gels: Bis-Tris pre-cast polyacrylamide gels (Invitrogen, USA) or in-house made SDS PAGE gels:

Resolving gel	7.5%	10%	12%
ddH_20	7.2 mls	5.5 mls	4.2 mls
1M Tris HCL pH 8.8	7.5 mls	7.5 mls	7.5 mls
30% Bis Acrylamide (37.5:1) (Sigma-Aldrich, UK)	5 mls	6.7 mls	8 mls
10% SDS	200 µL	200 µL	200 µL
10% APS	200 µL	200 µL	200 µL
TEMED (Bio-Rad, UK)	13 µL	13 µL	13 µL

Stacking gel	
ddH_20	6 mls
0.5M Tris HCL pH 6.8	2.5 mls
30% Bis Acrylamide (37.5:1) (Sigma-Aldrich, UK)	1.33 mls
10% SDS	100 µL
10% APS	50 µL
TEMED (Bio-Rad, UK)	20 µL

Table 2.2 – Composition of various %age gels used for western blotting:
Volumes represent required amounts for two 1.5mm gels.

Precision Plus Protein Dual Color Standards (Bio-Rad, UK)

10x Running buffer stock: 250mm Tris-Base, 1.9M Glycine, 1% of 10% SDS, ddH_20 to make 1L. Used at 1x concentration, diluted in ddH_20.

10x Transfer buffer stock: 250mm Tris-Base, 1.9M Glycine, ddH_20 to make 1L. Used at 1x concentration made up of 100mls 10x transfer buffer, 200ml MeOH and 700mls ddH_20.

Immobilon roll PVDF transfer membrane (Millipore, UK)

Wash buffer: 1x TBS plus 01% Tween (Sigma-Aldrich, UK) (i.e TBS-T)

Block buffer: 1x TBS plus 4% milk (Sigma-Aldrich, UK)

Primary antibody solutions diluted in 1x TBS-T and 4% BSA (Sigma-Aldrich, UK)

Detection reagent, high sensitivity for chemiluminescent detection (GE Healthcare, UK)

2.1.9 Reagents for cell and exosomal RNA extraction

TRIzol reagent (Invitrogen, USA)

Chloroform (HPLC) (Fisher Scientific, UK)

100% Ethanol (Sigma-Aldrich, UK)

PureLink RNA Mini Kit buffers I and II (Invitrogen, USA)

Ultra-Pure DNAase/RNAase-free distilled water (Invitrogen, USA)

2.1.10 Reagents for cell immunocytochemistry

PBS (Gibco, UK)

4% paraformaldehyde (PFA) solution in PBS (Sigma-Aldrich, UK)

0.1% Triton X-100 (Sigma-Aldrich, UK) in 1x TBS

0.1% BSA (Sigma-Aldrich, UK) in TBS for block and antibody dilution

Hoechst (Invitrogen, USA) at 1:10000 in TBS

Vectashield mounting medium (VWR, USA)

Immersol 510 immersion oil (Zeiss)

2.1.11 Reagents for cell and exosome staining for FLIM

HCL 37% (Sigma)

PBS (Gibco, UK) and 1x TBS for wash

4% paraformaldehyde (PFA) solution in PBS (Sigma-Aldrich, UK)

0.2% Tween (Sigma-Aldrich, UK) in 1x TBS

Sodium borohydride at 1mg/ml in 1x TBS

0.1% BSA (Sigma-Aldrich, UK) in TBS for block and antibody dilution

10% Mowiol 4-88, 25% glycerol, 100 mM Tris-HCL pH 8.5 (Calbiochem)

99% TDE (Sigma)

Immersol 510 immersion oil (Zeiss)

2.1.12 Reagents for frozen tissue immunofluorescence

Methanol (Sigma-Aldrich, UK)

Acetone (Sigma-Aldrich, UK)

TBS

2% BSA (Sigma-Aldrich, UK) in TBS for block and antibody dilution

Hoechst (Invitrogen, USA) at 1:10000 in TBS

Vectashield mounting medium (VWR, USA)

Immersol 510 immersion oil (Zeiss)

2.1.13 Reagents for tissue immunofluorescence for FLIM

Xylene (Fisher Scientific, UK)

100% Ethanol (Sigma-Aldrich, UK)

TBS

1% Tween (Sigma-Aldrich, UK) in 1x TBS

Sodium borohydride at 1mg/ml in 1x TBS

2% BSA (Sigma-Aldrich, UK) in TBS for block and antibody dilution

10% Mowiol 4-88, 25% glycerol, 100 mM Tris-HCL pH 8.5 (Calbiochem)

DABCO (Sigma-Aldrich, UK)

2.1.14 Primary Antibodies

anti-AR N-20, rabbit polyclonal (Santa Cruz Biotechnology, USA)

anti-AR N-19, rabbit polyclonal (Santa Cruz Biotechnology, USA)

anti-AR 441, mouse monoclonal conjugated to Alexa Fluor 488 (Santa Cruz Biotechnology, USA)

anti-EGFR D38B1, rabbit monoclonal (Cell Signaling Technology, USA)

anti-EGFR, clone F4 (from CRUK repository) conjugated to Alexa Fluor 546 (in house and provided by Dr Gregory Weitsman)

anti-HER2/ErbB2 29D8, rabbit monoclonal (Cell Signaling Technology, USA)

anti-HER2, clone Ab17, mouse monoclonal, conjugated to CY5 (in house and provided by Dr Gregory Weitsman)

anti-HER3/ErbB3 D22C5, rabbit monoclonal (Cell Signaling Technology, USA)

anti-HER3, clone 2F12 (Thermo Scientific) conjugated to Alexa Fluor 546 (in house and provided by Dr Gregory Weitsman)

anti-HER3, clone 2F12 (Thermo Scientific) conjugated to CY5 (in house and provided by Dr Gregory Weitsman)

anti-HER4 111B2, rabbit monoclonal (Cell Signaling Technology, USA)

anti-AKT (pan) C67E7, rabbit monoclonal (Cell Signaling Technology, USA)

anti-ERK 44/42, rabbit monoclonal (Cell Signaling Technology, USA)

anti-PSMA 1H8H5, mouse monoclonal (Invitrogen, USA)

anti-S6 5G10, rabbit monoclonal (Cell Signaling Technology, USA)

anti-HIF1α EP1215Y, rabbit monoclonal (Abcam, UK)

anti-phospho EGFR (Tyr1068), rabbit monoclonal (Cell Signaling Technology, USA)

anti-phospho HER2 (Tyr1248), rabbit monoclonal (Cell Signaling Technology, USA)

anti-phospho HER3 (Tyr1289) 21D3, rabbit monoclonal (Cell Signaling Technology, USA)

anti-phospho AKT (Thr308) D25E6, rabbit monoclonal (Cell Signaling Technology, USA)

anti-phospho AKT (Ser473) D9E, rabbit monoclonal (Cell Signaling Technology, USA)

anti-phospho ERK (Thr202/Tyr204), rabbit monoclonal (Cell Signaling Technology, USA)

anti-phospho S6 (Ser235/236), rabbit monoclonal (Cell Signaling Technology, USA)

anti-Tubulin, mouse monoclonal (Abcam, UK)

anti-GAPDH 71.1, mouse monoclonal (Sigma, UK)

2.1.15 Secondary Antibodies

For immunoblotting:

Polyclonal goat anti-mouse/rabbit at 1:2000/1:3000 (DAKO)

For immunofluorescence:

Goat anti-mouse IgG-Alexa 488 at 1:100 (Invitrogen, USA)

Goat anti-rabbit IgG-Alexa 568 at 1:100 (Invitrogen, USA)

2.1.16 Reagents for *in vivo* xenograft model establishment and experiments

Male nude athymic mice, Charles River Laboratories (UK)

Matrigel Basement Matrix, VWR International Ltd

PBS (Gibco, UK)

DS7423: small molecule inhibitor against PI3K and mTOR (mTORC1/2); used at 3mg/kg/day in 0.05% Methylcellulose solution (Daiichi-Sankyo Company Ltd, Tokyo, Japan)

Liquid nitrogen

70% Ethanol: made from 100% Ethanol diluted in ddH_2O (Sigma-Aldrich, UK)

10% Formalin solution, neutral buffered (Sigma-Aldrich, UK)

Dry ice

2.1.17 Reagents for exosome isolation

Exo-FBS (exosome-depleted FBS media) (System Biosciences, USA)

PBS (Gibco, UK)

2.2 Methods

2.2.1 Plasmid purification

100µL of chemically competent cells were transformed with 1µL of plasmid and incubated on ice for 20 minutes followed by heat-shock at 42°C for 45 seconds on a thermomixer. The cells were then chilled back on ice for another 2 minutes and 1 ml of LB broth was added to each sample before the cells were allowed

to recover at 37°C with shaking at 600 RPM for 1 hour. The cells were then spread on agar plates containing ampicillin (100 µg/ml; as selection antibiotic) for incubation at 37°C overnight. For amplification, a colony was picked and grown in a conical flask containing 50 mls of LB broth with antibiotics. This was incubated overnight in shaker at 37°C at 210-220 RPM. Plasmids were purified using the QIAGEN Plasmid Midi kit according to manufacturer's instructions (cells were harvested by centrifugation; cells were lysed; precipitation buffer was added to the lysates; precipitated lysates were allowed to flow-through an equilibrated midi column; the column was washed through with buffer and the flow-through was discarded; DNA was eluted into a flask using elution buffer; isopropanol was added to precipitate DNA prior to centrifugation; the DNA pellet was washed in 70% ethanol prior to further centrifugation; the pellet was air-dried before resuspension in water. The DNA concentration was determined using a nanodrop spectrophotometer.

2.2.2 Stable transfection

Viral particles (including transfer vector, packaging vector, enveloping vector and Rev expressing vector) with specific shRNA or non-targeting were generated by transfection in 293T cell culture. The supernatants which contained viral particles, were collected and added to target LNCaP cells (seeded in a 6 well plate) for infection. 48 hours post infection, media were refreshed daily with puromycin containing RPMI media (at 1µg/ml) for 7 days for the selection of antibiotic resistant cells due to expression of a resistant gene associated with shRNA. From here onwards cells were cultured in RPMI media

containing 0.5µg/ml puromycin to maintain the protein knockdown and scaled up to T75 flasks for use in further experiments.

2.2.3 Cell culture

LNCaP, CWR22, PC3 and DU145 parental cells were grown in RPMI full media. Cells were maintained at 37°C in a water saturated incubator with an atmosphere containing 5% CO_2. Adherent cells were grown in culture until 70-80% confluent, typically in a T75 tissue culture flask. The growth medium was aspirated, cells were washed with 10 mls PBS and then incubated with 3 mls trypsin/EDTA at 37°C for 3-5 minutes. 7 mls of full media was then added to the cells to inactivate the trypsin/EDTA. LNCaP and DU145 cells were split at 1:4 dilution 2 times every week. CWR22 were split at 1:4 dilution 2-3 times every week. PC3 cells were split at 1:6-1:8 dilution 2-3 times every week.

LNCaP NTC and HER3kd cells were grown in a similar fashion but the RPMI full media also contained Puromycin antibiotic at 0.125 µg/ml. They were split at the same dilution and frequency.

22Rv1 cells were grown in a similar way as described above but in Phenol-red free RPMI media with 10% charcoal-stripped FBS. They were split at 1:4 dilution ratio 2-3 times every week.

2.2.4 Cell treatments

Cell stimulation was performed with Heregulin-B1 (or NRG-1) at 50ng/ml for initial experiments between 2-120 minutes and thereafter at 5 minute timepoint.

Cell stimulation using EGF at 100ng/ml was performed at 5 minute timepoint and stimulation with the mibolerone was done at 1 nM concentration for 24 hours. Inhibition using DS7423 was done in initial experiments at increasing concentrations (from 1-1000 nM) for 48 hours as well as at single concentration (1000 nM) at increasing timepoints between 1-48 hours. Combination experiments using DS7423 and mibolerone were performed using DS7423 first with the addition of mibolerone 24 hours later. In the case of patritumab, this was used at concentration of 10 μg/ml both alone and in combination with DS7423. Lapatinib treatment concentration was 10 μM for 24 hours alone or in combination with DS7423.

Furthermore, GDC0068, GDC0941 and everolimus were used at 100 nM, 1000nM and 100nM respectively for 48 hours.

Finally, enzalutamide was used alone at 10 μM at timepoints 2 and 7 days.

The treated cells were always incubated for the indicated timepoints at 37°C.

In all experiments where the AR levels or cellular localisation were assessed RPMI media with 10% charcoal-stripped FBS was supplements for at least 24 hours prior to cell lysis or cell fixation on coverslips.

2.2.5 Western blot

Cells were cultured until 80% confluent in 6 well dishes and then stimulated or inhibited as described above. Cells were then washed with ice-cold PBS and lysed on ice by scraping into 150-200 μl NP40 lysis buffer. The lysates were incubated on ice after scraping for further 10 minutes before centrifuging at 4°C

at 10,000g for 10 minutes to clear the debris. The total protein concentration was determined using the BCA assay (Pierce).

Aliquots of equal protein concentration from each treatment condition were loaded into 10% gels (Bis-Tris pre-cast or in-house made SDS PAGE gels). Gels were run on an Invitrogen X-cell mini-gel system. The gels were subjected to constant voltage electrophoresis at 30 mAmp per gel, until the protein marker for 25 kDa reached the bottom of the gel. After separation on the 10% gel, proteins were electrophoretically transferred onto PVDF membranes using the Invitrogen XCell II^{TM} transfer apparatus (arrangement: 2 sponges, 2 filter papers, gel, membrane, 2 filter papers, 2 sponges).

The membranes were then blocked using 4% milk in TBS for 1 hour at room temperature with shaking, the incubated with primary antibodies diluted in 4% BSA in TBS at 4°C overnight. Membranes were washed twice in TBS-T for 5 minutes each time on a roller, prior to incubation with secondary antibodies in blocking buffer for one hour at room temperature. They were then washed a further 3 times as before. The membranes were then placed on a clear folder, covered with enhanced chemiluminescent (ECL) substrate and developed using a CCD-based camera (Syngene).

2.2.6 RNA extraction

The growth medium was removed from cells and these were washed once with PBS. 600µL of Trizol was added to cells in 6-well plates and allowed to lyse the cells for 5 minutes at room temperature. The cells were then transferred to 1.5ml eppendorfs and 120µL of Chloroform was added and the mixture was

vortexed for 10 seconds at room temperature. This was allowed to incubate for 2 minutes at room temperature and then centrifuged at 12,000g for 5 minutes at 4°C. The supernatant was transferred to RNAase-free tubes and an equal volume of 70% ETOH was added followed by 10 seconds of vortexing at room temperature. 700µL of the sample was transferred to a spin cartridge and centrifuged at 12,000g for 15 seconds at room temperature. The follow-through was discarded and the spin cartridge was re-inserted into the same tube. This centrifugation step was repeated until the whole sample was processed. Once this was complete 700µL of wash buffer I was added to the spin cartridge and centrifuged at 12,000g for 15 seconds at room temperature. The follow-through was again discarded together with the collection tube and the spin cartridge was inserted into a new collection tube. 500µL of wash buffer II (that contained ETOH) was added to the spin cartridge and this was centrifuged at 12,000g for 15 seconds at room temperature. The follow-through was discarded and the spin cartridge was re-inserted into the same collection tube. Another 500µL of wash buffer II (with ETOH) was added to the spin cartridge and the whole centrifugation process was repeated. Following that, the cartridge was centrifuged at 12,000g for 1 minute at room temperature to dry the membrane with attached RNA. The collection tube was discarded and the spin cartridge was inserted into the recovery tube. 50µL of RNA-free water was added to the centre of the spin cartridge and this was allowed to incubate for 1 minute. The spin cartridge was centrifuged for 2 minutes at 12,000g at room temperature, then another 50µL of RNA-free water was added to the attached RNA and the

process was repeated. In total 100µL of cellular RNA was collected and stored at -80°C until further use.

(N.B – in the case of RNA extraction from exosome pellets 250µL of Trizol was added for lysis followed by 50µL of Chloroform i.e at 1:5 ratio. The final RNA elute was suspended in 50µL of RNA-free water. Otherwise the procedure was as described above.)

2.2.7 Quantitative Reverse Transcription Polymerase Chain Reaction

The RNA samples obtained from the various treatment condition were quantified using the NanoDrop instrument. All the samples were then diluted with RNA-free water to make all samples at equal concentration at 500ng/µL prior to use. For the conversion of RNA to complementary DNA a mixture of RNA, RNA-free water dNTPs and oligoDT was prepared to run the PCR programme at 65°C for the first 5 minutes initially. This was paused to add buffer, DTT, RNAase out and SSIII so that the PCR program was restarted to run as follows: 50°C for 60 minutes, then at 70°C for 15 minutes followed by the last step at 4°C for ∞. The complementary DNA samples were then diluted at 1:5 to make a total of 100µL sample and mixture solutions using complementary DNA, Sybr Green, forward and reverse primers and water were prepared to allow triplicate samples from each condition to be tested. 20µL of each sample was placed in 96-well plates for PCR and sealed with a membrane, centrifuged and placed in the quantitative PCR machine to run at

the appropriate settings. The data was exported and analysed for interpretation of the results.

2.2.8 Preparation of cells for imaging (immunofluorescence and FLIM)

Cells were seeded in 6-well plates with coverslips as described previously under control or treatment conditions. When ready to prepare for imaging coverslips were removed from plates and placed on parafilm. They were washed once with PBS, then fixed with 4% PFA for 15 minutes at room temperature, followed by further 3 washes with PBS. The cells were then incubated in 0.1% Triton in TBS for 15 minutes at room temperature, washed once with TBS and incubated with block buffer (0.1% BSA in TBS) for 1 hour at room temperature. Finally, the block buffer was aspirated and primary antibodies were added at the appropriate dilution. After overnight incubation at 4°C primary antibodies were aspirated and secondary antibodies were added at the appropriate dilution for incubation for 90 minutes at room temperature. The antibodies were then washed off with PBS, incubated for 10 minutes in Hoechst (1:10000 in PBS) and washed 3 times with PBS followed by H_20. The coverslips were then mounted on slides using Vectashield medium and allowed to solidify at room temperature overnight. The slides were then stored at -20°C until imaging.

Samples for FLIM were prepared in a similar way with the difference that after fixation with PFA, permeabilisation was performed using 0.2% Tween for 10

minutes (instead of Triton-X), followed by further incubation for 15 minutes in fresh sodium borohydride in TBS (used at 1mg/ml) to reduce background autofluorescence. Incubation with conjugated antibodies was done overnight at 4°C. Mowiol was used instead as mounting medium.

2.2.9 Formalin-fixed paraffin-embedded mouse tissue staining for FLIM

FFPE tissue were incubated at 37°C for 1 hour, then baked at 60°C for another hour, followed by normalisation at room temperature. Dewaxing was then carried out by immersing slides in xylene for 7.5 minutes twice, followed by absolute ethanol twice for 5 minutes each, 70% ethanol for 5 minutes and washing in distilled water for 3-5 minutes. This was followed by heat mediated antigen retrieval using the Ventana system. Slides were immediately cooled for 20 minutes, washed using TBS thrice and incubated with TBS-T buffer for 15 minutes. This process was repeated 3 times. Incubation with sodium borohydride (1mg/ml) was done for 15 minutes at room temperature, to quench autofluorescence, followed by further 3 washes with TBS. Slides were blocked with filtered 2% BSA in TBS for 30 minutes, followed by incubation with the fluorophore-conjugated antibody of interest, diluted in filtered 2% BSA in TBS, overnight at 4°C. Slides were then washed 3 times using TBS, for 5 minutes each time, followed by distilled water. Coverslips were applied with Mowiol medium containing DABCO and left overnight at room temperature prior to storage at -20°C.

2.2.10 Frozen mouse tissue staining for immunofluorescence

Frozen tissue slides were removed from -80°C and sample borders were demarcated with a pen. These were immediately placed in methanol-acetone solution for fixation at -20°C for 20 minutes and then washed 3 times for 5 minutes each time in TBS on a rocker. The slides were then incubated in block solution with 2% BSA in TBS for 20 minutes at room temperature and after that in primary antibody solution which was diluted in 2% BSA in TBS. After overnight incubation at 4°C the slides were washed 3 times in TBS and incubated with secondary antibodies (where needed) for 1 hour at room temperature. Again, the samples were washed 3 times in TBS and Hoechst (1:10000 in TBS) stain was added for 30 minutes incubation at room temperature, followed by TBS washes 3 times and final wash with H20. The slides were then mounted using coverslips with Vectaschield medium and allowed to solidify overnight at room temperature prior to storage at -20°C until imaging.

2.2.11 *In vivo* prostate cancer xenograft model establishment for PSMA-PET imaging

Animal studies were carried out in accordance with UK Research Council's and Medical Research Charities' guidelines on Responsibility in the Use of Animals in Bioscience Research, under UK Home Office Licence. Animals were maintained in either the Rockefeller (UCL) or St Thomas' Hospital BSU (KCL). Male nude athymic mice, 4-6 weeks old in age were purchased from Charles River Laboratories (UK). The animals were maintained under sterile conditions

in filter topped cages on sterile bedding and fed an irradiated diet of standard mouse chow.

Mycoplasma negative CWR22 and 22Rv1 cells were inoculated subcutaneously to establish in vivo tumour models for treatment with DS7423 and PSMA-PET imaging. To establish subcutaneous tumour models 4-5 million cells of each cell line were suspended in 200µL Matrigel:PBS (1:1) and injected into the flank(s) of each mouse on Day 0 (Matrigel was thawed overnight at 4°C). The mice were monitored post inoculation, the day after and thereafter at least twice weekly. Subcutaneous tumours were measured using callipers (mm) and volume was calculated using the formula Volume = [(major axis*minor axis)^2/2]. Mouse monitoring comprised of the assessment of weight, behaviour and palpable tumour size up to three times a week. In accordance with the PPL evidence of weight loss greater than 10%, moderate signs of behavioural distress and/or palpable tumour diameter >15mm (single or combined tumours) precipitated humane killing by Schedule 1 method.

2.2.12 Preparation and administration of DS7423 by oral gavage

DS7423 for oral gavage was prepared at 0.6mg/ml concentration by dilution in 0.05% methylcellulose solution. To ensure efficient dilution sonication was performed for 5 minutes interrupted by intermittent vortexing. The dissolved DS7423 solution was stored on a rocker at 4°C until use.

Oral gavage of DS7423 was performed after mouse xenografts were established, about 3 weeks post tumour cell inoculation. Mouse weight was

measured and DS7423 was administered at 3mg/kg/day dose in a volume not to exceed 10ml/kg.

In the first pilot experiment the mice received daily DS7423 for 5 days, followed by 1 day of break and further treatment of another 5 consecutive days until the experiment was terminated. In the subsequent PSMA-PET experiment the mice received DS7423 on 4 consecutive days starting 5 days prior to imaging.

Following administration of DS7423 the mice were observed for at least 10 mins for detection of potential complications.

2.2.13 Tissue preservation

2.2.13.1 Frozen tissue

Tissues (e.g. primary tumours) were dissected out and wrapped in foil. They were immediately immersed in liquid nitrogen for flash freezing. After 30 minutes the snap frozen tissue was removed from the liquid nitrogen and transferred to a pre-chilled container for storage at -80°C freezer until further use. Frozen tumours were cut into 4mm sections with a cryostat for immunofluorescence staining.

2.2.13.2 Formalin-fixed paraffin-embedded tissue

Dissected tissue was placed in 70% ethanol and incubated overnight at room temperature. Subsequently, the ethanol was removed and the tissue was immersed in 10% Formalin solution for fixation until further processing that involved embedding in a paraffin block ready for sectioning.

2.2.14 Frozen tissue lysates

Frozen tissue was placed in a mortar containing liquid nitrogen and cut in smaller pieces. The tissue to be used for cell lysis was weighed by placing in previously chilled eppendorfs. The frozen tissue was then transferred back in the mortar which was kept cool on dry ice. The tumour was smashed into powder form, transferred to a chilled eppendorf and 150 µL of NP40 lysis buffer was added and allowed to homogenise on dry ice for 15 minutes. This was then vortexed and further allowed to incubate on dry ice for about 1 hour. Finally, the lysed tumour tissue was centrifuged at 10,000g for 10 minutes at 4°C and the supernatant (lysate) was collected into a new tube and stored at -80°C to be used for western blot.

2.2.15 PSMA-PET imaging

Mice were transferred to the preclinical laboratory about 1 hour prior to imaging. THP-PSMA was radiolabelled in hot lab with Ga-68 using instructions as described by Blower et al in a previous publication (225). Radiochemical purity (RCP) was checked by ITLC (>95%). Syringes with 10 Mbq Ga-THP-PSMA in 150 µL saline were prepared (dose should be 1-2 µg).

Once ready, bed heating was turned on at 36 °C and mice were placed in the induction box of 3.5% isoflurane and oxygen at 1L/min. Once anaesthetised tail veins were cannulated and the anaesthetised mice were transferred to nanoPET double bed in groups of 2. Anaesthesia was maintained with 2.5% isoflurane and oxygen flow at 2L/min. Once in the nanoPET double bed scanning was performed using a BioScan nanoPET-CT PLUS (Mediso). Mice

were imaged with CT for about 15 minutes before radiotracer administration and when this was completed the radiotracer was injected in a total maximum volume of 150-200 µL. Dynamic PET data was collected for the first hour after injection. At completion of the experiment mice were euthanised by cervical dislocation and tumours were harvested, weighed and γ-counted.

2.2.16 Exosome isolation by ultracentrifugation from cell culture supernatant

Cells were scaled up in 6-8 T175 flasks and when at about 70% confluence media was replaced by RPMI containing 10% Exo-free FBS (plus L-glutamine and Pen/Strep) for another 24 hours. In the case of cell treatment prior to exosome extraction, drug was added at this point and allowed to incubate for the indicated time as done in *in vitro* experiments described previously.

Once ready, about 100-134mls of cell culture supernatant was collected and transferred to 50 ml Falcon tubes. Media was centrifuged initially at 2000g for 20 minutes to pellet any contaminating cells and cell debris. The supernatant was collected with a syringe and filtered through a 0.45 µm filter cartridge into a fresh Falcon tube for further centrifugation at 12,200g for 45 minutes at 4°C. At the end of the centrifugation, using a 10ml pipette the supernatant was again transferred to UC Beckman tick wall centrifuge tubes. A vertical line was drawn with a marker on the side of the tube where the exosome pellet should form and the tubes were orientated in the rotor using this line that should face exteriorly (the tube remains in place during the spin and the line gives an indication where the pellet should be). Prior to placing into the rotor the tubes

were also balanced to the nearest 10^{th} of a gram prior to centrifugation (using the 71 Ti rotor) at 100,000g for 2 hours at 4°C. After the centrifugation run the supernatant was removed carefully and completely without disrturbing the exosome pellet (invisible) and the tubes were inverted onto a tissue paper for 1-2 minutes to ensure drain off of any excess media. The exosome pellets were then resuspended in volume of 500µL of sterile PBS and finally transferred to a single 1.5 ml Eppendorf tube for storage at -80°C.

The UC Beckman tubes were washed with ddH_2O, then with 70% ethanol and ddH_2O again and allowed to dry until further use.

2.2.17 Exosome isolation by ultracentrifugation from serum samples

The principle of exosome extraction is the same as when the starting material is cell culture conditioned media but because of the viscosity of some body fluids it is necessary to dilute them and to increase the speed and length of centrifugations.

1-3 mls of serum is diluted with an equal volume of PBS (1:1 dilution) and transferred to appropriate tube according to working volume. This is centrifuged at 2,000g for 30 minutes at 4°C. The supernatant is then transferred to clear centrifuge tubes without pellet contamination and further centrifuged at 12,000g for 45 minutes at 4°C. Then, the supernatant is transferred to ultracentrifuge tubes with the addition of PBS to ensure equal volume in all tubes. These are centrifuged at 100,000g for 2 hours at 4°C. The supernatant is discarded and the exosome pellets resuspended in 1ml of PBS for further ultracentrifugation

at 100,000g for 90 minutes at 4°C. Again, the supernatant is discarded and the final exosome pellet resuspended in 200µL PBS and stored at -80°C until further use.

2.2.18 Nanosight tracking analysis

Vesicles present in purified samples were analysed by nanosight tracking analysis using the Nanosight LM14 system (Malvern, Worcestershire UK), configured with a laser and a high sensitivity digital camera system. Videons were collected and analysed using the NTA-software (version 2.3) with the minimal expected particle size and minimum track length, all set to automatic. Camera shutter speed was fixed to 30.01ms and camera gain was set to 500. Camera sensitivity and detection threshold were set close to maximum (15 or 16) and minimum (3 or 4), respectively to reveal small particles. Ambient temperature was recorded automatically, ranging from 24 to 27°C. Each sample was diluted 1:100 in sterile PBS and were adminstered and recorded under controlled flow, using the Nanosight syringe pump and script control system, and for each sample five videos of 30 seconds duration were recorded, with a 10 second delay between recordings, generating five replicate histograms that were averaged to calculate the concentration of exosomes in each preparation.

2.2.19 Staining of exosomes for FLIM

A 96-well glass bottom plate was used and pre-treated prior to exosome placement with 37% HCL and 60%/90% ETOH for half hour at room

temperature. This was then followed by multiple washes with ddH_20 and PBS. Exosomes were then placed in the well at 1:30 dilution in PBS at a total volume of 40µL and were incubated at room temperature for 45 minutes to attach to the plate. Unbound exosomes were aspirated followed by 3 washes using PBS. The exosomes were then incubated for 30 minutes at room temperature in block solution using 1% BSA in TBS (100µL per well). Fluorescently-labelled antibodies were diluted in 1% BSA at 3µg/ml concentration for the donor antibody and at 10µg/ml for the acceptor antibody. Antibodies were spun at 12,000g at 4°C for 2 minutes prior to use to eliminate any aggregates and precipitate. 50µL of fluorescently-labelled antibodies were used per well and allowed to incubate at 4°C overnight. Finally, exosomes were washed twice with TBS and mounted using 99% TDE media (50µL per well) prior to imaging.

2.3 Analytical methods

2.3.1 Statistical analysis

Microsoft Excel and GraphPad were used to calculate mean, standard deviation and standard error of the mean and generate graphs for visual comparison of groups in experiments. For parametric data, means of two independent groups were compared using the Student's t-test.

2.3.2 FRET-FLIM analysis

The FLIM images obtained with our lifetime microscope were batch analysed by a PC workstation running in-house exponential fitting software (TRI2) written by Dr Paul Barber. This program outputs files where all the fitting parameters

are recorded for each image pixel into Excel format. These files are then analysed to produce a distribution of lifetime, and an average lifetime, from which FRET efficiency can be calculated using the equation below:

$FRET_{eff} = 1 - \tau(DA)/\tau(D)$, where $\tau(DA)$ is the fluorescent lifetime of the donor fluorophore in the prescence of the acceptor and $\tau(D)$ is the fluorescent lifetime of the donor fluorophore alone.

All data is fitted with a single exponential decay analysis.

Chapter 3: HER3-dependent AR upregulation in metastatic prostate cancer upon PI3K-mTOR inhibition in PTEN mutant setting

3.1 Introduction

The activation and heterodimerisation properties of the ErbB receptors and especially the potent activation of the PI3K-AKT-mTOR pathway by HER3 heterodimers make a very strong rationale for the study of their significance in metastatic prostate cancer, especially as mechanisms of resistance to other targeted therapies used for this malignancy.

Culig et al, have already shown that the AR can be activated by EGF and other growth factors in a low-androgen environment (122). The use of the TKI PKI-166 against EGFR and HER2 was also studied to evaluate its effect on AR signalling and prostate cancer cell growth. This demonstrated that EGFR-HER2 pathway inhibition in prostate cancer leads to decrease in the transcriptional activity of AR and that the main effector of this AR pathway modulation is HER2 via its association with other ErbB members (125). The ability of HER2 to heterodimerise preferentially with HER3 makes a strong argument for the role for HER2-HER3 dimer in the regulation of AR.

With the knowledge that ErbB overexpression occurs in metastatic prostate cancer, it makes sense to investigate the effect of PI3K-AKT-mTOR pathway inhibitors in metastatic prostate cancer since the ErbB pathway exerts its oncogenic activity through intracellular signalling pathways and particularly through the PI3K-AKT-mTOR pathway. Subsequently, there are various clinical trials currently that are investigating the role of these inhibitors and their ability to achieve desirable clinical responses in patients with metastatic CRPC (**Table 1.2** in introduction). In addition to PI3K pathway activation via ErbB activation, prostate cancers are associated with genetic alterations involving the PI3K pathway that enables sustained survival of prostate cancer cells. About 40% of primary and 70% of metastatic prostate cancers have genomic alterations in the PI3K signalling pathway, mostly through loss of PTEN, the negative regulator of the PI3K signalling pathway that when present acts as a tumour suppressor (153).

Preclinical studies in mice with PTEN deletion as well as work in prostate cancer cell lines with stable PTEN silencing using RNA interference have demonstrated that the loss of PTEN promotes resistance to castration (226). In addition, therapeutic inhibition with the PI3K-mTOR inhibitor BEZ235 can activate the AR pathway in a PTEN-null prostate cancer model and that *in vitro* treatment of LNCaP cells, that have a mutated PTEN gene, with BEZ235 was able to upregulate HER3 levels concurrently with AR (6). Combined PI3K and AR pathway inhibition was subsequently shown to be able to lead to profound tumour regressions. As discussed in **table 1.2**, current clinical trials exploring

the utility of PI3K pathway inhibitors in metastatic CRPC are used in combination with anti-AR agents. Consistent with this data in prostate cancer, it has also been described in breast cancer cell lines that PI3K inhibition is able to upregulate HER3 (227). The HER3 upregulation observed in this setting is an important mechanism of resistance and it is highly likely that this RTK acts through its heterodimerization with HER2.

What still remains unexplored in metastatic CRPC however, is the efficacy of combined pharmacologic inhibition of both the PI3K-AKT-mTOR pathway and ErbB. In addition, despite targeting these pathways pharmacologically, the heterodimerisation between HER3 and HER2 could be evaluated within clinical trials as an exploratory endpoint to predict resistance to treatment and/or disease progression. The ability to detect HER3 heterodimerisation in patient tissue samples has already been demonstrated by our laboratory in collaboration with Dr Baselga's group at Memorial Sloan Kettering in 2014. HER3 overexpression was associated with upregulation of EGFR-HER3 dimer by FLIM and FRET analysis in residual tumours of breast cancer patients treated with either panitumumab or cetuximab and suggested that this molecular rewiring mechanism prevents complete response to targeted therapies (228).

We hypothesised that HER3 heterodimerisation in the setting of metastatic prostate cancer might be an important resistance mechanism to targeted PI3K-AKT-mtor inhibition, especially in the setting of PTEN loss. We wished to

evaluate the heterodimerisation patterns of HER3 once it is overexpressed as a response to treatment and to consider whether this could be abrogated pharmacologically with agents against HER2 and HER3 that would inhibit heterodimer formation and could thus provide rational combined therapies to overcome treatment resistance and enable the robust inhibition of cell proliferation and disease progression.

3.2 Results

3.2.1 ErbB expression and responses to stimulation in LNCaP cell line

The LNCaP cells have a recognised mono-allelic mutation of the PTEN gene. PTEN mRNA and protein are expressed, however, the mutated PTEN protein is truncated, lacks the phosphatase domain and is therefore not fully active (229). In order to investigate the heterodimerisation of ErbB in prostate cancer it was important to establish the relative protein expression levels of these kinases in my model system. Western blots were performed on whole cell lysates with antibodies against ErbB family receptors and against tubulin as loading control. As depicted in **figure 3.1(a)** different prostate cancer cell lines exhibit distinct patterns of ErbB kinase expression. The LNCaP cells display expression of EGFR, HER2 and HER3 but the expression of all three ErbB members is not seen in the other two cells lines. The findings in LNCaP cells is consistent with previous reports regarding the expression of these ErbB members *in vitro* (230). The DU145 and PC3 cell lines are referred to as the "classical" cells lines used in prostate cancer research. The PC3 cell line was

used here due to its known loss of PTEN, however it is not an appropriate cell line to use for the hypothesis of this project since the cells do not express AR and PSA and their proliferation is independent of androgen (231). Similar to the PC3 cells, the DU145 cells do not express AR and PSA, however they express WT PTEN (232). Therefore, the absence of AR as well as the lack of expression of all ErbB members in the DU145 and PC3 cell lines makes their use inappropriate to investigate the proposed hypothesis of this project.

Further experiments in LNCaP cells following starvation and subsequent stimulation with the HER3 ligand NRG-1 used at 50ng/ml concentration at the indicated timepoints showed immediate phosphorylation of HER3 at 2 minutes and persistence in the level of total HER3 as compared to AKT that was used as a loading control in this experiment (**figure 3.1(b)**). The persistent HER3 levels upon ligand binding suggest that this RTK is not degraded and is able to continue signalling as a heterodimer with EGFR and HER2. NRG-1 in LNCaP cells enhances the activation of pAKT throughout the treatment timecourse. Signalling via the MAPK pathway is also induced in LNCaP cells after NRG-1 phosphorylation however this does not persist, supporting the idea that HER3 primarily signals through the PI3K-AKT pathway and that the mutational status of these cells, harbouring a PTEN mutation, defines to an extent their ability to signal downstream of HER3 via the PI3K-AKT pathway.

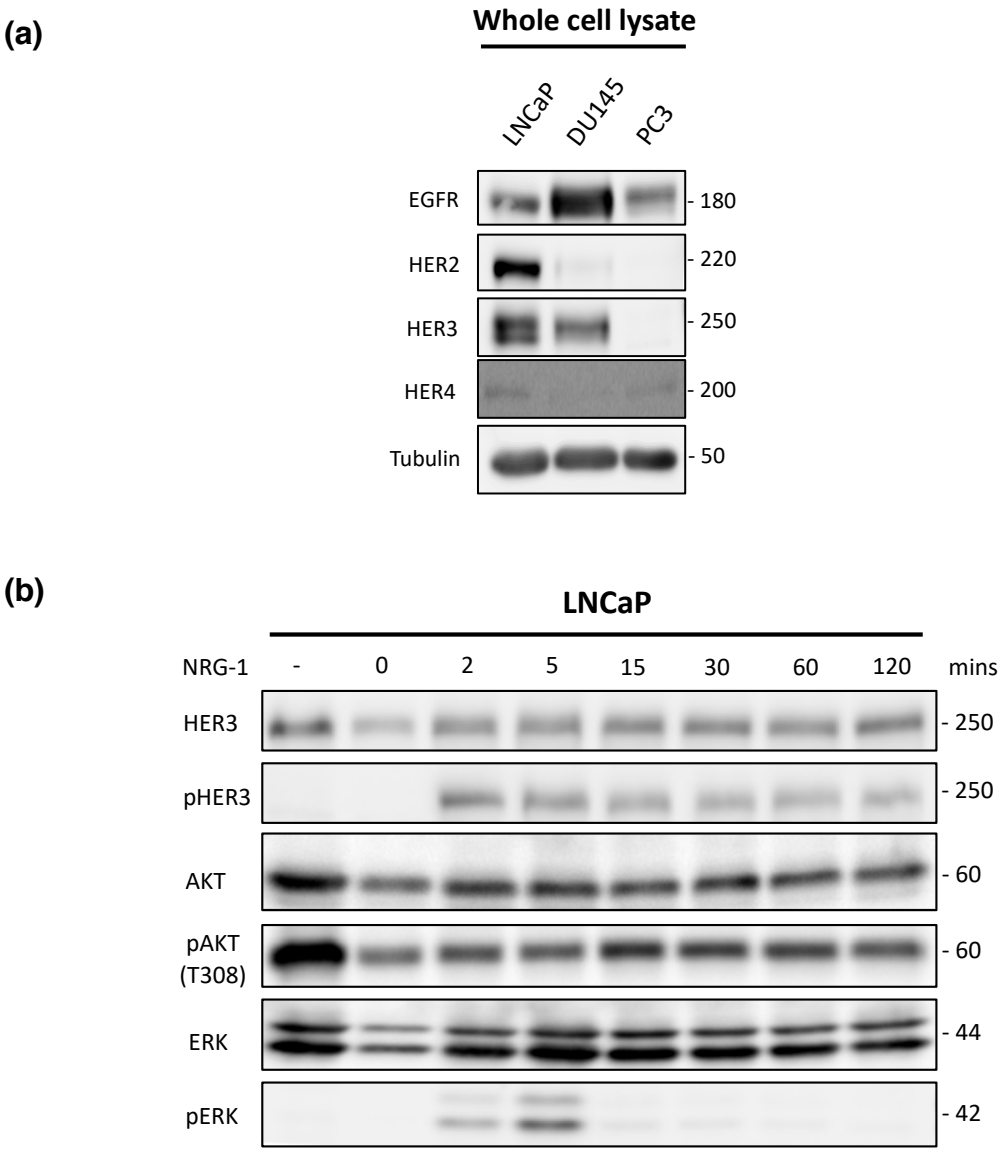

Figure 3.1 – ErbB expression in metastatic prostate cancer cell lines and the response of HER3 phosphorylation to NRG-1 stimulation:

(a) Whole cell lysate from LNCaP, DU145 and PC3 cells at baseline conditions was blotted with primary antibodies against the ErbB receptors as indicated. β-tubulin was used a loading control to compare expression of ErbB members (n=1).

(b) LNCaP cells were serum starved in 0% FBS RPMI for 24 hrs (except in the first lane where cell lysate was extracted after the cells were grown in full RPMI media) prior to treatment with NRG-1 at 50ng/ml at increasing timepoints to observe the effects on HER3 phosphorylation and the downstream pathways (n=1).

In addition to the expression of ErbB receptors and their known PTEN status, the LNCaP cells form an ideal set of cells to study the effect of PI3K-mTOR inhibition based on their metastatic potential and expression of the androgen receptor as shown by the use of N- and C-terminus antibodies. Both N-terminus and C-terminus AR antibodies recognise the main isoform of the AR at ~110 kDa. Any isoforms detected below that molecular weight using the N-terminus antibody could represent alternatively spliced forms of the AR that are extensively described in the literature (233). The use of these AR antibodies in the DU145 and PC3 cell lines demonstrated the very weak expression of androgen receptor in these cells since they are known to also be androgen independent as discussed earlier (**figure 3.2**).

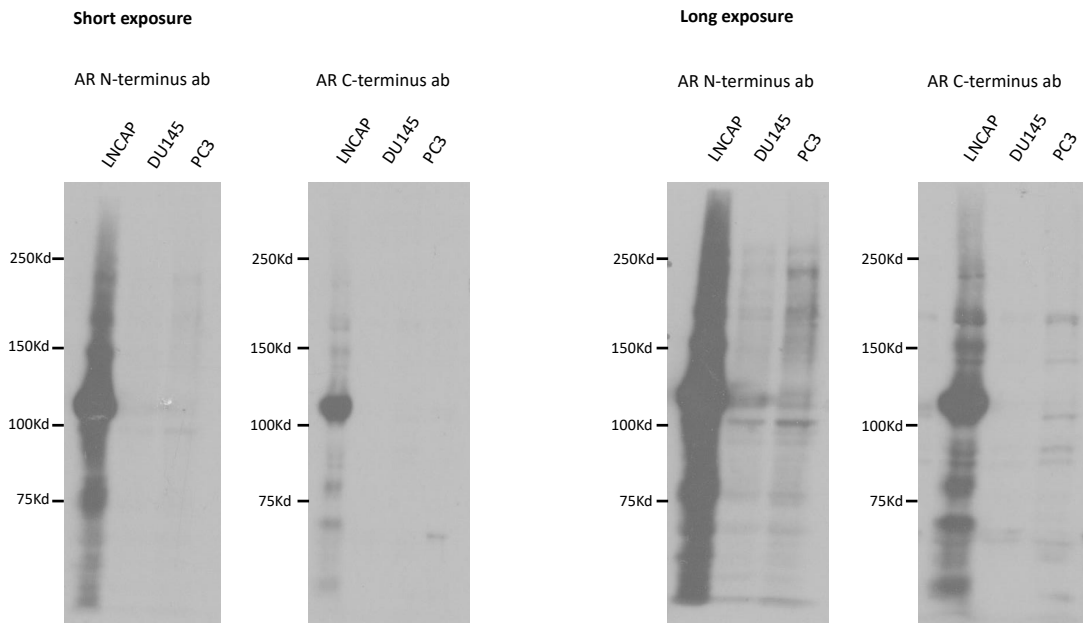

Figure 3.2 – The expression of AR N- and C-terminus antibodies in metastatic prostate cancer cell lines:

LNCaP cells show high expression of the AR protein on western blot. DU145 and PC3 cells only express AR at very low levels. Short and long exposure of the same films are shown on left and right respectively. In each lane 25µg for protein lysate was loaded and this represents a single experiment as proof of what is known in the literature about the AR expression in these cell lines.

Furthermore, treatment of LNCaP cells with EGF and NRG-1 for five minutes also reveals that these cells respond to stimulation by the ErbB ligands to upregulate phosphorylation of ErbB receptors differentially according to which ligand is used each time. For example, stimulation by EGF leads to phosphorylation of EGFR and HER2 and when NRG-1 is used the cells phosphorylate HER2 and HER3 (**Figure 3.3**). Tal-Or et al, demonstrate the same response to EGF and NRG stimulation in LNCaP cells (230) and this would suggest that respective heterodimers are preferentially formed and that specific ligands can define the downstream signalling of cells upon stimulation. The LNCaP cells have constitutive activation of the PI3K-AKT pathway as shown by expression of pAKT (T308) at control conditions. They sustain this upon ligand stimulation and in the case of NRG-1 stimulation additional activation of the MAPK pathway is noted with the upregulation of pERK suggesting that these cells are able to promote intracellular oncogenic signalling by utilising this pathway as well **(Figure 3.3)**.

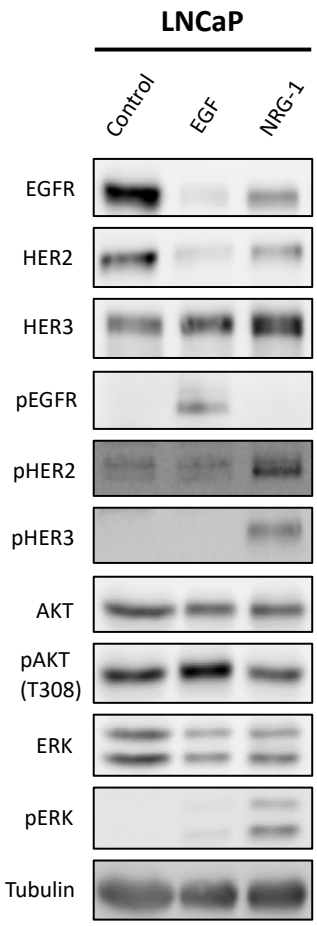

Figure 3.3 – LNCaP cell transphosphorylation:
LNCaP cells were treated with EGF (100ng/ml) and NGR-1 (50ng/ml) for 5 minutes to demonstrate the effect of transphosphorylation of the ErbB receptors with each respective ligand (n=1).

3.2.2 LNCaP cytotoxic treatment using dual PI3K-mTOR inhibitor (DS7423)

The dual PI3K-mTOR inhibitor DS7423 was used in *in vitro* experiments with LNCAP cells. DS7423 is a novel, small molecule compound that inhibits both PI3K and mTOR (mTORC1/2). It inhibits all class I PI3K isoforms with greater potency against p110α than against the other p110 isoforms (234). At the beginning of my project the compound was being evaluated in a Phase I Clinical trial in solid tumours. This study finished without reaching the maximum

tolerated dose. In addition no objective response was observed but stable disease was achieved in 10 out of 26 patients (235).

Treatment with DS7423 at increasing concentrations (1-1000 nM) for 24 hours showed adequate inhibition of the pathway downstream of mTOR by the decrease and complete loss of pS6 levels, a marker of MTOR activity, at 100 nM and 1000 nM concentrations respectively. Concomitant with that, AR levels also increased upon PI3K-mTOR pathway inhibition as suggested by previous data (6) (**Figure 3.4(a)**). Treatment with 1000 nM dose of DS7423 in **figure 3.4(b)** at increasing timepoints also reveals that the inhibition of downstream signalling, as indicated by the loss of pS6 levels occurs within 1 hour of treatment. In addition, there is a noted time-dependent feedback upregulation of HER3 levels, reaching a maximum at 24 hours after which the HER3 levels return back to baseline at the 48 hours timepoint. In addition, in the case of AR the protein levels continue to increase with DS7423 up to the maximum treatment timepoint of 48 hours. This coincides with the reverse effect observed in the levels of PSMA. The inverse relationship between AR and PSMA has already been described in the literature and these results showing AR upregulation and PSMA downregulation confirm this (236). In conclusion, I selected the 1000 nM dose of DS7423 at 48 hours treatment in LNCaP cells since this dose and timepoint confirms that AR upregulation occurs in conjunction with adequate inhibition of downstream signalling as shown in **figure 3.4(c)** with a 3.7 times increase in AR levels.

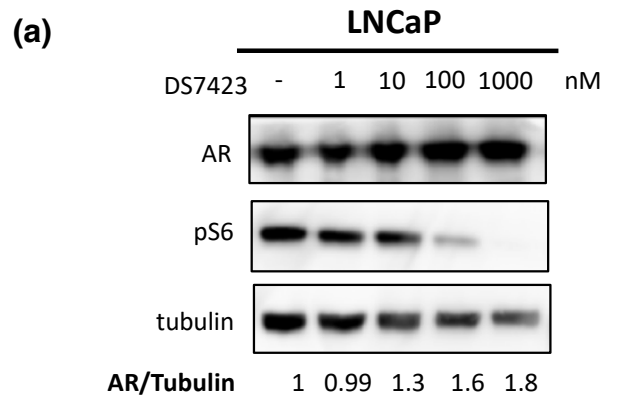
(a)
LNCaP
DS7423 - 1 10 100 1000 nM
AR
pS6
tubulin
AR/Tubulin 1 0.99 1.3 1.6 1.8

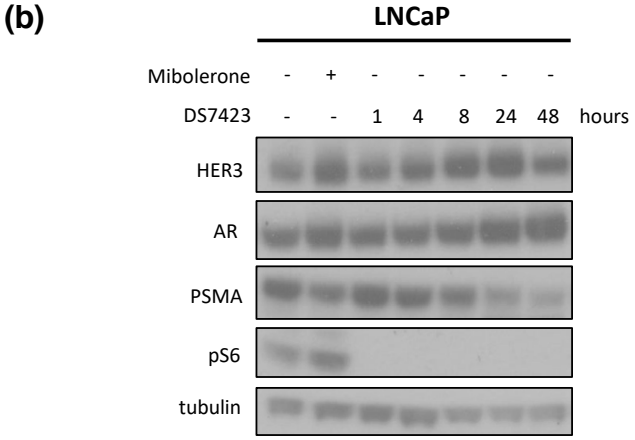
(b)
LNCaP
Mibolerone - + - - - - -
DS7423 - - 1 4 8 24 48 hours
HER3
AR
PSMA
pS6
tubulin

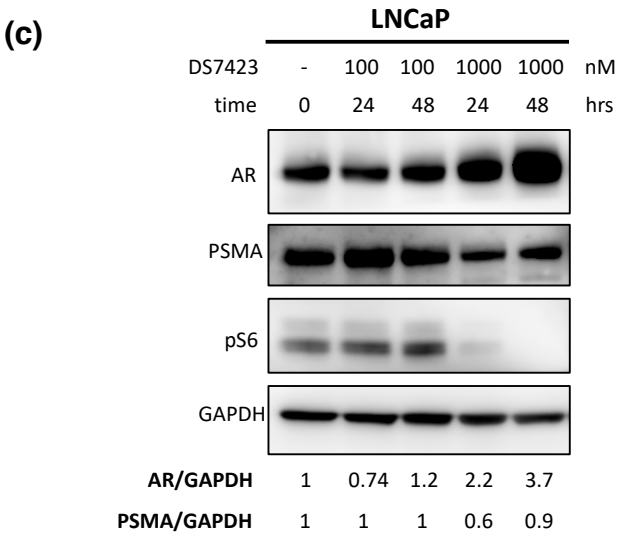
(c)
LNCaP
DS7423 - 100 100 1000 1000 nM
time 0 24 48 24 48 hrs
AR
PSMA
pS6
GAPDH
AR/GAPDH 1 0.74 1.2 2.2 3.7
PSMA/GAPDH 1 1 1 0.6 0.9

Figure 3.4 – The effect of PI3K-mTOR inhibition on expression of AR and HER3 in LNCaP cells:

(a) Western blot of LNCaP cells treated at increasing concentrations of DS7423 for 48 hrs. AR levels show 80% increase in expression compared to baseline when 1000 nM concentration of DS7423 is used (n=3).

(b) DS7423 was used at 1000 nM concentration at increasing timepoints (1 to 48 hrs). Mibolerone used at 1 μM for 24 hrs was a positive control for AR overexpression and subsequent PSMA downregulation (n=1).

(c) DS7423 was used at 100 and 1000 nM for 24 and 48 hrs to confirm the appropriate concentration and timepoint for use in subsequent experiments (n=3).

3.2.3 Generation of stable HER3 knockdown and cytotoxic treatments using LNCaP NTC and HER3kd cells

A stable HER3kd LNCaP cell line was generated using shRNA interference and viral transduction to be able to establish the dependence of AR upregulation upon PI3K-mTOR inhibition on HER3. The transfection efficiency achieved for HER3 knockdown in LNCaP cells was 74% (shRNA #3) compared to the LNCaP NTC cell line as demonstrated by the western blot quantification performed in all three clones generated **(Figure 3.5)**.

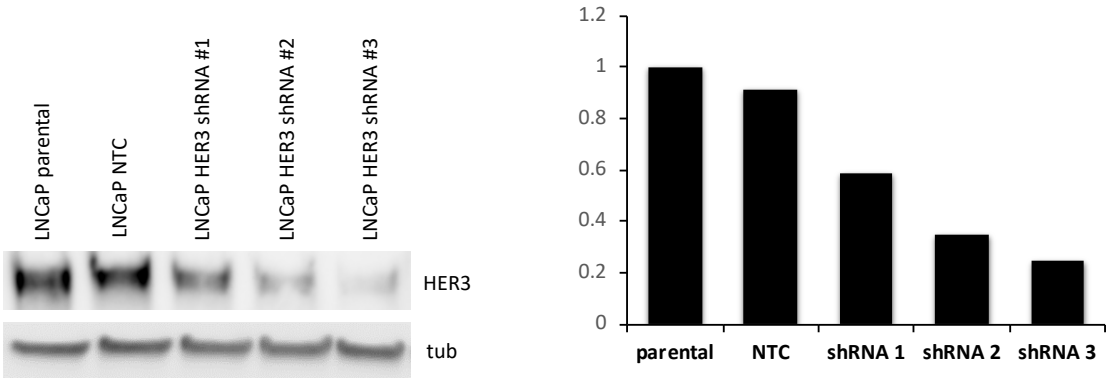

Figure 3.5 – The generation of HER3 knockdown LNCaP cell line:
Left panel shows HER3 western blot in parental and stably shRNA-transduced LNCaP cells. Right panel demonstrates the quantification of HER3 knockdown (n=1).

Treatment of the LNCaP NTC and HER3kd cells either with Mibolerone, a potent androgenic steroid with high affinity and selectivity for the AR at 1 nM concentration, and DS7434 alone or in combination with Mibolerone demonstrated an increase in AR protein levels in the LNCaP NTC cells. In the absence of HER3 the effect on AR is not seen (**Figure 3.6**). The increase in AR levels in LNCaP NTC from control to treatment with DS7423 alone is statistically significant (p=0.045) and the difference in AR upregulation between LNCaP NTC and HER3kd cells upon combined treatment with DS7423 and Mibolerone is also statistically significant (p=0.035). The use of patritumab, a monoclonal antibody against HER3, was used alone and in combination with DS7423, to observe whether its use could reverse the effect seen on AR protein levels, similar to when HER3 is knocked-down. From my *in vitro* experiments, however, the use of patritumab was not found to be sufficient in altering the observed AR upregulation.

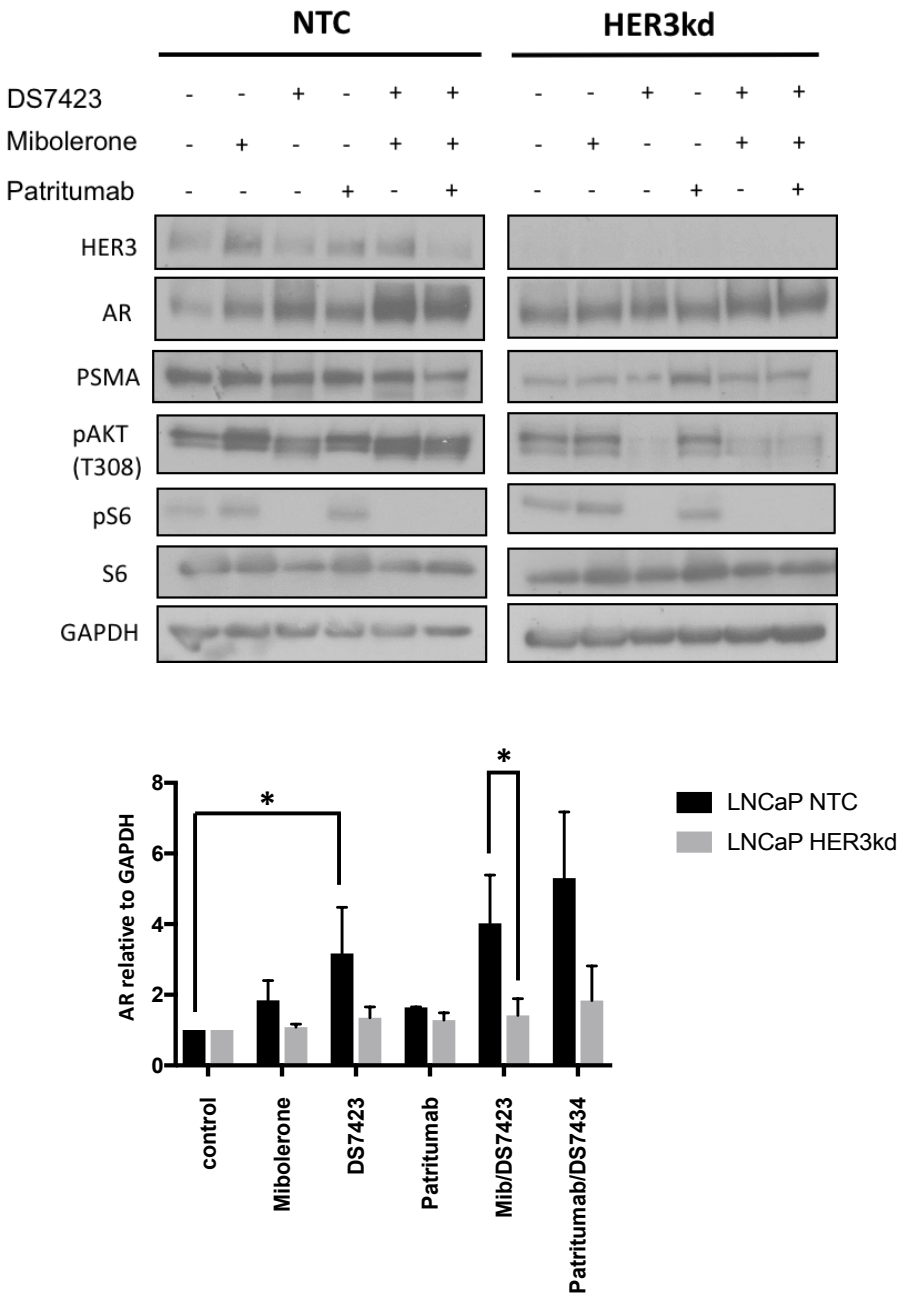

Figure 3.6 – The effect of DS7423 in LNCaP NTC versus LNCaP HER3kd cells on AR:

Top panel: DS7423 was used at 1000 nM for 48 hrs alone or in combination with Mibolerone (at 1 μM) with/without Patritumab (at 10μg/ml). Expression of HER3, AR and other proteins was assessed by western blot analysis.

Bottom panel: The histogram demonstrates the relative AR expression normalised to the loading control (GAPDH) in both cells lines under all 6 treatment conditions performed in this experiment. Results are shown as mean +/- SEM (n=3), * = $p<0.05$. Black bars = LNCaP NTC, Grey bars = LNCaP HER3kd.

Of further note is the inability to abrogate pAKT (T308) levels in the LNCAP NTC cells upon dual PI3K-mTOR inhibition alone and in combination with Mibolerone compared to the LNCaP HER3kd cells under the same treatment conditions, where pAKT levels are not sustained and in fact are depressed (**Figure 3.7**). The relative pAKT (T308) ratio between DS7423-treated and untreated cells compared in both LNCaP NTC and HER3kd cell lines shows sustained and slightly enhanced signalling via PI3K-AKT pathway in LNCaP NTC versus HER3kd cells (1.09 vs 0.82; p-value=0.083). More specifically, the pAKT relative ratio difference is 25% between the 2 cells lines.

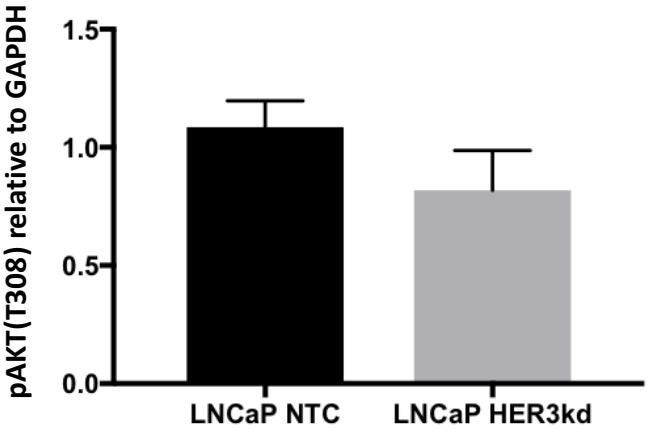

Figure 3.7 – Sustained pAKT signalling in LNCaP cells despite DS7423 treatment: PAKT (T308) quantification in LNCAP NTC and HER3kd cells post DS7423 treatment for 48 hours. Results are shown as mean +/- SEM (n=3).

To validate the effect seen on AR in LNCAP NTC versus HER3kd cells, it was important to compare DS7423 with other inhibitors of the PI3K-AKT-mTOR pathway. GDC0068 is a highly selective ATP-competitive pan-AKT inhibitor (237), currently being evaluated within a Phase III clinical trial in metastatic CRPC (NCT03072238) (238). The Phase Ib/II trial showed that GDC0068 (or

ipatasertib) in combination with abiraterone improves radiographic progression-free survival (rPFS) versus abiraterone alone, with greater benefit in patients with PTEN loss tumours (170). GDC0941, a thienopyrimide derivative, is a pan-class I PI3K inhibitor with equipotent activity against p-110α and p-110δ enzymes and exhibits inhibitory action against p-110β and p-110γ at low nanomolar concentrations (239). In a Phase I clinical trial in patients with advanced solid malignancies (that included patients with prostate cancer), GDC0941 showed evidence of pharmacodynamic activity (240) and further clinical trials using this drug are currently investigating its effect in various tumour types including breast and lung cancer. Finally, everolimus is an mTOR inhibitor which is selectively more potent against mTORC1 and has little impact against mTORC2 (241). The use of everolimus in CRPC has been tested in a Phase II clinical trial in combination with bicalutamide, unfortunately with negative results showing failure to achieve PSA response compared to bicalutamide alone (242). In addition, single-agent everolimus was used within another Phase II clinical trial in unselected patients with metastatic CRPC and showed moderate activity (PSA response in 35% of patients; 95% confidence interval 20-53). In this study retrospective analysis of PTEN status showed that PTEN loss was associated with prolonged PFS and PSA response (243). Despite the negative results, there is still high interest in testing the efficacy of everolimus with the newer second generation anti-androgens and also with prospective evaluation of the correct biomarkers for better patient stratification to maximize the efficacy within the correct subgroups of patients that are more likely to respond.

The effect on AR upregulation in LNCAP NTC cells was observed with all inhibitors used, however this was more pronounced with everolimus and DS7423, suggesting that it is the inhibitory effect on mTORC1, as shown by the complete inhibition of the pS6 kinase by these two inhibitors, that plays an important role in the regulation of the feedback loop between the PI3K-AKT-mTOR pathway and AR. In addition, HER3 upregulation upon PI3K-AKT-mTOR pathway inhibition is observed with DS7423 and GDC0068 treatments but under both treatment conditions HER3 upregulation was not statistically significant. This does not correlate with overexpression of HER2 in the LNCAP NTC cells upon inhibition of the PI3K-AKT-mTOR pathway. Finally, the effects on PSMA from inhibition of the PI3K-AKT-mTOR pathway in LNCAP NTC and HER3kd cells shows a downward trend when compared to baseline. In LNCaP NTC cells this is consistent with the upregulation observed in AR levels, however in the case of LNCaP HER3kd cells, it remains unclear whether the absence of the HER3 RTK would have any effect on PSMA, both in terms of its expression and also its function (**Figure 3.8(a)**). There are no reports currently in the literature suggesting that RTKs can interact with PSMA, however this would be intriguing to explore in the future.

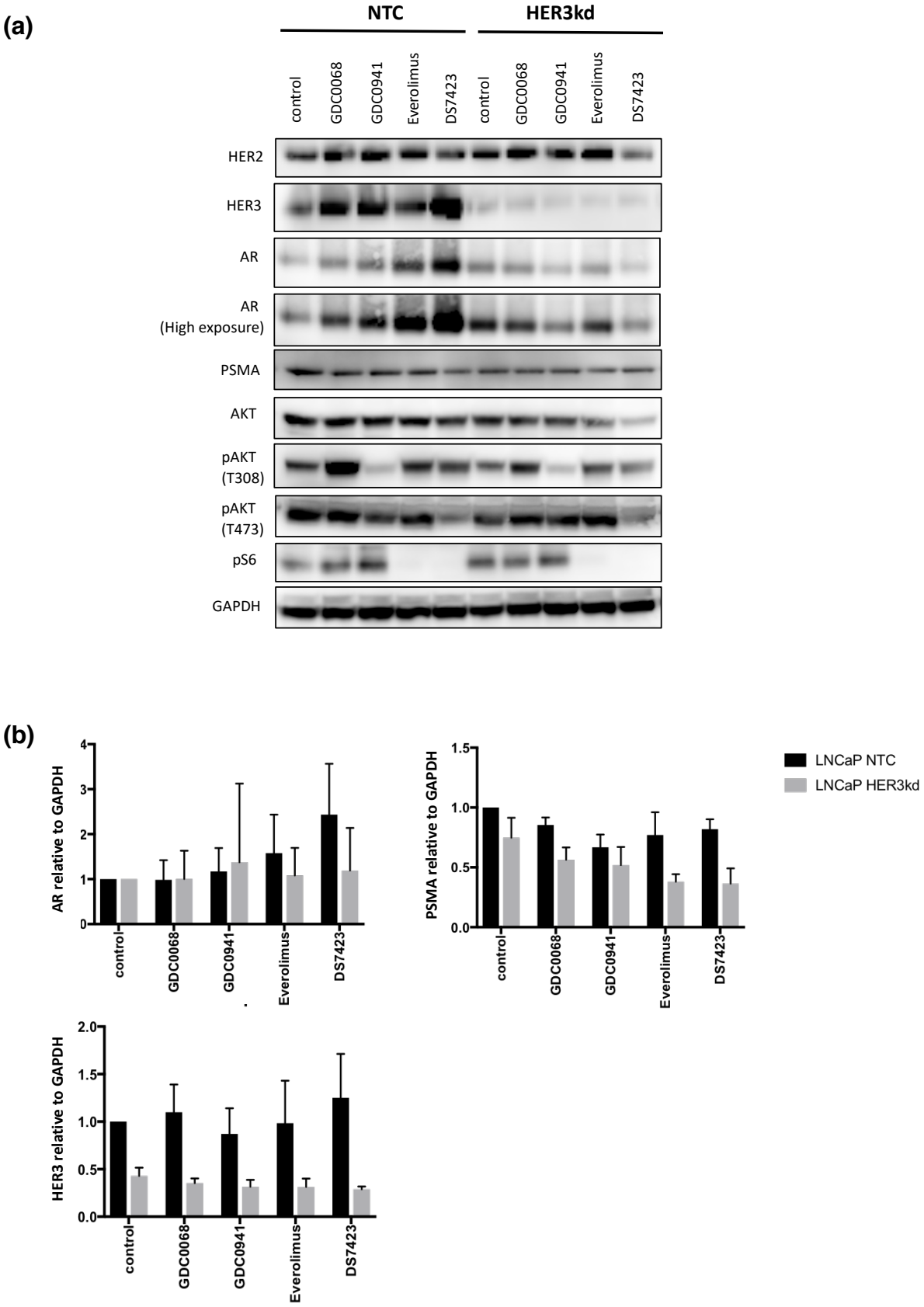
(a)
NTC
HER3kd
control
GDC0068
GDC0941
Everolimus
DS7423
control
GDC0068
GDC0941
Everolimus
DS7423
HER2
HER3
AR
AR
(High exposure)
PSMA
AKT
pAKT
(T308)
pAKT
(T473)
pS6
GAPDH
(b)
AR relative to GAPDH
PSMA relative to GAPDH
HER3 relative to GAPDH
LNCaP NTC
LNCaP HER3kd
control
GDC0068
GDC0941
Everolimus
DS7423

Figure 3.8 – The use of other PI3K-AKT-mTOR pathway inhibitors in LNCaP NTC and HER3kd cells demonstrate similar effects on AR levels and that these are dependent on HER3:

(a) Western blot in LNCaP NTC and HER3kd cells for the indicated antibodies. GDC0068, GDC0941 and Everolimus were added to individual wells for 48 hrs and these were used at 100, 1000 and 100 nm respectively.

(b) Histograms demonstrating AR, PSMA and HER3 expression upon all treatment conditions in both cell lines. Values are mean +/- SEM and are representative of 3 independent experiments (n=3). Black bars = LNCaP NTC, Grey bars = LNCaP HER3kd.

Consistent with the findings above, qRT-PCR of cDNA from LNCAP NTC and HER3kd cells treated with GDC0068, GDC0941, everolimus and DS7423 at the same concentrations and for 48 hours showed that PSA (or KLK3) gene expression correlated with the upregulation of AR on western blot experiments and that the upregulated AR protein is functionally active despite the use of culture media deprived of androgen (**Figure 3.9**). cDNA extracted from LNCAP NTC and HER3kd cells following stimulation with the androgen ligand Mibolerone was used in this experiment as a positive control. The maximum PSA gene upregulation was seen with the use of DS7423 and this was 3.6 times-fold compared to baseline expression in the absence of androgen and any drug. The effect of DS7423 on PSA gene expression was even higher than that seen with the use of Mibolerone suggesting that the enhanced AR protein observed upon DS7423 correlated with a functionally active AR. The degree of PSA gene upregulation with GDC0068, GDC0941 and everolimus was also in correlation with the western blot results of AR protein expression. The expression of PSA is mainly induced by androgens and regulated by the AR at the transcriptional level (244). The observed AR protein and PSA gene upregulation in these experiments demonstrate the androgen-independent

activation of AR upon inhibition of the PI3K-AKT-mTOR pathway and provide rationale for the combined use of these inhibitors with drugs that target the AR signalling pathway. Furthermore, despite the dual targeting of metastatic prostate cancer within clinical trials where PI3K-AKT-mTOR inhibitors are used, no data is available to provide information about the time when androgen-independent AR signalling overcomes the suppression from this AR targeted therapeutic approach and whether other biomarkers could provide additional insights about the exact mechanisms involved and the timing when this occurs.

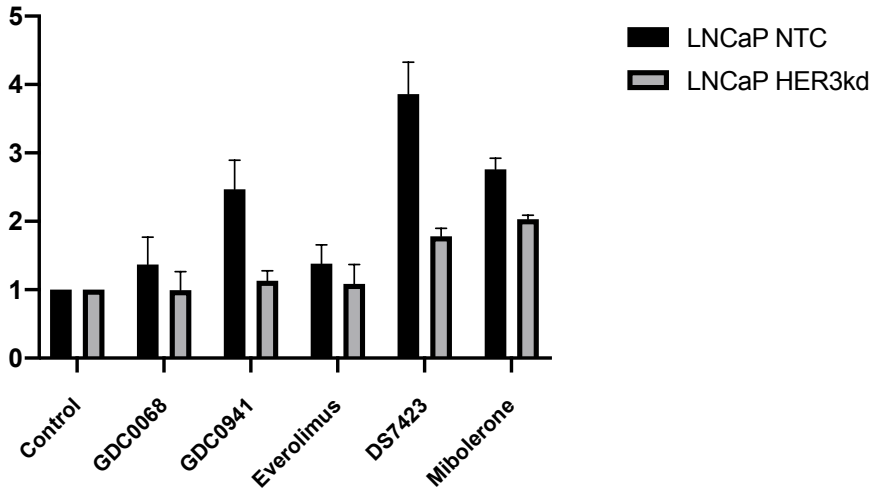

Figure 3.9 – The AR upregulation observed upon inhibition of PI3K-AKT-mtor pathway in LNCAP NTC cells is associated with increase of its function as seen by PSA overexpression:

cDNA from LNCaP NTC and HER3kd cells was used for quantitative RT-PCR to quantify the expression of KLK3 gene using forward and reverse primers for KLK3 and GAPDH genes to evaluate the relative expression on PSA (as compared to GAPDH loading control) under the treatment conditions of interest (n=3).

Further experiments concentrated on establishing the cellular localisation of AR upon treatment with DS7423. AR is localised in the cytoplasm in the absence of androgen and translocates to the nucleus upon ligand stimulation. I used a directly-labelled antibody of AR (AR-N20 that recognises an epitope on the N-terminus) with Alexa488 and cultured LNCaP parental cells in RPMI media with 10% charcoal-stripped FBS (deprived of androgen and growth factors) for 24 hours in control conditions and prior to any DS7423 treatment. At baseline and in media deprived of androgen LNCaP cells show that AR is primarily localised in the cytoplasm. At 8 and 24 hours, the AR is seen to localise in the nucleus as well. Interestingly, at 48 hours post treatment with DS7423 the AR relocates to the cytoplasm. HER3 under the same conditions remains in the membrane primarily and to an extent in the cell cytoplasm (**Figure 3.10**). LNCaP and PC-3 cells were used as positive and negative controls respectively for demonstration of the expected localisation of AR following staining with the directly-labelled anti-AR antibody at control conditions and following treatment with Mibolerone (**Figure 3.11**).

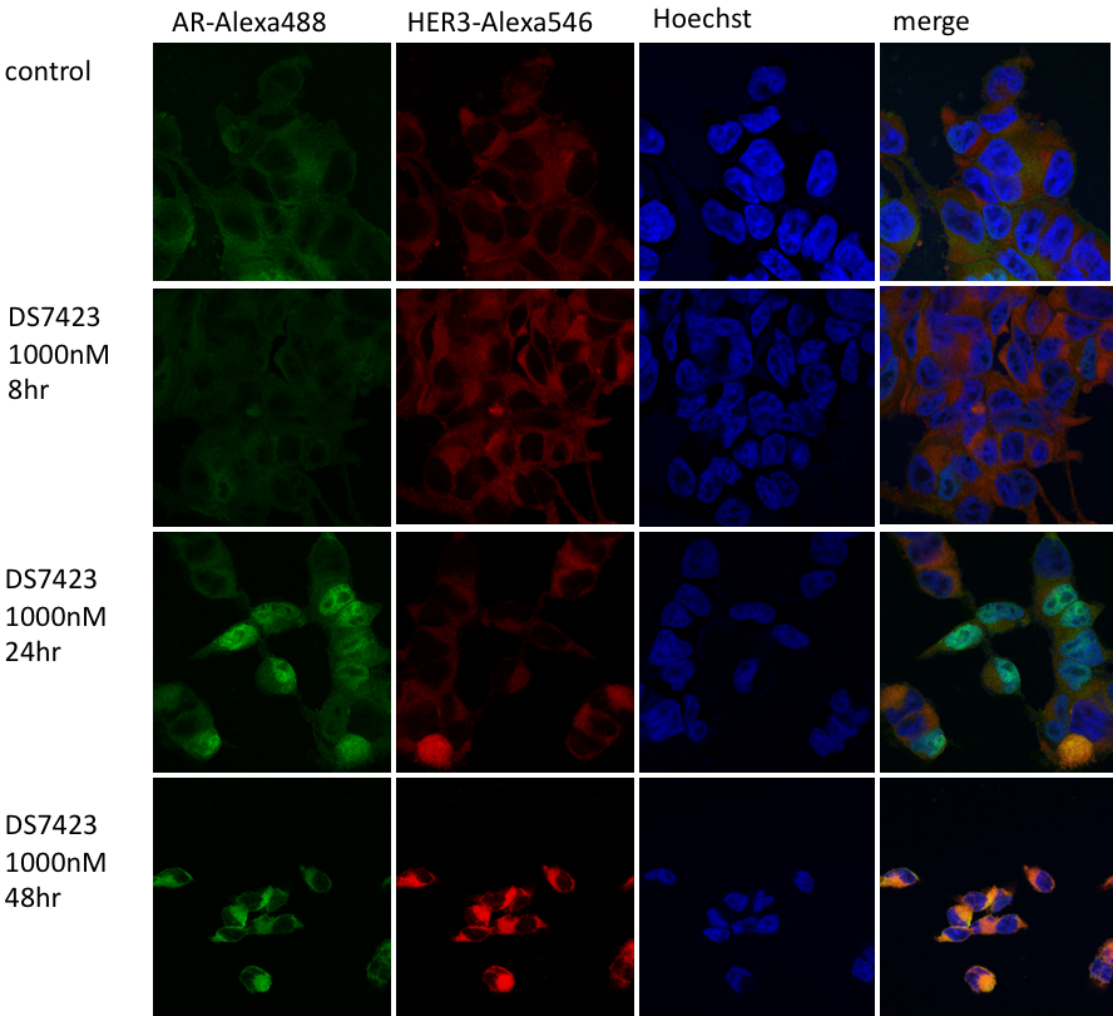

Figure 3.10 – AR and HER3 cellular localisation upon DS7423 treatment in LNCaP parental cells:

LNCaP parental cells were grown in RPMI media with 10% charcoal-stripped FBS in all conditions. The cells were treated with DS7423 for 8, 24 and 48 hour timepoints. Immunocytochemistry was performed for AR, HER3 and Hoechst using the protocol described in methods and images were acquired using confocal microscopy with x63 oil objective. The images are representative of triplicate experiments.

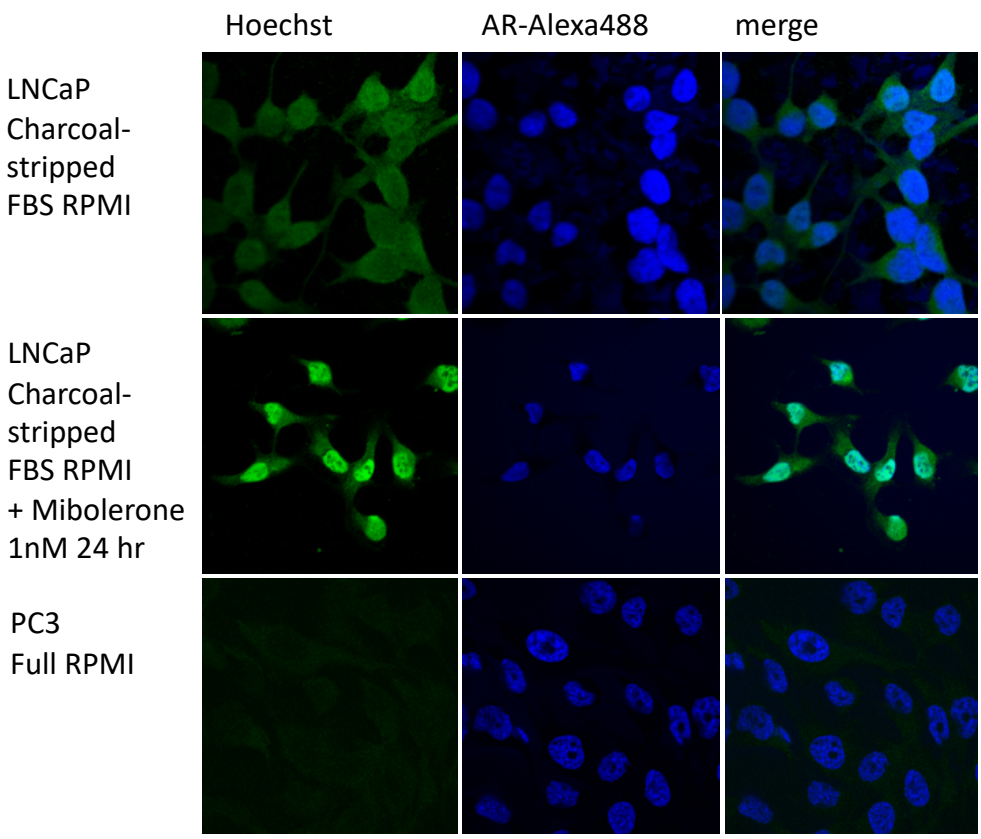

Figure 3.11 – LNCaP and PC-3 cells used for positive and negative control experiments for AR-Alexa 488 antibody:

LNCaP cells were grown in RPMI with 105% charcoal-stripped FBS and stimulated with 1nM Mibolerone for 24 hours. PC3 cells were grown in full RPMI without AR ligand stimulation. Immunohistochemistry was performed for AR and Hoechst using the protocol described in methods and images were acquired using confocal microscopy with x63 oil objective. Images are representative of experiments repeated 3 times.

3.2.4 The effect of PI3K-mTOR inhibition on ErbB dimerization

In order to assess the effect of DS7423 on ErbB dimer formation I used FLIM to measure direct receptor-receptor interaction by FRET, between HER3-Alexa 546 and HER2-Cy5. For the acquisition of data and the measurement of lifetime, 5 fields of view were used for each treatment condition within each replicate experiment. DS7423 induced stabilisation of the HER2-HER3

heterodimer, as an observed 2.2-fold increase in FRET efficiency compared to the untreated baseline LNCaP cells. The measured FRET efficiency in LNCaP cells treated with DS7423 was 13.1% compared to 6% when cells are at baseline without any treatment, despite this not being statistically significant. **Figure 3.12** shows representative images of cells at baseline and post treatment and cumulative histogram of FRET efficiency that is calculated by the following equation and averaged in each cell; FRET efficiency = 1-[Tau(DA)/Tau(D)].

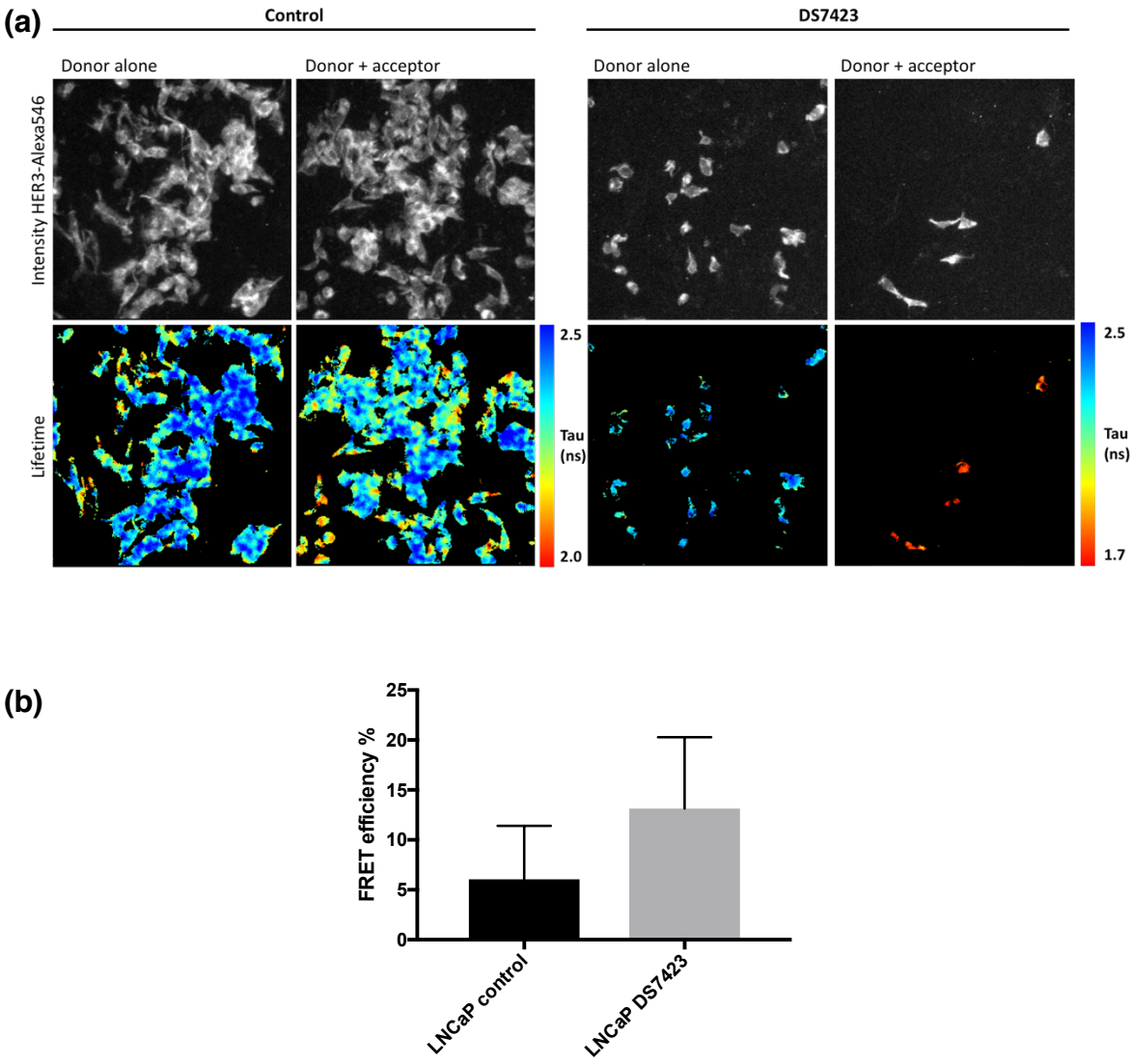

Figure 3.12 – HER2-HER3 heterodimer formation is enhanced upon PI3K-mTOR inhibition in LNCaP cells:

(a) Donor alone and donor + acceptor intensity and fluorescence lifetime images representative of experiments done in LNCaP parental cells stained with directly labelled antibodies for HER2 and HER3 before and after treatment with DS7423 for 48 hrs (used at 1000 nM concentration). The intensity images shown are those of the donor only fluorophore. The pseudocolour fluorescence lifetime images demonstrate the range of lifetimes; between 2-2.5 ns in the control conditions and 1.7-2.5 ns in the treated conditions (Tau=lifetime).

(b) Quantification of average FRET efficiencies for control and treatment groups. Data is shown as the mean FRET efficiencies, n=3 for each condition and error bars represent SEM.

The role of HER2-HER3 dimer in metastatic prostate cancer has not been explored yet, however preclinical and clinical work done in breast cancer in our laboratory shows that it has a role in driving cellular proliferation and in being predictive of recurrence of disease (208).

These results confirm the relevance of HER3 in mediating resistance to targeted treatments against the PI3K-mTOR pathway in metastatic hormone-sensitive prostate cancer. HER3 heterodimerisation in this setting adds to sustained positive stimulation on cancer cell proliferation by enhanced activity through the PI3K-AKT-mTOR pathway, despite its pharmacologic inhibition.

3.2.5 The effect of ErbB targeting on AR upregulation in LNCaP NTC cells

The use of lapatinib, a TKI that interrupts EGFR and HER2 pathways, and patritumab, a monoclonal antibody against HER3, were used alone and in combination with DS7423 in LNCaP NTC cells to observe their effect, if any, in disrupting AR upregulation in response to PI3K-mTOR inhibition. AR protein levels on western blot were not restored to those pre-DS7423 treatment by either lapatinib or patritumab (**Figure 3.13**). The use of lapatinib has been recently shown to induce HER2-HER3 dimer stabilisation in breast cancer (245). If PI3K-mTOR inhibition is able to enhance the presence and signalling of an established HER2-HER3 dimer in this cell line, then further stabilisation

of this heterodimer by lapatinib might provide reasonable explanation as to why the AR levels are not effectively abrogated. On the other hand, the use of patritumab demonstrates a decrease in relative levels of HER3 when used in combination with DS7423, despite the upregulation of this ErbB receptor seen originally by PI3K-mTOR inhibition (33% decrease in HER3 levels; p=0.0238). Patritumab works by binding to the extracellular ligand-binding domain of HER3. Literature shows that LNCaP cells do not express heregulin and I was also able to demonstrate that in RNA extracted from LNCaP cells at control conditions and treatment with DS7423 there was no detectable HRG (done in collaboration with Molecular MD; HRG mRNA assay) (246). This suggests that the presence of a heregulin autocrine loop in these cells is an unlikely explanation for the observed HER3 upregulation responsible for AR activation. Since the full mechanisms of action of patritumab have not entirely elucidated, it is possible that patritumab-mediated HER3 receptor endocytosis and degradation is responsible for the downregulation of HER3 levels reversing the effect of DS7423. HER3 degradation and endocytosis is known to be followed by frequent recycling back to the plasma membrane a mechanism shown to contribute to signal amplification (247) and this might be a likely explanation as to why, in this case, the AR levels are not restored to those seen at baseline.

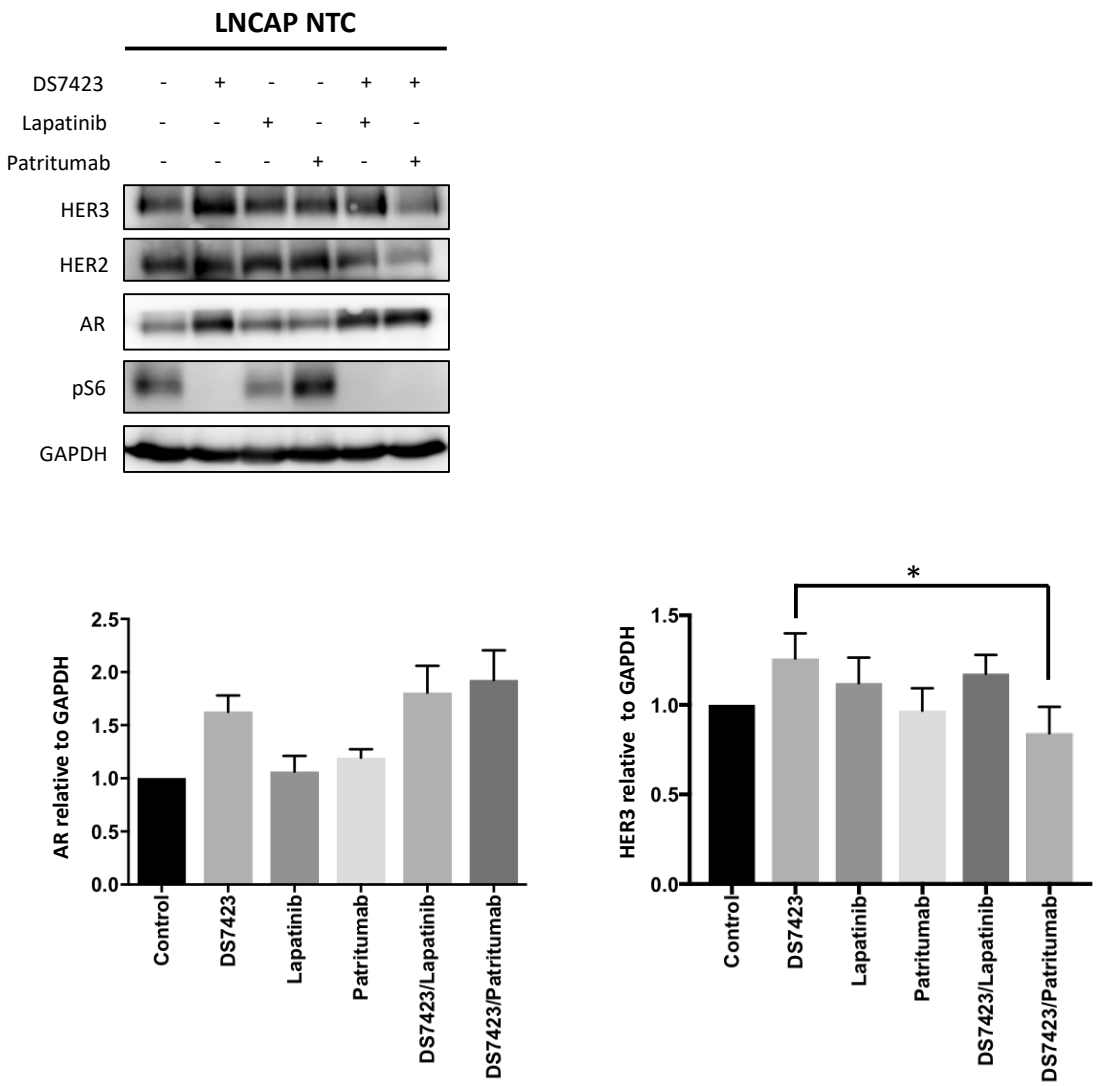

Figure 3.13 – HER2 and HER3 targeting in LNCaP NTC cells does not reverse the effect of DS7423 on AR upregulation:

Top panel: DS7423 in LNCaP NTC cells was used at 1000 nM concentration for 48 hrs. Lapatinib was used at 10 μM and patritumab at 10μg/ml for 24 hrs. Western blot was performed using the presented antibodies.

Bottom panel: The histograms show mean (+/- SEM) AR and HER3 levels normalised to GAPDH upon the treatment conditions as in the western blot and represent three biological replicates.

3.3 Discussion

The role of an activated HER2-HER3 heterodimer in metastatic prostate cancer has been proposed as a mechanism of ligand-independent activation of AR, due to its strong ability to signal intracellularly primarily via the PI3K-AKT-mTOR pathway (103). Furthermore, clinical and preclinical data over the years has demonstrated the activation of the PI3K-AKT-mTOR pathway in metastatic and castrate-resistant prostate cancer, mainly due to the high frequency of PTEN loss. PTEN is the negative regulator of the PI3K pathway and its inactivation by mutation or deletion is identified in ~20% of primary prostate tumour samples at radical prostatectomy and in as many as 50% of metastatic and castrate-resistant tumours (153). Several clinical trials are currently evaluating the clinical responses using inhibitors of the PI3K-AKT pathway in combination with anti-androgens in metastatic CRPC patients (see **table 1.2**, page 44). The presence of a reciprocal feedback loop leading to upregulation of AR via HER3 activation has been suggested to exist upon PI3K-AKT inhibition (6).

The data derived from this project shows that ErbB receptors are expressed in the metastatic hormone sensitive cell line LNCaP which has constitutive AKT phosphorylation as a result of PTEN mutation. LNCaP cells are able to enhance signalling upon NRG-1 stimulation both via the PI3K-AKT pathway but also through the MAPK pathway and to phosphorylate ErbB receptors upon EGF and NRG-1 ligand binding. Consistent with my findings in LNCaP cells that HER3 levels persist upon ligand stimulation, data from others demonstrates that HER3 has reduced internalisation, downregulation and degradation when

compared to the kinetics of EGFR (248). HER3 is endocytosed in a clathrin-dependent manner, in the absence of ligand and independently of its tyrosine phosphorylation (249). The endocytosis of HER3 upon ligand binding, however, is more controversial with some evidence suggesting very low rate of ligand-induced HER3 internalisation (250) while others demonstrate that this occurs within 20 minutes (247). It is generally believed that the C-terminal tail of HER3 and co-receptor activation (e.g. HER2) maybe important factors in determining the trafficking of HER3 (251). Our main knowledge on the kinetics of ErbB members mainly comes from the extensive work done to study EGFR. Data available on EGFR trafficking shows that EGFR homodimers display more efficient internalisation and degradation of the receptor, as opposed to when EGFR forms heterodimers with either HER2 or HER3 (252, 253). As a result, EGFR signalling is prolonged in the case of heterodimerisation. In addition, EGFR heterodimers once internalised do not become sorted within lysosomes but are recycled to the cell membrane (253) and signalling of endocytosed ErbB receptors is not confined to the plasma membrane but can continue after the receptors are internalised within endosomes (254-256). The demonstration that HER3 levels in LNCaP cells persist upon stimulation are most likely a reflection of their heterodimer formation and ability to sustain prolonged signalling intracellularly.

Furthermore, the enhanced activation of pAKT by NRG-1 stimulation in LNCaP cells shows additional PI3K pathway activation that occurs most likely through induction of HER2-HER3 heterodimer formation. This is well established in

breast cancer models upon HRG stimulation (257). In addition, other studies show that AR can be phosphorylated by AKT on two residues in an androgen-independent way and that this is a mechanism by which AR transactivation is enabled leading to promotion of cell survival *in vitro* (258, 259) **(Figure 3.1)**. Also, the analysis of clinical specimens for the expression of pAKT has shown that this kinase has a strong role in prostate cancer progression (158). What this evidence is suggesting therefore, is that AKT activity in prostate cancer probably acts independently of AR to promote cell growth and survival. Moreover, the aberrant status of the PI3K pathway in LNCaP cells as seen by the levels of activated pAKT at baseline, despite correlating with PI3K dependence, does not robustly predict response to PI3K-AKT inhibition (260).

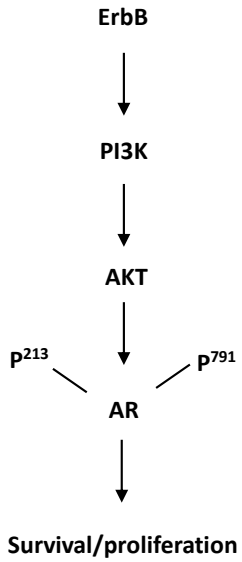

Figure 3.14 – The model of HER2 activation of the AKT-AR pathway that promotes survival and proliferation of androgen-dependent prostate cancer cells upon androgen deprivation.

The transphosphorylation patterns observed in LNCaP cells upon EGF and NRG-1 stimulation shows their ability to sustain and enhance oncogenic downstream signalling. According to the literature, EGF has been identified as an autocrine/paracrine growth factor in prostate cancer tumours and cell lines. It activates EGFR and plays an important role in prostate cancer cell proliferation (261, 262). On the other hand, NRG is not expressed in the LNCaP cell line and prostate cancer tumours (144, 262) and previous studies also demonstrate that in LNCaP cells NRG inhibits their growth when cultured in complete medium (262). Since NRG has a known function in inducing differentiation and apoptosis, its absence in prostate cancer tumours maybe a reason for the uncontrolled growth in these tumours. Indeed, *in vitro* data shows that in the absence of androgen, NRG induces death of LNCaP cells whereas EGF induces cell growth and survival under the same conditions. The NRG-induced LNCaP cell death was dependent on PI3K pathway activation in this study (230). Of note, in breast cancer the expression and effect of NRG has been reported to have both stimulatory and growth inhibitory effects (263-265). The ability of NRG to induce various biological processes is probably a cell dependent process, but it might also depend on the equilibrium between other growth factors and ligands as well as the respective expression of RTKs in each system.

Cytotoxic treatments with DS7423, a novel small molecule inhibitor against PI3K and mTOR (mTORC1/2) showed the upregulation of AR protein in LNCaP parental cells, an increase that correlated with upregulation of HER3, consistent

with the relief of ErbB feedback inhibition upon PI3K-mTOR pathway targeting. Arteaga et al, report a similar effect in HER3 levels in response to PI3K inhibition in a breast cancer model with constitutive PI3K activation, despite adequate inhibition of pAKT and pS6. PI3K pathway inhibition relieves the suppression of RTKs and their activity and therefore limits the sustained inhibition of the pathway and attenuates responses in relation to their use (112). The significance of this increase in HER3 is that it can engage with the p85 subunit of PI3K to reactivate the pathway and induce partial recovery of pAKT and pS6. Of course, the catalytic activity HER2 is paramount for the HER3 and p85 association, therefore the known expression of this ErbB in my cell model and also in breast cancer models is an important pre-requisite for this compensatory feedback. The patterns of HER2 expression in response to inhibition with DS7423 were not studied in this setting mainly because when this data was being generated our attempts were to understand whether therapeutic targeting of HER3 would have been successful in abrogating this feedback upregulation originally observed. Ideally cell proliferation assays performed using the LNCaP parental and HER3 knockdown cells would also provide us with additional information about the phenotypic changes at baseline and upon inhibition with DS7423, however the work in this project concentrated on describing the potential heterodimerisation patterns in ErbB receptors in response to targeted treatment.

My initial findings therefore suggest that the emergence of AR activation as a resistance mechanism following PI3K-mTOR inhibition in this setting is HER3

dependent. Potential therapeutic targeting of HER3 with monoclonal antibodies against HER3 could be beneficial upon the emergence of resistance. This therapeutic strategy has not been explored yet in metastatic or castrate-resistant disease. The creation of a HER3 knockdown stable LNCaP cell line allowed us to demonstrate that in the absence of this RTK, AR upregulation occurs to a smaller degree, most likely consistent with the incomplete knockdown achieved, but also provides evidence that the upregulated AR levels correlate with the presence and upregulation of HER3.

The mechanisms by which AR upregulation occurs in the presence of upregulated HER3 involve mainly the ability of HER3 to form a heterodimer with HER2, to re-activate AKT signalling and enhance AR activity via a ligand-independent mechanism. There is some evidence in the literature suggesting that HER3 is responsible for the ligand-independent increase in AR activation. HER2-HER3 heterodimers, but not EGFR-HER2, modulated AR transcriptional activity by stabilising the AR protein and enhancing binding to its cognate AREs (125). To further support the above statement, a preclinical study also showed that Ebp1, a protein known to interact with HER3, regulates expression of AR and AR regulated genes in the LNCaP cell line. Upon NRG-1 stimulation Ebp1 dissociated from HER3 and translocated to the nucleus to regulate gene transcription (266). Upon interaction with the AR it acts as a corepressor and inhibits the transcription of AR-responsive gene promoters (131). Its expression levels in the setting of HER3 upregulation and activation might be another

possible mechanism to explain the enhanced AR transcription observed in the setting of PI3K-mTOR inhibition in this project.

The enhanced AKT phosphorylation observed in LNCaP cells does not abide by what has been observed before with the use of DS7423 *in vitro* in ovarian cancer models with PIK3CA mutations and, therefore, constitutive activation of pAKT (T308) at baseline as seen in the case of LNCaP cells as well. Here treatment with DS7423 at 625 nM concentration was effective at completely suppressing AKT phosphorylation in those cell lines (234). These findings further enhance the notion that HER3 plays an important role in the regulation of the AR-AKT feedback loop that determines resistance to PI3K-AKT-mTOR pathway inhibition. Targeting HER3 might have an important role in sensitising cells to PI3K-mTOR inhibition by abrogating more effectively the signalling via AKT. Also, independently of the HER3 and its important role, AR is probably able to further maintain cell survival independently of transcription, which is enhanced by PI3K-AKT signalling. The observed increase in pAKT levels seen with Mibolerone treatment alone in both the LNCAP NTC and HER3kd cells is consistent with reports in the literature that show direct interaction between ligand-activated AR and PI3K in the cytosol, mediated by binding of phosphotyrosine residues on the AR NTD to SH2 domain of p85α regulatory subunit of PI3K leading to subsequent activation of AKT (267).

We also show that the effect on AR upregulation seen in LNCaP NTC is observed with other inhibitors of the PI3K-AKT-mTOR pathway and not solely

with DS7423, reinforcing this initial observation. The AR target gene PSA is also overexpressed and correlates with the increase in AR protein levels observed, showing that the upregulated AR is transcriptionally active. This represents a ligand-independent mechanism of AR upregulation and could have important implications in PTEN mutated or null metastatic prostate cancers both at the hormone-sensitive and castrate-resistant setting.

The inability of patritumab to reverse AR upregulation upon PI3K-mTOR inhibition can be explained knowing that monoclonal antibodies against the extracellular ligand-binding domain of HER3 do not completely block or alter the formation of HER3 heterodimers with other members of the ErbB family. In addition, anti-HER3 monoclonal antibodies have been found to be most effective in cancers with high expression of the HER3 ligand, HRG. For example, the human prostate cancer cell line DU145 harbours a strongly-activating HER3-HRG autocrine loop and treatment with the HER3 monoclonal antibody MM-121 showed efficient response in inhibiting HER3, AKT and ERK phosphorylation (268). In addition, recent evidence suggests that HER3 has the ability to bind to ATP and autophosphorylate its intracellular domain when clustered to the cell's membrane (100). While its kinase activity is very low (about 1000-fold lower than of EGFR), it is sufficient for the initial autophosphorylation steps to allow HER3 to efficiently phosphorylate other ErbB members such as EGFR and HER2. Thus, a weakly catalytic HER3 can still lead to the phosphorylation of downstream signalling substrates. Unfortunately, it still remains difficult to target the function of this RTK because

the overall kinase activity is so low compared to its function within heterodimer formation and scaffolding (269). In summary, it would make sense that drugs able to disrupt HER3 heterodimerisation would be more effective at inhibiting the effect of HER3 than monoclonal antibodies and that this is a strategy important to explore in the future especially in the setting of HER3 upregulation.

With regard to the cellular localisation changes that we describe with DS7423 treatment in LNCap cells, data exists describing the regulation of AR nuclear import and export in relation to androgen ligand. The AR contains both nuclear localisation signals (NLS) and nuclear export signals (NES) whose activities are regulated by androgen directly or indirectly. The activity of the respective NLS and NES is important in AR nuclear to cytoplasmic shuttling and are governed by an equilibrium that is driven by the presence or absence of ligand (270). The ligand-dependent nuclear import of AR has been shown to be rapid and is almost complete within 60 minutes. Furthermore, upon androgen withdrawal the AR is exported back outside in the cytoplasm where it is competent to undertake subsequent rounds of hormonal signalling (271). This ability of one molecule of AR to undertake multiple rounds of androgen signalling is very unlike the oestrogen receptor that undergoes proteasomal degradation (272). Consequently, the ability of AR to translocate to the nucleus in the androgen-deprived setting as seen with my work upon treatment with PI3K-mTOR inhibitor raises the question about the ligand-independent nuclear-to-cytoplasmic shuttling of AR and its significance in resistance such therapies and in the promotion of castration-refractory disease. A likely explanation into

the mechanism of how this is achieved is the ligand-independent AR phosphorylation and activation due to signalling downstream of an activated ErbB heterodimer.

Together with the possibility for therapeutic targeting of HER3 overexpression to abrogate resistance to PI3K-mTOR inhibition, assays such as FLIM that are optimised on tumour tissue could complement current techniques to evaluate PTEN as a predictive biomarker of response to PI3K-mTOR inhibition. The Phase II clinical trial with ipatasertib (GDC0068) showed that patients with PTEN loss had superior radiological PFS with the combined ipatasetib and abiraterone treatment compared to the abiraterone only group. PTEN status was assessed using expression level in tumours by IHC and genomic loss by FISH and NGS (170). My data demonstrates that HER2-HER3 heterodimerisation is present in the LNCaP metastatic hormone-sensitive cell line at baseline, prior to any treatment and that using our FLIM assay we can detect the emergence of enhanced HER2-HER3 dimerisation (FRET efficiency from 6% to 13% after treatment with DS7423 for 48 hours) that coincides with AR upregulation and transcriptional activation. Therefore, with this data we suggest that the additional assessment of HER2-HER3 heterodimerisation via FRET-FLIM done on patient tumours at baseline and along the course of treatment with drugs targeting the PI3K-AKT-mTOR pathway could provide additional information to complement PTEN expression to predict response and resistance to these targeted treatments. Further, the detection of ErbB dimerization in patient-derived exosomes could provide a promising way to

monitor this resistance mechanism in a non-invasive way, in the form of a liquid biopsy.

Moreover, we know that AR activation by EGF and other growth factors occurs in a low-androgen environment (122). Therefore, if we accept that ErbB receptors/dimers can activate AR without the need for its ligand, then the role of the various potential ErbB dimerization partners in enhancing prostate cancer cell further metastatic potential and proliferation, but also and very importantly their significance in driving castration-resistant metastatic prostate cancer would allow us to use the detection and evaluation of ErbB dimers as predictive biomarkers of disease progression from the metastatic hormone-sensitive setting to castrate-resistant phenotype and also to predict response and resistance to targeted treatments. In addition, the observed changes in dimerization stability as measured by FRET efficiency in response to treatments would also be important to study within a cohort of patient tumours where relevant clinical information would be available to make correlations between changes in ErbB heterodimerisation within a heterogeneous patient population and the respective effects on clinical outcome. This way we will be able to make true inferences about the role of ErbB heterodimerisation as a predictive biomarker in this disease.

Finally, the use of lapatinib and patritumab showed that the effect on AR upon PI3K-mTOR inhibition is not reversed by the use of these drugs. In fact, under both combined treatment conditions a further degree of increase in AR protein

level is observed. The combination of DS7423 and lapatinib enhances AR levels by 29% compared to DS7423 alone treated cells and the combination of DS7423 and patritumab shows a further increase of 48%. Lapatinib has been shown by previous work done in our laboratory to stabilise the HER2-HER3 dimer (245). In addition, lapatinib inhibits HER2 phosphorylation and prevents receptor ubiquitination leading to the accumulation of marked numbers of inactive HER2 receptors on the cell surface (273). It is likely that the increase observed in HER2-HER3 heterodimer upon PI3K-mTOR treatment in LNCaP cells is further stabilised by lapatinib, and that this allows the cells to proliferate due to sustained signalling downstream the PI3K pathway as well as due to AR signalling due to the observed enhanced AR levels. In the case of patritumab, the upregulated HER3 levels decrease to below baseline most likely as a result of receptor endocytosis and degradation. We hypothesise that the use of the monoclonal antibody against HER3 might perturb the ligand-induced heterodimerisation process and encourage the formation of HER3 homodimers. HER3 homodimers will preferentially by internalised and degraded. The HER2-HER3 heterodimer is thus impaired most likely due to patritumab use but this might enable the cells to form other ErbB heterodimers, such as EGFR-HER2 that is also known to have a potent effect on oncogenic cell signalling (274, 275). The small further increase in AR levels, therefore, might reflect this switch in ErbB dimer formation.

In conclusion, the results of this chapter provide additional preclinical evidence that PI3K-AKT-mTOR pathway targeting could be efficacious in the hormone-

sensitive metastatic setting, despite the predominant AR signalling driving the disease at this stage. In addition, it would be very interesting to evaluate the predictive significance of HER2-HER3 heterodimerisation performed as surrogate pre-treatment biomarker in patient tissue and exosome samples within a clinical trial targeting PI3K-AKT-mTOR pathway therapeutically, as well as at various timepoints along the treatment to identify whether subgroups of patients preferentially up- or down-regulate HER2-HER3 heterodimer with treatment and how the changes in ErbB heterodimerisation inform us on clinical outcome. It would also be intriguing to identify, within a heterogeneous patient population, the proportion of patients with metastatic hormone sensitive and castrate-resistant disease that express HER2-HER3 dimer at baseline and whether patients without basal HER2-HER3 dimerisation respond differently to treatments, have better survival outcomes or have to ability to utilise the formation of a new ErbB heterodimer as a resistance mechanism at occurs during the time-course of their treatment using targeted inhibition of the PI3K-AKT-mTOR pathway. Furthermore, the combination of FLIM for HER2-HER3 heterodimerisation and PTEN status, already assessed by IHC in clinical trials, might prove to be a more robust predictive model of response or resistance to therapeutic targeting.

Chapter 4: PI3K-mTOR inhibition in PTEN functional metastatic prostate cancer is dependent on ErbB family to upregulate PSMA

4.1 Introduction

PSMA is a type II integral cell-surface membrane protein whose expression density and carboxypeptidase enzymatic activity are increased progressively in prostate cancer compared to normal prostate epithelium. PSMA is an ideal target for monoclonal antibody imaging and therapy and studies published more recently show that PSMA also has a functional role in prostate cancer (171).

The single correlation between PSMA and HER2 in prostate cancer has been described in a clinical study looking at radical prostatectomy specimens compared to normal tissue. PSMA expression by IHC was higher in prostate cancers and correlated with tumour stage, high Gleason score, PSA level and HER2 expression ($p<0.0001$ each) (276). As discussed previously, a new role for PSMA was recently described; this is the ability of PSMA to regulate cellular signaling via the PI3K-AKT pathway (193) through mGLUR1 (195).

Given that PI3K pathway signalling is so relevant in metastatic prostate cancer and PI3K-AKT inhibitors are currently being investigated in metastatic CRPC we further wished to investigate the changes in PSMA expression levels *in vitro*

and *in vivo* by using the PI3K-mTOR inhibitor DS7423. The heterogeneity of prostate cancers makes it very difficult to anticipate whether inhibition of PI3K-AKT signaling would benefit patients. Additionally, many biological sequelae of PI3K-AKT-mTOR inhibition, such as HER3 and AR upregulation described in the previous chapter of this work, undermine the potential therapeutic gain. For example, the work done using the LNCaP cell line which has a mutated PTEN gene, leading to deficient function of the PTEN tumour suppressor, demonstrated downregulation of PSMA consistent with the overexpression of AR seen in the LNCaP NTC cells (**see Figure 3.9**).

The CWR22 and 22Rv1 cells were used to investigate the effect of PI3K-mTOR inhibition in the PTEN wild-type setting of metastatic prostate cancer. The CWR22 cell line was originally established from transplantable human CWR22 prostate tumours (277). The tumours were derived from a Gleason score 9 primary prostate cancer with bone metastases (278). CWR22 cells, as with the tumour counterparts, respond very promptly to androgen deprivation showing marked tumour regression after castration, mimicking the course of the human disease (279). The 22Rv1 cell line is the androgen-independent derivative established from hormone refractory recurrent CWR22 tumours (280). CWR22 cells express EGFR, HER2 and HER3 as well as NRG-1, the ligand for HER3 and HER4, suggesting that the ErbB receptors play a significant role in the growth of these cells (278). Furthermore, the CWR22 and 22Rv1 cell lines are known to express wild type PTEN and have low/undetectable levels of pAKT in

the absence of upstream activation by RTKs (281, 282). Finally, the 22Rv1 cell line exhibits a truncated AR that was demonstrated to be AR-V7 (283).

In this section, we wished to investigate the expression of PSMA and AR in the metastatic and castrate-resistant prostate cancer settings where the PTEN tumour suppressor is still expressed and functional. The recent demonstration of the link between PSMA and the PI3K pathway makes this relevant, despite the presence of WT PTEN. Furthermore, we wished to investigate whether any changes in PSMA could be presented by radiological imaging using PSMA-PET *in vivo* as a means of detecting this in patients as well.

4.2 Results

4.2.1 Effects of RTK stimulation in CWR22 and 22Rv1 cells

Both CWR22 and 22Rv1 cells show strong levels of phosphorylation of EGFR upon EGF stimulation, which coincides with phosphorylation of HER2 and to a smaller degree with HER3 phosphorylation as well (**Figure 4.1**). An increase in phosphorylated ERK levels is seen predominantly upon EGF stimulation in both cell lines, showing that MAPK is the principal pathway signalling downstream of EGFR activation. On the other hand, phosphorylated AKT (T308) is only mildly activated in the setting of EGF stimulation. Further, when NRG-1 is used, both cell lines are able to phosphorylate HER3. HER2 phosphorylation, but not of EGFR, is seen in both CWR22 and 22Rv1 cells upon NRG-1 stimulation suggesting that HER3 preferentially forms heterodimers with HER2 when

activated to enhance downstream signaling via the PI3K-AKT pathway as seen by the strong phosphorylation of AKT at threonine 308. Activation of MAPK pathway in response to NRG-1 stimulation is only modest when compared to the effect seen upon EGF stimulation. Finally, both cell lines demonstrate increase in AR levels upon EGF and NRG-1 stimulation, that could indicate that activation of RTKs can lead to subsequent activation of AR in metastatic prostate cancer. My findings are consistent with results reported in the CWR-R1 cell line, where HRG stimulation activated HER2 and HER3 and increased androgen-dependent AR transactivation of reporter genes (121). Finally, EGF and NRG-1 stimulation in both cell lines does not appear to stimulate PSMA activation. In conclusion, EGFR, HER2 and HER3 activation in metastatic hormone-sensitive and castrate-resistant prostate cancer are associated with elevated kinase signalling and AR activation, most likely through the formation of ErbB heterodimers.

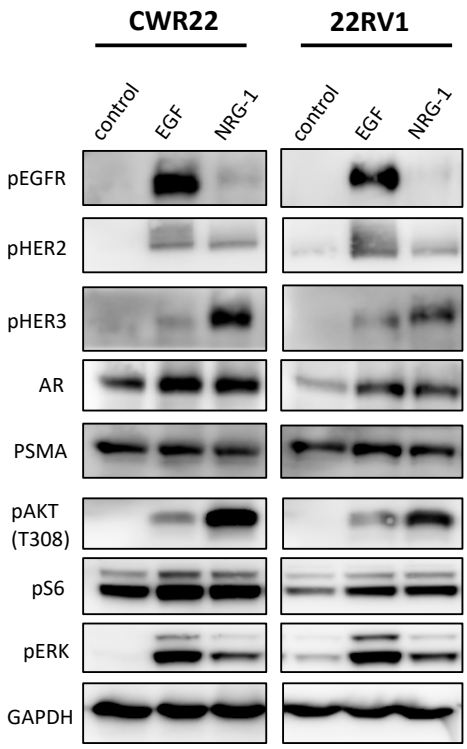

Figure 4.1 – ErbB phosphorylation in CWR22 and 22Rv1 cell lines following EGF and NRG-1 stimulation:

Western blot showing the response of RTKs and downstream signalling targets, as indicated by the antibodies used in the figure, to EGF (used at 100ng/ml for 5 mins) and NRG-1 (used at 50ng/ml for 5 mins).

The use of Enzalutamide at two timepoints, 2 and 7 days, showed that AR expression decreases in both hormone-sensitive and castrate-resistant cell lines and that HER2 expression follows the same trend (**Figure 4.2**). In the CWR22 cells the effect on AR expression is seen at a greater magnitude (58% decrease in AR levels seen after Day 7 post Enzalutamide) compared to the 22Rv1 cells (AR decrease by 10%). Interestingly though, the degree of HER2 downregulation in both these cells lines is similar; 32% and 36% in CWR22 and 22Rv1 cells respectively. On the contrary, PSMA in these cell lines is upregulated upon Enzalutamide use for 7 days and this might represent a

resistance mechanism to androgen inhibition since it does not occur as an immediate effect. These findings also show that in response to anti-androgens PSMA is upregulated irrespective of ErbB signaling to allow oncogenic signaling when the AR pathway is inhibited in a ligand-dependent way. However, the relationship of PSMA and ErbB signaling in response to PI3K-mTOR inhibition has not been described at all and further experiments planned wished to describe the relationship between these and how they can be utilized together as biomarkers in the setting of targeted treatment against the PI3K-AKT-mTOR pathway.

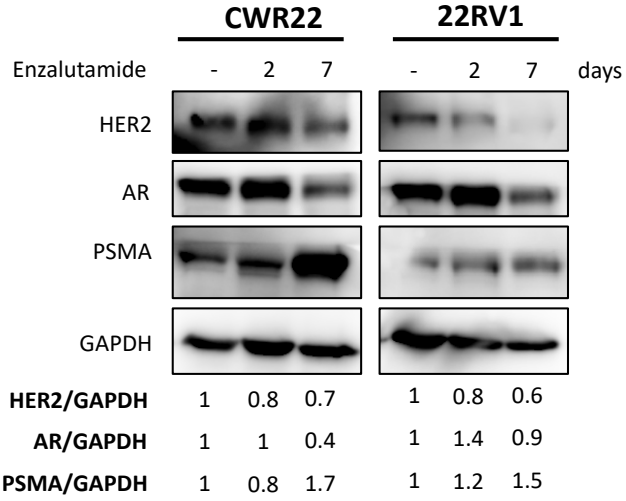

Figure 4.2 – Enzalutamide treatment leads to AR and HER2 downregulation in CWR22 and 22Rv1 cells:

Enzalutamide was used at 10 μM concentration at the indicated timepoints. The quantification of PSMA, HER2 and AR (relative to GAPDH) is also shown in the panels.

4.2.2 PSMA upregulation in PTEN WT prostate cancer cell lines upon inhibition of PI3K-mTOR pathway

The CWR22 and 22Rv1 isogenic pair of cell lines were treated with DS7423, alongside other inhibitors of the PI3K-AKT-mTOR pathway as done in the LNCaP cells, to look for the effects on AR and PSMA. Interestingly, upon 48 hours of treatment with DS7423 at 1000 nM, there is observed overexpression of the PSMA protein in both cell lines that coincides with upregulation of HER2 (**Figure 4.3 and Figure 4.4**). PSMA overexpression was observed in both hormone-sensitive and castration-resistant cell lines by 42% and 35% respectively upon PI3K-mTOR inhibition. The PSMA upregulation is statistically significant (p-value 0.0046 in CWR22 cells and 0.006 in 22Rv1 cells) (**Figure 4.5**). In addition, the use of GDC0941 and everolimus also leads to PSMA upregulation in the castrate-resistant 22Rv1 cells, however this is not statistically significant. The effect on PSMA is not observed in the hormone-sensitive CWR22 cell line upon treatment with these drugs. Notably, the expression of AR is suppressed upon DS7423 treatment in contrary to what has been observed in the LNCaP NTC cells before, but consistent with previous literature demonstrating the inverse relationship between AR and PSMA (236).

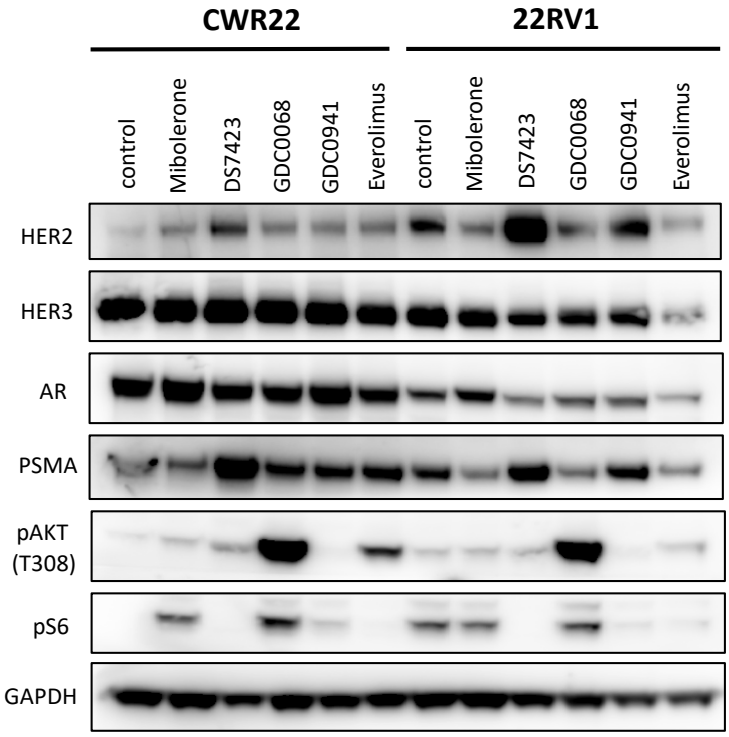

Figure 4.3 – PI3K-mTOR inhibition in PTEN WT prostate cancer cell lines upregulates PSMA:

CWR22 and 22Rv1 cells were treated with Mibolerone and inhibitors of the PI3K-AKT-mTOR pathway for 48 hrs. Mibolerone was used at 1 nM concentration. DS7423, GDC0068, GDC0941 and Everolimus were used at 1000 nM, 100 nM, 1000nM and 100 nM respectively.

Interestingly, HER2 upregulation coincides with the effects observed in PSMA under the conditions described above and in the respective cell lines. In contrary however, HER3 levels remain at baseline or even show mild downregulation with the use of inhibitors that target the PI3K-AKT-mTOR pathway.

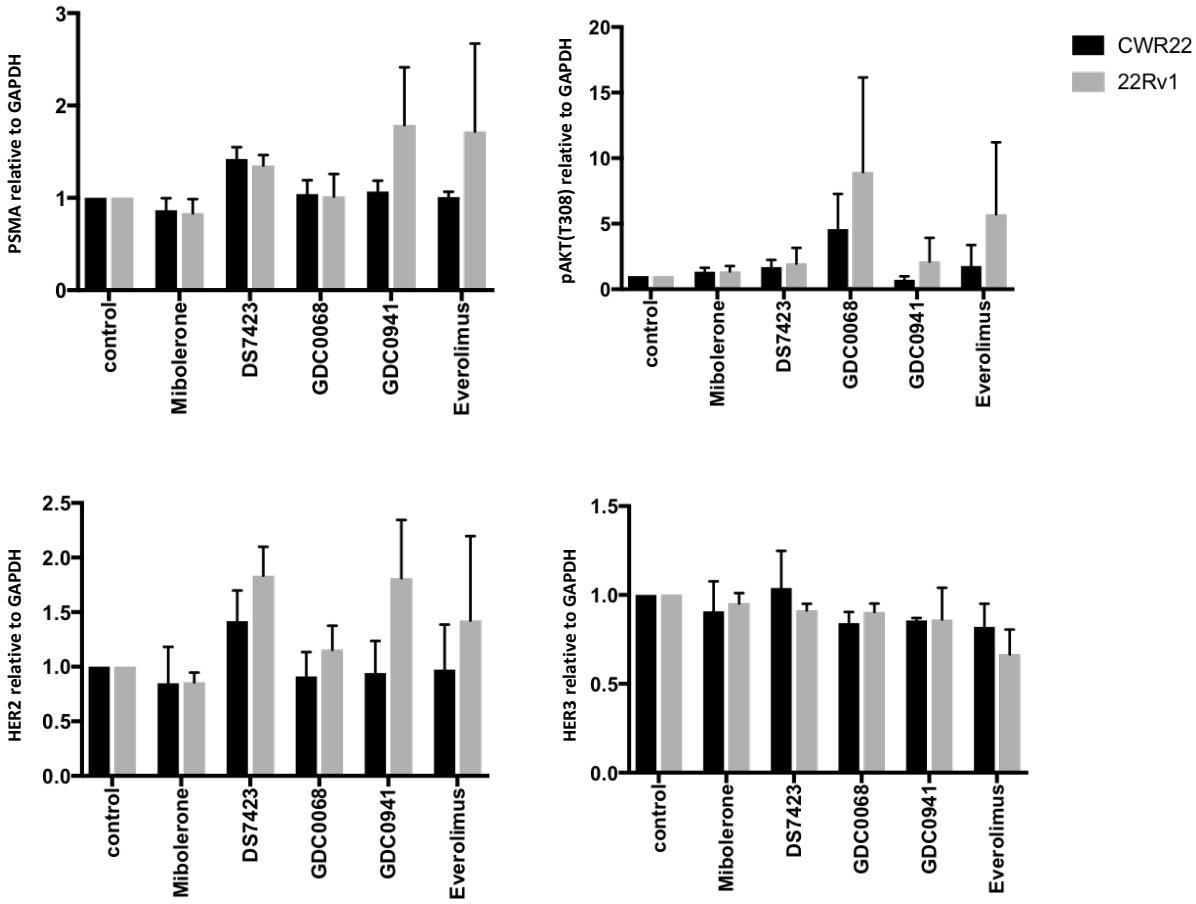

Figure 4.4 – PSMA, pAKT(T308), HER2 and HER3 quantification upon treatment: Histograms demonstrate changes in the proteins of interest in both cell lines relative to GAPDH. Values are mean +/- SEM (n=3). Black bars = CWR22, Grey bars = 22Rv1.

The levels of pAKT (T308) are also enhanced in both CWR22 and 22Rv1 cell lines upon DS7423 treatment, supporting the hypothesis that PSMA upregulation enables the emergence of resistance by signalling through the PI3K pathway (**Figure 4.4**). In 22Rv1 cells, consistent with PSMA and HER2 upregulation upon GDC0941 and Everolimus, pAKT also shows markedly elevated levels suggesting that sustained signalling of the PI3K-AKT-mTOR pathway occurs as a resistance mechanism to targeted inhibition. The effect observed with the use of GDC0068, in that pAKT (T308) levels are induced upon AKT inhibition reflects a homeostatic feedback mechanism in response to

this allosteric inhibitor and has previously been shown with other similar AKT inhibitors (284, 285) before.

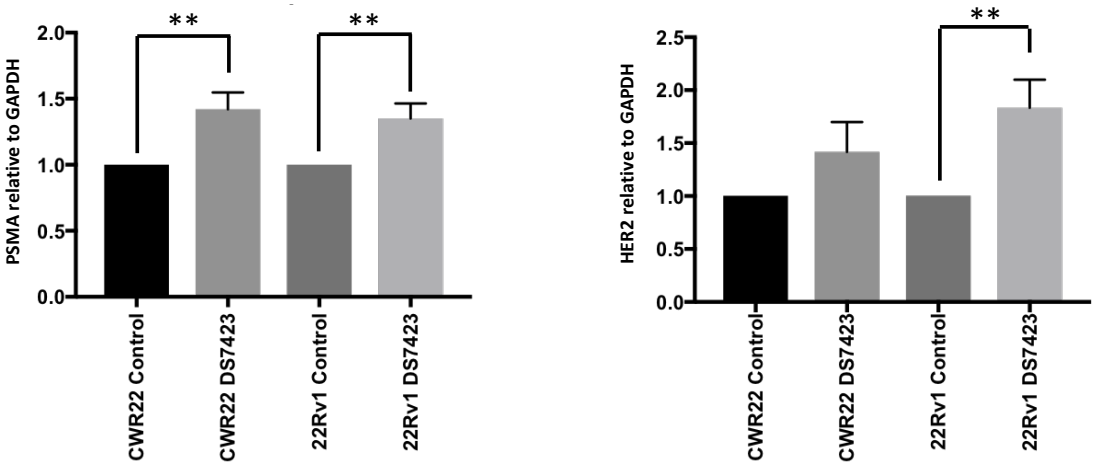

Figure 4.5 – PSMA and HER2 quantification post DS7423 in CWR22 and 22Rv1 cells: Histograms represent the quantification of DS7423 effect on PSMA (left panel) and HER2 (right panel) levels in CWR22 and 22Rv1 cells after 48 hrs of treatment. Total levels of each protein were expressed as a ratio relative to GAPDH used as loading control. Values are mean +/- SEM (n=3), ** = $p<0.01$.

Based on the findings identified by immunoblot after treatment of cells *in vitro* I wanted to observe the localisation of HER2 and HER3 in CWR22 and 22Rv1 by confocal microscopy. This was done at control (10% charcoal-stripped FBS in RPMI; i.e media deprived of androgens) and treatment conditions with DS7423 at 1000 nM for 48 hours. In CWR22 cells we observe re-localisation of HER2 from the cell surface membrane to the nucleus upon treatment. HER3 on the other hand remains located in the cell surface membrane under both conditions. In 22Rv1 cells both HER2 and HER3 showed continuous expression in the cell surface membrane (**Figure 4.6**) at control and upon treatment.

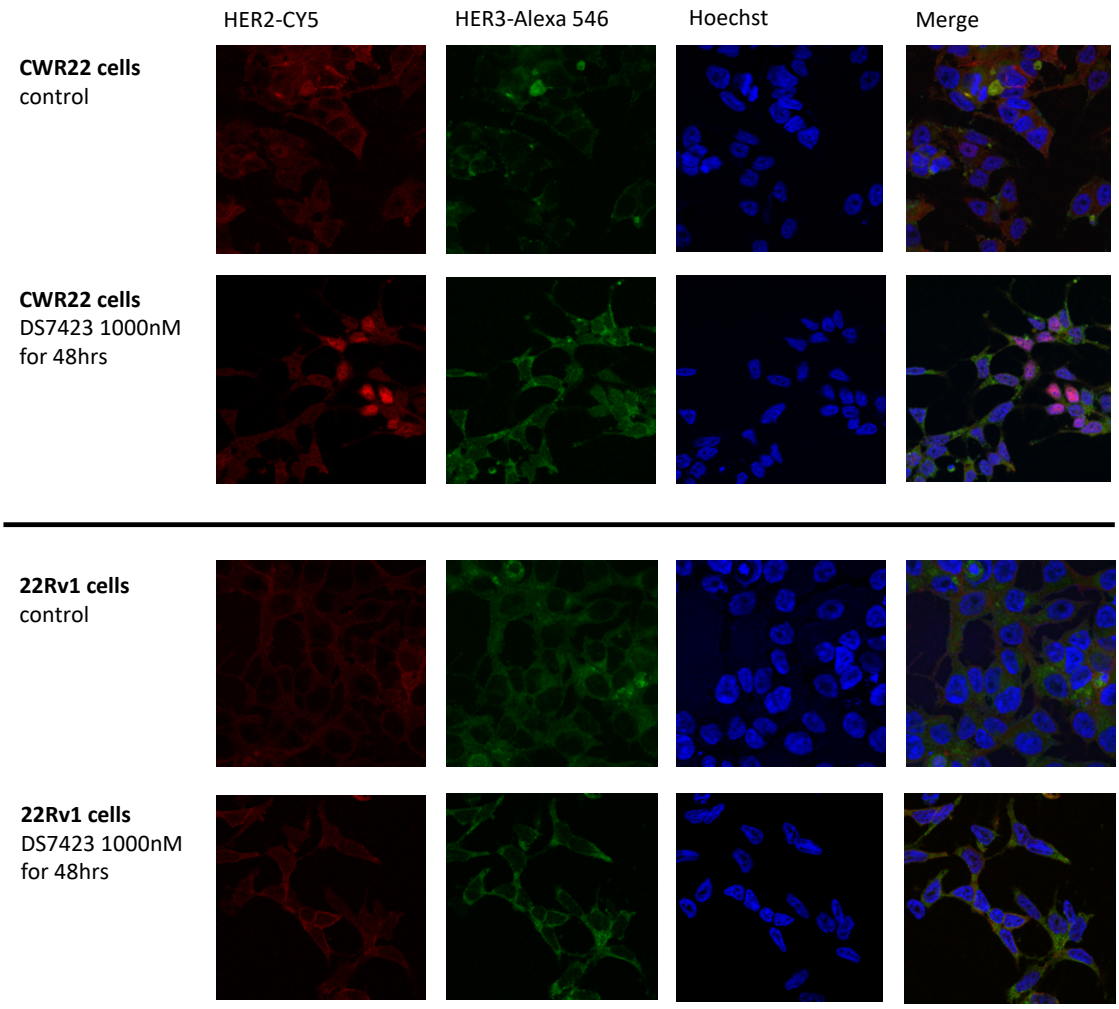

Figure 4.6 – The cellular localisation of HER2 and HER3 upon DS7423 treatment in CWR22 and 22Rv1 cells:

Cells were stained with directly-labelled fluorescent antibodies for HER2 and HER3 and imaged by confocal microscopy at the indicated timepoints. Panels also represent Hoechst staining as an indicator of cell nuclear staining and merged images.

I then proceeded with treatments in CWR22 and 22Rv1 cells treated with lapatinib and patritumab, alone and in combination with DS7423, as done in the LNCaP cells in the previous chapter. HER2 and PSMA upregulation is demonstrated again in both cell lines upon DS7423 treatment (**Figure 4.7**). The use of lapatinib and patritumab alone in CWR22 and 22Rv1 cells does not lead to significant changes in PSMA expression levels.

When DS7423 is used in combination with lapatinib in the CWR22 cell line we observe decrease in PSMA upregulation and return to PSMA expression levels similar to baseline prior to DS7423 treatment (**Figure 4.7**). Specifically, there is a 20% decrease in PSMA levels between CWR22 cells treated with DS7423 alone and those with combined DS7423 and lapatinib. 33% decrease in PSMA expression levels is seen in 22Rv1 cells between DS7423 treatment alone and the combined treatment with lapatinib. The combined use of DS7423 and patritumab, on the other hand, resulted in only a very modest abrogation of the overexpressed PSMA levels in the CWR22 cells, while the same combination had no effect in reversing the DS7423 induced PSMA upregulation in 22Rv1, where on the contrary, PSMA levels are seen to increase even further.

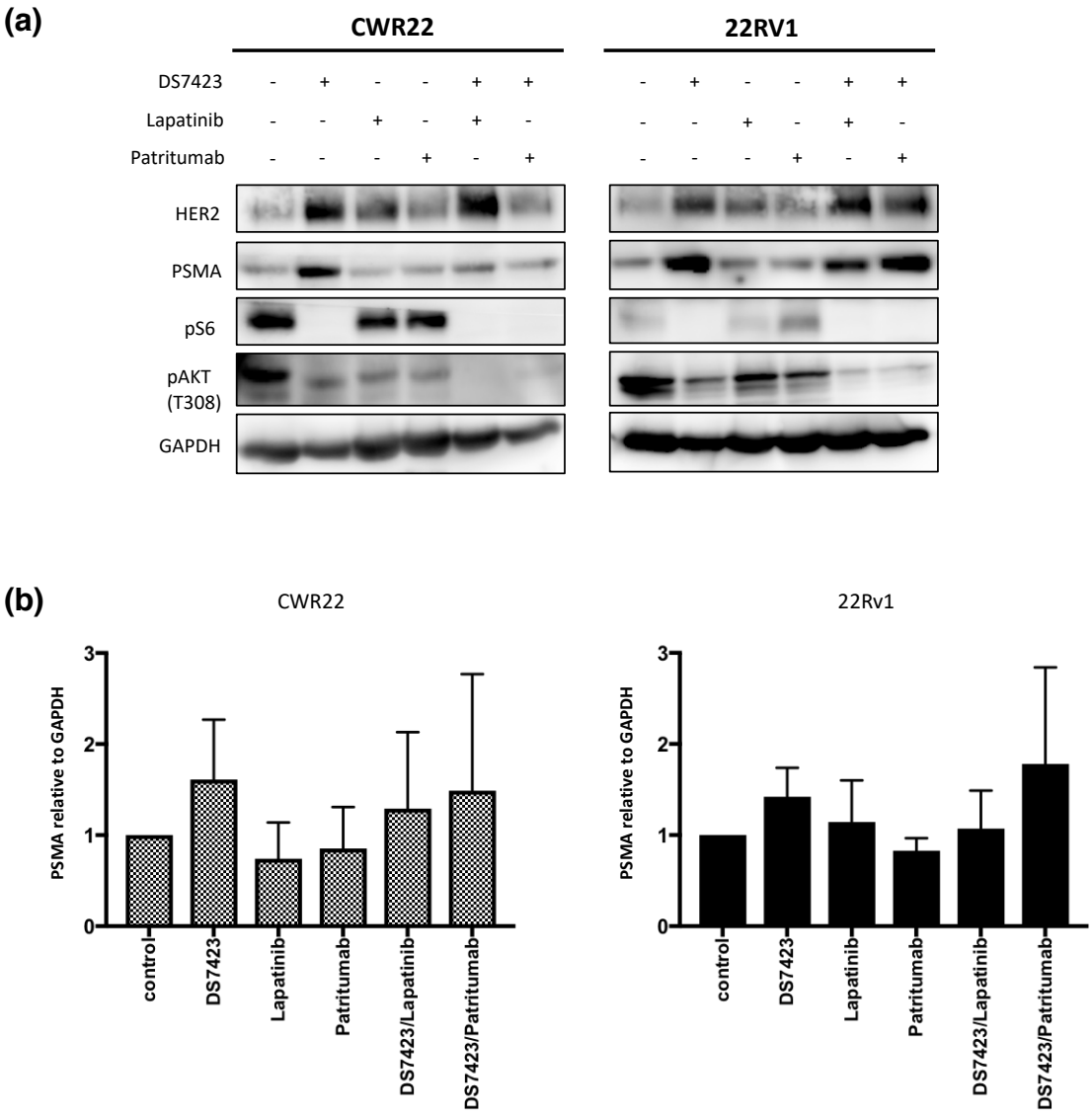

Figure 4.7 – The effects of ErbB targeting in PTEN WT prostate cancer cell lines, alone and in combination with PI3K-mTOR inhibition:

(a) CWR22 and 22Rv1 cells were treated with DS7423, lapatinib and patritumab alone and in combination. In the combination treatments, the cells were treated for the first 24 hrs with DS7423 at 1000 nM, followed by the addition of lapatinib (at 10 μM) or patritumab (at 10 μg/ml) for another 24.

(b) Histograms show the quantitative effect of single and combined treatments on PSMA expression relative to GAPDH loading control. The data is representative of mean +/ SEM (n=3).

Furthermore, the use of lapatinib in both cell lines leads to increase in HER2 levels (**Figure 4.8**) and this finding is consistent with data in breast cancer cell lines overexpressing HER2 (273) and is most likely due to the accumulation of HER2 on the cell plasma membrane. When lapatinib is added to cells already being treated with DS7423 we observe that HER2 levels are sustained but do not increase further and that HER3 levels decrease in conjunction with the decrease in PSMA upregulation when compared to DS7423 treatment alone. As discussed already above, the PSMA levels do not return to baseline but the feedback effect in its levels in response to PI3K-mTOR inhibition that is mediated by HER2 upregulation is lessened to an extent. It is not clear whether this reflects PSMA dependency on HER2 phosphorylation that is diminished in the presence of lapatinib or whether HER3 is also required, potentially as part of a complex with PSMA that is essential to maintain its levels. When we observe the effects of patritumab addition on the other hand, it appears that the two cell lines behave in an opposite fashion with regards to PSMA levels. Combined DS7423 and patritumab treatment in CWR22 cells allows small decrease in PSMA levels, however the 22Rv1 cells show further overexpression of this protein. Interestingly, and in a way that coincides with the rest of our findings, the HER2 and HER3 levels are downregulated by patritumab in the CWR22 cells, whereas in 22Rv1 cells HER2 demonstrates further overexpression. These results support our knowledge that PSMA and HER2 are closely linked. Furthermore, HER3 monoclonal antibody in CWR22 cells enables decrease in HER2 expression, probably suggesting that these cells activate HER2 via NRG-1 stimulated HER3 activation. The regulation of

HER2 in the castrate-refractory 22Rv1 cells appears to be less dependent on HER3 ligand levels for its activation and function.

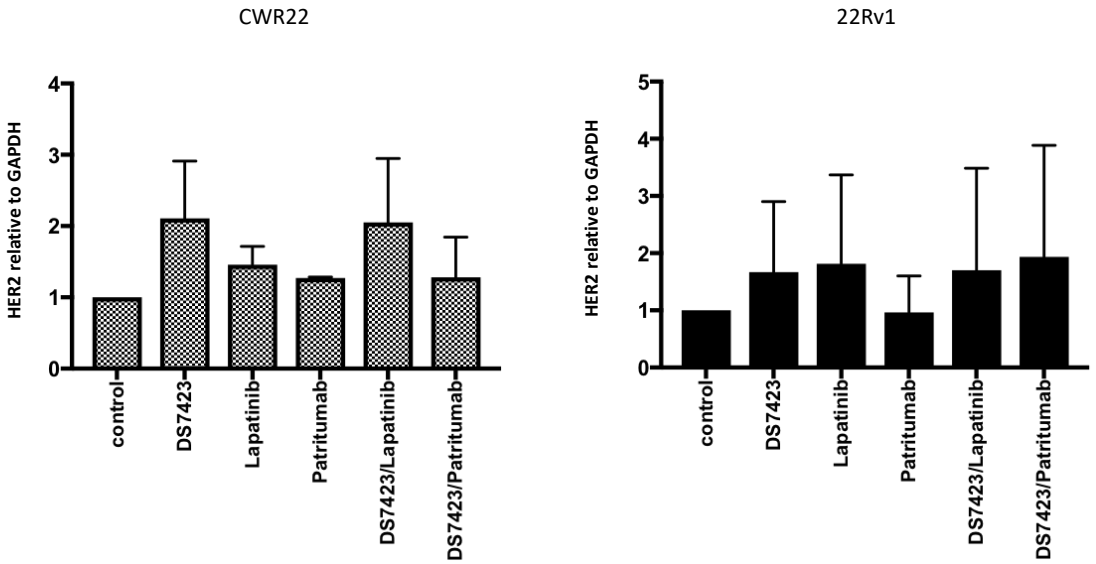

Figure 4.8 – HER2 regulation upon DS7423 and combined treatments in CWR22 and 22Rv1 cells:

Histogram representation of the HER2 changes upon DS7423 treatment alone and in combination with lapatinib or patritumab after triplicate repetition and expressed relative to GAPDH as control.

4.2.3 In vivo evaluation of DS7423 treatment in PTEN WT prostate cancer mouse xenografts

Following the findings from the *in vitro* use of PI3K-AKT-mTOR inhibition in CWR22 and 22Rv1 cells I wished to evaluate this *in vivo*, within frozen tumour lysates and if successful by PSMA PET scan. We used a subcutaneous mouse xenograft model in nude athymic male mice to treat with DS7423 by daily oral gavage for 10 days (schedule as in **Figure 4.9(a)**) that would allow us to investigate these. The graphs in **Figure 4.9(b)** represent the tumour growth curves in CWR22 and 22Rv1 xenograft mice, as recorded as tumour volume

measurements. Despite the initial observed decrease in tumour volume at the initiation of treatment between D0 and D2 (days 21 and 23 post inoculation), the tumours in both models continue to grow despite PI3K-mTOR inhibition demonstrating that resistance develops early, and that this correlates with PSMA upregulation. It is therefore very possible that PSMA upregulation acts as one important mechanism that allows the PI3K pathway to continue its oncogenic signalling to enhance prostate cancer cell proliferation.

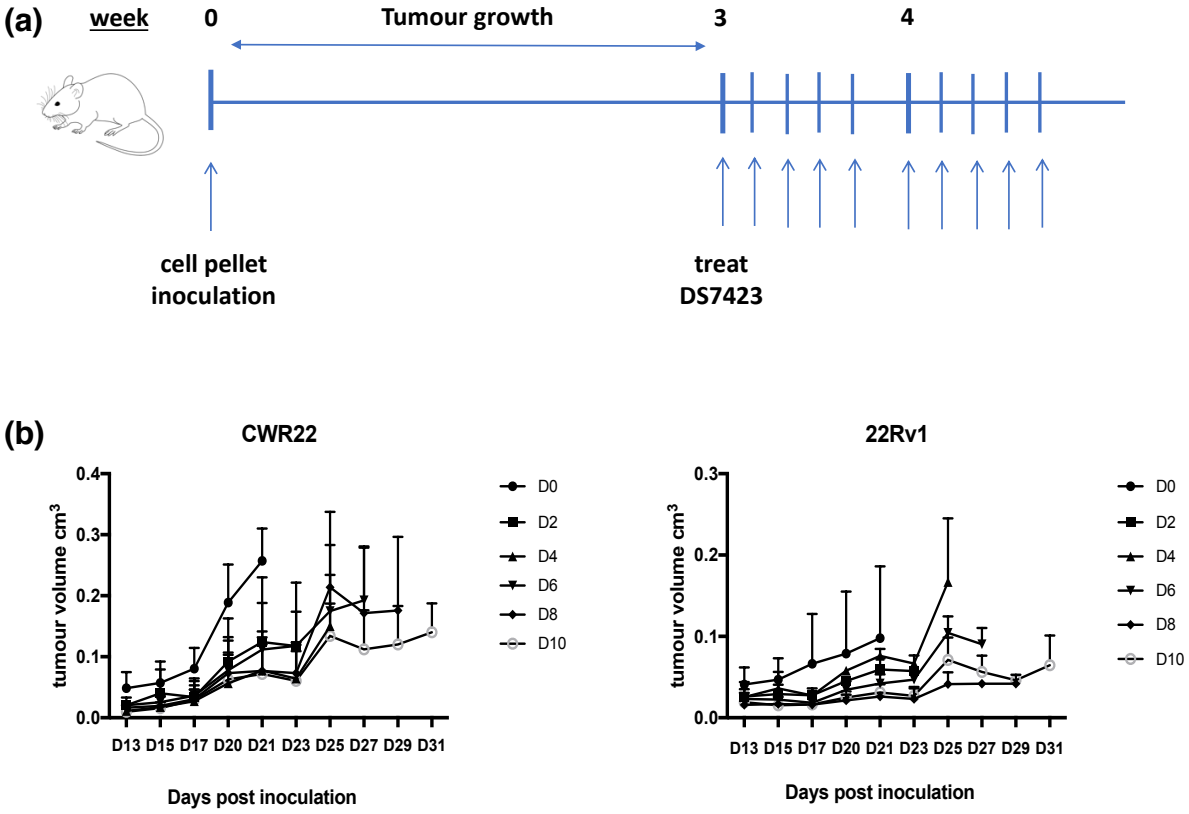

Figure 4.9 – *In vivo* growth and assessment of prostate cancer xenografts upon DS7423 treatment in nude mice:

(a) Bilateral subcutaneous CWR22 and 22Rv1 xenografts were grown in nude athymic male mice. At 3 weeks when the tumours were established the mice were treated with DS7423 by oral gavage at 3mg/kg/day for 5 days of the week for 2 weeks. At the end of the week mice were culled and tumours collected and stored for further experiments.

(b) Growth curves of mice treated with DS7423. Treatment days are shown as days 21-31 (post inoculation). Each cell line xenograft included 12 mice and 2 mice were sacrificed every 2 days (from D21 onwards) post treatment for collection of tumours for further analysis. Tumour volumes were calculated using the formula [(major axis)*(minor axis)^2/2]/1000 cm^3.

Similarly to what has been observed *in vitro*, the tumour lysates from CWR22 and 22Rv1 mice treated with DS7423 upregulated PSMA by day 4 and 6 respectively following treatment with the drug. Interestingly, the HER2 upregulation observed *in vitro* following PI3K-mTOR inhibition that correlates

with PSMA overexpression is only seen in 22Rv1 tumours **(Figure 4.10)**. This can be explained by the fact that HER2 has been shown to relocalise to the nucleus in the CWR22 tumours and that the NP-40 based lysis buffer used to extract protein from lysed frozen tumours has decreased ability to detect nuclear extracts within tumour tissue as compared to cells in culture (286).

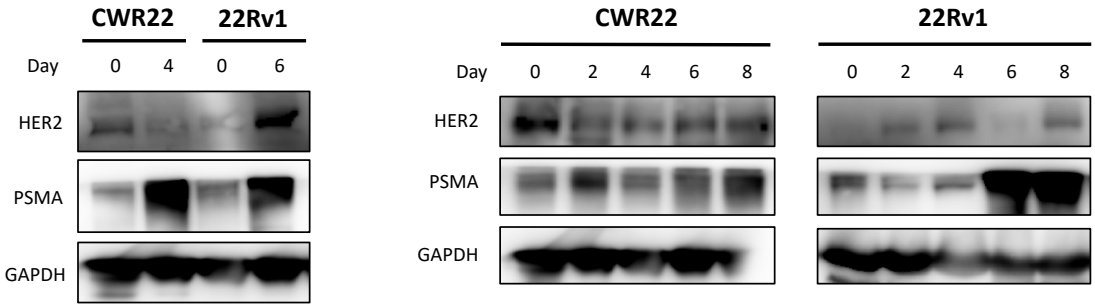

Figure 4.10 – Assessment of HER2 and PSMA levels in mouse xenograft tumours post DS7423 treatment:

Left panel: Frozen tumours were lysed and used for western blot electrophoresis to assess the levels of HER2 and PSMA at timepoints day 0 and 4/6 of DS7423 treatment.

Right panel: shows frozen tumour lysates blotted on timepoints 0-8 days of treatment to demonstrate the changes in HER2 and PSMA (GAPDH immunoblot images are not available due to inability to obtain clear image from experiments but equal protein was loaded as changes in protein level expression should only represent effect of drug use).

Further evaluation of mouse xenograft paraffin-embedded tissue with FLIM to look for baseline HER2-HER3 dimerisation was performed in the tumour samples obtained at day 0 to show that in the CWR22 tumours HER2-HER3 heterodimerisation is not present prior to treatment as the calculated FRET efficiency % is 0.003. On the contrary, the 22Rv1 tumours exhibit a basal level of HER2-HER3 heterodimerisation with FRET efficiency % of 2.32, suggesting that HER2-HER3 heterodimerisation in PTEN WT models of metastatic

prostate cancer occurs as the disease progresses from a hormone-sensitive to a castrate-resistant phenotype (**Figure 4.11**). Of course, this needs further evaluation within a bigger cohort of patient-derived tissue at these stages of their disease, which is not always possible to obtain. However, establishing the presence of HER2-HER3 dimerisation and their potential relationship to PSMA expression would be important within clinical trial where prospective sampling of tissue can be planned for surrogate biomarker evaluation.

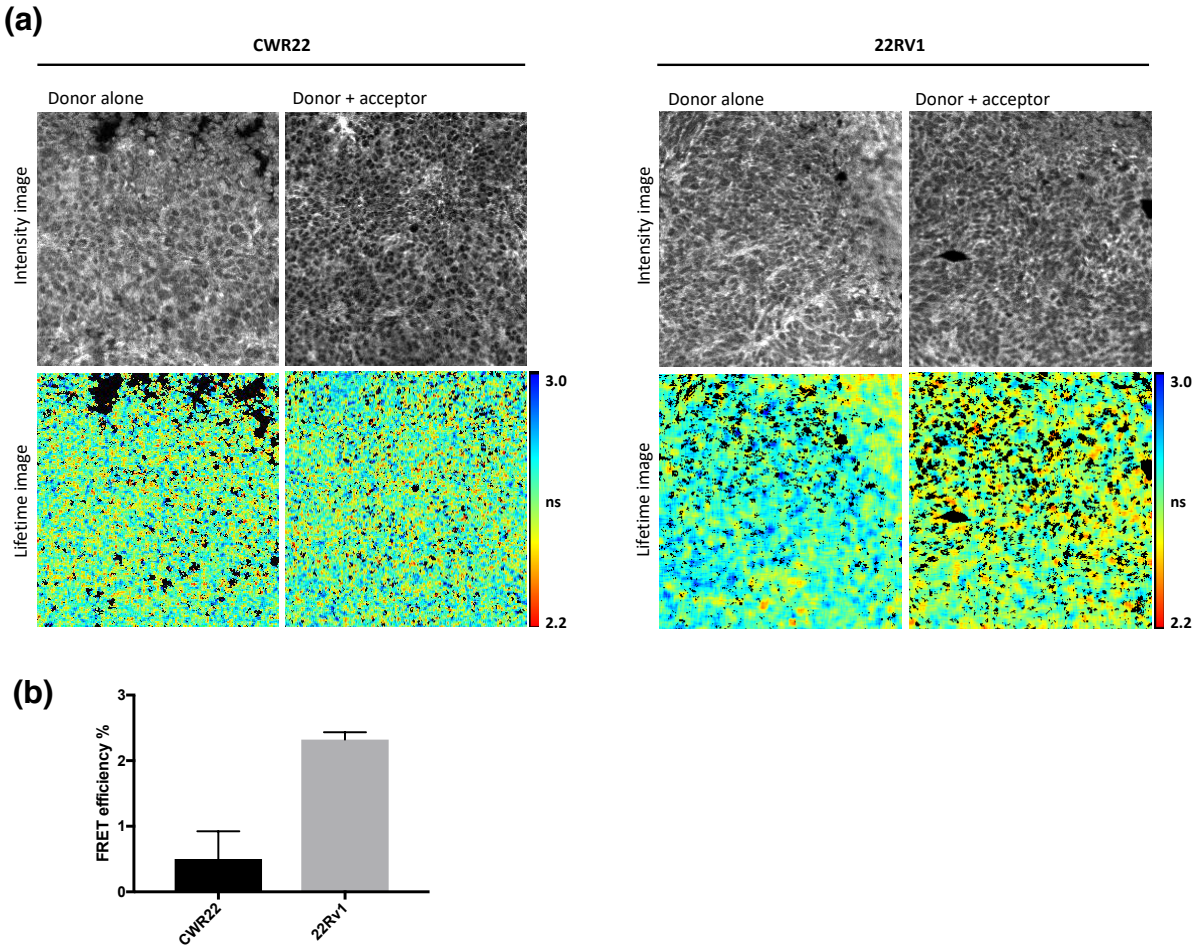

Figure 4.11 - HER2-HER3 heterodimer detection in CWR22 and 22Rv1 mouse xenograft tissue at baseline:

(a) Donor alone and donor + acceptor intensity and fluorescence lifetime images representative of experiments done in paraffin-embedded tissue of CWR22 and 22Rv1 mouse xenograft tumours stained with directly labelled antibodies for HER2 and HER3. The intensity images shown are those of the donor and donor + acceptor fluorophores. The pseudocolour fluorescence lifetime images demonstrate the range of lifetimes; between 2.2-3.0 ns (Tau=lifetime).

(b) Quantification of average FRET efficiencies. Data is shown as the mean FRET efficiencies, n=3 for each condition and error bars represent SEM.

When HER2-HER3 heterodimerisation was assessed in tumour tissue following treatment with DS7423 at Day 4 and 6 timepoints (respectively for CWR22 and 22Rv1 tumours) this demonstrated no change in HER2-HER3 dimer in the

CWR22 tumour tissue. In 22Rv1 tumour tissue FRET efficiency showed an increase of 46% between untreated (2.32%) and day 6 (3.38%) tumours and this increase, despite modest, was statistically significant (p=0.0267) (Figure 4.12).

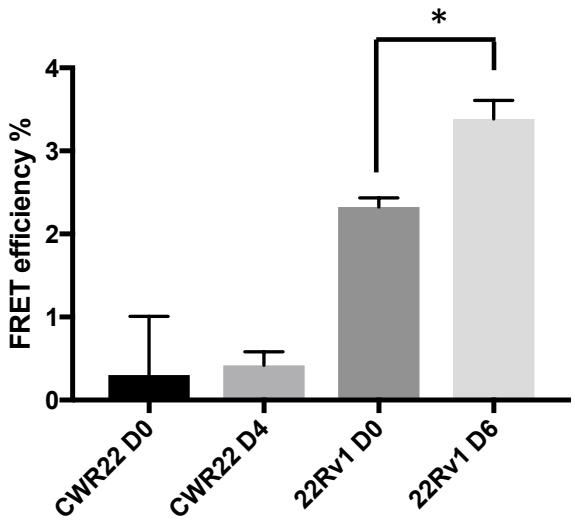

Figure 4.12 - HER2-HER3 heterodimer detection in CWR22 and 22Rv1 mouse xenograft tissue after DS7423 treatment:
Quantification of average FRET efficiencies for control and treatment groups. Data is shown as the mean FRET efficiencies, N=3 for each condition and error bars represent SEM (* = p<0.05). Replicates are technical and represent 3 tissue samples from the same mouse tumour at each treatment condition.

The frozen tumours collected from the *in vivo* study of DS7423 in CWR22 and 22Rv1 mouse xenografts were also used to stain with antibodies of interest for immunofluorescence confocal microscopy (**Figure 4.13**). CWR22 tumours prior to any treatment with DS7423 show expression of PSMA and HER2 as expected. More specifically, by frozen tumour immunofluorescence, CWR22 xenograft tissue at Day 0 of treatment demonstrates strong and heterogeneous PSMA staining that is localised in the membranous and cytoplasmic areas of

tumour cells, consistent with what has been described in literature so far. The HER2 pattern appears more homogenous with some areas of more intense staining, and is also expressed mainly in the membranous region of the prostate cancer tumour cells, consistent with IHC reports in metastatic prostate cancer models where the cellular localisation of HER2 is described as cytoplasmic, membranous or a combination of both (287).

Furthermore, HIF1α demonstrates very low intensity staining at baseline in CWR22 tumours. The interest in studying the staining pattern of HIF1α in these tumours comes from the knowledge that HIF has an important role in tumour angiogenesis where this occurs not only in response to hypoxia but it is also induced by growth promoting stimuli, oncogenic pathways (such as EGFR and MAPK) and tumour suppressor mutations, most strikingly that involving VHL (288). Since PSMA is present in the neovasculature of tumours it is thought to be important in the regulation of angiogenesis. Therefore, it is reasonable to hypothesise that PSMA and HIF1α upregulation might occur simultaneously in these tumours especially after treatment with PI3K-mTOR inhibitor to regulate angiogenesis, possibly via mechanisms that modulate VEGF expression.

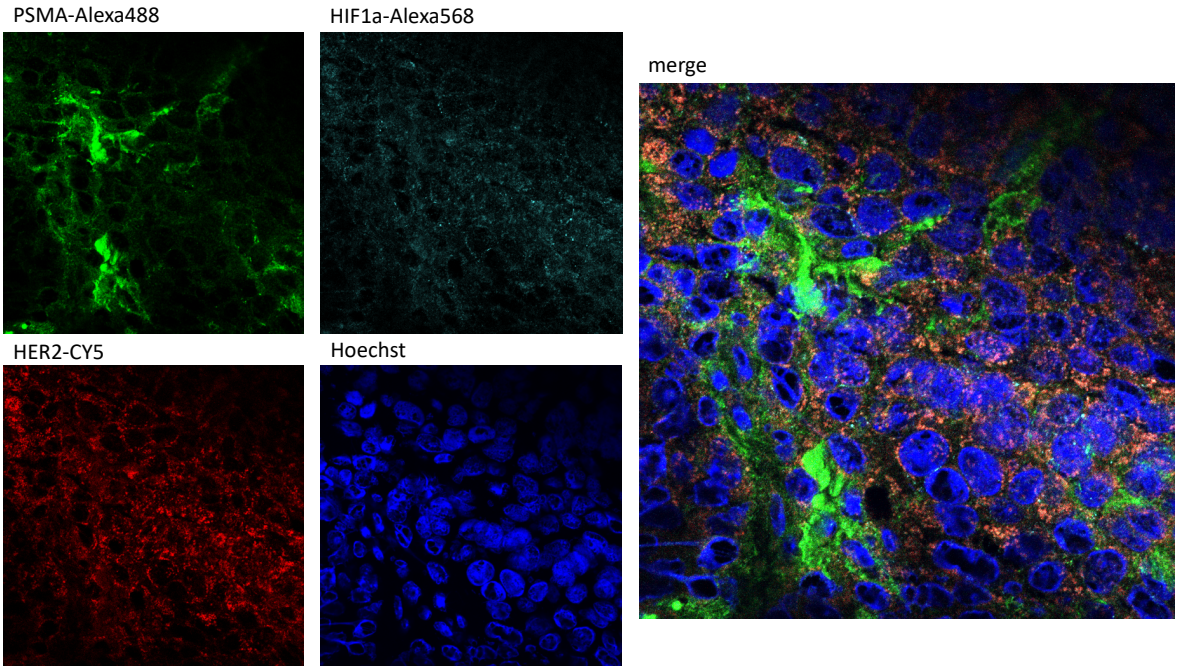

Figure 4.13 – Triple immunofluorescence staining of prostate cancer xenograft CWR22 tumours:

CWR22 frozen tumours at baseline prior to any treatment with DS7423 (Day 0) were stained with the indicated antibodies to study the cellular localisation of these markers in metastatic prostate cancer tumours. Tumours were imaged with x63 oil objective using confocal microscope.

When tumours from CWR22 mouse xenograft at treatment Day 8 (**Figure 4.14**) were examined the HER2 expression pattern remained the same, with an observed diffuse expression of this oncogene throughout the tumour tissue. It is also observed that there are areas of more intense staining suggesting that enhanced expression occurs within a heterogeneneous population of tumour cells. Similarly, the expression of PSMA remains heterogenous but more diffuse within the tumour and at some areas appears to be expressed around structures resembling vasculature. PSMA is known to be expressed in endothelial cells of tumour neovasculature, but not established vasculature. The expression of PSMA within endothelial cells of tumour neovasculature

demonstrated co-localisation with HIF1α expression as well, supporting the hypothesis that via the upregulation of PSMA, prostate cancer cells might be able to develop resistance to PI3K-mTOR inhibition by mechanisms that involve tumour angiogenesis as well. HIF1α expression in tumour endothelial cells plays as significant role in the migration of cancer cells and their metastatic potential (289).

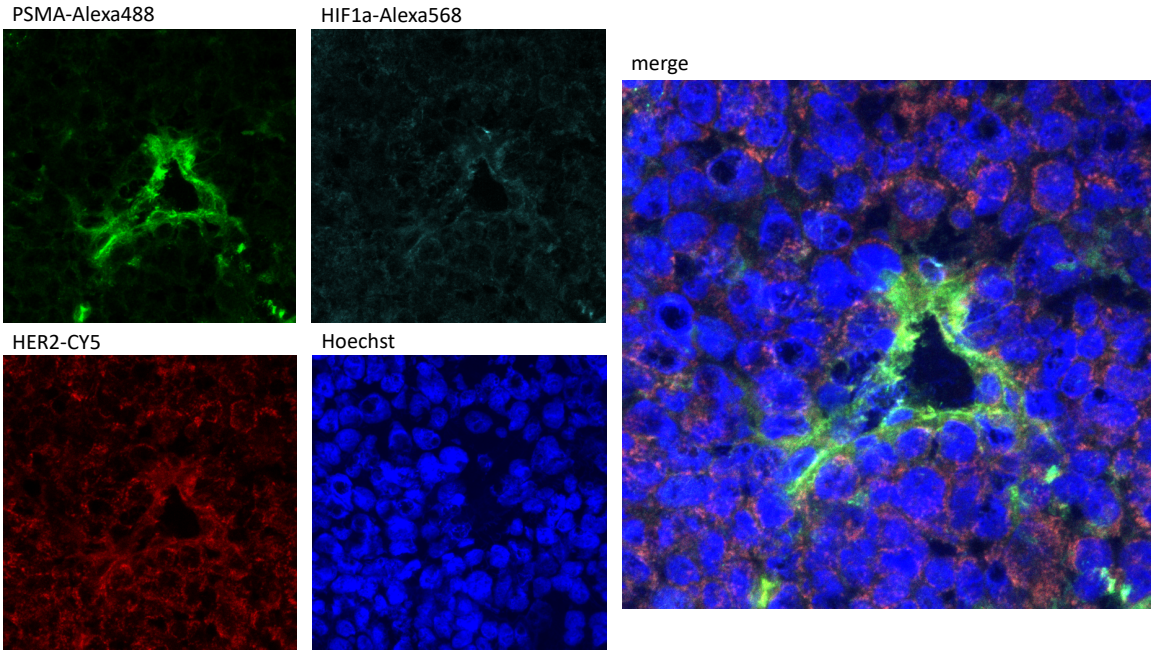

Figure 4.14 – Triple immunofluorescence staining of prostate cancer xenograft CWR22 tumours after DS7423 treatment:

CWR22 frozen xenograft tumours at D8 of treatment with DS7423 were imaged using confocal microscopy for the antibodies as indicated above. Tumours were imaged using x63 objective of the confocal microscope.

4.2.4 PSMA-PET in CWR22 and 22Rv1 mouse xenografts post PI3K-mTOR treatment

The mouse subcutaneous tumour xenograft study in CWR22 and 22Rv1 models described above was repeated to evaluate PSMA upregulation by PSMA-PET. As demonstrated in the schema below (**Figure 4.15**) after the establishment of subcutaneous tumours, mice were treated with DS7423 by daily oral gavage for 4 days and then imaged with ^{68}Ga-THP-PSMA by PET at day 5. Using tumour ex-vivo values we demonstrate the basal uptake in PSMA-expressing tumours prior to any treatment and show enhanced PSMA uptake in the tumours of mice after 4-day treatment with DS7423, which is consistent with the biochemical results we have presented so far (**Figure 4.16**). The ratios between treated-to-untreated values for PSMA uptake (presented as %ID/g) are 1.36 and 1.28 in the CWR22 and 22Rv1 models respectively. Unfortunately, we experienced death of mice during imaging when the mice were anaesthetised and the data presented here is only pilot data, as we were unable to complete this in equal numbers per group, proving that the detection of PSMA upregulation is possible by PSMA-PET. The experiment described in this section is going to be repeated for future presentation purposes and to obtain statistically significant data.

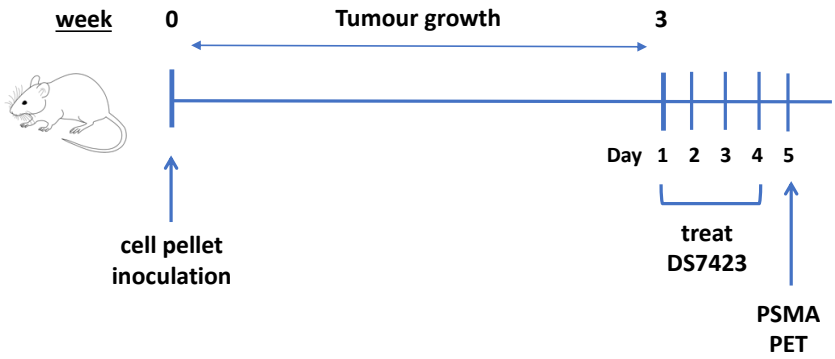

Figure 4.15 – Schematic representation of the mouse xenograft tumour growth and treatment schedule with DS7423 prior to PSMA-PET imaging.

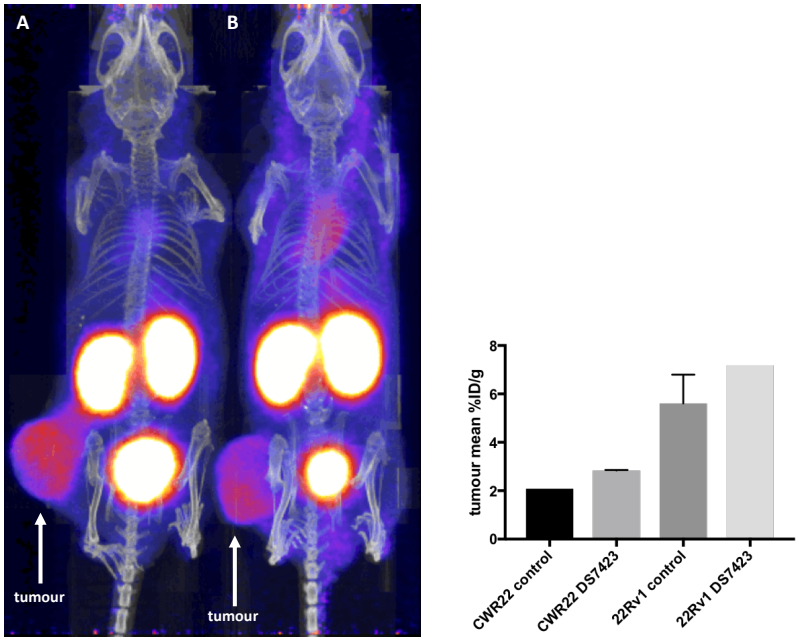

Figure 4.16 – Representative PET-CT images of mice bearing 22Rv1 xenografts at 40-60 mins after injection.

Left panel: A shows ^{68}Ga-THP-PSMA in mouse bearing tumour post treatment with DS7423 and B shows ^{68}Ga-THP-PSMA mouse bearing tumour without any treatment.

Right panel: The ex-vivo uptake of ^{68}Ga-THP-PSMA in CWR22 and 22Rv1 mice tumours (culled 1 hour after injection) pre- and post-treatment with DS7423.

4.3 Discussion

The rationale for the use of PI3K-mTOR inhibitors in the PTEN wild-type cell lines CWR22 and 22Rv1 comes from the knowledge that the AR can activate signalling pathways, including PI3K-AKT and MAPK, upon its activation by the binding of ligand. This occurs in the cytoplasm through non-nuclear signalling and is rapid in onset as compared to the classical AR signalling that requires AR conformational change and nuclear localisation (168).

These actions of non-genomic signalling of AR are able to enhance cell proliferation and survival by rapid signal transduction. In more detail, direct interactions between ligand-activated AR and PI3K in the cytoplasm are mediated by phosphotyrosine residues on the AR NTD to the SH2 domain of p85α regulatory subunit of PI3K. The associated of AR/p85α promotes the activation of p110 catalytic subunit and the generation of PIP3 to induce activation of AKT kinase, leading to the regulation of transcription factors to inhibit apoptosis pathways and promote cell survival. Therefore, it is clear that AR is able to maintain cell survival independently of transcription which is achieved through activation of the PI3K-AKT pathway (267).

As a result, it is not unexpected to observe clinical responses with inhibitors of the PI3K-AKT pathway in patients enrolled in clinical trials where stratification did not occur based on PTEN status, as seen in the Phase II study with GDC0068 in combination with abiraterone (170). Results from some of the

other Phase II clinical trials are also awaited to help make more observations of the clinical responses seen with PI3K-AKT inhibitors.

In this chapter, the work focused on describing the effects of PI3K-mTOR inhibition in the PTEN WT prostate cancer cell lines, CWR22 and 22Rv1. Both cell lines show expression of ErbB RTKs and ability to respond to stimulation by the respective ligands of EGFR and HER3. When the dual PI3K-mTOR inhibitor is used in this setting we observe upregulation of HER2 levels in both cell lines by 42% and 83% in CWR22 and 22Rv1 cells respectively. This increase in HER2 level expression coincides with upregulation of the transmembrane glycoprotein PSMA. In fact, PSMA upregulation in this setting is shown to be dependent on HER2 levels. In addition, the effect on PSMA appears to be independent of HER3, the levels of which do not show a similar trend potentially suggesting that the absence or disruption of HER2-HER3 dimer enables PSMA upregulation through mechanisms that require HER2 alone. The identification of HER2 translocation from the cytoplasm to the nucleus in the CWR22 cells (hormone-sensitive setting), but not in the 22Rv1 cells, is also an important finding further suggesting that the HER2-HER3 heterodimer is not important in the PTEN WT hormone-sensitive setting, and that the nuclear localization of HER2 has an important role in driving resistance, by mechanisms that we have not identified in this work. The membrane localisation of both HER2 and HER3 in the 22Rv1 castrate-resistant cells further supports that HER2 upregulation in this setting acts via different

mechanisms to drive resistance and that the stabilization of HER2-HER3 dimer might have a more important role here.

As already described in previous sections of this work, HER2 is a membrane receptor whose overexpression in prostate cancer has been described and is associated with aggressive phenotype and disease progression. Insights into further understanding of the HER2 biology has demonstrated that HER2 can migrate from the cell membrane to the nucleus where it acts as a transcription factor. Specifically, HER2 in the nucleus of cultured cells forms a complex with cyclooxygenase enzyme COX-2 gene promoter and is able to stimulate its transcription (290). In another study, HER2 nuclear translocation was shown to form a transcriptional complex with Stat3 and to function as a coactivator of Stat3 to enhance breast cancer cell proliferation (291). Furthermore, the nuclear translocation of HER2 in trastuzumab resistant breast cancer cells can assembly in a transcriptional complex to include HER3 and Stat3 to encourage further cell growth (292). Finally, nuclear HER2 in clinical patient TMA samples with invasive breast cancer was demonstrated to be an independent adverse prognostic factor of poor clinical outcome in HER2 positive disease (293). The observed HER2 nuclear translocation seen here upon PI3K-mTOR inhibition in metastatic prostate cancer might suggest that this RTK is able to promote resistance by acting as a transcription regulator of genes responsible for cell proliferation and might potentially also associate with AR in the cell nucleus.

The detection of concurrent HER2 and PSMA upregulation in the PTEN WT setting upon PI3K-mTOR inhibition is also intriguing. There are no reports in the literature showing an association between HER2 and PSMA to date in metastatic prostate cancer. Certainly, HER2 overexpression in prostate cancer is associated with androgen-independent growth and clinical progression of the disease (124). The same applies to PSMA, with numerous reports showing that its expression is present is all stages of the disease and that this increases as the disease progresses to the castrate-refractory phenotype (191, 294). Our results also indicate that HER2 overexpression is necessary to increase PSMA-mediated signaling through the PI3K-AKT pathway independently of HER3. It is therefore acceptable to postulate that HER2 works cooperatively with PSMA and that their communication might lead to the formation of a more complex receptor complex in association with HER3, but also without, to promote activation of common downstream signalling pathways, such as the PI3K pathway, contributing to resistance to targeted inhibition. Along these lines, it has recently been shown that the cell membrane clustering of PSMA in LNCaP cells and subsequent PSMA activity needed to stimulate the PI3K and MAPK pathways was dependent on the assembly of a macromolecular complex including filamin A, beta1 integrin, p130CAS, c-SRC and EGFR (295). Another explanation could be that the heterodimerisation pattern between HER2 and HER3 and its changes upon treatment might be a mechanism by which PSMA levels and activity are regulated on the cell surface membrane in prostate cancer cells.

The data also demonstrates that the mechanisms of resistance to PI3K-mTOR inhibition in the PTEN WT metastatic prostate cancer setting do not involve the AR, as observed in the PTEN MT cell line, suggesting that the PTEN status of the cells has the ability to dictate the emergence of resistance pathways in metastatic prostate cancer cells upon PI3K-AKT-mTORtor inhibition and that further targeted therapies could be guided based on this knowledge and the ability to detect resistance pathway emergence robustly within clinical samples.

Furthermore, we show that the observed PSMA upregulation upon PI3K-AKT-mTOR inhibition is able to sustain and enhance pAKT (T308) despite targeting of the PI3K pathway, suggesting that the enzymatic activity of the upregulated PSMA protein is able to activate the PI3K-AKT pathway as a resistance mechanism. It has recently been shown that PSMA can induce activation of the PI3K-AKT signalling axis by acting enzymatically to release glutamate and activate the mGLUR1 receptor (195). Some preliminary experiments done by myself at the completion of this work support this as transient knockdown of the mGLUR1 receptor with siRNA interference demonstrate deficiency of PSMA upregulation with DS7423 treatment that coincides with absence of HER2 level upregulation. Furthermore, hyperactivation of AKT can also result due to deregulated signalling of cell surface receptors (296), therefore the amplification of HER2 following PI3K-AKT-mTOR treatment is also partly responsible for the enhanced AKT phosphorylation seen in these cells. In any case, both constitutive and inducible AKT activation has been associated with resistance to chemotherapeutic and targeted agents (297). Through the results

of this work we have identified PSMA and HER2 as being responsible in driving PI3K-AKT pathway re-activation and that these proteins can be utilised both therapeutically and as predictive biomarkers along the treatment course to enhance outcomes of PI3K-AKT-mTOR pathway inhibitors and to better stratify patients to further treatments or treatment combinations. In addition to downstream targets of the PI3K pathway and PSMA as described in this work so far, it would also be interesting to evaluate the role Ki67 as a proliferation marker that might reflect HER2-HER3 heterodimerisation. This could serve as a biological predictive biomarker of response and resistance to targeted inhibition and might enable better patient subgroup classification.

The dual inhibition using DS7423 and lapatinib stabilises HER2 levels in cells, an effect that has been shown with lapatinib monotherapy and combined therapy in breast cancer cells before (273). However, this demonstrates a negative effect on PSMA levels and lapatinib addition to DS7423 is therefore able to partially abrogate the upregulation of PSMA to levels that are still more elevated than cells without any treatment. The observed HER2 stabilisation upon the addition of lapatinib has been shown to be due to prevention of ubiquitination of the receptor which leads to the accumulation of inactive receptors on the cell membrane (273). This can explain the partial abrogation of PSMA levels in both these cell lines. Furthermore, when we inhibit HER3 ligand with the addition of patritumab to DS7423, we observe a return of PSMA levels to those below baseline in the CWR22 cell line, an effect seen to coincide with decrease in HER2 and HER3 expression. In the castrate-resistant cell line

22Rv1, HER2 levels are sustained with patritumab leading to further increase in PSMA, suggesting that possibly in castration-resistance additional mechanisms are recruited that are able to allow the cells to continue to proliferate and express these oncogenic proteins.

All the results from the *in vitro* work taken together suggest that in the metastatic androgen-sensitive PTEN WT CWR22 cells PSMA upregulation upon inhibition of the PI3K-mTOR pathway, is dependent on HER2 but not so much on HER3. When HER2 phosphorylation is blocked by lapatinib or when patritumab inhibits NRG-1 ligand binding to HER3, then HER2 activation via phosphorylation or heterodimerisation is impaired and this subsequently abrogates the upregulation of PSMA. While this is also the case with the combined use of DS7423 and lapatinib in the metastatic castrate-refractory PTEN WT 22Rv1 cell line, the use of patritumab is not sufficient to suppress HER2 levels and PSMA remains upregulated. One explanation for this might be the preferential formation of EGFR-HER2 heterodimers instead that can continue to signal as potent oncogenic units. As already proposed by Yarden et al, HER2 acts as a preferred heterodimeric partner for all ErbB receptors and its overexpression can bias heterodimer formation and broaden ligand specificity (298). In addition, it is known that the 22Rv1 cell line is highly responsive to stimulation by EGF (280), which might be another reason why these cells upon patritumab treatment might be able to enhance their ability to enable EGFR-HER2 heterodimerisation instead.

Therefore, pharmacological targeting of HER2 either in combination with PI3K-AKT-mTOR pathway inhibitors or at detection of resistance could provide more potent control over the signalling pathways involved in prostate cancer cell proliferation and growth. In addition, these findings confirm that HER2 upregulation and its heterodimerisation status can be very useful biomarkers in the metastatic hormone sensitive and castration-resistant settings and that assays that can detect its heterodimerisation patterns could be assessed within relevant clinical trials to evaluate their utility as predictive biomarkers for more optimal treatment stratification. Furthermore, the use of PSMA targeted therapeutic agents is also rapidly advancing and is considered a milestone in the management of this disease. Specifically, ^{177}Lu-labelled PSMA radiopeptidomimetic therapy (299, 300) has been tested within small clinical trials with promising results. In addition, PSMA-targeting BiTE (bispecific T cell engager) immunotherapies (301, 302) and PSMA-directed CAR-T cell therapies (303) are currently being evaluated within Phase I clinical trials and the results of these will be awaited in the years to come. Based on the findings from this work, the combined and/or sequential use of PI3K-AKT-mTOR pathway inhibitors with PSMA-targeted therapies can be timed at the time of upregulation of PSMA expression and might provide more robust responses to the therapies and enhance clinical outcomes.

In vivo use of DS7423 in prostate cancer CWR22 and 22Rv1 mouse xenografts demonstrates similar upregulation of PSMA within frozen tumour lysates, which is heterogeneously expressed in tumours when these are stained for

immunofluorescence microscopy. We also demonstrate within a small cohort of mice that PSMA upregulation can be detected successfully pre- and post-treatment using PSMA-PET. In contrary, HER2 is expressed more homogeneously in tumours of these xenografts. We also demonstrate that the PSMA upregulation in prostate cancer tumours derived from our *in vivo* study occurs in conjunction with enhanced expression of HIF1α and that these proteins show co-localisation and are seen around vascular structures in the tumour tissue. PSMA is known to be expressed on the apical surface of endothelial cells (179, 304) and in the neovasculature of numerous solid malignancies (182). It is also weakly expressed in normal prostate tissue but strongly upregulated in prostate cancer (304). In prostate cancer, there are various patterns of PSMA expression described by IHC studies including apical, apical/cytoplasmic, cytoplasmic with membranous accentuation and cytoplasmic only. The first 3 patterns have been shown to be very specific for prostate cancer (305). In general, PSMA is highly specific (94.5%) and fairly sensitive (65.9%) for the diagnosis of prostate cancer (305). When expressed in prostate cancer though, it is associated with higher grade and development of castration resistance suggesting that it has a functional role in disease progression, despite the fact that the mechanism for this has not described yet (306, 307). Within prostate cancer tumours, the localisation of PSMA has been described in the glandular epithelium, cytoplasm and membrane (267). PSMA, therefore, has an important role in metastatic prostate cancer upon inhibition of the PI3K-mTOR pathway to promote resistance mechanisms via prostate cancer cell proliferation and angiogenesis.

In conclusion, the results of this work encourage the belief, as shown by others, that PSMA has an important functional role in activating cell signalling pathways involved in prostate cancer cell proliferation and angiogenesis and that it is not solely an important biomarker to utilise for the detection of disease through the use of radiolabelled agents that conjugate with PSMA. In addition, it is preferentially upregulated in PTEN functional (WT) prostate cancer cell lines that are treated pharmacologically with inhibitors of the PI3K-AKT-mTOR pathway, an effect not seen in the PTEN null setting, thus demonstrating that the understanding and detection of the relevant resistant mechanisms will allow correct stratification of patients in the future to PSMA-targeted therapies that are currently in clinical development.

Chapter 5: The development of exosome based biomarkers to monitor disease evolution in prostate cancer

5.1 Introduction

As discussed previously, exosomes are a heterogeneous class of extracellular vesicles released by exocytosis by virtually all cells types in the body. Unlike larger types of extracellular vesicles such as apoptotic bodies or microvesicles, exosomes are nano-scaled (40-150 nm) and are released in physiological and pathological conditions. Exosomes play critical roles in intercellular communication and can be found in the circulation. They can be directly released in biological fluids where their cargo is stable and protected from enzymatic degradation thanks to their lipid membrane envelope. Because their molecular content reflects the composition of the cell of origin, they have recently emerged as a promising source of biomarkers in cancer (308). Direct enumeration of tumour-derived exosomes and/or profiling of their molecular cargo in patient body fluids has been shown to provide valuable information about the biology of the tumour (309). While exosomal profiling offers significant advantages because of the complex cargo they contain (proteins, lipids, nucleic acids) which could be interrogated simultaneously, discriminating cancer-derived exosomes from non-cancer ones is still a very challenging area.

Exosomes in prostate cancer have been shown to support tumourigenesis by promoting angiogenesis (310) and those secreted within the tumour microenvironment are important regulators of prostate cancer cell survival, proliferation, angiogenesis and the evasion of immune surveillance (310-312). Protein profiling in plasma, serum and other biological fluids is limited by an intrinsic high dynamic range and by the fact that most biomarkers are at least five orders of magnitude lower than albumin and other abundant serum proteins, making it challenging to characterise exosomal protein cargo in prostate cancer directly from patient body fluids. Many preliminary studies, therefore, have been conducted in prostate cancer cell line-derived exosomes (308).

5.2 The use of FRET-FLIM in prostate cancer exosomes

The use of fluorescence lifetime imaging microscopy for the analysis of protein expression, function and protein-protein complex formation in cancer cell lines, fresh tumour tissue and FFPE tissue is now well established in our laboratory (228, 313-317). These advanced imaging techniques have now been adapted for blood-derived exosomes, as a novel and minimally invasive means of monitoring the onset of tumour resistance using liquid biopsies from patients. Detection of specific protein-protein interactions in patients' biopsies can be used for prognostic and predictive information and to monitor response and resistance to treatment at a molecular level in order to allow better patient selection for targeted therapy (206). More recently, in our laboratory we have optimised assays for the use of antibodies for FLIM against EGFR and HER3.

Our data demonstrated that exosomal EGFR-HER3 dimer can change within 3 weeks in head and neck cancer patients commencing anti-ErbB therapy in combination with chemotherapy and that these changes in EGFR-HER3 dimerisation can predict RECIST in a multivariate analysis of a prospective Phase 2 clinical trial (318).

As part of our hypothesis and results already presented, we sought to study HER3 heterodimerisation as a 'rewiring' mechanism in metastatic prostate cancer upon treatment pressure using PI3K-mTOR inhibition, as a resistance mechanism that could be detected within exosomes. In order to assess the role of HER3 heterodimerisation within prostate cancer patient serum-derived exosomes prospectively, one needs to do this within a clinical trial where the longitudinal blood sampling occurs at pre-determined timepoints to match whole-body imaging modalities, such as CT, MRI and PET, that are used as a tool to provide information of clinical disease burden and outcome.

5.3 Exosomal miR-21 in prostate cancer:

MicroRNAs are small non-coding RNAs that have been identified as post-transcriptional regulators of gene expression (319) and evidence has shown that they can have significant role in biological processes (320). Their deregulation has been observed in cancer where they can function both as tumour suppressors or oncogenes (321). Studies have shown their participation in the resistance to chemotherapeutic agents in cancer cells (322, 323). Furthermore, the presence of nucleic acids in exosomes allows them to be

protected from degradation making the study of genomic alterations, aberrant transcripts and non-coding RNAs in exosomes very interesting.

In preclinical studies using prostate cancer models, elevated levels of miR-21 were able to enhance growth in androgen-sensitive prostate cancer cells and to promote resistance to castration-mediated growth arrest, suggesting that this microRNA has a role in prostate cancer pathogenesis and treatment resistance (324). In another study, miR-21 expression was associated with resistance to docetaxel chemotherapy in PC3 prostate cancer cells (325). Finally, the role of miR-21 in mediating pro-metastatic inflammatory responses leading to cancer cell growth and metastasis has also been described (326).

In the following section I will describe the work that has been carried out to evaluate the changes in cell-line derived exosomes in response to treatment with DS7434 and also the work done to translate our preclinical FRET-FLIM assay for EGFR-HER3 heterodimerisation, to measure endogenous protein-protein interactions in archived patient serum-derived exosomes. We hypothesised that combining whole-body multi-parametric MRI information with circulating exosomal EGFR-HER3 dimer and microRNA information we would be able to create a multivariate statistical model that will predict the likelihood of occurrence of metastases in prostate cancer patients who present with biochemical relapse following previous localised therapy for prostate cancer (within the LOCATE clinical trial) (327). Examining circulating tumour-derived exosomes for the aforementioned EGFR-HER3 activated dimer, has the

potential to help us understand prostate cancer cell progression and treatment resistance through the time-dependent, treatment responsive evolution of its protein network. (More details on the LOCATE trial can be found in the protocol provided in **Appendix 1**).

5.4 Results

5.4.1 The extraction, purification and characterisation of prostate cancer exosomes

Exosomes from prostate cancer cell lines were extracted using differential ultracentrifugation which is one of the gold standard techniques for the enrichment of exosome populations. Other techniques such as using exosome precipitation kits offer some advantages when it comes to exosomal yield. However, for our intention of conducting exosomal imaging, ultracentrifugation is the only method that preserves the exosome membrane protein interactions in a way that allows us to study receptor dimerization. To validate the purified exosomal fractions obtained, I performed nanoparticle tracking analysis (NTA) using a state-of-the-art Nanosight LM14 equipment. NTA allowed us to confirm the successful extraction of exosomes from prostate cancer cell line culture supernatant based on their size distribution. Characterisation of the concentration of exosomes present in each preparation was also provided by NTA. **Figure 5.1(a)** shows NTA graphs of CWR22 cell line exosomes extracted from cells cultured in exosome-free RPMI media only or exosome-free RPMI

media that was supplemented with DS7423 at 1000 nM for 48 hours. Under both conditions, NTA detects particles with modal diameter around 140 nm, consistent with reports in the literature that describes the size of exosomes to lie within the 40-150 nm range. The absence of other peaks at higher particle diameter confirms that the extraction has purified exosomes and does not contain other extracellular vesicles such as microvesicles (200-1000 nm) or apoptotic bodies (600-2000 nm) which would contaminate further analyses.

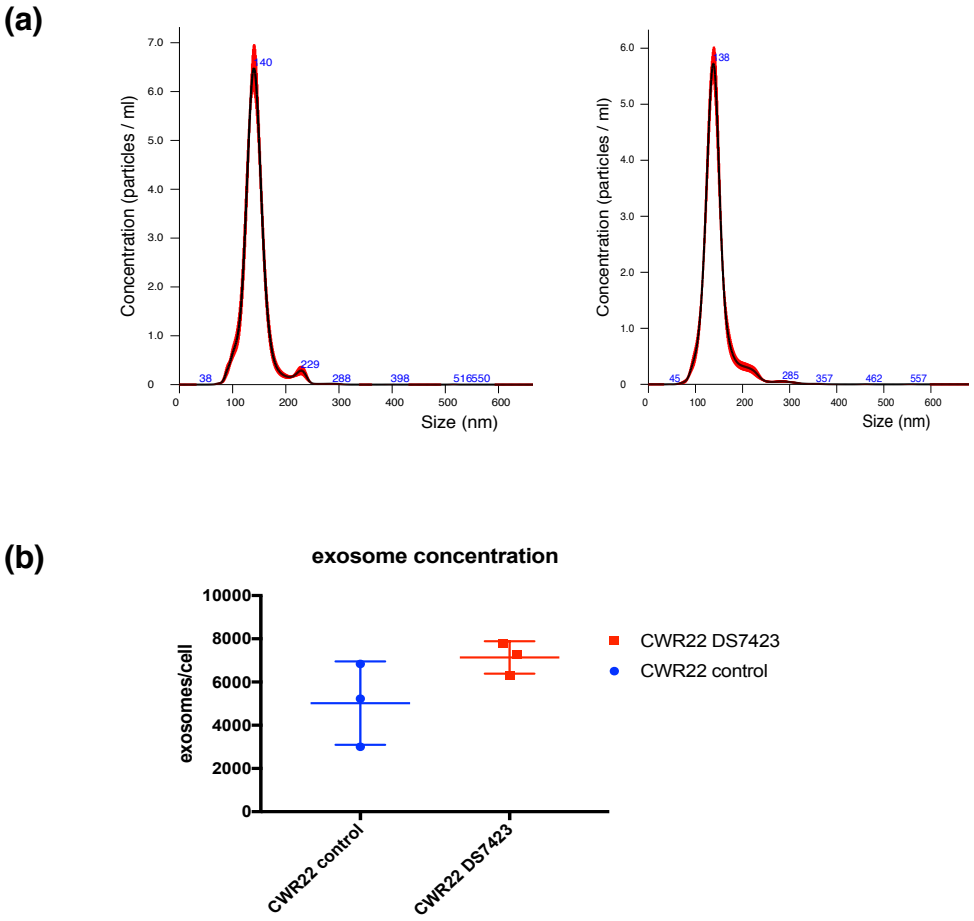

Figure 5.1 – CWR22 cells release exosomes both under control and treatment conditions with DS7423:

(a) Nanoparticle tracking analysis (NTA) showing the size distribution of exosomes isolated from CWR22 cell culture supernatants under control (left) and treatment conditions with DS7423 for 48 hours (right). Each trace is representative of NTA performed on individual samples and is a summary of five tracks of 30 seconds done for each preparation.

(b) The ratio of exosome concentration per cell shows a higher number of particles extracted under conditions of treatment with DS7423.

NTA utilises the properties of both light scattering and Brownian motion in order to obtain particle size distribution of samples in a liquid suspension. A laser beam passes through the sample chamber and the particles in suspension and visualised through a perpendicularly placed x20 magnification microscope onto which is mounted a video camera. The camera captures a video file of the

particles moving under Brownian motion. The NTA software tracks many particles individually and using the Stoked Einstein equation it calculates their hydrodynamic diameters.

Further evaluation of the exosomal preparation obtained from three independent exosome extraction experiments performed under both treatment conditions in the CWR22 cells demonstrated that the exosome particle concentration per cell was higher when the cells were treated with DS7423 (**Figure 5.1(b)**). The significance of this is does not necessarily have to do with exosome enumeration pre- and post- treatment but mainly on the constitution of their cargo. One hypothesis might be that the exosomes secreted from prostate cancer cells after exposure to PI3K-mTOR inhibition might be more pro-tumourigenic by enabling sustained proliferative signalling via the mechanisms that have been described in the *in vitro* experiments performed as part of this project.

Based on available resources in the literature I modified the protocol for exosome extraction and purification from cell culture supernatant so that exosome extraction would be achieved from patient-derived serum and plasma. This was done in order for us to be able to utilise these protocols within retrospective and prospective clinical trials where patient blood samples are available. Biomarkers identified within patient-derived exosomes could serve as valuable liquid biopsies in these settings.

Control individual and prostate cancer patient serum available to us via the SUN study protocol (through an MTA between King's College and University of Surrey; see details in appendix) was used for exosome extraction and purification using the protocol described in the methods chapter of this thesis. I used 1ml of serum from each serum sample to demonstrate that exosomes can be extracted from this volume and that the particle numbers in prostate cancer patients are higher than those in healthy individuals (mean exosome particle number in prostate cancer patients = $3.443x10^8$/ml vs from healthy individuals = $1.379x10^8$/ml) (**Figure 5.2**), again suggesting that exosomes transfer proteins and RNA that represent the burden of disease and that these can be detected when the appropriate assay is used.

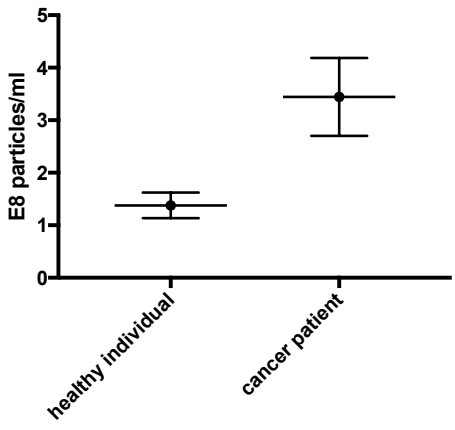

Figure 5.2 – Exosome extraction from serum of healthy individuals and prostate cancer patients:

Data represent mean and individual exosome particle concentration derived from 1ml of serum of healthy individuals and prostate cancer patients and error bars represent +/- SEM, n=3.

5.4.2 The extraction and purification of exosomal RNA

Further downstream applications of exosomal samples from both cell line culture supernatant and patient serum would involve the evaluation of exosomal RNA cargo. Based on available literature I opted to extract cell line-derived exosomal RNA using the combined phenol (Trizol) and column based approach, using an adapted protocol described in the methodology section. This was done due to our main interest to optimise methodology for the extraction and purification of patient-derived exosomal RNA for further microRNA analysis and the combined phenol and column technique was shown to be superior in extracting small RNA compared to other kits (328).

Cellular and exosomal RNA was extracted from the same preparation of cells prior to exosome extraction, therefore the data presented here matches exactly the cellular origin of the exosomal RNA. Cellular RNA concentration (µg/µL) extracted pre- and post-DS7423 treatment in LNCaP NTC cells shows decrease in RNA concentration per cell. However, from the same cellular preparations, the exosomal RNA that was extracted using the same kit demonstrates a consistent increase in RNA concentration per cell (pg/µL) (**Figure 5.3**). Information available in the literature suggests that exosomes released from cancer cells after exposure to cytotoxic and targeted therapies are able to mediate specific cell-to-cell interactions and activate signalling pathways in cells. Exosomal RNAs are heterogeneous in size but enriched in small RNAs such as microRNAs. In the primary tumour microenvironment cancer-secreted exosomes and microRNAs can be internalised by other cells

at the local vicinity or by transfer within the systemic circulation. MicroRNAs loaded within these exosomes might be transferred to recipient cells to exert genome-wide regulation of gene expression. The way that exosomal microRNAs contribute to the development of drug resistance has not been fully described however (215).

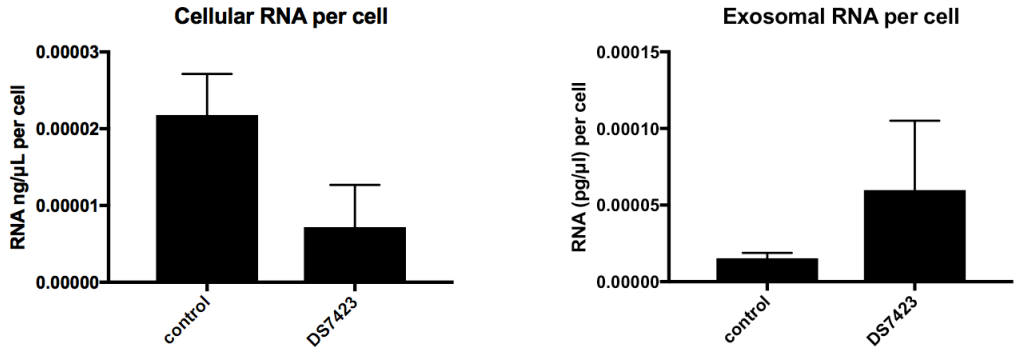

Figure 5.3 – Cellular and exosomal RNA per cell extracted from LNCaP NTC cells pre- and post-DS7423 treatment:

Left panel shows cellular RNA concentration (ng/µL) and right panel exosomal RNA concentration (pg/µL) per cell. Values represent mean+/-SEM, n=3.

Further information obtained from a high sensitivity Agilent bioanalyser demonstrate that the exosomal RNA isolation method under both control and treatment conditions enabled the extraction of RNA with a broad size distribution that also included RNA in the range of microRNAs as seen by the early peaks in the electropherograms (**Figure 5.4)**.

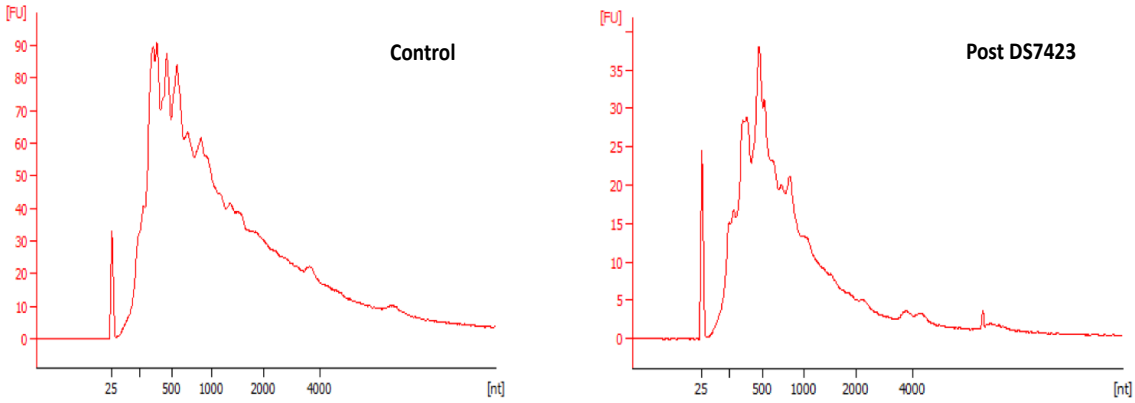

Figure 5.4 – Bioanalyser analysis of total RNA samples from LNCaP NTC cell line exosomes pre and post treatment with DS7423:
Representative electropherograms showing the size distribution in nucleotides (nt) and fluorescence intensity (FU) of total exosomal RNA in control (left panel) and treatment (right panel) samples. The peak at 25 nt is an internal standard and the 18S and 28S ribosomal peaks are absent as expected for exosome preparations.

Samples from the LOCATE clinical trial cohort were then used for the extraction and purification of serum-derived exosomes from a group of 10 patients, identified by the research team but their clinical information was blinded to myself at the time of the experiments. The table below shows information about total particle count, protein and RNA concentration of exosomes extracted from 3mls of patient serum and the variability in total protein and RNA concentration observed within this cohort from equal volume of starting material (**Table 5.1**).

LOCATE Patient ID	Total Nanosight count (particles/ml)	Total Protein concentration (µg/ml)	Total RNA Concentration (pg/µl)
001	7.54×10^{10}	214.1	3,385
002	7.81×10^{10}	391.1	430
003	5.68×10^{10}	273.5	972
004	5×10^{10}	374.3	615
005	5.14×10^{10}	290.8	1,500
006	3.92×10^{10}	350.9	1,865
007	1.22×10^{11}	777.3	4,580
008	8.08×10^{10}	400.1	305
012	1.07×10^{12}	952.8	2,010
015	3.2×10^{11}	835.9	10,475

Table 5.1 – LOCATE patient serum-derived exosomes were evaluated by NTA, protein concentration and RNA concentration prior to further downstream applications.
3mls of serum led to the extraction of exosomes that were suspended in 200µL of PBS. Total amount of protein and RNA in 200µL total volume available can be calculated from the above concentrations.

We then sought to determine whether microRNAs could be detected within a cohort of prostate cancer patients recruited in the LOCATE trial due to detection of biochemical relapse of previously treated prostate cancer. Specifically, we decided to design assays for the detection of miR-21 within this cohort of prostate cancer patients. miR-21 was identified as a microRNA target that was interesting because of its previously identified oncogenic activity in other cancers.

Using miR-21 taqman probes in exosomal RNA samples extracted from this cohort of 10 prostate cancer patients, digital-droplet PCR analysis was done as an initial pilot experiment to establish whether we would be able to detect this microRNA in exosomal RNA derived from clinical samples. Indeed, as we show below we were able to detect miR-21 in 3 of these 10 patients (**Figure 5.5**).

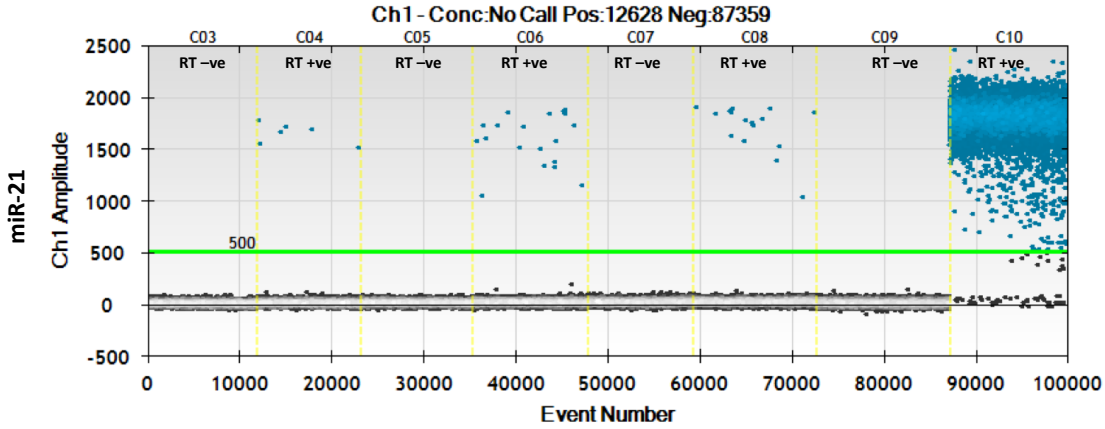

Figure 5.5 – Fluorescence amplitude plotted for the 3 positive RNA samples:
The unbroken green line represents the threshold, above which are positive droplets (blue) with PCR amplification and below which are negative droplets (gray) without any amplification. For each exosomal RNA sample RT -ve and RT +ve samples are shown (C04-C08) and compared to positive control cellular RNA sample from H1975 lung cancer cell lines (C09-C10).

To conduct further analysis as part of these pilot experiments to characterise patient-derived exosomal samples, we tested our in-house built FRET-FLIM technology that has been optimised for use in exosomes. The ability to detect ErbB heterodimerisation in patient-derived exosomes coupled with exosomal microRNA information in combination with clinical data and multiparametric MRI imaging (done within LOCATE) will allow us to create a multivariate

statistical model to predict the occurrence of metastases and future treatment resistance in prostate cancer patients presenting with biochemical relapse.

Optimised assays for the detection of EGFR-HER3 dimer in exosome samples by FRET-FLIM were applied in patient-derived serum exosomes in suspension in PBS to evaluate whether there was detectable FRET efficiency within this cohort of patients, the variability of lifetime range and FRET efficiency and whether these values correlated with any of the available clinical data that was blinded to us at the time of this pilot study. FRET efficiency was evaluated in 6 out of 10 patients. Four patients were not evaluable due to very high auto-fluorescence in the images that did not allow us to measure FRET efficiency reliably. We saw a range of FRET efficiencies from 0.01-10.2% suggesting that EGFR-HER3 heterodimerisation can be detected within the exosomes of patients with prostate cancer and new biochemical relapse (**Figure 5.6**).

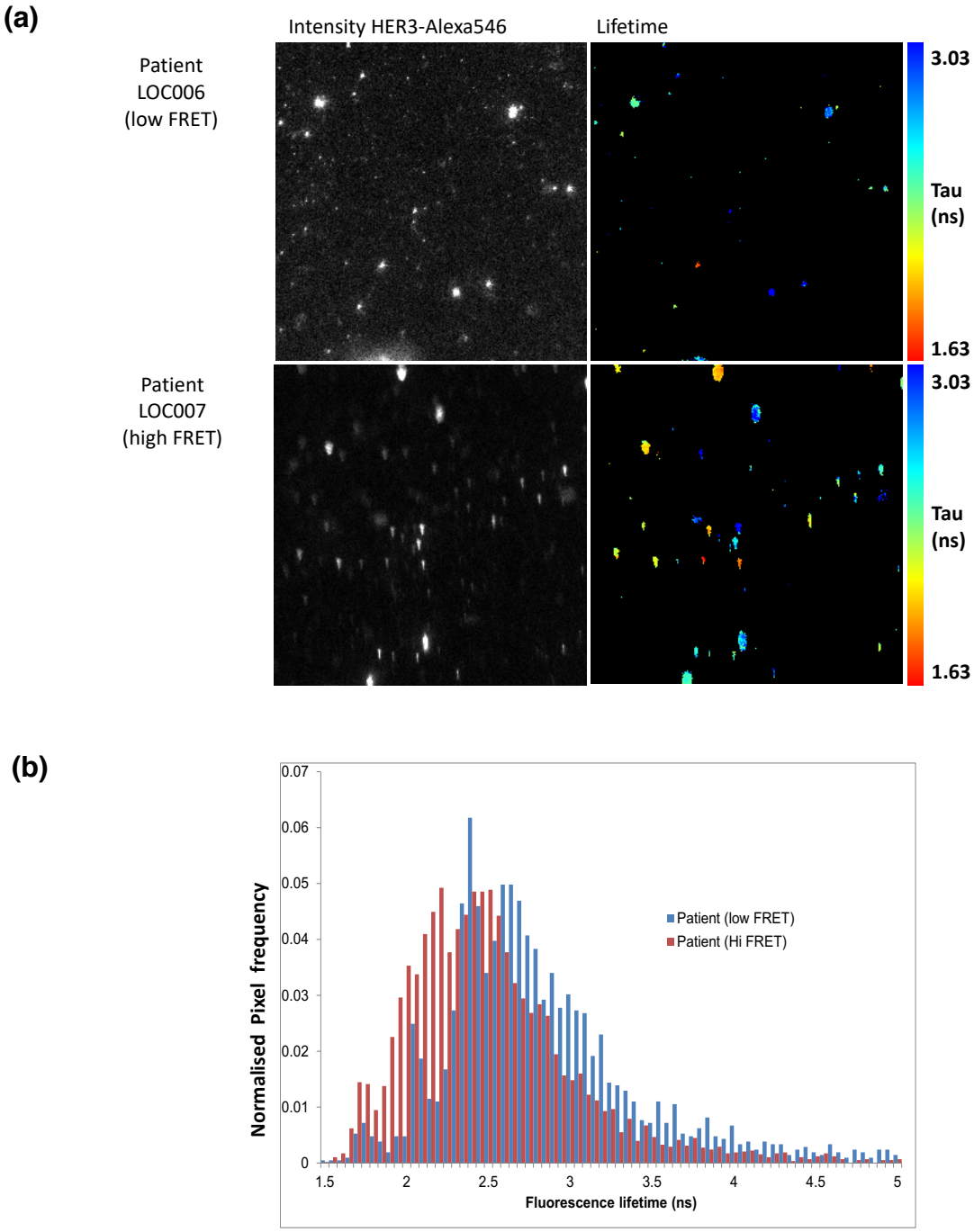

Figure 5.6 – EGFR-HER3 heterodimerisation by FLIM in patient-derived exosomes:

(a) Fluorescence lifetime from exosome samples was determined using global lifetime analysis with tri-exponential filter. The images are representative of the lifetime in two patients demonstrating high and low FRET efficiency values that was calculated using the equation FRET=1-(τDA/τD). The pseudocolour lifetime image is a visual representation of the decrease in lifetime (ns) in patient LOC007 when compared to LOC006.

(b) the histograms depict the fluorescence lifetime (ns) distribution normalised per pixel frequency in the 2 patients as in **(a)** showing the shift to lower lifetimes predominantly per normalised pixel frequency in each all samples analysed from each patient.

Figure 5.7 shows that when radiological findings were un-blinded to us the low FRET efficiency percentage values (<1%) were associated with the absence of detectable disease by CT and MRI imaging. Higher FRET efficiency percentage values were detected in patients whose radiological examinations show evidence of lymph node and metastatic disease at the time of biochemical relapse. In other words, the presence of EGFR-HER3 heterodimerisation in patient serum-derived exosomes shows correlation with the detection of disease relapse in prostate cancer and warrants further evaluation within a bigger cohort to determine whether this could serve as a valuable biomarker when assessing patients clinically.

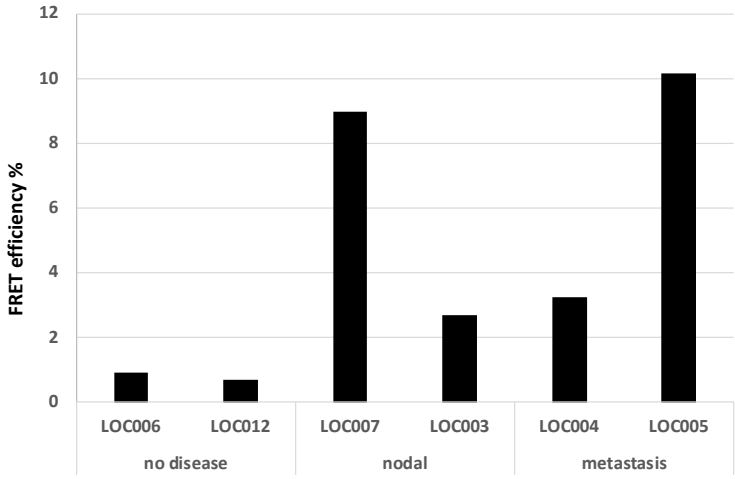

Figure 5.7 – FRET efficiency % values in 6 prostate cancer patients presenting with biochemical relapse in LOCATE trial: EGFR-HER3 dimer heterogeneity correlates with volume of disease.

In addition, **table 5.2** shows FRET efficiency percentage and its relevance with PSA value and radiological findings. The data, despite done in a small cohort of patients, suggests that percentage FRET efficiency in patient serum-derived

exosomes could have important prognostic and predictive biomarker value, both in the prediction of diagnosis of relapsed and/or metastatic disease as well as potential predictive information with regards to treatment response and resistance. The FRET-FLIM assay in exosomes therefore, needs to be evaluated in the full LOCATE patient cohort to be able to obtain statistically robust results about the value of EGFR-HER3 dimerisation as a predictive biomarker in this cohort of patients. Furthermore, we would like to correlate the FRET efficiency percentage value at the 1-year follow-up timepoint, and assess its correlation with the clinical responses in the patients that have started androgen-deprivation therapy due to newly diagnosed metastatic disease, to see whether it is predictive of resistance. Finally, in the very small proportion of LOCATE patients where tumour or metastatic tissue was obtained at the time of recruitment to the trial, the correlation of FRET efficiency between exosomal and tumour samples would be interesting to study.

LOCATE patient ID	Average FRET efficiency (%)	PSA value (ng/ml)	Clinical outcome/Staging
LOC003	2.7	3.7	N1M0
LOC004	3.2	6.09	N1M1
LOC005	10.2	3.68	N1M1*
LOC006	0.9	1.24	N0M0
LOC007	8.9	4.5	N1M0
LOC012	0.7	2.83	N0M0

Table 5.2 – LOCATE patient FRET efficiency, PSA values and radiological staging.

5.5 Discussion

Here we show that treatment of prostate cancer cells *in vitro* with DS7423 leads to increase in the numbers of exosomes per cell, suggesting that these nanoparticles might have the ability to transfer information as part of their cargo to encourage other cells to acquire proteins and RNA that will enable resistance to treatment and cell aggressiveness. Exosome enumeration done by Kharaziha et al, provided evidence that exosomal numbers reported by nanoparticle tracking analysis was enhanced in DU145 cells that acquired resistance to docetaxel when compared to docetaxel sensitive parental DU145 cells. Additionally, docetaxel-resistant DU145 exosomes were enriched with specific proteins that could serve as predictive biomarkers of treatment response and drug resistance within further studies in the future (329). It might well be the case that elevated PSMA protein level expression, that has been detected by our *in vitro* work as a response to treatment using PI3K-mTOR inhibition in a subgroup of prostate cancer cells, might be packaged within exosomes as part of their cargo, transferred to other cells in the vicinity and encourage resistance to targeted therapies. Liu et al, have demonstrated that PSMA at the protein level is enriched in exosomes and that the exosomal PSMA is able to retain its functional enzymatic activity (330).

Literature search reveals that proteomic analysis of exosomes from the metastatic cell line PC-3 identified 266 proteins known to have variable cellular functions including transport, cell organisation and biogenesis, metabolism, response to stimulus and regulation of biological processes. The tetraspanin

protein CD151 and the glycoprotein CUB domain-containing protein 1 were identified. Their roles in tumour progression and invasiveness suggest that these can be used as promising biomarkers for prostate cancer (331). The work from another group used exosomes extracted from the DU145 prostate cancer cell line compared to the contents of the cell lysate from the same cell line. Within this study about 100 proteins were identified to be enriched in exosomes relative to cells, and these could be used as novel putative extracellular markers for prostate cancer (332). In another study, the identification of ITGA3 and ITGB1 in LNCaP and PC-3 cell-derived exosomes indicate that these proteins as part of exosomal cargo can manipulate non-cancer cells in the vicinity by enhancing migration and invasion (333).

Mass spectrometry using urinary exosomes of patients was also performed to identify proteins that are differentially expressed in prostate cancer patients compared to healthy male controls. This study identified 246 to be differentially expressed in the two groups with the majority being upregulated in exosomes from prostate cancer patients. Several of these proteins had high sensitivity and specificity for prostate cancer as individual biomarkers and combining them within a multi-panel test showed the potential to be able to fully differentiate prostate cancer patients from non-disease controls (334). Regarding the detection of canonical prostate cancer biomarkers in exosomes, PSA and TMPR22-ERG fusion mRNA are found as well in these extracellular vesicles. In addition, δ-catenin was detected in exosomes extracted from PC-3 cell culture supernatant and urine of prostate cancer patients (335) and survivin

was expressed at higher levels in exosomes from prostate cancer patients compared to healthy controls (336).

We were also able to show that serum-derived exosomes can be extracted successfully from samples obtained from patients and that the detection of miR-21 and EGFR-HER3 heterodimerisation can be utilised within bigger patient cohorts to provide predictive biomarker information of recurrence and response to treatment.

Our preliminary work showing detection of miR-21 is the first record to our knowledge of this microRNA being identified in a subgroup of prostate cancer patient-derived exosomes and its predictive biomarkers significance might be important especially if demonstrated within the full LOCATE clinical trial patient cohort. Apart from miR-21 literature search reveals the detection of other exosomal microRNAs in prostate cancer that might attract work in the future within translational research. For example, exosomal miR-34a was shown to regulate response to docetaxel and to correlate strongly with prostate cancer progression and poor prognosis (337). Exosomal RNA sequencing screening in a cohort of patients with CRPC identified miR-375 and miR-1290 as having prognostic significance. These were identified and validated in a bigger cohort of 100 patients. Interestingly, despite their prognostic ability when detected in exosomes of patients, their exosomal levels did not always correlate with their expression in tissue, demonstrating that the identification of cancer-derived molecules in biological fluids might not always be coming directly from the

tumours but from the interaction of tumour cell with the microenvironment or immune system (338).

Exosomes also contain double-stranded DNA (dsDNA) reflecting the genomic DNA (gDNA) of the originating cell. Studies in pancreatic, melanoma and lung cancer show that KRAS (339), BRAF and EGFR (340) mutations can be detected in exosomes by PCR. Similarly, detection of PSMA mRNA within exosomes, using digital droplet PCR, and its relative expression levels pre- and post-targeted treatments could be a useful tool to use as a non-invasive liquid biopsy to detect the point of the emergence of resistance and the possible need for change in therapy. However, additional work is needed to understand the functional distribution of extracellular DNA in different exosome populations that might preferentially accommodate specific types and amounts of DNA. For example, the genomic aberrations in PI3K pathway that includes PTEN mutations and deletions would be an ideal area to research to measure the PTEN copy number as an exosomal-based circulating DNA assay. The standardisation of these assays using patient-derived exosomal material is still in its early days and further work will help to advance this field.

Finally, the use of exosomal FRET-FLIM for the detection of EGFR-HER3 dimerisation has been utilised in our laboratory to show its importance as a predictive signature when used in combination with exosomal immune profiling within a multivariate statistical model where the decrease of EGFR-HER3 interaction after targeted treatment in head and neck cancer correlated with

worse short term RECIST best overall response outcome (318). My preliminary data within the LOCATE patient cohort also demonstrates that EGFR-HER3 dimerisation can be predictive of recurrence of prostate cancer and/or metastatic disease and the combined use of exosomal FRET-FLIM with microRNA profiling and PSMA mRNA expression could allow us to create a robust model of prediction that would correlate with radiological findings.

.

Chapter 6: Summary and future directions

6.1 Summary

Blockade of androgen receptor signalling in advanced and metastatic prostate cancer represents a very effective antitumour strategy. This leads to remissions for about 2-3 years, however the disease inevitably progresses to castration-resistant prostate cancer which is associated with poor prognosis and poses considerable therapeutic challenges (341). Recent advances in next-generation sequencing and RNA interference screening have provided considerable understanding in prostate cancer biology, apart from the androgen receptor signalling, and have allowed the identification of novel pharmacological approaches to targeting prostate cancer (153). As a result, personalised approaches in the treatment of advanced prostate cancer patients are now possible, an approach that is really relevant given the high intra- and inter-patient heterogeneity (342). More specifically, alterations in the PI3K-AKT pathway are identified within a significant proportion of prostate cancer patients at all stages of the disease. These can be targeted pharmacologically with PI3K pathway inhibitors and various combination studies are currently underway (see **table 1.2**).

Within this project, I aimed to investigate the resistance pathways that emerge through targeted inhibition of PI3K-AKT-mTOR pathway, especially those involving rewiring of ErbB receptors, as a means of understanding failure to treatment and to allow better patient stratification within a prospective future

clinical trial. I have demonstrated that PI3K-AKT-mTOR inhibition upregulates HER2 or HER3 in prostate cancer cell lines and that depending on the PTEN status, differential upregulation of AR or PSMA is observed that are shown to be dependent on ErbB feedback reactivation. These resistance mechanisms, irrespective of the PTEN status, have shown enhanced signalling of the PI3K-AKT-mTOR pathway as demonstrated by sustained and increased AKT phosphorylation levels, despite targeted inhibition of the pathway. Using shRNA interference to develop stable knockdown of HER3 in the LNCaP PTEN MT cell line I was able to demonstrate that AR upregulation following PI3K-AKT-mTOR inhibition is dependent on HER3. Furthermore, using FRET-FLIM technology in our laboratory I have shown for the first time that strong HER2-HER3 heterodimerisation occurs after 48 hours treatment with PI3K-AKT-mTOR inhibitor in LNCaP parental cells as a mechanism of resistance by enabling sustained signalling of the PI3K pathway. In the PTEN WT setting, the use of lapatinib was able to abrogate the observed PSMA upregulation that occurs in both hormone-sensitive and castrate-resistance cell lines demonstrating that HER2 activation via phosphorylation is an important feedback mechanism in enabling PSMA upregulation. Interestingly, the HER2-mediated upregulation of PSMA does not depend on HER2-HER3 heterodimerisation in this setting. The ErbB heterodimerisation patterns in metastatic prostate cancer have not been fully described and we lack information about their significance in the hormone-sensitive and castrate-resistant settings in allowing prostate cancer cell growth, however our work provides evidence that this is determined by PTEN status. It is possible, that the full complexity between the ErbB and AR/PSMA signaling

pathways is not at all fully decoded and further research needs to be done to understand the patient heterogeneity leading to ErbB upregulation and how this determines further pathway activation and sensitivity/resistance to targeted treatment (121).

Finally, I have used patient serum to extract exosomes successfully and demonstrate that these can be used as liquid biopsies to detect ErbB heterodimerisation and to assess microRNA expression as important biomarkers in patients within clinical trials to allow their initial stratification to treatment but also as a means of monitoring their responses to targeted therapies.

6.2 Future directions

Understanding why and how the anti-proliferative effects of PI3K-AKT pathway inhibition can be overcome with upregulation of important targets is an important area to focus on since this pathway is so frequently upregulated in prostate cancer. Our finding of PSMA upregulation in a subset of prostate cancer upon PI3K-AKT-mTOR inhibition has not been described before. There is strong belief currently that PSMA has an important role functionally in prostate cancer and that its significance is not limited to its detection as a prognostic biomarker. Our work has enhanced this view and we are interested in performing further work to define the targets downstream of PSMA that could be exploited both pharmacologically and as biomarkers of resistance to targeted treatment. In addition, we are working on optimising assays by the use of mass spectrometry techniques for the detection of glutamate substrates in

order to be able to measure changes in these metabolites in metastatic prostate cancer upon PI3K-mTOR inhibitor as a result of PSMA upregulation. Establishing these assays using preclinical material from this project could enable further utilisation of such techniques in clinical samples in the future. Furthermore, PI3K-mTOR driven upregulation of PSMA can lead to an increase in angiogenesis via HIF1α and mGLUR1 and this is also another area we would like to work on in the future. Collectively, targeting the PSMA-dependent mechanisms driving prostate cancer progression may provide a novel paradigm for the development of therapeutic strategies that target both tumour progression and vascularization (194).

Assays within liquid-biopsies that are able to detect PSMA expression at baseline and upon its upregulation as a resistance mechanism following targeted treatment are important to develop as PSMA expression level might have significant predictive power of clinical outcomes, especially in the PTEN WT setting.

Furthermore, the quantification of EGFR-HER3 dimer formation within prostate cancer patient serum-derived exosomes is an area of work in our group. The FRET-FLIM assay is being applied to serum-derived exosomes from the LOCATE trial cohort, to correlate dimer formation with the detection of metastatic disease and clinical outcome in terms of treatment resistance. In order to maximise prognostic capacity, it is important to fully profile the disease of each patient. The combination of data from multiparametric MRI radiological biomarker information and established clinicopathological factors together with

the output from our proteomic and microRNA exosome data should provide a better prognostic model for outcome. The availability of archival or new prostate biopsy samples from the LOCATE patient cohort will also enable us to apply the FRET-FLIM assay in a subset of patients from this trial to observe whether any correlation between tissue and exosomal dimer exists. Further improvements in protein-based biomarkers within exosomes are also being sought to detect PSMA and other proteins with key relevance to our findings. Simultaneously, we aim to describe the tumour microenvironment and immune response, in order to fully profile all the relevant factors involved in metastasis and treatment resistance. The generation of all this data will be challenging and will require collaboration with bioinformatics and computational statistical modelling. Once validated, high-throughput technology will need to be developed to enable the use of these assays in routine clinical practice.

Although some predictive tools already exist, we hope to improve the prediction of outcome by these methods, especially where targeted therapies are used in metastatic prostate cancer. Firstly, validation of our exosomal assay must be carried out within the LOCATE patient cohort but we are also very interested to also take this forward within a clinical trial using targeted inhibition of the PI3K pathway. Ideally this should be done prospectively in a cohort of patients receiving targeted treatment against the PI3K pathway, we would be interested in obtaining information of the PTEN status by IHC either from archival samples or by the acquisition of fresh biopsies at the time of recruitment.

Finally, in collaboration with Crescendo Biologics we aim to perform further work using their bispecific CD137-PSMA Humabody. This is designed so that it delivers highly potent T cell costimulatory activity by clustering and activating CD137 on T cells only in the tumour microenviroment (TME) and then it has the ability to rapidly accumulate in the tumours that are expressing PSMA, to activate tumour-specific T-cells in the tumour microenvironment. Data from this exciting approach suggests that the targeted costimulatory molecule has potential as a platform in its own right. We propose to utilise the cryopreserved PBMCs from anonymised samples of prostate cancer patients from the LOCATE cohort to investigate whether this CD137-PSMA bispecific Humabody has the ability to target and kill PSMA positive prostate cancer cell lines in co-culture. This will be carried out as an in vitro cell growth/viability assay using serial dilutions of the bispecific Humabody in prostate cancer cell lines with known positive expression of PSMA. The demonstration of a positive outcome in the killing of PSMA-expressing cells in vitro will confirm that the CD137-PSMA bispecific Humabody is capable of engaging tumours from patients by binding to PSMA and in doing so, it is able to initiate T-cell mediated killing in a tumour-specific manner. It will also lead to further in vivo evaluation of this effect as well as and move towards to the future design of a clinical trial that will aim to assess clinically relevant endpoints in patients with PSMA positive prostate cancer following biochemical relapse upon treatment with anti-androgen and other targeted therapies that are able to upregulate PSMA as a resistance mechanism.

In summary, we aim to define the best predictive biomarkers for use in patients to improve clinical outcomes and responses to therapies as well as to minimize patient morbidity, toxicities and financial burden. Development of minimally invasive methods, by the use of exosomes, for obtaining information about the whole tumour proteome and transcriptome will prove invaluable for tumour surveillance, both during and after treatment. The ultimate goal will be to provide therapies to which patients will respond and at the right time along the timecourse of their disease.

References:

1. UK CR. Prostate Cancer Key facts [Available from: http://www.cancerresearchuk.org/cancer-info/ cancerstats/keyfacts/prostate-cancer.
2. Galazi M, Rodriguez-Vida A, Ng T, Mason M, Chowdhury S. Precision medicine for prostate cancer. Expert Rev Anticancer Ther. 2014;14(11):1305-15.
3. Huggins C, Hodges CV. Studies on Prostatic Cancer. I. The Effect of Castration, of Estrogen and of Androgen Injection on Serum Phosphatases in Metastatic Carcinoma of the Prostate. Cancer Research. 1941;1(4):293-7.
4. Ferraldeschi R, Welti J, Luo J, Attard G, de Bono JS. Targeting the androgen receptor pathway in castration-resistant prostate cancer: progresses and prospects. Oncogene. 2015;34(14):1745-57.
5. Massard C, Fizazi K. Targeting continued androgen receptor signaling in prostate cancer. Clin Cancer Res. 2011;17(12):3876-83.
6. Carver BS, Chapinski C, Wongvipat J, Hieronymus H, Chen Y, Chandarlapaty S, et al. Reciprocal feedback regulation of PI3K and androgen receptor signaling in PTEN-deficient prostate cancer. Cancer cell. 2011;19(5):575-86.
7. Robinson D, Van Allen EM, Wu YM, Schultz N, Lonigro RJ, Mosquera JM, et al. Integrative clinical genomics of advanced prostate cancer. Cell. 2015;161(5):1215-28.
8. Beck S, Ng T. C2c: turning cancer into chronic disease. Genome Medicine. 2014;6(5):38-.
9. Watson PA, Arora VK, Sawyers CL. Emerging mechanisms of resistance to androgen receptor inhibitors in prostate cancer. Nature reviews Cancer. 2015;15(12):701-11.
10. van Poppel H, Nilsson S. Testosterone surge: rationale for gonadotropin-releasing hormone blockers? Urology. 2008;71(6):1001-6.
11. Nguyen PL, Alibhai SM, Basaria S, D'Amico AV, Kantoff PW, Keating NL, et al. Adverse effects of androgen deprivation therapy and strategies to mitigate them. European urology. 2015;67(5):825-36.
12. Berthold DR, Pond GR, Soban F, de Wit R, Eisenberger M, Tannock IF. Docetaxel plus prednisone or mitoxantrone plus prednisone for advanced prostate cancer: updated survival in the TAX 327 study. J Clin Oncol. 2008;26(2):242-5.
13. de Bono JS, Logothetis CJ, Molina A, Fizazi K, North S, Chu L, et al. Abiraterone and increased survival in metastatic prostate cancer. N Engl J Med. 2011;364(21):1995-2005.
14. Scher HI, Fizazi K, Saad F, Taplin ME, Sternberg CN, Miller K, et al. Increased survival with enzalutamide in prostate cancer after chemotherapy. N Engl J Med. 2012;367(13):1187-97.
15. de Bono JS, Oudard S, Ozguroglu M, Hansen S, Machiels JP, Kocak I, et al. Prednisone plus cabazitaxel or mitoxantrone for metastatic castration-resistant prostate cancer progressing after docetaxel treatment: a randomised open-label trial. Lancet (London, England). 2010;376(9747):1147-54.
16. Parker C, Nilsson S, Heinrich D, Helle SI, O'Sullivan JM, Fossa SD, et al. Alpha emitter radium-223 and survival in metastatic prostate cancer. N Engl J Med. 2013;369(3):213-23.

17. Fizazi K, Carducci M, Smith M, Damiao R, Brown J, Karsh L, et al. Denosumab versus zoledronic acid for treatment of bone metastases in men with castration-resistant prostate cancer: a randomised, double-blind study. Lancet (London, England). 2011;377(9768):813-22.
18. Kantoff PW, Higano CS, Shore ND, Berger ER, Small EJ, Penson DF, et al. Sipuleucel-T immunotherapy for castration-resistant prostate cancer. N Engl J Med. 2010;363(5):411-22.
19. Kirby M, Hirst C, Crawford ED. Characterising the castration-resistant prostate cancer population: a systematic review. International journal of clinical practice. 2011;65(11):1180-92.
20. Potter GA, Barrie SE, Jarman M, Rowlands MG. Novel steroidal inhibitors of human cytochrome P45017 alpha (17 alpha-hydroxylase-C17,20-lyase): potential agents for the treatment of prostatic cancer. Journal of medicinal chemistry. 1995;38(13):2463-71.
21. Jung ME, Ouk S, Yoo D, Sawyers CL, Chen C, Tran C, et al. Structure-activity relationship for thiohydantoin androgen receptor antagonists for castration-resistant prostate cancer (CRPC). Journal of medicinal chemistry. 2010;53(7):2779-96.
22. Ryan CJ, Smith MR, de Bono JS, Molina A, Logothetis CJ, de Souza P, et al. Abiraterone in metastatic prostate cancer without previous chemotherapy. N Engl J Med. 2013;368(2):138-48.
23. Beer TM, Armstrong AJ, Rathkopf DE, Loriot Y, Sternberg CN, Higano CS, et al. Enzalutamide in metastatic prostate cancer before chemotherapy. N Engl J Med. 2014;371(5):424-33.
24. Antonarakis ES, Drake CG. Current status of immunological therapies for prostate cancer. Current opinion in urology. 2010;20(3):241-6.
25. Fong PC, Boss DS, Yap TA, Tutt A, Wu P, Mergui-Roelvink M, et al. Inhibition of poly(ADP-ribose) polymerase in tumors from BRCA mutation carriers. N Engl J Med. 2009;361(2):123-34.
26. Bryant HE, Schultz N, Thomas HD, Parker KM, Flower D, Lopez E, et al. Specific killing of BRCA2-deficient tumours with inhibitors of poly(ADP-ribose) polymerase. Nature. 2005;434(7035):913-7.
27. Castro E, Goh C, Olmos D, Saunders E, Leongamornlert D, Tymrakiewicz M, et al. Germline BRCA mutations are associated with higher risk of nodal involvement, distant metastasis, and poor survival outcomes in prostate cancer. J Clin Oncol. 2013;31(14):1748-57.
28. Mateo J, Carreira S, Sandhu S, Miranda S, Mossop H, Perez-Lopez R, et al. DNA-Repair Defects and Olaparib in Metastatic Prostate Cancer. N Engl J Med. 2015;373(18):1697-708.
29. Sweeney CJ, Chen YH, Carducci M, Liu G, Jarrard DF, Eisenberger M, et al. Chemohormonal Therapy in Metastatic Hormone-Sensitive Prostate Cancer. N Engl J Med. 2015;373(8):737-46.
30. James ND, Sydes MR, Clarke NW, Mason MD, Dearnaley DP, Spears MR, et al. Addition of docetaxel, zoledronic acid, or both to first-line long-term hormone therapy in prostate cancer (STAMPEDE): survival results from an adaptive, multiarm, multistage, platform randomised controlled trial. Lancet (London, England). 2016;387(10024):1163-77.

31. Fizazi K, Tran N, Fein L, Matsubara N, Rodriguez-Antolin A, Alekseev BY, et al. Abiraterone plus Prednisone in Metastatic, Castration-Sensitive Prostate Cancer. N Engl J Med. 2017;377(4):352-60.
32. James ND, de Bono JS, Spears MR, Clarke NW, Mason MD, Dearnaley DP, et al. Abiraterone for Prostate Cancer Not Previously Treated with Hormone Therapy. N Engl J Med. 2017;377(4):338-51.
33. McNamara M, Sweeney C, Antonarakis ES, Armstrong AJ. The evolving landscape of metastatic hormone-sensitive prostate cancer: a critical review of the evidence for adding docetaxel or abiraterone to androgen deprivation. Prostate Cancer Prostatic Dis. 2017.
34. Lundwall A, Clauss A, Olsson AY. Evolution of kallikrein-related peptidases in mammals and identification of a genetic locus encoding potential regulatory inhibitors. Biological chemistry. 2006;387(3):243-9.
35. D'Amico AV, Kantoff P, Loffredo M, Renshaw AA, Loffredo B, Chen MH. Predictors of mortality after prostate-specific antigen failure. International journal of radiation oncology, biology, physics. 2006;65(3):656-60.
36. Kwak C, Jeong SJ, Park MS, Lee E, Lee SE. Prognostic significance of the nadir prostate specific antigen level after hormone therapy for prostate cancer. The Journal of urology. 2002;168(3):995-1000.
37. Armstrong AJ, Garrett-Mayer E, Ou Yang YC, Carducci MA, Tannock I, de Wit R, et al. Prostate-specific antigen and pain surrogacy analysis in metastatic hormone-refractory prostate cancer. J Clin Oncol. 2007;25(25):3965-70.
38. D'Amico AV, Whittington R, Malkowicz SB, Schultz D, Blank K, Broderick GA, et al. Biochemical outcome after radical prostatectomy, external beam radiation therapy, or interstitial radiation therapy for clinically localized prostate cancer. Jama. 1998;280(11):969-74.
39. Eggener SE, Scardino PT, Walsh PC, Han M, Partin AW, Trock BJ, et al. Predicting 15-year prostate cancer specific mortality after radical prostatectomy. The Journal of urology. 2011;185(3):869-75.
40. Stephenson AJ, Scardino PT, Eastham JA, Bianco FJ, Jr., Dotan ZA, DiBlasio CJ, et al. Postoperative nomogram predicting the 10-year probability of prostate cancer recurrence after radical prostatectomy. J Clin Oncol. 2005;23(28):7005-12.
41. Partin AW, Kattan MW, Subong EN, Walsh PC, Wojno KJ, Oesterling JE, et al. Combination of prostate-specific antigen, clinical stage, and Gleason score to predict pathological stage of localized prostate cancer. A multi-institutional update. Jama. 1997;277(18):1445-51.
42. Boehm K, Larcher A, Beyer B, Tian Z, Tilki D, Steuber T, et al. Identifying the Most Informative Prediction Tool for Cancer-specific Mortality After Radical Prostatectomy: Comparative Analysis of Three Commonly Used Preoperative Prediction Models. European urology. 2016;69(6):1038-43.
43. Dalela D, Loppenberg B, Sood A, Sammon J, Abdollah F. Contemporary Role of the Decipher(R) Test in Prostate Cancer Management: Current Practice and Future Perspectives. Reviews in urology. 2016;18(1):1-9.
44. Prolaris Cell Cycle Progression Test for Localized Prostate Cancer: A Health Technology Assessment. Ontario health technology assessment series. 2017;17(6):1-75.

45. Albala D, Kemeter MJ, Febbo PG, Lu R, John V, Stoy D, et al. Health Economic Impact and Prospective Clinical Utility of Oncotype DX(R) Genomic Prostate Score. Reviews in urology. 2016;18(3):123-32.
46. Liu W, Laitinen S, Khan S, Vihinen M, Kowalski J, Yu G, et al. Copy number analysis indicates monoclonal origin of lethal metastatic prostate cancer. Nature medicine. 2009;15(5):559-65.
47. Gundem G, Van Loo P, Kremeyer B, Alexandrov LB, Tubio JMC, Papaemmanuil E, et al. The evolutionary history of lethal metastatic prostate cancer. Nature. 2015;520(7547):353-7.
48. de Bono JS, Scher HI, Montgomery RB, Parker C, Miller MC, Tissing H, et al. Circulating tumor cells predict survival benefit from treatment in metastatic castration-resistant prostate cancer. Clin Cancer Res. 2008;14(19):6302-9.
49. Romanel A, Gasi Tandefelt D, Conteduca V, Jayaram A, Casiraghi N, Wetterskog D, et al. Plasma AR and abiraterone-resistant prostate cancer. Sci Transl Med. 2015;7(312):312re10.
50. Efstathiou E, Titus M, Wen S, Hoang A, Karlou M, Ashe R, et al. Molecular characterization of enzalutamide-treated bone metastatic castration-resistant prostate cancer. European urology. 2015;67(1):53-60.
51. Antonarakis ES, Lu C, Wang H, Luber B, Nakazawa M, Roeser JC, et al. AR-V7 and resistance to enzalutamide and abiraterone in prostate cancer. N Engl J Med. 2014;371(11):1028-38.
52. Ferraldeschi R, Nava Rodrigues D, Riisnaes R, Miranda S, Figueiredo I, Rescigno P, et al. PTEN protein loss and clinical outcome from castration-resistant prostate cancer treated with abiraterone acetate. European urology. 2015;67(4):795-802.
53. Barchetti F, Panebianco V. Multiparametric MRI for recurrent prostate cancer post radical prostatectomy and postradiation therapy. BioMed research international. 2014;2014:316272.
54. Murphy AM, Berkman DS, Desai M, Benson MC, McKiernan JM, Badani KK. The number of negative pelvic lymph nodes removed does not affect the risk of biochemical failure after radical prostatectomy. BJU international. 2010;105(2):176-9.
55. Heidenreich A, Bastian PJ, Bellmunt J, Bolla M, Joniau S, van der Kwast T, et al. EAU guidelines on prostate cancer. Part II: Treatment of advanced, relapsing, and castration-resistant prostate cancer. European urology. 2014;65(2):467-79.
56. Hu JC, Chang E, Natarajan S, Margolis DJ, Macairan M, Lieu P, et al. Targeted prostate biopsy in select men for active surveillance: do the Epstein criteria still apply? The Journal of urology. 2014;192(2):385-90.
57. Hoeks CM, Barentsz JO, Hambrock T, Yakar D, Somford DM, Heijmink SW, et al. Prostate cancer: multiparametric MR imaging for detection, localization, and staging. Radiology. 2011;261(1):46-66.
58. Turkbey B, Choyke PL. Multiparametric MRI and prostate cancer diagnosis and risk stratification. Current opinion in urology. 2012;22(4):310-5.
59. Afshar-Oromieh A, Zechmann CM, Malcher A, Eder M, Eisenhut M, Linhart HG, et al. Comparison of PET imaging with a (68)Ga-labelled PSMA ligand and (18)F-choline-based PET/CT for the diagnosis of recurrent prostate cancer. European journal of nuclear medicine and molecular imaging. 2014;41(1):11-20.

60. Eiber M, Maurer T, Souvatzoglou M, Beer AJ, Ruffani A, Haller B, et al. Evaluation of Hybrid (6)(8)Ga-PSMA Ligand PET/CT in 248 Patients with Biochemical Recurrence After Radical Prostatectomy. Journal of nuclear medicine : official publication, Society of Nuclear Medicine. 2015;56(5):668-74.
61. Ost P, Reynders D, Decaestecker K, Fonteyne V, Lumen N, De Bruycker A, et al. Surveillance or Metastasis-Directed Therapy for Oligometastatic Prostate Cancer Recurrence: A Prospective, Randomized, Multicenter Phase II Trial. J Clin Oncol. 2018;36(5):446-53.
62. Gelmann EP. Molecular biology of the androgen receptor. J Clin Oncol. 2002;20(13):3001-15.
63. Prescott J, Coetzee GA. Molecular chaperones throughout the life cycle of the androgen receptor. Cancer letters. 2006;231(1):12-9.
64. Jenster G, van der Korput HA, van Vroonhoven C, van der Kwast TH, Trapman J, Brinkmann AO. Domains of the human androgen receptor involved in steroid binding, transcriptional activation, and subcellular localization. Molecular endocrinology (Baltimore, Md). 1991;5(10):1396-404.
65. He B, Kemppainen JA, Wilson EM. FXXLF and WXXLF sequences mediate the NH2-terminal interaction with the ligand binding domain of the androgen receptor. J Biol Chem. 2000;275(30):22986-94.
66. Ikonen T, Palvimo JJ, Janne OA. Interaction between the amino- and carboxyl-terminal regions of the rat androgen receptor modulates transcriptional activity and is influenced by nuclear receptor coactivators. J Biol Chem. 1997;272(47):29821-8.
67. Weigel NL. Steroid hormone receptors and their regulation by phosphorylation. Biochemical Journal. 1996;319(Pt 3):657-67.
68. Heery DM, Kalkhoven E, Hoare S, Parker MG. A signature motif in transcriptional co-activators mediates binding to nuclear receptors. Nature. 1997;387(6634):733-6.
69. van Royen ME, Cunha SM, Brink MC, Mattern KA, Nigg AL, Dubbink HJ, et al. Compartmentalization of androgen receptor protein-protein interactions in living cells. The Journal of cell biology. 2007;177(1):63-72.
70. Dehm SM, Tindall DJ. Molecular regulation of androgen action in prostate cancer. Journal of cellular biochemistry. 2006;99(2):333-44.
71. Lu S, Jenster G, Epner DE. Androgen induction of cyclin-dependent kinase inhibitor p21 gene: role of androgen receptor and transcription factor Sp1 complex. Molecular endocrinology (Baltimore, Md). 2000;14(5):753-60.
72. Tyagi RK, Lavrovsky Y, Ahn SC, Song CS, Chatterjee B, Roy AK. Dynamics of intracellular movement and nucleocytoplasmic recycling of the ligand-activated androgen receptor in living cells. Molecular endocrinology (Baltimore, Md). 2000;14(8):1162-74.
73. Lee JH, Lee MJ. Emerging roles of the ubiquitin-proteasome system in the steroid receptor signaling. Archives of pharmacal research. 2012;35(3):397-407.
74. Sheflin L, Keegan B, Zhang W, Spaulding SW. Inhibiting proteasomes in human HepG2 and LNCaP cells increases endogenous androgen receptor levels. Biochem Biophys Res Commun. 2000;276(1):144-50.
75. Lin HK, Wang L, Hu YC, Altuwaijri S, Chang C. Phosphorylation-dependent ubiquitylation and degradation of androgen receptor by Akt require Mdm2 E3 ligase. The EMBO journal. 2002;21(15):4037-48.

76. Murata S, Minami Y, Minami M, Chiba T, Tanaka K. CHIP is a chaperone-dependent E3 ligase that ubiquitylates unfolded protein. EMBO reports. 2001;2(12):1133-8.
77. Xu K, Shimelis H, Linn DE, Jiang R, Yang X, Sun F, et al. Regulation of Androgen Receptor Transcriptional Activity and Specificity by RNF6-Induced Ubiquitination. Cancer cell.15(4):270-82.
78. Qi J, Tripathi M, Mishra R, Sahgal N, Fazli L, Ettinger S, et al. The E3 ubiquitin ligase Siah2 contributes to castration-resistant prostate cancer by regulation of androgen receptor transcriptional activity. Cancer cell. 2013;23(3):332-46.
79. Scher HI, Sawyers CL. Biology of progressive, castration-resistant prostate cancer: directed therapies targeting the androgen-receptor signaling axis. J Clin Oncol. 2005;23(32):8253-61.
80. Buchanan G, Irvine RA, Coetzee GA, Tilley WD. Contribution of the androgen receptor to prostate cancer predisposition and progression. Cancer metastasis reviews. 2001;20(3-4):207-23.
81. Steinkamp MP, O'Mahony OA, Brogley M, Rehman H, Lapensee EW, Dhanasekaran S, et al. Treatment-dependent androgen receptor mutations in prostate cancer exploit multiple mechanisms to evade therapy. Cancer Res. 2009;69(10):4434-42.
82. Sack JS, Kish KF, Wang C, Attar RM, Kiefer SE, An Y, et al. Crystallographic structures of the ligand-binding domains of the androgen receptor and its T877A mutant complexed with the natural agonist dihydrotestosterone. Proc Natl Acad Sci U S A. 2001;98(9):4904-9.
83. Locke JA, Guns ES, Lubik AA, Adomat HH, Hendy SC, Wood CA, et al. Androgen levels increase by intratumoral de novo steroidogenesis during progression of castration-resistant prostate cancer. Cancer Res. 2008;68(15):6407-15.
84. Heemers HV, Tindall DJ. Androgen receptor (AR) coregulators: a diversity of functions converging on and regulating the AR transcriptional complex. Endocrine reviews. 2007;28(7):778-808.
85. Lonergan PE, Tindall DJ. Androgen receptor signaling in prostate cancer development and progression. Journal of carcinogenesis. 2011;10:20.
86. Zhu ML, Kyprianou N. Androgen receptor and growth factor signaling cross-talk in prostate cancer cells. Endocrine-related cancer. 2008;15(4):841-9.
87. Watson PA, Chen YF, Balbas MD, Wongvipat J, Socci ND, Viale A, et al. Constitutively active androgen receptor splice variants expressed in castration-resistant prostate cancer require full-length androgen receptor. Proceedings of the National Academy of Sciences. 2010;107(39):16759-65.
88. Chan SC, Li Y, Dehm SM. Androgen receptor splice variants activate androgen receptor target genes and support aberrant prostate cancer cell growth independent of canonical androgen receptor nuclear localization signal. J Biol Chem. 2012;287(23):19736-49.
89. Tran C, Ouk S, Clegg NJ, Chen Y, Watson PA, Arora V, et al. Development of a second-generation antiandrogen for treatment of advanced prostate cancer. Science (New York, NY). 2009;324(5928):787-90.

90. Smith MR, Saad F, Chowdhury S, Oudard S, Hadaschik BA, Graff JN, et al. Apalutamide Treatment and Metastasis-free Survival in Prostate Cancer. N Engl J Med. 2018;378(15):1408-18.
91. ClinicalTrials.gov. Efficacy and safety study of BAY1841788 (ODM-201) in men with high-risk non-metastatic castration-resistant prostate cancer (ARAMIS). 2017 [Available from: https://clinicaltrials.gov/ct2/show/NCT02200614.
92. Moilanen AM, Riikonen R, Oksala R, Ravanti L, Aho E, Wohlfahrt G, et al. Discovery of ODM-201, a new-generation androgen receptor inhibitor targeting resistance mechanisms to androgen signaling-directed prostate cancer therapies. Scientific reports. 2015;5:12007.
93. Schreiber AB, Libermann TA, Lax I, Yarden Y, Schlessinger J. Biological role of epidermal growth factor-receptor clustering. Investigation with monoclonal anti-receptor antibodies. J Biol Chem. 1983;258(2):846-53.
94. Jura N, Endres NF, Engel K, Deindl S, Das R, Lamers MH, et al. Mechanism for activation of the EGF receptor catalytic domain by the juxtamembrane segment. Cell. 2009;137(7):1293-307.
95. Yarden Y, Sliwkowski MX. Untangling the ErbB signalling network. Nat Rev Mol Cell Biol. 2001;2(2):127-37.
96. Olayioye MA, Neve RM, Lane HA, Hynes NE. The ErbB signaling network: receptor heterodimerization in development and cancer. The EMBO journal. 2000;19(13):3159-67.
97. Cho HS, Leahy DJ. Structure of the extracellular region of HER3 reveals an interdomain tether. Science (New York, NY). 2002;297(5585):1330-3.
98. Ogiso H, Ishitani R, Nureki O, Fukai S, Yamanaka M, Kim JH, et al. Crystal structure of the complex of human epidermal growth factor and receptor extracellular domains. Cell. 2002;110(6):775-87.
99. Yarden Y, Pines G. The ERBB network: at last, cancer therapy meets systems biology. Nature reviews Cancer. 2012;12(8):553-63.
100. Shi F, Telesco SE, Liu Y, Radhakrishnan R, Lemmon MA. ErbB3/HER3 intracellular domain is competent to bind ATP and catalyze autophosphorylation. Proc Natl Acad Sci U S A. 2010;107(17):7692-7.
101. Cho HS, Mason K, Ramyar KX, Stanley AM, Gabelli SB, Denney DW, Jr., et al. Structure of the extracellular region of HER2 alone and in complex with the Herceptin Fab. Nature. 2003;421(6924):756-60.
102. Pinkas-Kramarski R, Soussan L, Waterman H, Levkowitz G, Alroy I, Klapper L, et al. Diversification of Neu differentiation factor and epidermal growth factor signaling by combinatorial receptor interactions. The EMBO journal. 1996;15(10):2452-67.
103. Hynes NE, Lane HA. ERBB receptors and cancer: the complexity of targeted inhibitors. Nature reviews Cancer. 2005;5(5):341-54.
104. Citri A, Yarden Y. EGF-ERBB signalling: towards the systems level. Nat Rev Mol Cell Biol. 2006;7(7):505-16.
105. Soltoff SP, Carraway KL, 3rd, Prigent SA, Gullick WG, Cantley LC. ErbB3 is involved in activation of phosphatidylinositol 3-kinase by epidermal growth factor. Molecular and cellular biology. 1994;14(6):3550-8.

106. Lee-Hoeflich ST, Crocker L, Yao E, Pham T, Munroe X, Hoeflich KP, et al. A central role for HER3 in HER2-amplified breast cancer: implications for targeted therapy. Cancer Res. 2008;68(14):5878-87.
107. Mendelsohn J, Baselga J. Status of epidermal growth factor receptor antagonists in the biology and treatment of cancer. J Clin Oncol. 2003;21(14):2787-99.
108. Baselga J, Swain SM. Novel anticancer targets: revisiting ERBB2 and discovering ERBB3. Nature reviews Cancer. 2009;9(7):463-75.
109. Carraway KL, 3rd, Cantley LC. A neu acquaintance for erbB3 and erbB4: a role for receptor heterodimerization in growth signaling. Cell. 1994;78(1):5-8.
110. Engelman JA, Zejnullahu K, Mitsudomi T, Song Y, Hyland C, Park JO, et al. MET amplification leads to gefitinib resistance in lung cancer by activating ERBB3 signaling. Science (New York, NY). 2007;316(5827):1039-43.
111. Sergina NV, Rausch M, Wang D, Blair J, Hann B, Shokat KM, et al. Escape from HER-family tyrosine kinase inhibitor therapy by the kinase-inactive HER3. Nature. 2007;445(7126):437-41.
112. Chakrabarty A, Sanchez V, Kuba MG, Rinehart C, Arteaga CL. Feedback upregulation of HER3 (ErbB3) expression and activity attenuates antitumor effect of PI3K inhibitors. Proc Natl Acad Sci U S A. 2012;109(8):2718-23.
113. Chandarlapaty S, Sawai A, Scaltriti M, Rodrik-Outmezguine V, Grbovic-Huezo O, Serra V, et al. AKT inhibition relieves feedback suppression of receptor tyrosine kinase expression and activity. Cancer cell. 2011;19(1):58-71.
114. Turke AB, Song Y, Costa C, Cook R, Arteaga CL, Asara JM, et al. MEK inhibition leads to PI3K/AKT activation by relieving a negative feedback on ERBB receptors. Cancer Res. 2012;72(13):3228-37.
115. Lemoine NR, Barnes DM, Hollywood DP, Hughes CM, Smith P, Dublin E, et al. Expression of the ERBB3 gene product in breast cancer. Br J Cancer. 1992;66(6):1116-21.
116. Jaiswal BS, Kljavin NM, Stawiski EW, Chan E, Parikh C, Durinck S, et al. Oncogenic ERBB3 mutations in human cancers. Cancer cell. 2013;23(5):603-17.
117. Ciardiello F, Kim N, Saeki T, Dono R, Persico MG, Plowman GD, et al. Differential expression of epidermal growth factor-related proteins in human colorectal tumors. Proc Natl Acad Sci U S A. 1991;88(17):7792-6.
118. Beji A, Horst D, Engel J, Kirchner T, Ullrich A. Toward the prognostic significance and therapeutic potential of HER3 receptor tyrosine kinase in human colon cancer. Clin Cancer Res. 2012;18(4):956-68.
119. Iorio MV, Casalini P, Piovan C, Di Leva G, Merlo A, Triulzi T, et al. microRNA-205 regulates HER3 in human breast cancer. Cancer Res. 2009;69(6):2195-200.
120. Scott GK, Goga A, Bhaumik D, Berger CE, Sullivan CS, Benz CC. Coordinate suppression of ERBB2 and ERBB3 by enforced expression of micro-RNA miR-125a or miR-125b. J Biol Chem. 2007;282(2):1479-86.
121. Gregory CW, Whang YE, McCall W, Fei X, Liu Y, Ponguta LA, et al. Heregulin-induced activation of HER2 and HER3 increases androgen receptor transactivation and CWR-R1 human recurrent prostate cancer cell growth. Clin Cancer Res. 2005;11(5):1704-12.
122. Culig Z, Hobisch A, Cronauer MV, Radmayr C, Trapman J, Hittmair A, et al. Androgen receptor activation in prostatic tumor cell lines by insulin-like growth

factor-I, keratinocyte growth factor, and epidermal growth factor. Cancer Res. 1994;54(20):5474-8.
123. Sirotnak FM, She Y, Lee F, Chen J, Scher HI. Studies with CWR22 xenografts in nude mice suggest that ZD1839 may have a role in the treatment of both androgen-dependent and androgen-independent human prostate cancer. Clin Cancer Res. 2002;8(12):3870-6.
124. Craft N, Shostak Y, Carey M, Sawyers CL. A mechanism for hormone-independent prostate cancer through modulation of androgen receptor signaling by the HER-2/neu tyrosine kinase. Nature medicine. 1999;5(3):280-5.
125. Mellinghoff IK, Vivanco I, Kwon A, Tran C, Wongvipat J, Sawyers CL. HER2/neu kinase-dependent modulation of androgen receptor function through effects on DNA binding and stability. Cancer cell. 2004;6(5):517-27.
126. Kuhn EJ, Kurnot RA, Sesterhenn IA, Chang EH, Moul JW. Expression of the c-erbB-2 (HER-2/neu) oncoprotein in human prostatic carcinoma. The Journal of urology. 1993;150(5 Pt 1):1427-33.
127. Ross JS, Sheehan CE, Hayner-Buchan AM, Ambros RA, Kallakury BV, Kaufman RP, Jr., et al. Prognostic significance of HER-2/neu gene amplification status by fluorescence in situ hybridization of prostate carcinoma. Cancer. 1997;79(11):2162-70.
128. Sadasivan R, Morgan R, Jennings S, Austenfeld M, Van Veldhuizen P, Stephens R, et al. Overexpression of Her-2/neu may be an indicator of poor prognosis in prostate cancer. The Journal of urology. 1993;150(1):126-31.
129. Mendoza N, Phillips GL, Silva J, Schwall R, Wickramasinghe D. Inhibition of ligand-mediated HER2 activation in androgen-independent prostate cancer. Cancer Res. 2002;62(19):5485-8.
130. Agus DB, Akita RW, Fox WD, Lewis GD, Higgins B, Pisacane PI, et al. Targeting ligand-activated ErbB2 signaling inhibits breast and prostate tumor growth. Cancer cell. 2002;2(2):127-37.
131. Zhang Y, Linn D, Liu Z, Melamed J, Tavora F, Young CY, et al. EBP1, an ErbB3-binding protein, is decreased in prostate cancer and implicated in hormone resistance. Molecular cancer therapeutics. 2008;7(10):3176-86.
132. Canil CM, Moore MJ, Winquist E, Baetz T, Pollak M, Chi KN, et al. Randomized phase II study of two doses of gefitinib in hormone-refractory prostate cancer: a trial of the National Cancer Institute of Canada-Clinical Trials Group. J Clin Oncol. 2005;23(3):455-60.
133. Gross M, Higano C, Pantuck A, Castellanos O, Green E, Nguyen K, et al. A phase II trial of docetaxel and erlotinib as first-line therapy for elderly patients with androgen-independent prostate cancer. BMC cancer. 2007;7:142.
134. Ziada A, Barqawi A, Glode LM, Varella-Garcia M, Crighton F, Majeski S, et al. The use of trastuzumab in the treatment of hormone refractory prostate cancer; phase II trial. The Prostate. 2004;60(4):332-7.
135. Whang YE, Armstrong AJ, Rathmell WK, Godley PA, Kim WY, Pruthi RS, et al. A phase II study of lapatinib, a dual EGFR and HER-2 tyrosine kinase inhibitor, in patients with castration-resistant prostate cancer. Urologic oncology. 2013;31(1):82-6.
136. Agus DB, Sweeney CJ, Morris MJ, Mendelson DS, McNeel DG, Ahmann FR, et al. Efficacy and safety of single-agent pertuzumab (rhuMAb 2C4), a human epidermal

growth factor receptor dimerization inhibitor, in castration-resistant prostate cancer after progression from taxane-based therapy. J Clin Oncol. 2007;25(6):675-81.
137. de Bono JS, Bellmunt J, Attard G, Droz JP, Miller K, Flechon A, et al. Open-label phase II study evaluating the efficacy and safety of two doses of pertuzumab in castrate chemotherapy-naive patients with hormone-refractory prostate cancer. J Clin Oncol. 2007;25(3):257-62.
138. Carrion-Salip D, Panosa C, Menendez JA, Puig T, Oliveras G, Pandiella A, et al. Androgen-independent prostate cancer cells circumvent EGFR inhibition by overexpression of alternative HER receptors and ligands. International journal of oncology. 2012;41(3):1128-38.
139. Choi BK, Fan X, Deng H, Zhang N, An Z. ERBB3 (HER3) is a key sensor in the regulation of ERBB-mediated signaling in both low and high ERBB2 (HER2) expressing cancer cells. Cancer medicine. 2012;1(1):28-38.
140. Leung HY, Weston J, Gullick WJ, Williams G. A potential autocrine loop between heregulin-alpha and erbB-3 receptor in human prostatic adenocarcinoma. British journal of urology. 1997;79(2):212-6.
141. Soler M, Mancini F, Meca-Cortes O, Sanchez-Cid L, Rubio N, Lopez-Fernandez S, et al. HER3 is required for the maintenance of neuregulin-dependent and -independent attributes of malignant progression in prostate cancer cells. Int J Cancer. 2009;125(11):2565-75.
142. Koumakpayi IH, Diallo JS, Le Page C, Lessard L, Gleave M, Begin LR, et al. Expression and nuclear localization of ErbB3 in prostate cancer. Clin Cancer Res. 2006;12(9):2730-7.
143. Chen L, Siddiqui S, Bose S, Mooso B, Asuncion A, Bedolla RG, et al. Nrdp1-mediated regulation of ErbB3 expression by the androgen receptor in androgen-dependent but not castrate-resistant prostate cancer cells. Cancer Res. 2010;70(14):5994-6003.
144. Lyne JC, Melhem MF, Finley GG, Wen D, Liu N, Deng DH, et al. Tissue expression of neu differentiation factor/heregulin and its receptor complex in prostate cancer and its biologic effects on prostate cancer cells in vitro. The cancer journal from Scientific American. 1997;3(1):21-30.
145. Ghosh PM, Malik S, Bedolla R, Kreisberg JI. Akt in prostate cancer: possible role in androgen-independence. Current drug metabolism. 2003;4(6):487-96.
146. Vanhaesebroeck B, Guillermet-Guibert J, Graupera M, Bilanges B. The emerging mechanisms of isoform-specific PI3K signalling. Nat Rev Mol Cell Biol. 2010;11(5):329-41.
147. Kaplan DR, Whitman M, Schaffhausen B, Pallas DC, White M, Cantley L, et al. Common elements in growth factor stimulation and oncogenic transformation: 85 kd phosphoprotein and phosphatidylinositol kinase activity. Cell. 1987;50(7):1021-9.
148. Zhao L, Vogt PK. Class I PI3K in oncogenic cellular transformation. Oncogene. 2008;27(41):5486-96.
149. Wick MJ, Dong LQ, Riojas RA, Ramos FJ, Liu F. Mechanism of phosphorylation of protein kinase B/Akt by a constitutively active 3-phosphoinositide-dependent protein kinase-1. J Biol Chem. 2000;275(51):40400-6.
150. Aoki M, Blazek E, Vogt PK. A role of the kinase mTOR in cellular transformation induced by the oncoproteins P3k and Akt. Proc Natl Acad Sci U S A. 2001;98(1):136-41.

151. Li J, Yen C, Liaw D, Podsypanina K, Bose S, Wang SI, et al. PTEN, a putative protein tyrosine phosphatase gene mutated in human brain, breast, and prostate cancer. Science (New York, NY). 1997;275(5308):1943-7.
152. Maehama T, Dixon JE. The tumor suppressor, PTEN/MMAC1, dephosphorylates the lipid second messenger, phosphatidylinositol 3,4,5-trisphosphate. J Biol Chem. 1998;273(22):13375-8.
153. Taylor BS, Schultz N, Hieronymus H, Gopalan A, Xiao Y, Carver BS, et al. Integrative genomic profiling of human prostate cancer. Cancer cell. 2010;18(1):11-22.
154. Vivanco I, Sawyers CL. The phosphatidylinositol 3-Kinase AKT pathway in human cancer. Nature reviews Cancer. 2002;2(7):489-501.
155. Jiao J, Wang S, Qiao R, Vivanco I, Watson PA, Sawyers CL, et al. Murine cell lines derived from Pten null prostate cancer show the critical role of PTEN in hormone refractory prostate cancer development. Cancer Res. 2007;67(13):6083-91.
156. Reid AH, Attard G, Ambroisine L, Fisher G, Kovacs G, Brewer D, et al. Molecular characterisation of ERG, ETV1 and PTEN gene loci identifies patients at low and high risk of death from prostate cancer. Br J Cancer. 2010;102(4):678-84.
157. Stambolic V, Suzuki A, de la Pompa JL, Brothers GM, Mirtsos C, Sasaki T, et al. Negative regulation of PKB/Akt-dependent cell survival by the tumor suppressor PTEN. Cell. 1998;95(1):29-39.
158. Kreisberg JI, Malik SN, Prihoda TJ, Bedolla RG, Troyer DA, Kreisberg S, et al. Phosphorylation of Akt (Ser473) is an excellent predictor of poor clinical outcome in prostate cancer. Cancer Res. 2004;64(15):5232-6.
159. Malik SN, Brattain M, Ghosh PM, Troyer DA, Prihoda T, Bedolla R, et al. Immunohistochemical demonstration of phospho-Akt in high Gleason grade prostate cancer. Clin Cancer Res. 2002;8(4):1168-71.
160. Graff JR, Konicek BW, Lynch RL, Dumstorf CA, Dowless MS, McNulty AM, et al. eIF4E activation is commonly elevated in advanced human prostate cancers and significantly related to reduced patient survival. Cancer Res. 2009;69(9):3866-73.
161. Shukla S, Maclennan GT, Hartman DJ, Fu P, Resnick MI, Gupta S. Activation of PI3K-Akt signaling pathway promotes prostate cancer cell invasion. Int J Cancer. 2007;121(7):1424-32.
162. Graff JR, Konicek BW, McNulty AM, Wang Z, Houck K, Allen S, et al. Increased AKT activity contributes to prostate cancer progression by dramatically accelerating prostate tumor growth and diminishing p27Kip1 expression. J Biol Chem. 2000;275(32):24500-5.
163. Jiang BH, Jiang G, Zheng JZ, Lu Z, Hunter T, Vogt PK. Phosphatidylinositol 3-kinase signaling controls levels of hypoxia-inducible factor 1. Cell growth & differentiation : the molecular biology journal of the American Association for Cancer Research. 2001;12(7):363-9.
164. Mahajan K, Coppola D, Challa S, Fang B, Chen YA, Zhu W, et al. Ack1 mediated AKT/PKB tyrosine 176 phosphorylation regulates its activation. PLoS One. 2010;5(3):e9646.
165. Gao M, Patel R, Ahmad I, Fleming J, Edwards J, McCracken S, et al. SPRY2 loss enhances ErbB trafficking and PI3K/AKT signalling to drive human and mouse prostate carcinogenesis. EMBO molecular medicine. 2012;4(8):776-90.

166. Pfeil K, Eder IE, Putz T, Ramoner R, Culig Z, Ueberall F, et al. Long-term androgen-ablation causes increased resistance to PI3K/Akt pathway inhibition in prostate cancer cells. The Prostate. 2004;58(3):259-68.
167. Mulholland DJ, Tran LM, Li Y, Cai H, Morim A, Wang S, et al. Cell autonomous role of PTEN in regulating castration-resistant prostate cancer growth. Cancer cell. 2011;19(6):792-804.
168. Leung JK, Sadar MD. Non-Genomic Actions of the Androgen Receptor in Prostate Cancer. Frontiers in endocrinology. 2017;8:2.
169. Crumbaker M, Khoja L, Joshua AM. AR Signaling and the PI3K Pathway in Prostate Cancer. Cancers. 2017;9(4).
170. Bono JSD, Giorgi UD, Massard C, Bracarda S, Kocak I, Font A, et al. Randomized phase II study of AKT blockade with ipatasertib (GDC-0068) and abiraterone (Abi) vs. Abi alone in patients with metastatic castration-resistant prostate cancer (mCRPC) after docetaxel chemotherapy (A. MARTIN Study). Journal of Clinical Oncology. 2016;34(15_suppl):5017-.
171. Wolf P. Prostate specific membrane antigen as biomarker and therapeutic target for prostate cancer. 2011.
172. Carter RE, Feldman AR, Coyle JT. Prostate-specific membrane antigen is a hydrolase with substrate and pharmacologic characteristics of a neuropeptidase. Proc Natl Acad Sci U S A. 1996;93(2):749-53.
173. O'Keefe DS, Su SL, Bacich DJ, Horiguchi Y, Luo Y, Powell CT, et al. Mapping, genomic organization and promoter analysis of the human prostate-specific membrane antigen gene. Biochimica et biophysica acta. 1998;1443(1-2):113-27.
174. Davis MI, Bennett MJ, Thomas LM, Bjorkman PJ. Crystal structure of prostate-specific membrane antigen, a tumor marker and peptidase. Proc Natl Acad Sci U S A. 2005;102(17):5981-6.
175. Ghosh A, Heston WD. Effect of carbohydrate moieties on the folate hydrolysis activity of the prostate specific membrane antigen. The Prostate. 2003;57(2):140-51.
176. Liu H, Rajasekaran AK, Moy P, Xia Y, Kim S, Navarro V, et al. Constitutive and antibody-induced internalization of prostate-specific membrane antigen. Cancer Res. 1998;58(18):4055-60.
177. Ghosh A, Heston WD. Tumor target prostate specific membrane antigen (PSMA) and its regulation in prostate cancer. Journal of cellular biochemistry. 2004;91(3):528-39.
178. Liu J, Kopeckova P, Buhler P, Wolf P, Pan H, Bauer H, et al. Biorecognition and subcellular trafficking of HPMA copolymer-anti-PSMA antibody conjugates by prostate cancer cells. Molecular pharmaceutics. 2009;6(3):959-70.
179. Israeli RS, Powell CT, Corr JG, Fair WR, Heston WD. Expression of the prostate-specific membrane antigen. Cancer Res. 1994;54(7):1807-11.
180. Lee SJ, Kim HS, Yu R, Lee K, Gardner TA, Jung C, et al. Novel prostate-specific promoter derived from PSA and PSMA enhancers. Molecular therapy : the journal of the American Society of Gene Therapy. 2002;6(3):415-21.
181. Bostwick DG, Pacelli A, Blute M, Roche P, Murphy GP. Prostate specific membrane antigen expression in prostatic intraepithelial neoplasia and adenocarcinoma: a study of 184 cases. Cancer. 1998;82(11):2256-61.

182. Chang SS, Reuter VE, Heston WD, Bander NH, Grauer LS, Gaudin PB. Five different anti-prostate-specific membrane antigen (PSMA) antibodies confirm PSMA expression in tumor-associated neovasculature. Cancer Res. 1999;59(13):3192-8.
183. Luthi-Carter R, Barczak AK, Speno H, Coyle JT. Molecular characterization of human brain N-acetylated alpha-linked acidic dipeptidase (NAALADase). The Journal of pharmacology and experimental therapeutics. 1998;286(2):1020-5.
184. Liu H, Moy P, Kim S, Xia Y, Rajasekaran A, Navarro V, et al. Monoclonal antibodies to the extracellular domain of prostate-specific membrane antigen also react with tumor vascular endothelium. Cancer Res. 1997;57(17):3629-34.
185. Conway RE, Petrovic N, Li Z, Heston W, Wu D, Shapiro LH. Prostate-specific membrane antigen regulates angiogenesis by modulating integrin signal transduction. Molecular and cellular biology. 2006;26(14):5310-24.
186. Lapidus RG, Tiffany CW, Isaacs JT, Slusher BS. Prostate-specific membrane antigen (PSMA) enzyme activity is elevated in prostate cancer cells. The Prostate. 2000;45(4):350-4.
187. Burger MJ, Tebay MA, Keith PA, Samaratunga HM, Clements J, Lavin MF, et al. Expression analysis of delta-catenin and prostate-specific membrane antigen: their potential as diagnostic markers for prostate cancer. Int J Cancer. 2002;100(2):228-37.
188. Kawakami M, Nakayama J. Enhanced expression of prostate-specific membrane antigen gene in prostate cancer as revealed by in situ hybridization. Cancer Res. 1997;57(12):2321-4.
189. Ross JS, Sheehan CE, Fisher HA, Kaufman RP, Jr., Kaur P, Gray K, et al. Correlation of primary tumor prostate-specific membrane antigen expression with disease recurrence in prostate cancer. Clin Cancer Res. 2003;9(17):6357-62.
190. Cao KY, Mao XP, Wang DH, Xu L, Yuan GQ, Dai SQ, et al. High expression of PSM-E correlated with tumor grade in prostate cancer: a new alternatively spliced variant of prostate-specific membrane antigen. The Prostate. 2007;67(16):1791-800.
191. Mannweiler S, Amersdorfer P, Trajanoski S, Terrett JA, King D, Mehes G. Heterogeneity of prostate-specific membrane antigen (PSMA) expression in prostate carcinoma with distant metastasis. Pathology oncology research : POR. 2009;15(2):167-72.
192. Colombatti M, Grasso S, Porzia A, Fracasso G, Scupoli MT, Cingarlini S, et al. The prostate specific membrane antigen regulates the expression of IL-6 and CCL5 in prostate tumour cells by activating the MAPK pathways. PLoS One. 2009;4(2):e4608.
193. Guo Z LY, Du T, Zhang Y, Chen J, Bi L, Lin T, Liu T, Wang W, Xu K, Jiang C, Han J, Zhang C, Dong W, Huang J, Huang H. Prostate specific membrane antigen knockdown impairs the tumorigenicity of LNCaP prostate cancer cells by inhibiting the phosphatidylinositol 3-kinase/Akt signaling pathway. Chin Med J (Engl). 2014;127(5):929-36.
194. Caromile LA, Dortche K, Rahman MM, Grant CL, Stoddard C, Ferrer FA, et al. PSMA redirects cell survival signaling from the MAPK to the PI3K-AKT pathways to promote the progression of prostate cancer. Sci Signal. 2017;10(470).
195. Kaittanis C, Andreou C, Hieronymus H, Mao N, Foss CA, Eiber M, et al. Prostate-specific membrane antigen cleavage of vitamin B9 stimulates oncogenic signaling through metabotropic glutamate receptors. The Journal of experimental medicine. 2018;215(1):159-75.

196. Ahmadzadehfar H, Rahbar K, Kurpig S, Bogemann M, Claesener M, Eppard E, et al. Early side effects and first results of radioligand therapy with (177)Lu-DKFZ-617 PSMA of castrate-resistant metastatic prostate cancer: a two-centre study. EJNMMI research. 2015;5(1):114.
197. Ahmadzadehfar H, Eppard E, Kurpig S, Fimmers R, Yordanova A, Schlenkhoff CD, et al. Therapeutic response and side effects of repeated radioligand therapy with 177Lu-PSMA-DKFZ-617 of castrate-resistant metastatic prostate cancer. Oncotarget. 2016;7(11):12477-88.
198. Rahbar K, Bode A, Weckesser M, Avramovic N, Claesener M, Stegger L, et al. Radioligand Therapy With 177Lu-PSMA-617 as A Novel Therapeutic Option in Patients With Metastatic Castration Resistant Prostate Cancer. Clinical nuclear medicine. 2016;41(7):522-8.
199. Baum RP, Kulkarni HR, Schuchardt C, Singh A, Wirtz M, Wiessalla S, et al. 177Lu-Labeled Prostate-Specific Membrane Antigen Radioligand Therapy of Metastatic Castration-Resistant Prostate Cancer: Safety and Efficacy. Journal of nuclear medicine : official publication, Society of Nuclear Medicine. 2016;57(7):1006-13.
200. Rahbar K, Ahmadzadehfar H, Kratochwil C, Haberkorn U, Schafers M, Essler M, et al. German Multicenter Study Investigating 177Lu-PSMA-617 Radioligand Therapy in Advanced Prostate Cancer Patients. Journal of nuclear medicine : official publication, Society of Nuclear Medicine. 2017;58(1):85-90.
201. Brauer A, Grubert LS, Roll W, Schrader AJ, Schafers M, Bogemann M, et al. (177)Lu-PSMA-617 radioligand therapy and outcome in patients with metastasized castration-resistant prostate cancer. European journal of nuclear medicine and molecular imaging. 2017;44(10):1663-70.
202. Ahmadzadehfar H, Wegen S, Yordanova A, Fimmers R, Kurpig S, Eppard E, et al. Overall survival and response pattern of castration-resistant metastatic prostate cancer to multiple cycles of radioligand therapy using [(177)Lu]Lu-PSMA-617. European journal of nuclear medicine and molecular imaging. 2017;44(9):1448-54.
203. von Eyben FE, Roviello G, Kiljunen T, Uprimny C, Virgolini I, Kairemo K, et al. Third-line treatment and (177)Lu-PSMA radioligand therapy of metastatic castration-resistant prostate cancer: a systematic review. European journal of nuclear medicine and molecular imaging. 2018;45(3):496-508.
204. Study of 177Lu-PSMA-617 In Metastatic Castrate-Resistant Prostate Cancer (VISION).
205. Galsky MD, Eisenberger M, Moore-Cooper S, Kelly WK, Slovin SF, DeLaCruz A, et al. Phase I trial of the prostate-specific membrane antigen-directed immunoconjugate MLN2704 in patients with progressive metastatic castration-resistant prostate cancer. J Clin Oncol. 2008;26(13):2147-54.
206. Kelleher MT, Fruhwirth G, Patel G, Ofo E, Festy F, Barber PR, et al. The potential of optical proteomic technologies to individualize prognosis and guide rational treatment for cancer patients. Targeted oncology. 2009;4(3):235-52.
207. Albrecht C. Joseph R. Lakowicz: Principles of fluorescence spectroscopy, 3rd Edition. Analytical and Bioanalytical Chemistry. 2008;390(5):1223-4.
208. Weitsman G, Barber PR, Nguyen LK, Lawler K, Patel G, Woodman N, et al. HER2-HER3 dimer quantification by FLIM-FRET predicts breast cancer metastatic relapse independently of HER2 IHC status. Oncotarget. 2016;7(32):51012-26.

209. Melo SA, Luecke LB, Kahlert C, Fernandez AF, Gammon ST, Kaye J, et al. Glypican-1 identifies cancer exosomes and detects early pancreatic cancer. Nature. 2015;523(7559):177-82.
210. Chowdhury R, Ganeshan B, Irshad S, Lawler K, Eisenblatter M, Milewicz H, et al. The use of molecular imaging combined with genomic techniques to understand the heterogeneity in cancer metastasis. The British journal of radiology. 2014;87(1038):20140065.
211. Rak J. Microparticles in cancer. Seminars in thrombosis and hemostasis. 2010;36(8):888-906.
212. Raposo G, Stoorvogel W. Extracellular vesicles: exosomes, microvesicles, and friends. The Journal of cell biology. 2013;200(4):373-83.
213. Kowal J, Arras G, Colombo M, Jouve M, Morath JP, Primdal-Bengtson B, et al. Proteomic comparison defines novel markers to characterize heterogeneous populations of extracellular vesicle subtypes. Proc Natl Acad Sci U S A. 2016;113(8):E968-77.
214. Kowal J, Tkach M, Thery C. Biogenesis and secretion of exosomes. Current opinion in cell biology. 2014;29:116-25.
215. Valadi H, Ekstrom K, Bossios A, Sjostrand M, Lee JJ, Lotvall JO. Exosome-mediated transfer of mRNAs and microRNAs is a novel mechanism of genetic exchange between cells. Nature cell biology. 2007;9(6):654-9.
216. Mathivanan S, Fahner CJ, Reid GE, Simpson RJ. ExoCarta 2012: database of exosomal proteins, RNA and lipids. Nucleic acids research. 2012;40(Database issue):D1241-4.
217. Higginbotham JN, Demory Beckler M, Gephart JD, Franklin JL, Bogatcheva G, Kremers GJ, et al. Amphiregulin exosomes increase cancer cell invasion. Curr Biol. 2011;21(9):779-86.
218. Hedlund M, Nagaeva O, Kargl D, Baranov V, Mincheva-Nilsson L. Thermal- and oxidative stress causes enhanced release of NKG2D ligand-bearing immunosuppressive exosomes in leukemia/lymphoma T and B cells. PLoS One. 2011;6(2):e16899.
219. Nilsson J, Skog J, Nordstrand A, Baranov V, Mincheva-Nilsson L, Breakefield XO, et al. Prostate cancer-derived urine exosomes: a novel approach to biomarkers for prostate cancer. Br J Cancer. 2009;100(10):1603-7.
220. Li Z, Ma YY, Wang J, Zeng XF, Li R, Kang W, et al. Exosomal microRNA-141 is upregulated in the serum of prostate cancer patients. OncoTargets and therapy. 2016;9:139-48.
221. Kalluri R. The biology and function of exosomes in cancer. The Journal of clinical investigation. 2016;126(4):1208-15.
222. Greening DW, Gopal SK, Xu R, Simpson RJ, Chen W. Exosomes and their roles in immune regulation and cancer. Seminars in cell & developmental biology. 2015;40:72-81.
223. Ribeiro MF, Zhu H, Millard RW, Fan GC. Exosomes Function in Pro- and Anti-Angiogenesis. Current angiogenesis. 2013;2(1):54-9.
224. Mu W, Rana S, Zoller M. Host matrix modulation by tumor exosomes promotes motility and invasiveness. Neoplasia (New York, NY). 2013;15(8):875-87.
225. Young JD, Abbate V, Imberti C, Meszaros LK, Ma MT, Terry SYA, et al. (68)Ga-THP-PSMA: A PET Imaging Agent for Prostate Cancer Offering Rapid, Room-

Temperature, 1-Step Kit-Based Radiolabeling. Journal of nuclear medicine : official publication, Society of Nuclear Medicine. 2017;58(8):1270-7.
226. Gao H, Ouyang X, Banach-Petrosky WA, Shen MM, Abate-Shen C. Emergence of androgen independence at early stages of prostate cancer progression in Nkx3.1; Pten mice. Cancer Res. 2006;66(16):7929-33.
227. Yao E, Zhou W, Lee-Hoeflich ST, Truong T, Haverty PM, Eastham-Anderson J, et al. Suppression of HER2/HER3-mediated growth of breast cancer cells with combinations of GDC-0941 PI3K inhibitor, trastuzumab, and pertuzumab. Clin Cancer Res. 2009;15(12):4147-56.
228. Tao JJ, Castel P, Radosevic-Robin N, Elkabets M, Auricchio N, Aceto N, et al. Antagonism of EGFR and HER3 enhances the response to inhibitors of the PI3K-Akt pathway in triple-negative breast cancer. Sci Signal. 2014;7(318):ra29.
229. Vlietstra RJ, van Alewijk DC, Hermans KG, van Steenbrugge GJ, Trapman J. Frequent inactivation of PTEN in prostate cancer cell lines and xenografts. Cancer Res. 1998;58(13):2720-3.
230. Tal-Or P, Di-Segni A, Lupowitz Z, Pinkas-Kramarski R. Neuregulin promotes autophagic cell death of prostate cancer cells. The Prostate. 2003;55(2):147-57.
231. Tai S, Sun Y, Squires JM, Zhang H, Oh WK, Liang CZ, et al. PC3 is a cell line characteristic of prostatic small cell carcinoma. The Prostate. 2011;71(15):1668-79.
232. van Bokhoven A, Varella-Garcia M, Korch C, Johannes WU, Smith EE, Miller HL, et al. Molecular characterization of human prostate carcinoma cell lines. The Prostate. 2003;57(3):205-25.
233. Wadosky KM, Koochekpour S. Androgen receptor splice variants and prostate cancer: From bench to bedside. Oncotarget. 2017;8(11):18550-76.
234. Kashiyama T, Oda K, Ikeda Y, Shiose Y, Hirota Y, Inaba K, et al. Antitumor activity and induction of TP53-dependent apoptosis toward ovarian clear cell adenocarcinoma by the dual PI3K/mTOR inhibitor DS-7423. PLoS One. 2014;9(2):e87220.
235. Yokota T TT, Kenmotsu H, et al. PHASE I CLINICAL TRIAL OF DS-7423, AN ORAL PI3K/MTOR DUAL INHIBITOR, IN JAPANESE PATIENTS WITH ADVANCED SOLID TUMORS. Annals of Oncology. 2014.
236. Evans MJ, Smith-Jones PM, Wongvipat J, Navarro V, Kim S, Bander NH, et al. Noninvasive measurement of androgen receptor signaling with a positron-emitting radiopharmaceutical that targets prostate-specific membrane antigen. Proc Natl Acad Sci U S A. 2011;108(23):9578-82.
237. Lin J, Sampath D, Nannini MA, Lee BB, Degtyarev M, Oeh J, et al. Targeting activated Akt with GDC-0068, a novel selective Akt inhibitor that is efficacious in multiple tumor models. Clin Cancer Res. 2013;19(7):1760-72.
238. Ipatasertib Plus Abiraterone Plus Prednisone/Prednisolone, Relative to Placebo Plus Abiraterone Plus Prednisone/Prednisolone in Adult Male Patients With Metastatic Castrate-Resistant Prostate Cancer (IPATential150).
239. Folkes AJ, Ahmadi K, Alderton WK, Alix S, Baker SJ, Box G, et al. The identification of 2-(1H-indazol-4-yl)-6-(4-methanesulfonyl-piperazin-1-ylmethyl)-4-morpholin-4-yl-t hieno[3,2-d]pyrimidine (GDC-0941) as a potent, selective, orally bioavailable inhibitor of class I PI3 kinase for the treatment of cancer. Journal of medicinal chemistry. 2008;51(18):5522-32.

240. Sarker D, Kristeleit R, Mazina KE, Ware JA, Yan Y, Dresser M, et al. A phase I study evaluating the pharmacokinetics (PK) and pharmacodynamics (PD) of the oral pan-phosphoinositide-3 kinase (PI3K) inhibitor GDC-0941. Journal of Clinical Oncology. 2009;27(15S):3538-.
241. Arriola Apelo SI, Neuman JC, Baar EL, Syed FA, Cummings NE, Brar HK, et al. Alternative rapamycin treatment regimens mitigate the impact of rapamycin on glucose homeostasis and the immune system. Aging Cell. 2016;15(1):28-38.
242. Nakabayashi M, Werner L, Courtney KD, Buckle G, Oh WK, Bubley GJ, et al. Phase II trial of RAD001 and bicalutamide for castration-resistant prostate cancer. BJU international. 2012;110(11):1729-35.
243. Templeton AJ, Dutoit V, Cathomas R, Rothermundt C, Bartschi D, Droge C, et al. Phase 2 trial of single-agent everolimus in chemotherapy-naive patients with castration-resistant prostate cancer (SAKK 08/08). European urology. 2013;64(1):150-8.
244. Kim J, Coetzee GA. Prostate specific antigen gene regulation by androgen receptor. Journal of cellular biochemistry. 2004;93(2):233-41.
245. Claus J, Patel G, Autore F, Colomba A, Weitsman G, Soliman TN, et al. Inhibitor-induced HER2-HER3 heterodimerisation promotes proliferation through a novel dimer interface. eLife. 2018;7.
246. Mendell J, Freeman DJ, Feng W, Hettmann T, Schneider M, Blum S, et al. Clinical Translation and Validation of a Predictive Biomarker for Patritumab, an Anti-human Epidermal Growth Factor Receptor 3 (HER3) Monoclonal Antibody, in Patients With Advanced Non-small Cell Lung Cancer. EBioMedicine. 2015;2(3):264-71.
247. Waterman H, Sabanai I, Geiger B, Yarden Y. Alternative intracellular routing of ErbB receptors may determine signaling potency. J Biol Chem. 1998;273(22):13819-27.
248. Baulida J, Kraus MH, Alimandi M, Di Fiore PP, Carpenter G. All ErbB receptors other than the epidermal growth factor receptor are endocytosis impaired. J Biol Chem. 1996;271(9):5251-7.
249. Sak MM, Breen K, Ronning SB, Pedersen NM, Bertelsen V, Stang E, et al. The oncoprotein ErbB3 is endocytosed in the absence of added ligand in a clathrin-dependent manner. Carcinogenesis. 2012;33(5):1031-9.
250. Baulida J, Carpenter G. Heregulin degradation in the absence of rapid receptor-mediated internalization. Experimental cell research. 1997;232(1):167-72.
251. Waterman H, Alroy I, Strano S, Seger R, Yarden Y. The C-terminus of the kinase-defective neuregulin receptor ErbB-3 confers mitogenic superiority and dictates endocytic routing. The EMBO journal. 1999;18(12):3348-58.
252. Worthylake R, Opresko LK, Wiley HS. ErbB-2 amplification inhibits down-regulation and induces constitutive activation of both ErbB-2 and epidermal growth factor receptors. J Biol Chem. 1999;274(13):8865-74.
253. Lenferink AE, Pinkas-Kramarski R, van de Poll ML, van Vugt MJ, Klapper LN, Tzahar E, et al. Differential endocytic routing of homo- and hetero-dimeric ErbB tyrosine kinases confers signaling superiority to receptor heterodimers. The EMBO journal. 1998;17(12):3385-97.

254. Puri C, Tosoni D, Comai R, Rabellino A, Segat D, Caneva F, et al. Relationships between EGFR signaling-competent and endocytosis-competent membrane microdomains. Molecular biology of the cell. 2005;16(6):2704-18.
255. Wiley HS. Trafficking of the ErbB receptors and its influence on signaling. Experimental cell research. 2003;284(1):78-88.
256. Carpentier JL, White MF, Orci L, Kahn RC. Direct visualization of the phosphorylated epidermal growth factor receptor during its internalization in A-431 cells. The Journal of cell biology. 1987;105(6 Pt 1):2751-62.
257. Wallasch C, Weiss FU, Niederfellner G, Jallal B, Issing W, Ullrich A. Heregulin-dependent regulation of HER2/neu oncogenic signaling by heterodimerization with HER3. The EMBO journal. 1995;14(17):4267-75.
258. Lin HK, Yeh S, Kang HY, Chang C. Akt suppresses androgen-induced apoptosis by phosphorylating and inhibiting androgen receptor. Proc Natl Acad Sci U S A. 2001;98(13):7200-5.
259. Wen Y, Hu MC, Makino K, Spohn B, Bartholomeusz G, Yan DH, et al. HER-2/neu promotes androgen-independent survival and growth of prostate cancer cells through the Akt pathway. Cancer Res. 2000;60(24):6841-5.
260. Kirouac DC, Du J, Lahdenranta J, Onsum MD, Nielsen UB, Schoeberl B, et al. HER2+ Cancer Cell Dependence on PI3K vs. MAPK Signaling Axes Is Determined by Expression of EGFR, ERBB3 and CDKN1B. PLoS computational biology. 2016;12(4):e1004827.
261. Fong CJ, Sherwood ER, Mendelsohn J, Lee C, Kozlowski JM. Epidermal growth factor receptor monoclonal antibody inhibits constitutive receptor phosphorylation, reduces autonomous growth, and sensitizes androgen-independent prostatic carcinoma cells to tumor necrosis factor alpha. Cancer Res. 1992;52(21):5887-92.
262. Grasso AW, Wen D, Miller CM, Rhim JS, Pretlow TG, Kung HJ. ErbB kinases and NDF signaling in human prostate cancer cells. Oncogene. 1997;15(22):2705-16.
263. Peles E, Bacus SS, Koski RA, Lu HS, Wen D, Ogden SG, et al. Isolation of the neu/HER-2 stimulatory ligand: a 44 kd glycoprotein that induces differentiation of mammary tumor cells. Cell. 1992;69(1):205-16.
264. Bacus SS, Yarden Y, Oren M, Chin DM, Lyass L, Zelnick CR, et al. Neu differentiation factor (Heregulin) activates a p53-dependent pathway in cancer cells. Oncogene. 1996;12(12):2535-47.
265. Aguilar Z, Akita RW, Finn RS, Ramos BL, Pegram MD, Kabbinavar FF, et al. Biologic effects of heregulin/neu differentiation factor on normal and malignant human breast and ovarian epithelial cells. Oncogene. 1999;18(44):6050-62.
266. Sithanandam G, Anderson LM. The ERBB3 receptor in cancer and cancer gene therapy. Cancer gene therapy. 2008;15(7):413-48.
267. Baron S, Manin M, Beaudoin C, Leotoing L, Communal Y, Veyssiere G, et al. Androgen receptor mediates non-genomic activation of phosphatidylinositol 3-OH kinase in androgen-sensitive epithelial cells. J Biol Chem. 2004;279(15):14579-86.
268. Schoeberl B, Faber AC, Li D, Liang MC, Crosby K, Onsum M, et al. An ErbB3 antibody, MM-121, is active in cancers with ligand-dependent activation. Cancer Res. 2010;70(6):2485-94.
269. Jathal MK, Chen L, Mudryj M, Ghosh PM. Targeting ErbB3: the New RTK(id) on the Prostate Cancer Block. Immunology, endocrine & metabolic agents in medicinal chemistry. 2011;11(2):131-49.

270. Saporita AJ, Zhang Q, Navai N, Dincer Z, Hahn J, Cai X, et al. Identification and characterization of a ligand-regulated nuclear export signal in androgen receptor. J Biol Chem. 2003;278(43):41998-2005.
271. Roy AK, Tyagi RK, Song CS, Lavrovsky Y, Ahn SC, Oh TS, et al. Androgen receptor: structural domains and functional dynamics after ligand-receptor interaction. Ann N Y Acad Sci. 2001;949:44-57.
272. Nawaz Z, Lonard DM, Smith CL, Lev-Lehman E, Tsai SY, Tsai MJ, et al. The Angelman syndrome-associated protein, E6-AP, is a coactivator for the nuclear hormone receptor superfamily. Molecular and cellular biology. 1999;19(2):1182-9.
273. Scaltriti M, Verma C, Guzman M, Jimenez J, Parra JL, Pedersen K, et al. Lapatinib, a HER2 tyrosine kinase inhibitor, induces stabilization and accumulation of HER2 and potentiates trastuzumab-dependent cell cytotoxicity. Oncogene. 2009;28(6):803-14.
274. Brandt BH, Roetger A, Dittmar T, Nikolai G, Seeling M, Merschjann A, et al. c-erbB-2/EGFR as dominant heterodimerization partners determine a motogenic phenotype in human breast cancer cells. FASEB journal : official publication of the Federation of American Societies for Experimental Biology. 1999;13(14):1939-49.
275. Chen X, Yeung TK, Wang Z. Enhanced drug resistance in cells coexpressing ErbB2 with EGF receptor or ErbB3. Biochem Biophys Res Commun. 2000;277(3):757-63.
276. Minner S, Wittmer C, Graefen M, Salomon G, Steuber T, Haese A, et al. High level PSMA expression is associated with early PSA recurrence in surgically treated prostate cancer. The Prostate. 2011;71(3):281-8.
277. Dagvadorj A, Tan S-H, Liao Z, Cavalli LR, Haddad BR, Nevalainen MT. Androgen-regulated and highly tumorigenic human prostate cancer cell line established from a transplantable primary CWR22 tumor. Clinical cancer research : an official journal of the American Association for Cancer Research. 2008;14(19):6062-72.
278. Wainstein MA, He F, Robinson D, Kung HJ, Schwartz S, Giaconia JM, et al. CWR22: androgen-dependent xenograft model derived from a primary human prostatic carcinoma. Cancer Res. 1994;54(23):6049-52.
279. Nagabhushan M, Miller CM, Pretlow TP, Giaconia JM, Edgehouse NL, Schwartz S, et al. CWR22: the first human prostate cancer xenograft with strongly androgen-dependent and relapsed strains both in vivo and in soft agar. Cancer Res. 1996;56(13):3042-6.
280. Sramkoski RM, Pretlow TG, 2nd, Giaconia JM, Pretlow TP, Schwartz S, Sy MS, et al. A new human prostate carcinoma cell line, 22Rv1. In vitro cellular & developmental biology Animal. 1999;35(7):403-9.
281. Festuccia C, Muzi P, Millimaggi D, Biordi L, Gravina GL, Speca S, et al. Molecular aspects of gefitinib antiproliferative and pro-apoptotic effects in PTEN-positive and PTEN-negative prostate cancer cell lines. Endocrine-related cancer. 2005;12(4):983-98.
282. Fraser M, Zhao H, Luoto KR, Lundin C, Coackley C, Chan N, et al. PTEN deletion in prostate cancer cells does not associate with loss of RAD51 function: implications for radiotherapy and chemotherapy. Clin Cancer Res. 2012;18(4):1015-27.

283. Tepper CG, Boucher DL, Ryan PE, Ma AH, Xia L, Lee LF, et al. Characterization of a novel androgen receptor mutation in a relapsed CWR22 prostate cancer xenograft and cell line. Cancer Res. 2002;62(22):6606-14.
284. Han EK, Leverson JD, McGonigal T, Shah OJ, Woods KW, Hunter T, et al. Akt inhibitor A-443654 induces rapid Akt Ser-473 phosphorylation independent of mTORC1 inhibition. Oncogene. 2007;26(38):5655-61.
285. Rhodes N, Heerding DA, Duckett DR, Eberwein DJ, Knick VB, Lansing TJ, et al. Characterization of an Akt kinase inhibitor with potent pharmacodynamic and antitumor activity. Cancer Res. 2008;68(7):2366-74.
286. Holden P, Horton WA. Crude subcellular fractionation of cultured mammalian cell lines. BMC research notes. 2009;2:243.
287. Day KC, Lorenzatti Hiles G, Kozminsky M, Dawsey SJ, Paul A, Broses LJ, et al. HER2 and EGFR Overexpression Support Metastatic Progression of Prostate Cancer to Bone. Cancer Res. 2017;77(1):74-85.
288. Pugh CW, Ratcliffe PJ. Regulation of angiogenesis by hypoxia: role of the HIF system. Nature medicine. 2003;9(6):677-84.
289. Branco-Price C, Zhang N, Schnelle M, Evans C, Katschinski DM, Liao D, et al. Endothelial cell HIF-1alpha and HIF-2alpha differentially regulate metastatic success. Cancer cell. 2012;21(1):52-65.
290. Wang SC, Lien HC, Xia W, Chen IF, Lo HW, Wang Z, et al. Binding at and transactivation of the COX-2 promoter by nuclear tyrosine kinase receptor ErbB-2. Cancer cell. 2004;6(3):251-61.
291. Beguelin W, Diaz Flaque MC, Proietti CJ, Cayrol F, Rivas MA, Tkach M, et al. Progesterone receptor induces ErbB-2 nuclear translocation to promote breast cancer growth via a novel transcriptional effect: ErbB-2 function as a coactivator of Stat3. Molecular and cellular biology. 2010;30(23):5456-72.
292. Cordo Russo RI, Beguelin W, Diaz Flaque MC, Proietti CJ, Venturutti L, Galigniana N, et al. Targeting ErbB-2 nuclear localization and function inhibits breast cancer growth and overcomes trastuzumab resistance. Oncogene. 2015;34(26):3413-28.
293. Schillaci R, Guzman P, Cayrol F, Beguelin W, Diaz Flaque MC, Proietti CJ, et al. Clinical relevance of ErbB-2/HER2 nuclear expression in breast cancer. BMC cancer. 2012;12:74.
294. Kusumi T, Koie T, Tanaka M, Matsumoto K, Sato F, Kusumi A, et al. Immunohistochemical detection of carcinoma in radical prostatectomy specimens following hormone therapy. Pathology international. 2008;58(11):687-94.
295. Perico ME, Grasso S, Brunelli M, Martignoni G, Munari E, Moiso E, et al. Prostate-specific membrane antigen (PSMA) assembles a macromolecular complex regulating growth and survival of prostate cancer cells "in vitro" and correlating with progression "in vivo". Oncotarget. 2016;7(45):74189-202.
296. Brugge J, Hung MC, Mills GB. A new mutational AKTivation in the PI3K pathway. Cancer cell. 2007;12(2):104-7.
297. Clark AS, West K, Streicher S, Dennis PA. Constitutive and inducible Akt activity promotes resistance to chemotherapy, trastuzumab, or tamoxifen in breast cancer cells. Molecular cancer therapeutics. 2002;1(9):707-17.

298. Tzahar E, Pinkas-Kramarski R, Moyer JD, Klapper LN, Alroy I, Levkowitz G, et al. Bivalence of EGF-like ligands drives the ErbB signaling network. The EMBO journal. 1997;16(16):4938-50.
299. Pfestroff A, Luster M, Jilg CA, Olbert PJ, Ohlmann CH, Lassmann M, et al. Current status and future perspectives of PSMA-targeted therapy in Europe: opportunity knocks. European journal of nuclear medicine and molecular imaging. 2015;42(13):1971-5.
300. Rahbar K, Afshar-Oromieh A, Jadvar H, Ahmadzadehfar H. PSMA Theranostics: Current Status and Future Directions. Molecular imaging. 2018;17:1536012118776068.
301. Hummel H-D, Kufer P, Grüllich C, Deschler-Baier B, Chatterjee M, Goebeler M-E, et al. Phase 1 study of pasotuxizumab (BAY 2010112), a PSMA-targeting Bispecific T cell Engager (BiTE) immunotherapy for metastatic castration-resistant prostate cancer (mCRPC). Journal of Clinical Oncology. 2019;37(15_suppl):5034-.
302. Bailis J, Deegen P, Thomas O, Bogner P, Wahl J, Liao M, et al. Preclinical evaluation of AMG 160, a next-generation bispecific T cell engager (BiTE) targeting the prostate-specific membrane antigen PSMA for metastatic castration-resistant prostate cancer (mCRPC). Journal of Clinical Oncology. 2019;37(7_suppl):301-.
303. Narayan V, Gladney W, Plesa G, Vapiwala N, Carpenter E, Maude SL, et al. A phase I clinical trial of PSMA-directed/TGFβ-insensitive CAR-T cells in metastatic castration-resistant prostate cancer. Journal of Clinical Oncology. 2019;37(7_suppl):TPS347-TPS.
304. Silver DA, Pellicer I, Fair WR, Heston WD, Cordon-Cardo C. Prostate-specific membrane antigen expression in normal and malignant human tissues. Clin Cancer Res. 1997;3(1):81-5.
305. Mhawech-Fauceglia P, Zhang S, Terracciano L, Sauter G, Chadhuri A, Herrmann FR, et al. Prostate-specific membrane antigen (PSMA) protein expression in normal and neoplastic tissues and its sensitivity and specificity in prostate adenocarcinoma: an immunohistochemical study using mutiple tumour tissue microarray technique. Histopathology. 2007;50(4):472-83.
306. Wright GL, Jr., Grob BM, Haley C, Grossman K, Newhall K, Petrylak D, et al. Upregulation of prostate-specific membrane antigen after androgen-deprivation therapy. Urology. 1996;48(2):326-34.
307. Sweat SD, Pacelli A, Murphy GP, Bostwick DG. Prostate-specific membrane antigen expression is greatest in prostate adenocarcinoma and lymph node metastases. Urology. 1998;52(4):637-40.
308. Minciacchi VR, Zijlstra A, Rubin MA, Di Vizio D. Extracellular vesicles for liquid biopsy in prostate cancer: where are we and where are we headed? Prostate Cancer Prostatic Dis. 2017;20(3):251-8.
309. Jansen FH, Krijgsveld J, van Rijswijk A, van den Bemd GJ, van den Berg MS, van Weerden WM, et al. Exosomal secretion of cytoplasmic prostate cancer xenograft-derived proteins. Molecular & cellular proteomics : MCP. 2009;8(6):1192-205.
310. Liu CM, Hsieh CL, Shen CN, Lin CC, Shigemura K, Sung SY. Exosomes from the tumor microenvironment as reciprocal regulators that enhance prostate cancer progression. International journal of urology : official journal of the Japanese Urological Association. 2016;23(9):734-44.

311. Shiao SL, Chu GC, Chung LW. Regulation of prostate cancer progression by the tumor microenvironment. Cancer letters. 2016;380(1):340-8.
312. De Marzo AM, Platz EA, Sutcliffe S, Xu J, Gronberg H, Drake CG, et al. Inflammation in prostate carcinogenesis. Nature reviews Cancer. 2007;7(4):256-69.
313. Patel GS, Kiuchi T, Lawler K, Ofo E, Fruhwirth GO, Kelleher M, et al. The challenges of integrating molecular imaging into the optimization of cancer therapy. Integrative biology : quantitative biosciences from nano to macro. 2011;3(6):603-31.
314. Weitsman G, Lawler K, Kelleher MT, Barrett JE, Barber PR, Shamil E, et al. Imaging tumour heterogeneity of the consequences of a PKCalpha-substrate interaction in breast cancer patients. Biochemical Society transactions. 2014;42(6):1498-505.
315. Ng T, Squire A, Hansra G, Bornancin F, Prevostel C, Hanby A, et al. Imaging protein kinase Calpha activation in cells. Science (New York, NY). 1999;283(5410):2085-9.
316. Coban O, Zanetti-Dominguez LC, Matthews DR, Rolfe DJ, Weitsman G, Barber PR, et al. Effect of phosphorylation on EGFR dimer stability probed by single-molecule dynamics and FRET/FLIM. Biophysical journal. 2015;108(5):1013-26.
317. Kiuchi T, Ortiz-Zapater E, Monypenny J, Matthews DR, Nguyen LK, Barbeau J, et al. The ErbB4 CYT2 variant protects EGFR from ligand-induced degradation to enhance cancer cell motility. Sci Signal. 2014;7(339):ra78.
318. Tony Ng FF-B, Giovanna Alfano, Paul Barber, Gregory Weitsman, Felix Wong, Jose Vicencio, Myria Galazi, Jana Doyle, Jonathan Greenberg, Martin David Forster, Anthonius Coolen. The use of exosome and immune profiling to analyze a phase 2 study on the addition of patritumab or placebo to cetuximab and a platinum agent for recurrent / metastatic head and neck cancer (R/M HNSCC) patients. J Clin Oncol 36, 2018 (suppl; abstr 6043). 2018
.
319. Bartel DP. MicroRNAs: genomics, biogenesis, mechanism, and function. Cell. 2004;116(2):281-97.
320. He L, Hannon GJ. MicroRNAs: small RNAs with a big role in gene regulation. Nature reviews Genetics. 2004;5(7):522-31.
321. Calin GA, Croce CM. MicroRNA signatures in human cancers. Nature reviews Cancer. 2006;6(11):857-66.
322. Fujita Y, Kojima K, Hamada N, Ohhashi R, Akao Y, Nozawa Y, et al. Effects of miR-34a on cell growth and chemoresistance in prostate cancer PC3 cells. Biochem Biophys Res Commun. 2008;377(1):114-9.
323. Song B, Wang Y, Xi Y, Kudo K, Bruheim S, Botchkina GI, et al. Mechanism of chemoresistance mediated by miR-140 in human osteosarcoma and colon cancer cells. Oncogene. 2009;28(46):4065-74.
324. Ribas J, Ni X, Haffner M, Wentzel EA, Salmasi AH, Chowdhury WH, et al. miR-21: an androgen receptor-regulated microRNA that promotes hormone-dependent and hormone-independent prostate cancer growth. Cancer Res. 2009;69(18):7165-9.
325. Shi GH, Ye DW, Yao XD, Zhang SL, Dai B, Zhang HL, et al. Involvement of microRNA-21 in mediating chemo-resistance to docetaxel in androgen-independent prostate cancer PC3 cells. Acta pharmacologica Sinica. 2010;31(7):867-73.

326. Fabbri M, Paone A, Calore F, Galli R, Gaudio E, Santhanam R, et al. MicroRNAs bind to Toll-like receptors to induce prometastatic inflammatory response. Proc Natl Acad Sci U S A. 2012;109(31):E2110-6.
327. Punwani S. Localising Occult Prostate Cancer Metastases With Advanced Imaging TEchniques (LOCATE). 2015.
328. Eldh M, Lotvall J, Malmhall C, Ekstrom K. Importance of RNA isolation methods for analysis of exosomal RNA: evaluation of different methods. Molecular immunology. 2012;50(4):278-86.
329. Kharaziha P, Chioureas D, Rutishauser D, Baltatzis G, Lennartsson L, Fonseca P, et al. Molecular profiling of prostate cancer derived exosomes may reveal a predictive signature for response to docetaxel. Oncotarget. 2015;6(25):21740-54.
330. Liu T, Mendes DE, Berkman CE. Functional prostate-specific membrane antigen is enriched in exosomes from prostate cancer cells. International journal of oncology. 2014;44(3):918-22.
331. Sandvig K, Llorente A. Proteomic analysis of microvesicles released by the human prostate cancer cell line PC-3. Molecular & cellular proteomics : MCP. 2012;11(7):M111.012914.
332. Webber J, Stone TC, Katilius E, Smith BC, Gordon B, Mason MD, et al. Proteomics analysis of cancer exosomes using a novel modified aptamer-based array (SOMAscan) platform. Molecular & cellular proteomics : MCP. 2014;13(4):1050-64.
333. Bijnsdorp IV, Geldof AA, Lavaei M, Piersma SR, van Moorselaar RJ, Jimenez CR. Exosomal ITGA3 interferes with non-cancerous prostate cell functions and is increased in urine exosomes of metastatic prostate cancer patients. Journal of extracellular vesicles. 2013;2.
334. Overbye A, Skotland T, Koehler CJ, Thiede B, Seierstad T, Berge V, et al. Identification of prostate cancer biomarkers in urinary exosomes. Oncotarget. 2015;6(30):30357-76.
335. Lu Q, Zhang J, Allison R, Gay H, Yang WX, Bhowmick NA, et al. Identification of extracellular delta-catenin accumulation for prostate cancer detection. The Prostate. 2009;69(4):411-8.
336. Khan S, Jutzy JM, Valenzuela MM, Turay D, Aspe JR, Ashok A, et al. Plasma-derived exosomal survivin, a plausible biomarker for early detection of prostate cancer. PLoS One. 2012;7(10):e46737.
337. Corcoran C, Rani S, O'Driscoll L. miR-34a is an intracellular and exosomal predictive biomarker for response to docetaxel with clinical relevance to prostate cancer progression. The Prostate. 2014;74(13):1320-34.
338. Huang X, Yuan T, Liang M, Du M, Xia S, Dittmar R, et al. Exosomal miR-1290 and miR-375 as prognostic markers in castration-resistant prostate cancer. European urology. 2015;67(1):33-41.
339. Kahlert C, Melo SA, Protopopov A, Tang J, Seth S, Koch M, et al. Identification of double-stranded genomic DNA spanning all chromosomes with mutated KRAS and p53 DNA in the serum exosomes of patients with pancreatic cancer. J Biol Chem. 2014;289(7):3869-75.
340. Thakur BK, Zhang H, Becker A, Matei I, Huang Y, Costa-Silva B, et al. Double-stranded DNA in exosomes: a novel biomarker in cancer detection. Cell research. 2014;24(6):766-9.

341. Yap TA, Smith AD, Ferraldeschi R, Al-Lazikani B, Workman P, de Bono JS. Drug discovery in advanced prostate cancer: translating biology into therapy. Nature reviews Drug discovery. 2016;15(10):699-718.
342. Yap TA, Zivi A, Omlin A, de Bono JS. The changing therapeutic landscape of castration-resistant prostate cancer. Nature reviews Clinical oncology. 2011;8(10):597-610.

Appendix 1

LOCATE

Localising Occult prostate Cancer metastasis with Advanced imaging TEchniques

Project Protocol Version 1
3rd of March 2015

Table of Contents

1.0 Investigators

Dr Shonit Punwani (Principal investigator)- Reader in Magnetic Resonance and Cancer Imaging (UCL) and Honarary Consultant Radiologist (UCLH)

Dr Simon Chowdhury- Consultant Medical Oncologist, Guys and St. Thomas Hospital

Professor Tony Ng- Professor of Cancer Research, Department of Cancer Research, King's College London

Mr Hashim Ahmed- MRC Clinician Scientist & Clinical Lecturer in Urology, UCL

Professor Anthony Coolen- Professor of Applied Mathematics, King's College London

Dr Manit Arya- Senior Lecturer and Honarary Consultant Urological Surgeon, UCL

Dr Haether Ann Payne- Consultant Oncologist, University College London Hospital

Dr Maria Lioumi- Project Manager, Kings College London

Professor Gary Cook- Professor of PET Imaging, Kings College London

Professor Stephen Morris, Professor of Health economics, UCL

Dr Athar Haroon, Consultant Radiologist and Nuclear Medicine Physician, St Bartholmew's hospital

Dr Sue Chua, Consultant radiologist and Nuclear Medicine Physician, Royal Marsden Hospital

Dr Jamshed Bomanji, Consultant Radiologist and Nuclear Medicine Physician, UCLH

Dr Alex Freeman, Consultant Histopathologist, UCLH

Dr Manuel Rodriguez-Justo, Consultant Histopathologist, UCLH

Dr Harbir Sidhu, Radiology Clinical Research Fellow, UCL, UCLH

Dr Arash Latifoltojar, Radiology Clinical Research Fellow, UCL

Dr Myria Galazi, Clinical Research Fellow, UCL Cancer Institute

Acronyms:

ADT: Androgen Deprivation Therapy

CT: Computed Tomography

EBRT: External Beam Radiotherapy Brachytherapy

EPI: Echo Planar Imaging

FN: False Negative

FORECAST: FOcal RECurrent Assessment and Salvage Treatment

GCP: Good Clinical Practice

HER: Human Epidermal growth Receptor

ICER: Incremental Cost Effectiveness Ratio

LOCATE: Localising Occult prostate Cancer metastasis with Advanced imaging TEchniques

MRI: Magnetic Resonance Imaging

PCUK: Prostate Cancer UK

PET: Positron Emission Tomography

PSA: Prostate Specific Antigen

QALY: Quality Adjusted Life Year

RIS: Radiology Information System

TP: True Positive

UCL: University College London

UCLH: University College London Hospital

WBMRI: Whole Body Magnetic Resonance Imaging

2.0 Protocol Summary

2.1 Summary of trial design

Title:	Whole body multi-parametric MRI: Accuracy in staging of biochemically relapsed prostate cancer
Short Title:	LOCATE: **L**ocalising **O**ccult prostate **C**ancer metastases with **A**dvanced imaging **TE**chniques
Sponsor Name:	UCL
Funder Name:	Prostate Cancer UK (PCUK)
Design:	Prospective cohort study
Overall Aim:	To prospectively compare diagnostic concordance of whole body multi-parametric Magnetic Resonance Imaging (MRI) with current conventional multi-modality reference standard imaging (CT scan, isotope bone scan +/- PET-CT scan) for staging of prostate cancer patients with biochemical relapse following external beam radiotherapy or brachytherapy of locally advanced prostate cancer
Primary outcome:	The per site sensitivity and specificity of whole body multi-parametric MRI for nodal and distant metastasis
Secondary outcomes:	1.0 Diagnostic performance of MRI for the assessment of the extent of the recurrent prostate cancer compared to choline PET-CT 2.0 Interobserver agreement of MRI for disease staging 3.0 Derivation and evaluation of quantitative MRI signal heterogeneity indices of metastatic disease as predictors of treatment response to androgen deprivation therapy (ADT) 4.0 Exploration of the Human Epidermal growth factor Receptor (HER) activated dimer in metastatic castration-resistant prostate cancer 5.0 Cost-effectiveness of whole-body multi-parametric MRI for metastatic disease staging compared with conventional staging with computed tomography and bone-scan

Recruitment target:	One-hundred and thirty patients
Planned Number of Sites:	**Two** - University College London Hospital - Guys and St Thomas Hospital
Inclusion and Exclusion Criteria:	**Inclusion Criteria:** 1.0 Men who have undergone previous external beam radiotherapy or brachytherapy with or without neo-adjuvant/adjuvant hormone therapy 2.0 Men who have radiorecurrent disease defined by biochemical failure – Phoenix definition (PSA nadir + 2 ng/ml) **Exclusion Criteria:** 1.0 Men unable to have MRI scan, or in whom artefact would significantly reduce quality of MRI 2.0 Men unable to give informed consent
Anticipated duration of recruitment:	Thirty-six months
Duration of patient follow up:	For one year or until death
Definition of end of trial:	*Recruitment:* Last patient undergoes staging MRI *Active:* Last recruited patients undergoes 1 year follow up MRI and/or undergoes suspected metastatic site biopsy

2.2 Trial Schema

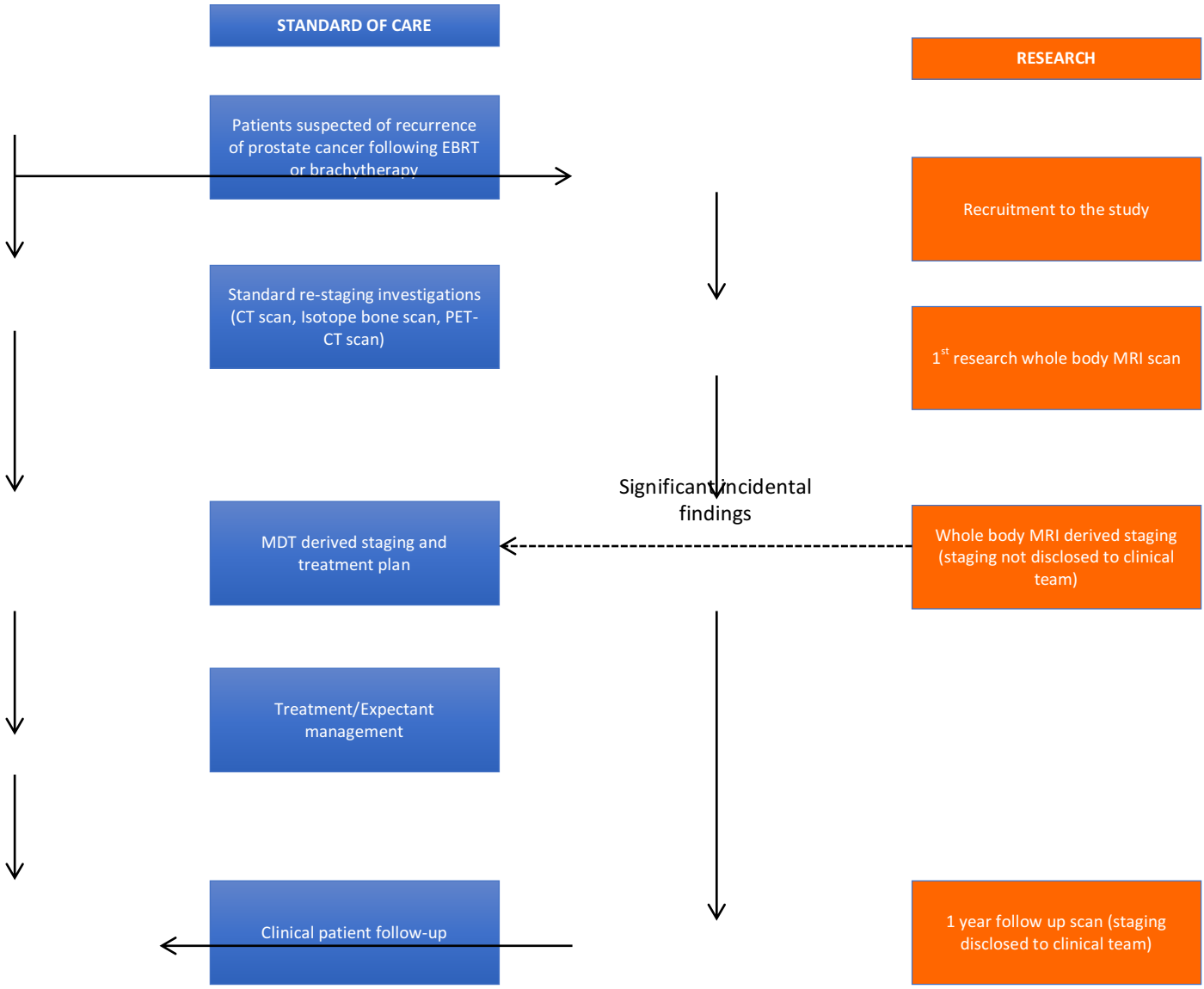

3.0 Introduction

3.1 Background

Locally advanced (T3/4; T (any), N1-2) and metastatic prostate cancer is a lethal disease and mortality within this group is primarily from prostate cancer rather than from other causes as previously thought [1]. Whilst locally advanced disease is often treated with local therapies (external beam radiotherapy (EBRT) / brachytherapy), biochemical failure of therapy occurs in 25% of treated men at 5 years [2]. Failure of local therapy initiates an imaging based assessment for metastatic disease; yet metastatic disease is difficult to detect on conventional imaging (CT and bone-scan) unless PSA level are very high (PSA > 20 ng/mL) [3], and so most men within this group have negative imaging findings and irrespective of biochemical failure undergo expectant management awaiting disease progression [4].

This is not an unreasonable strategy as escalation to androgen deprivation therapy (ADT) (if not previously administered) itself has potential toxicity such as hot flushes, breast tenderness/enlargement, lethargy; osteopenia, osteoporosis; cognitive impairment; and metabolic syndrome [5]. Where metastatic disease is detected on conventional imaging the UK STAMPEDE study suggests that with ADT alone median progression free survival (PFS) is only 12 months [6].

We hypothesize that the poor outcome in this group of patients is a consequence of poor patient stratification, with:

(i) An inability to select patients appropriately from within the biochemical failure group;

(ii) And an inability to predict whether any given patient will benefit from ADT.

This stems from the fact that biochemical monitoring does not necessarily provide the best reflection of disease status; with the over reliance on biochemical monitoring itself a consequence of flaws with conventional imaging staging methods:

- Sensitivity for metastatic disease detection on CT is low; sub-centimetre metastatic lymph nodes are incorrectly ascribed as normal and early bone lesions are not visible [7]
- Bone scan is insensitive for early disease detection as it images the reaction within bone of the presence of disease rather than the disease process itself [8]

There is a clearly recognised and pressing need for development of imaging biomarkers to better detect disease, monitor treatment and potentially predict response to guide therapy [9]. Magnetic Resonance Imaging (MRI) methods may offer a solution. Recent technological advances have enabled the reliable whole-body MRI staging of cancers within a reasonable scanning time [10,11]. Furthermore, multi-parametric MRI (T1, T2, contrast enhanced and diffusion weighted) of the

prostate shows promise for detection of local disease within the prostate and is set to revolutionise the management of early stage disease [12].

We have developed and assessed the feasibility of performing whole-body multi-parametric MRI for staging metastatic disease. We hypothesize that a whole body multi-parametric MRI will be more sensitive and specific than conventional imaging staging for detection of metastatic disease in patients with biochemical failure following local therapies. We therefore propose a comparative trial of conventional imaging verses whole-body multi-parametric MRI within this population of men. We would further like to explore whether heterogeneity between metastases of multi-parametric MRI signals can predict men unlikely to respond to ADT. We aim to enhance the main study by exploratory work on exosome, pathway and genomic analysis, the results of which could lead to complimentary imaging / non-imaging biomarker combinations of clinical utility for patient stratification Finally we will perform a health economic analysis to assess the cost-effectiveness of whole-body multi-parametric MRI for metastatic disease staging compared with conventional staging with computed tomography and bone-scans.

3.2 Proposed Trial

Multi-centre prospective cohort study of patients with prostate cancer, presenting with biochemical failure following external beam radiotherapy or brachytherapy, being evaluated for local recurrence and metastatic disease spread.

4.0 Aim/Outcomes

To prospectively compare diagnostic concordance of whole body multi-parametric Magnetic Resonance Imaging (MRI) with current conventional multi-modality reference standard imaging (CT scan, isotope bone scan +/- PET-CT scan) for staging of prostate cancer patients with biochemical relapse following external beam radiotherapy or brachytherapy of locally advanced prostate cancer.

4.1 Primary Outcome

The per site sensitivity and specificity of whole body multi-parametric MRI for nodal and distant metastasis

4.2 Secondary Outcomes

1.0 Diagnostic performance of MRI for the assessment of the extent of the recurrent prostate cancer compared to choline PET-CT

2.0 Interobserver agreement of MRI for disease staging

3.0 Derivation and evaluation of quantitative MRI signal heterogeneity indicies of metastatic disease as predictors of treatment response to androgen deprivation therapy (ADT)

4.0 Exploration of the significance of the Human Epidermal growth factor Receptor (HER) activated dimer in metastatic castration-resistant prostate cancer

5.0 Cost-effectiveness of whole-body multi-parametric MRI for metastatic disease staging compared with conventional staging with computed tomography and bone-scan

5.0 Cohort

5.1 Patient Eligibility

There will be no exception to the eligibility requirements. Queries in relation to the eligibility criteria should be addressed prior to enrollment. Patients are eligible for the trial if all the inclusion criteria are met and none of the exclusion criteria applies.

5.1.1 Patient Inclusion Criteria

- Men who have undergone previous external beam radiotherapy or brachytherapy with or without neo-adjuvant/adjuvant hormone therapy
- Men who have radiorecurrent disease defined by biochemical failure – Phoenix definition (PSA nadir + 2 ng/mL)

5.1.2 Patient Exclusion Criteria

- Men unable to have MRI scan, or in whom artefact would significantly reduce quality of MRI
- Men unable to give informed consent

6.0 Recruitment

There will be 3 entry points into the trial:

1. Patients already recruited to FORECAST study: As part of FORECAST trial (REC NO: 13/0204), patient with biochemical failure will undergo a baseline whole body MRI study. These patients will be identified by the FORECAST trial team and their details passed onto the LOCATE trial team (note that investigators overlap between the two studies). Potential participants for LOCATE will be approached for a repeat follow-up 1-year whole body MRI scan and blood tests.

2. Patients eligible for the LOCATE study that do not participate within the FORECAST trial will directly be enrolled from relevant clinics at UCLH
3. Patients eligible for the study, and expressing an interest to participate, will be identified at Guys and St Thomas NHS trust by Dr Simon Chowdhury (Consultant Oncologist, Guys and St Thomas NHS Trust). They will be provided the patient information sheet and sample consent for the LOCATE trial and referred to the UCLH oncology clinic (Dr Heather Payne, Consultant Oncologist, UCLH).

In all cases, patient information sheets and sample consent forms will be made available to patients a minimum of 24 hours prior to the consent procedure. Following dissemination of these, patients will be contacted to arrange an appointment for the MRI scan/blood test. Consent will be obtained at the time of the appointment and prior to commencement of any trial intervention. Patients will be asked to arrive half an hour before the scheduled time. They will be met and greeted by a nominated member of the trial team who will go through the patient information sheet and undertake written informed consent. A signed copy of the consent form will be stored in the site file and also be provided to patients for their records.

7.0 Intervention

7.1 Standard of care interventions

Recruited patients will undergo the standard imaging protocol employed at UCLH or Guys and St Thomas hospital. The standard imaging study compromise of the following:

7.1.1 Multi-parametric prostate MRI

A standard minimum mp-MRI protocol as defined by the UK consensus guidelines on prostate MRI [13] will be used. Conventional T1 and T2-weighted images are acquired of the prostate in accordance with the standard imaging protocol employed by each hospital site. Anatomical images are supplemented by diffusion weighted imaging (as per hospital site protocol); and +/- axial T1 images during dynamic contrast enhancement.

7.1.2 Computed Tomography

Routine CT staging scans of the chest/abdomen/pelvis will be performed with intravenous contrast using the standard staging protocol for CT scan at hospital site.

7.1.3 Isotope Bone Scan

Bone scans will be performed using Technetium-99m labelled diphosphonates administered through intravenous injection. For prostate cancer patients with suspected bony metastasis, the standard protocol employed at the hospital site will be used. As a guide, whole body imaging is conventionally performed with anterior and posterior views, 256 x 1024 matrix and energy window(s) of 140 KeV. Effective dose (ED) is 3mSv (or 5mSv for Cancer patients) and Diagnostic Reference Level (DRL) is 600 MBq (0r 800 for Cancer patients).

7.1.4 Positron Emission Tomography (PET)- CT Imaging

Where performed during routine clinical care, a choline PET-CT study will be obtained. As a guide, a dedicated combined PET/64-detector-CT (VCT-XT Discovery, GE-Healthcare Technology, Waukesha, WI), CT is performed (for attenuation correction) using 64x3.75 mm detectors, a pitch of 1.5 and a 5 mm collimation (140 kVp and 80 mA in 0.8 s). Maintaining the patient position, a whole-body Choline PET emission scan is performed and covers an area identical to that covered by CT. Acquisitions are carried out in 2D and 3D mode (4 min/bed position). Transaxial subsets expectation maximization with two iterations and 28 subsets will be used. The axial field of view is 148.75 mm, resulting in 47 slices per bed position.

7.2 Trial specific interventions

7.2.1 Multi-parametric whole-body MRI

Recruited patients will undergo a multi-parametric whole body MRI on presentation with biochemical failure (staging) and then at 12 months (follow-up). All MRIs will be performed at UCLH on a 3T MRI scanner. The MRI protocol will be limited to a maximum of 1 hour scan time and will be standardized. The following MRI sequences will be used:

Morphological (T1- weighted) Imaging

Pre-contrast T1 mDIXON breath-held coronal imaging with two flip angles (2.5 and 15 degrees) and multiple stacks covering head to mid-thigh will be acquired. This sequence is considered as morphological imaging in this protocol and provides a superior soft tissue and bone contrast images in a fairly short amount of time. By

using two flip angles, we can quantify T1 values at these flip angles for the comparison of changes at baseline and follow up whole body MRI imaging.

Morphological T2-weighted imaging

Axial T2 weighted turbo-spin-echo (TSE) anatomical images, covering head to mid-thigh will be acquired from patients in free breathing. These images are mainly provide excellent morphological data for investigating the nodal and extra-nodal involvement in recurrent prostate cancer and would be helpful for characterizing and localizing suspected metastasis identified on functional (DWI and post-contrast MRI) MRI sequences.

Diffusion Weighted MRI Imaging (DWI)

Axial fat suppressed free breathing echo planar imaging (EPI) DWI with 2-b values (b0 and b1000 s/mm^2) with matched resolution and coverage to axial T2 imaging will be acquired.

Diffusion-weighted MRI is sensitive to molecular diffusion due to random and microscopic translational motion of molecules, known as Brownian motion, because random motion in the field gradient produces incoherent phase shifts that result in signal attenuation. The areas involved with metastasis appear bright on diffusion weighted images which, when added to morphological images, aid in diagnosis of suspected area of involvement.

Post-Contrast T1-weighted imaging

After administration of intra venous (IV) gadolinium (Gd) based contrast agent at standard dose of 0.1 mmol/kg, a repeat T1 mDIXON breath-held imaging with one flip angle (15 degrees) will be performed covering vertex to toe. Post contrast MRI investigates the vascularity of tumours, as malignancies are often manifest by an

increase in new vessels formation and an increase uptake of contrast material. Gd reduces T1 relaxation time leading to diseased tissue appearing bright on post-contrast T1 weighted MRI.

7.2.2 Blood samples

Blood will be taken from recruited patients, by an appropriately trained member of the trial team, at the time of each multi-parametric whole body MRI (staging and then at 12 month follow-up). The cannula will be inserted for the injection of MRI contrast will be used to withdraw blood. Blood samples will be used for exosome and phenotypic (FACS analysis)/DNA-RNA analysis. In total a maximum of 50 ml of blood will be taken:

- up to 3 Acid Citrate Dextrose Solution (ACD)tubes (yellow-capped tubes): to collect ~25 ml blood for serum separation
- up to 4 EDTA containing (purple-capped) tubes for PBMC's isolation and further FACS analysis, functional assays, and DNA/RNA isolation.

Frozen aliquots-samples will be transported by courier service in dry ice-containing carrier boxes within 24 hours after obtaining the blood sample. Samples will be processed at UCL and KCL laboratories:

- UCL: Exosome purification and analysis. DNA-RNA isolation and analysis
- King's College London: PBMC's isolation, FACS analysis and functional assays

7.2.3 Health economic data collection

For the health economic analysis, we will collect information on the use of standard imaging tests and whole body MRI and the incidence of adverse events associated with each imaging technique at the time of initial assessment. These data will be obtained from a retrospective review of patient notes for all patients included in the study.

At one year follow-up, after revealing results of whole body MRI, the consistency of patient management plans between standard staging and whole body will be assessed. If standard staging and whole body MRI staging produce the same treatment decisions there will be no differences in costs between the two options other than the imaging costs and the health economic analysis will consist of the imaging costs as described above. If there are differences the health economic analysis will additionally include the difference in cost of the management plans in terms of the following:

- Imaging investigations
- Medications
- Radiotherapy
- Surgery
- Outpatient visits
- Inpatient stays
- Day cases

The research associate in health economics will, in conjunction with appointed clinical research fellow, develop a care pathway and populate it with resource use data from published sources and from patient records.

8.0 Imaging Analysis

8.1 Disease reference standard

The pathway for establishing the reference standard for disease status is illustrated below:

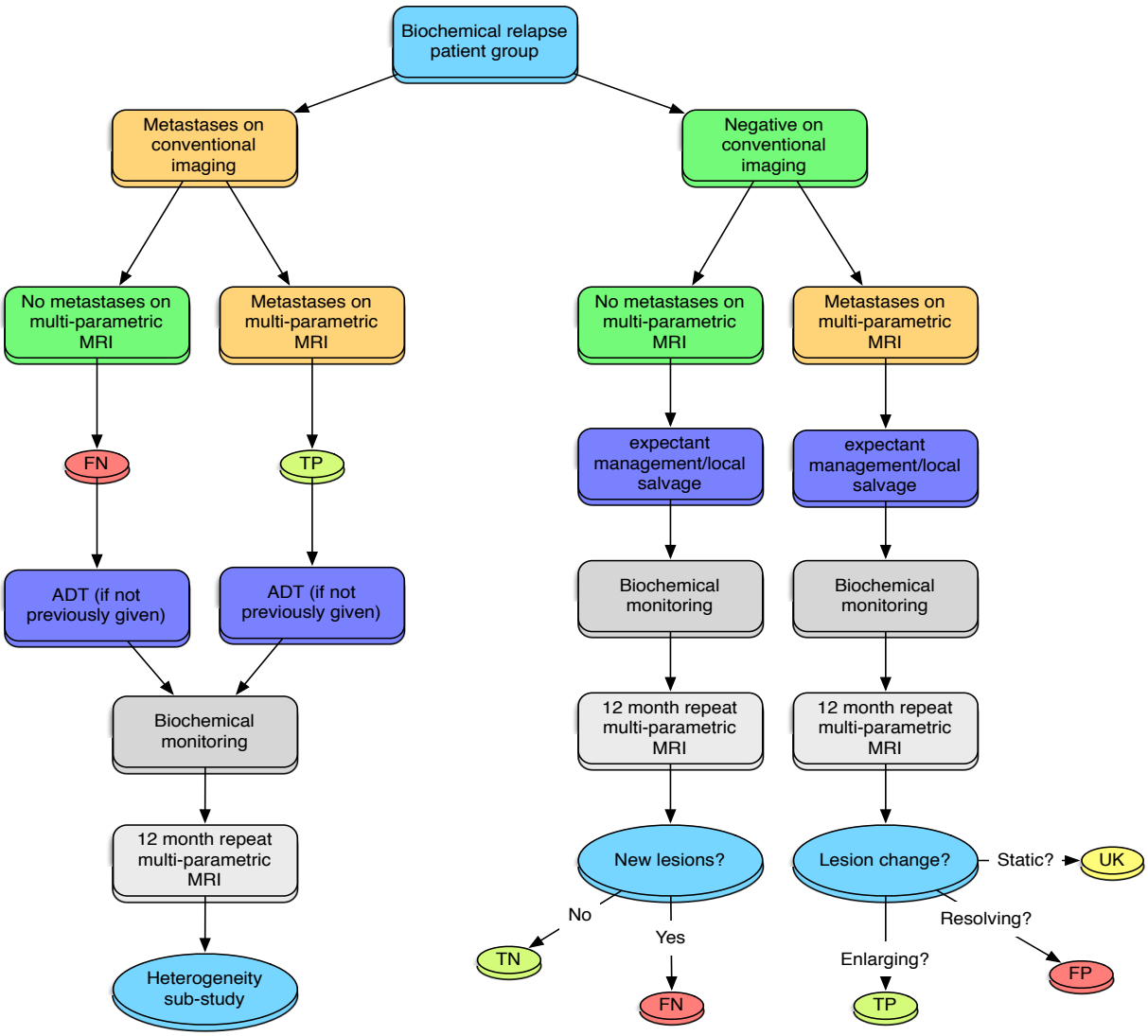

Figure 1: Outcome based reference standard flow chart

Flow charts key

FN: False Negative
TP: True Positive
ADT: Androgen Deprivation Therapy

As we expect the nodal and metastatic staging by whole body multi-parametric MRI to be superior to conventional imaging (CT CAP and bone scan), a reference standard based on conventional imaging alone would not be appropriate. This is a commonly faced problem in radiologic studies. Whilst biopsy could be performed in cases

where the MRI is suspicious for disease but conventional imaging negative, this would place patients at risk of potential 'unnecessary' biopsy related complications, as we do not know if the MRI findings could represent a true positive or false positive result. We have therefore opted to derive a 1-year follow-up outcome based reference standard as detailed above. The 12-month whole-body mp-MRI study will interpret the staging mp-MRI and thereby minimize the number of biopsies required for confirmation/exclusion of metastatic/nodal disease. Specifically:

(a) if conventional imaging staging is **positive** then conventional imaging alone will act as the reference standard (conventional imaging is highly specific, whilst not sensitive). These patients will be treated with ADT. All patients will undergo a 12-month follow-up MRI to assess lesion response.

(b) if conventional imaging staging is **negative** then patients will not have ADT and will be monitored using PSA (and repeat conventional imaging as clinically indicated); those within this group with:

- a ***positive staging whole-body mp-MRI*** may be a *false positive* or a *true positive* finding; and re-evaluation of these lesions will be performed at 12 months by follow-up whole-body mp-MRI.
    - Where the follow-up study demonstrates *a progressive lesion*, patients will undergo repeat conventional imaging +/- targeted biopsy, if clinically possible, and repeat conventional imaging remains negative. The repeat conventional imaging, if positive,

or the biopsy, if repeat conventional imaging is negative, will then define the reference standard.

- Where the follow-up study demonstrates *no lesion or a resolving lesion* the intial whole-body mp-MRI finding will be regarded as a false positive (as no treatment has been given in the interim). It would be unethical to biopsy these patients. Re-imaging with conventional methods may occur as clinically indicated.
- Where the follow-up study demonstrates *a static lesion*, patients will be managed as per best clinical practice. If the PSA is rising they will likely undergo repeat conventional imaging +/- biopsy as clinically indicated. If the PSA is stable, the patients may not undergo repeat conventional imaging or biopsy, in which case they will be excluded from analysis.

- a ***negative staging whole-body mp-MRI*** may be a *false negative* or a *true negative* finding; and a re-evaluation of these patients will be performed at 12 months by follow-up whole-body mp-MRI.
    - Where the follow-up study becomes positive, patients will undergo repeat conventional imaging +/- targeted biopsy (if clinically possible) of the lesion if conventional imaging remains negative. The repeat conventional imaging, if positive, or the biopsy, if repeat conventional imaging is negative, will then define the reference standard.

- Where the follow-up study remains negative the initial mp-MRI initial mp-MRI will be regarded as a true negative. No biopsy will be performed. Re-imaging with conventional methods may occur as clinically indicated.

8.2 Reporting of standard of care imaging

The reference standard imaging (CT CAP, Isotope Bone Scan +/- PET-CT) will be prospectively reported by two radiologists and nuclear medicine physicians, independently. The report will be transferred to a proforma and final nodal (N) and metastatic (M) stages will be derived base on the reported proforma.

8.3 Reporting of trial imaging

8.3.1 Staging whole-body mp-MRI

The study will be reported by two radiologists experienced in oncological and functional MR reporting, independently and then in consensus, blinded to all other imaging tests. The images are reviewed for the presence of nodal (N) and metastatic (M) disease and each radiologists will record the presence/absence of disease on the study specific proforma (see appendix 1). The staging of disease will not be revealed to the clinical team. Where a significant incidental (unrelated) finding is demonstrated this will be reported on the Radiology Information System (RIS) as per standard clinical practice. Where no significant incidental findings are noted the study will be reported on the RIS system as “Study performed as per LOCATE protocol. No significant incidental findings”.

8.3.2 12-month follow-up whole-body mp-MRI

The study will be reported in consensus by two radiologists experienced in oncological and functional MR reporting. The consensus proforma report for the staging whole-body mp-MRI will be made available to the reporting radiologists prior to review of the 12-month follow-up whole-body mp-MRI. The results follow-up study will be compared with the staging study. The radiologists will generate a consensus proforma report indicating sites of potential disease and also whether the site is new, progressing (=>20% increase in size of lesion and/or definite increase in conspicuity on functional imaging), regressing (<= 30% decrease in size of a lesion and/or definite reduced conspicuity on functional imaging), static (<20% increase or <30% decrease in the size of a lesion and equivocal/marginal change in conspicuity on functional imaging), or resolved. A RIS report with disease locations indicated will be generated on the RIS system and be made available to the clinical care team.

8.4 Comparison of standard of care imaging with whole-body mp-MRI

The research team will correlate the standard of care staging proforma with the staging mp-MRI proforma and follow-up mp-MRI proforma. A radiologist and NM physician in consensus will review all discrepancies, between standard of care and whole body mp-MRI. Anatomical matching errors resulting from discrepancies in ascribing disease location will be recorded and corrected. Residual discrepancies will be highlighted and statistically assessed.

The per site sensitivity and specificity will be determined against the disease reference standard. In addition, a sign test for paired data will be used to test for differences in patient staging (i.e. whether a difference between the disease reference standard and MRI exists in site specific staging).

8.5 Repeat conventional imaging +/- lesion biopsy

All highlighted discrepancies will be discussed with the clinical team at the weekly clinical prostate radiological/surgical meeting. Decisions/recommendations on subsequent patient management will be made as outlined in section 8.1 above. All decisions will be recorded and uploaded to the electronic health record system and discussed with the patient prior to action. If repeat conventional imaging is necessary, this will be performed as per standard clinical practice. If biopsy is required patients will be consented for this as per standard clinical practice. The best image guided biopsy approach to enable optimal sampling of the lesion will be undertaken as per standard clinical practice.

9.0 Health Economic Analysis

To compare the incremental cost and cost-effectiveness from an NHS perspective of whole-body multi-parametric MRI for metastatic disease staging compared with conventional staging with computed tomography and bone-scan, for men presenting with biochemical failure following external beam radiotherapy or brachytherapy of locally advanced prostate cancer.

All analyses will conform to accepted economic evaluation methods [14].

The care pathways for men who have previously been confirmed to have prostate cancer and have undergone local treatment can be divided into the *treatment decision* pathway and the *subsequent disease pathway*. The former includes the time from presentation to treatment decision by the clinician and includes the imaging tests received; the latter includes the time period following the treatment decision. The treatment decision pathway will be different between whole-body MRI and conventional staging, yielding different costs and potentially different treatment decisions. In patients for whom the treatment decision with whole-body MRI is the same as that with conventional staging, the subsequent disease pathways will be the same. Where the treatment decision with whole-body MRI is different, the disease pathway will be different, yielding potentially different costs and health outcomes.

If in the patients studied the concordance between the treatment decisions associated with whole-body MRI and conventional staging is high, then the economic analysis can focus on the cost of the treatment decision pathways only because the disease pathways will be no different. In this case the cost-effectiveness of whole-body MRI versus conventional staging depends only on the incremental cost (positive or negative) of whole-body MRI versus conventional staging in the treatment decision pathway.

Alternatively, if the concordance between the treatment decisions is low, then the economic analysis ought to focus on both the treatment decision pathways *and* the subsequent disease pathways because both of these will vary between whole-body

MRI and conventional staging. In this case the cost-effectiveness of whole-body MRI depends on the incremental cost of the whole-body MRI versus standard staging algorithms in the treatment decision pathway plus the incremental costs and health benefits of the two different disease pathways.

The precise nature of the economic analysis will therefore depend on the degree of concordance between treatment decisions provoked by whole-body MRI versus conventional staging, which will be assessed directly in the study.

Scenario1: there is *concordance* between the treatment decisions associated with whole-body MRI and conventional staging

In this case, the cost components included in the analysis will be:

- Conventional metastases imaging tests (e.g., abdominal and pelvic CT and bone-scan, plus additional tests as indicated by the conventional staging algorithm);
- Costs of treating adverse events associated with conventional staging;
- Whole-body MRI, plus additional tests generated by whole-body MRI;
- Costs of treating adverse events associated with whole-body MRI; and,
- MDT and other clinical meetings to determine the subsequent disease pathway.

The volume of resource use for each cost component will be measured directly in the study. Unit costs will be taken from standard published sources. Since the two algorithms yield the same treatment decisions cost-effectiveness depends on the incremental cost of whole-body MRI versus conventional staging in the treatment decision pathway.

Scenario 2: there is *discordance* between the treatment decisions associated with whole-body MRI and standard staging

In this case, cost-effectiveness depends on the incremental cost (positive or negative) of the treatment decision pathway and disease pathway associated with whole-body MRI versus conventional staging and the incremental health benefits (positive or negative). We will calculate cost-effectiveness in terms of the incremental cost per quality-adjusted life year (QALY) gained using one year and lifetime time horizons

Cost-effectiveness will be calculated as the mean cost difference between whole-body MRI versus conventional divided by the mean difference in outcomes (QALYs) to give the incremental cost-effectiveness ratio (ICER). Non-parametric methods for calculating confidence intervals around the ICER based on bootstrapped estimates of the mean cost and QALY differences will be used .The bootstrap replications will also be used to construct a cost-effectiveness acceptability curve, which will show the probability that whole-body MRI is cost-effective at one year for different values of the NHS' willingness to pay for an additional QALY. We will also subject the results to extensive deterministic (one-, two- and multi-way) sensitivity analysis.

10.0 Sub-study analysis

10.1 Comparison of whole-body multi-parametric MRI performance with Choline PET- CT

A separate retrospective comparative study will be set-up using this data and performed to determine the relative performance of both tests for detection of

metastatic disease and the combined performance of a PET-MRI protocol against the disease reference standard. The per site sensitivity and specificity and overall patient staging performance for individual and combined tests will be determined against the disease reference standard.

10.2 Heterogeniety across metastases of multi-parametric MRI signals for prediction of ADT response

For patients undergoing ADT treatment retrospective quantitative analysis of multi-parametric MRI signals will be performed to derive heterogeniety indices from confirmed true positive metastatic sites. The heterogeniety indices will inform Bayesian models to predict high-risk patients with aggressive disease that progress on ADT within 12-months of treatment.

10.3 The significance of the Human Epidermal growth factor Receptor (HER) activated dimer

This project aims to investigate the significance of the Human Epidermal growth factor Receptor (HER) activated dimer in metastatic castration-resistant prostate cancer. Up-regulation of the HER1 (EGFR)/HER3 dimer was recently found by the Ng laboratory, for the first time, to limit the efficacy of anti-EGFR treatment in human breast cancer, as directly shown by imaging of residual disease; suggesting the potential of combined EGFR/HER3-targeted treatment.

This molecular signaling rewiring is hypothesised to constitute a pathway of resistance to hormonal treatment in prostate cancer as well.

We intend to quantify the EGFR/HER3 heterodimer using Fluorescence lifetime imaging microscopy (FLIM) in formalin-fixed prostate cancer tissues as well as in matched circulating exosomes from patient-derived plasma. We will then correlate the heterodimer quantification with tumour genomic changes such as *PTEN* mutation/deletion . The patient-derived correlative experiments will be complemented by mechanistic *in vitro* experiments that investigate the effect of EGFR and PI3K/Akt inhibitors on HER dimer formation in castration-resistant and sensitive prostate cancer cells, and their exosomes released into the culture supernatants. In the clinical setting, the tissue- and exosome-derived HER dimer measurements will be combined with functional imaging (whole body multi-parametric MRI) to assess their value and translation as predictive biomarkers of clinical outcome and response to treatment.

11.0 Sample size

130 patients (based on 50% prevalence of metastases) will be required to demonstrate a minimum of a 20% difference in sensitivity for detection of metastases between multi-parametric and conventional imaging (power of 90% and statistical significance cut-off of 0.05).

12.0 Safety Reporting

The imaging techniques involved in this trial are well established and the risks of each are well known. In case of any adverse event, including ‘related’ or ‘unexpected’ SAEs, these will be reported and submitted to relevant regulatory organization(s).

13.0 Incident Reporting

Relevant regulatory bodies will be notified of all deviations from the protocol or GCP immediately. A report on the incident(s) might be required and a form will be provided if the organisation does not have an appropriate document (e.g. Trust Incident Form).

If site staffs are unsure whether a certain occurrence constitutes a deviation from the protocol or GCP, R&D can be contacted immediately to discuss.

14.0 Withdrawal of Patients

In consenting to the trial, patients are consenting to trial treatment, assessments, follow-up and data collection.

Discontinuation of Trial Intervention for clinical reasons

A patient may be withdrawn from trial intervention whenever continued participation is no longer in the patient's best interests, but the reasons for doing so must be recorded. Reasons for discontinuing intervention may include:

- Intercurrent illness which prevents further imaging
- Patients withdrawing consent to further trial participation
- Any alterations in the patient's condition which justifies the discontinuation of trial imaging in the site investigator's opinion

In these cases patients remain within the trial for the purposes of follow-up and data analysis.

Patient withdrawal from trial intervention

If a patient expresses their wish to withdraw from the trial, the site should explain the importance of remaining on trial follow-up, or failing this of allowing routine follow-up data to be used for trial purposes and for allowing existing collected data to be used. If patient gives a reason for their withdrawal, this should be recorded.

Withdrawal of Consent to Data Collection

If a patient explicitly states they do not wish to contribute further data to the trial their decision must be respected and recorded on the relevant CRF. In this event details should be recorded in the investigator site file and no further CRFs must be completed.

Losses to follow-up

If a patient moves from the area, every effort should be made for patient to be followed up via GP.

If a patient is lost to follow-up at a site every effort should be made to contact the patient's GP to obtain information on the patient's status.

15.0 Trial Closure

15.1 End of Trial

For regulatory purposes the end of the trial will be 1 year after the recruitment of 130 patients who have undergone the requisite imaging both at staging and treatment efficacy assessment as per protocol at which point the 'declaration of end of trial' form will be submitted to participating ethical committees, as required.

15.2 Archiving of Trial Documentation

At the end of the trial, all relevant documentation will be archived securely and all centrally held trial related documentation for a minimum of 5 years. Arrangements for confidential destruction will then be made. It is the responsibility of PIs to ensure data and all essential documents relating to the trial held at site are retained for a minimum of 5 years after the end of the trial, in accordance with national legislation and for the maximum period of time permitted by the site.

Essential documents are those which enable both the conduct of the trial and the quality of the data produced to be evaluated and show whether the site complied with the principles of GCP and all applicable regulatory requirements.

All archived documents must continue to be available for inspection by appropriate authorities upon request.

15.3 Early discontinuation of trial

The trial may be stopped before completion as an Urgent Safety Measure.

Sites and relevant regulatory bodies will be informed in writing of reasons for early closure and the actions to be taken with regards the treatment and follow up of patients.

15.4 Withdrawal from trial participation by a site

Should a site choose to close to recruitment the PI must inform the relevant regulatory bodies in writing. Follow up as per protocol must continue for all patients

recruited into the trial at that site and other responsibilities continue as per trial protocol.

16.0 Quality Assurance

A strict MRI quality assurance program will be in place to ensure acquisition of robust scan data including weekly phantom calibration. Scan acquisition will be overseen by a dedicated research radiographer and medical physicist to ensure explicit adherence to scan protocol. The QA program will run throughout the study.

17.0 Ethical and Regulatory Approvals

In conducting the trial, the Sponsor and Sites will comply with all laws and statutes, as amended from time to time, applicable to the performance of clinical trials including, but not limited to:

- The principles of ICH Harmonised Tripartite Guideline for Good Clinical Practice
- The Human Rights Act 1998
- The Data Protection Act 1998
- The Freedom of Information Act 2000
- The Human Tissue Act 2004
- The Research Governance Framework for Health and Social Care, issued by the UK Department of Health (Second Edition 2005) or the Scottish Health Department Research Governance Framework for Health and Community Care (Second Edition 2006)

17.1 Ethical Approval

The trial will be conducted in accordance with the World Medical Association Declaration of Helsinki entitled 'Ethical Principles for Medical Research Involving Human Subjects' (1996 version) and in accordance with the terms and conditions of the ethical approval given to the trial.

An annual Progress Reports to the REC will be submitted, which will commence one year from the date of ethical approval for the trial

17.2 Site Approval

Evidence of local Trust R&D approval will be provided prior to site activation. The trial will only be conducted at sites where all necessary approvals for the trial have been obtained.

17.3 Protocol Amendments

PI and nominated research fellow will be responsible for gaining ethical approval for amendments made to the protocol and other trial-related documents. Once approved, trial team will ensure that all amended documents are distributed to sites and CLRNs as appropriate.

Site staff will be responsible for acknowledging receipt of documents and for implementing all amendments.

17.4 Patient Confidentiality & Data Protection

All identifiable data will be stored in a secure manner and all efforts will be made to adhere with the Data Protection Act 1998.

17.5 University College London Insurance Indemnity

University College London holds insurance against claims from participants for harm caused by their participation in this clinical study. Participants may be able to claim compensation if they can prove that UCL has been negligent. However, if this clinical study is being carried out in a hospital, the hospital continues to have a duty of care to the participant of the clinical study. University College London does not accept liability for any breach in the hospital's duty of care, or any negligence on the part of hospital employees. This applies whether the hospital is an NHS Trust or otherwise."

18.0 References

1. Chowdhury et al. BJUi (in press)

2. Interval to Biochemical Failure Predicts Clinical Outcomes in Patients With High-Risk Prostate Cancer Treated by Combined-Modality Radiation Therapy. Shilkrut M, McLaughlin PW, Merrick GS, Vainshtein JM, Feng FY, Hamstra DA. Int J Radiat Oncol Biol Phys. 2013 May 9.

3. The Dilemma of Localizing Disease Relapse After Radical Treatment for Prostate Cancer: Which is The Value of The Actual Imaging Techniques? Schiavina R, Ceci F, Borghesi M, Brunocilla E, Vagnoni V, Gacci M, Castellucci P, Nanni C, Martorana G, Fanti S. Curr Radiopharm. 2013 Apr 16.

4. No immediate treatment after biochemical failure in patients with prostate cancer treated by external beam radiotherapy. Faria SL, Mahmud S, Souhami L, David M, Duclos M, Shenouda G, Makis W, Freeman CR. Urology. 2006 Jan;67(1):142-6.

5. Androgen deprivation for prostate cancer. Chi KN, Nguyen PL, Higano CS. Am Soc Clin Oncol Educ Book. 2013;2013:176-83.

6. STAMPEDE study; http://meetinglibrary.asco.org/content/115654-132.

7. Performance characteristics of computed tomography in detecting lymph node metastases in contemporary patients with prostate cancer treated with extended pelvic lymph node dissection. Briganti A, Abdollah F, Nini A, Suardi N, Gallina A, Capitanio U, Bianchi M, Tutolo M, Passoni NM, Salonia A, Colombo R, Freschi M, Rigatti P, Montorsi F. Eur Urol. 2012 Jun;61(6):1132-8

8. Prostate cancer imaging: what the urologist wants to know. Talab SS, Preston MA, Elmi A, Tabatabaei S. Radiol Clin North Am. 2012 Nov;50(6):1015-41.

9. Unmet needs in the prediction and detection of metastases in prostate cancer. Sartor O, Eisenberger M, Kattan MW, Tombal B, Lecouvet F. Oncologist. 2013;18(5):549-57.

10. Can whole-body magnetic resonance imaging with diffusion-weighted imaging replace Tc 99m bone scanning and computed tomography for single-step detection of metastases in patients with high- risk prostate cancer? Lecouvet FE, El Mouedden J, Collette L, Coche E, Danse E, Jamar F, Machiels JP, Vande Berg B, Omoumi P, Tombal B. Eur Urol. 2012 Jul;62(1):68-75.

11. Pediatric and adolescent lymphoma: comparison of whole-body STIR half-Fourier RARE MR imaging with an enhanced PET/CT reference for initial staging. Punwani S, Taylor SA, Bainbridge A, Prakash V, Bandula S, De Vita E, Olsen OE, Hain SF, Stevens N, Daw S, Shankar A, Bomanji JB, Humphries PD. Radiology. 2010 Apr;255(1):182-90.

12. Multi-parametric magnetic resonance imaging to rule-in and rule-out clinically importantprostate cancer in men at risk: a cohort study. Rouse P, Shaw G, Ahmed HU, Freeman A, Allen C, Emberton M. Urol Int. 2011;87(1):49-53.

13. Prostate MRI: Who, when, and how? Report from a UK consensus meeting. A.P.S. Kirkham, P. Haslam, J.Y. Keanie, I. McCafferty, A.R Padhani, S. Punwani et al. Clin Radiol. 2013 Oct;68(10):1016-23

14. National Institute for Health and Care Excellence (NICE). Guide to the methods of technology appraisal 2013. NICE: London, 2013

Appendix: Selection/Obligations of participating sites/investigators

Site selection

In this protocol trial **"Site"** refers to the hospital or site where trial-related activities are actually conducted.

Sites must be able to comply with:

1. Trial imaging, follow up schedules and all requirements of the trial protocol
2. Requirements of the Research Governance Framework
3. Data collection requirements

Selection of Principal Investigator and other investigators at sites

Sites must have an appropriate Principal Investigator (PI) i.e. a health care professional authorised by the site, ethics committee to lead and coordinate the work of the trial on behalf of the site. Other investigators at site wishing to participate in the trial will be trained and approved by the PI.

Training requirements for site staff

All site staff will be appropriately qualified by education, training and experience to perform the trial related duties allocated to them, which will be recorded on the site delegation log.

CVs for all staff must be kept up-to-date, signed and dated and copies held in the Investigator Site File (ISF). GCP training is required for all staff responsible for trial activities. The frequency of repeat training may be dictated by the requirements of their employing Institution, or 2 yearly where the Institution has no policy, and more frequently when there have been updates to the legal or regulatory requirements for the conduct of clinical trials

Site initiation and activation

Site initiation

Before a site is activated, the trial team will arrange a site initiation with the site which the PI and site research team must attend. The site will be trained in the day-to-day management of the trial and essential documentation required for the trial will be checked. Site initiation will be performed for each site-by-site visit.

Required documentation

The following documentations will be submitted by the site to relevant regulatory bodies prior to a site being activated by trial team:

1. Trial specific Declaration of Participation/Site Registration Form (identifying relevant local staff)

2. All relevant institutional approvals (e.g. local NHS permission)

3. A completed site delegation log that is signed and dated by the PI

4. A copy of the PI's current CV that is signed and dated

The trial team will ensure that:

1. If the site was not included in the original CSP application, the Part C is updated and the R&D form is resubmitted to CSP (who will notify the lead CLRN of the new site)

2. An SSI form is transferred to the site via IRAS

Site activation letter

Once the trial team has received all required documentation and the site has been initiated, a site activation letter will be issued to the PI, at which point the site may start to approach patients.

Once the site has been activated the PI is responsible for ensuring:

1. Adherence to the most recent version of the protocol

2. All relevant site staffs are trained in the protocol requirements

3. Appropriate recruitment and medical care of patients in the trial

4. Timely completion and return of CRFs

Trial Activation

Principal investigator and nominated research fellow will ensure that all trial documentation has been reviewed and approved by all relevant bodies and that the following have been obtained prior to activating the trial:

1. Adequate funding for central coordination
2. Confirmation of sponsorship
3. Adequate insurance provision
4. Research Ethics Committee approval ‘Adoption’ into NIHR portfoli

5. NHS permission

Appendix: Informed consent procedure

A screening log should be maintained by the site and kept in the Investigator Site File. This should record each patient screened for the trial identified with radio-recurrent prostate cancer and the reasons why they were not registered in the trial if this is the case.

Sites must ensure that all patients have been given the current approved version of the patient information sheet, are fully informed about the trial and have confirmed their willingness to take part in the trial.

The PI, or, where delegated by the PI, other appropriately trained site staff, are required to provide a full explanation of the trial and all relevant treatment options to each patient prior to trial entry and consent. During these discussions the current approved patient information sheet for the trial should be discussed with the patient. A minimum of twenty-four hours must be allowed, after reading the patient information sheet, for patients to consider participation within the trial. Written informed consent on the current approved version of the consent form for the trial must be obtained before any trial-specific procedures are conducted. The discussion

and consent process must be documented in the investigator site file along with a copy of approved GP letter.

The trial team will be responsible for:

- Checking that the correct (current approved) version of the patient information sheet and consent form are used
- Checking that information on the consent form is complete and legible
- Checking that the patient has completed/initialled all relevant sections and signed and dated the form
- Checking that an appropriate member of staff has countersigned and dated the consent form to confirm that they provided information to the patient
- Giving the patient a copy of their signed consent form, patient information sheet and patient contact card

Following enrollment:

- Adding the patient trial number to all copies of the consent form and storage within the investigator site file

The right of the patient to refuse to participate in the trial without giving reasons must be respected. All patients are free to withdraw at any time.

Appendix: Data Collection and Management

Data will be collected from sites on version controlled case report forms (CRFs) designed for the trial Data entered onto CRFs must reflect source data at site.

Where supporting documentation (e.g. autopsy report, pathology reports, CT scan images etc) is being submitted the patient's trial number will be clearly indicated on all material and any patient identifiers removed/blacked out prior to sending to maintain confidentiality. A nominated individual will take responsibility for data collection. Data 'cleaning' and database entry will also be performed by the trial administrator. An external audit of data will be performed according to standard operating procedures of the sponsor or their delegated body. Data will be held according to the Data Protection Act 1998 and pseudo-anonymised as necessary. Each participant will be given a study number and this will be used on all of their study records. The paper records will be retained for a minimum of 10 years after the end of the study. Any information that is transferred between trial centres or from general practitioners surgeries will be anonymised.

All case report forms (CRFs) will be completed and signed by staff who are listed on the site staff delegation log and authorised by the PI to perform this duty. The PI is responsible for the accuracy of all data reported in the CRF. Once completed the original CRFs will be filed and a copy kept at site. All entries will be clear, legible and written in ball point pen. The use of abbreviations and acronyms will be avoided.

Any corrections made to a CRF at site will be made by drawing a single line through the incorrect item ensuring that the previous entry is not obscured. Each correction will be dated and initialed. Correction fluid must not be used. The amended CRF must be filed and a copy retained at site.

To avoid the need for unnecessary data queries CRFs will be checked at site to ensure there are no blank fields before filing. When data is unavailable because a measure has not been taken or test not performed, enter “ND” for not done. If an item was not required at the particular time the form relates to, enter “NA” for not applicable. When data are unknown enter the value “NK” (only use if every effort has been made to obtain the data).

CRFs will be completed at site as soon as possible after patient visit/scans and within 4 weeks of the patient being scanned.

Prior to filing, data will be checked for legibility, completeness, accuracy and consistency, including checks for missing or unusual values. Queries will be sent to the data contact at site. When responding to a query, site staff must update the relevant CRF held at site, as applicable. The amended copy of the CRF will be attached to the query sheet with a copy at site. All amendments will be initialed and dated.

Appendix: Whole body MRI Proforma

LOCATE

Localising Occult prostate Cancer metastases with Advanced imaging TEchniques

CASE REPORT FORMS

WB-MRI IMAGING BOOKLET

Patient Initials	☐☐☐
Trial Number	L O C – ☐☐☐

Please send COMPLETED forms to:

LOCATE Co-ordinator
University College London
Level 3 East, 250 Euston Road
London, UK. NW1 2PG

General enquires: **0203 447 9094**
between 9.00am and 5.00pm (UK Time)

E-mail: **TBC**

PROSTATE CANCER UK

UCL

Additional instructions for completing forms

WB-MRI Imaging Guidance

To be completed by the trial radiologist when reporting the WB-MRI.
See table below for definitions for T, N and M staging.

T1	T2	T3	T4
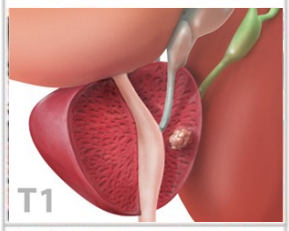			
T1 Clinically inapparent; tumor not palpable or visible by imaging **T1a** Incidental finding during transurethral resection of prostate; < 5% of tissue resected **T1b** Incidental finding during transurethral resection of prostate; > 5% of tissue resected **T1c** Tumor identified by needle biopsy (e.g. because of elevated PSA)	**T2** Tumor confined within prostate (palpable or visible on TRUS) **T2a** Involves half of a lobe or less **T2b** Involves more than half of a lobe one lobe but not both lobes **T2c** Tumor involves both lobes	**T3** Tumor extends through prostatic capsule, bladder neck or seminal capsule **T3a** Unilateral extracapsular extension **T3b** Bilateral extracapsular extension **T3c** Tumor invades seminal vesicle(s)	**T4** The tumor has spread or attached to tissues next to the prostate (other than the seminal vesicles). **T4a** The tumor has spread to the neck of the bladder, the external sphincter (muscles that help control urination), or the rectum. **T4b** The tumor has spread to the floor and/or the wall of the pelvis.

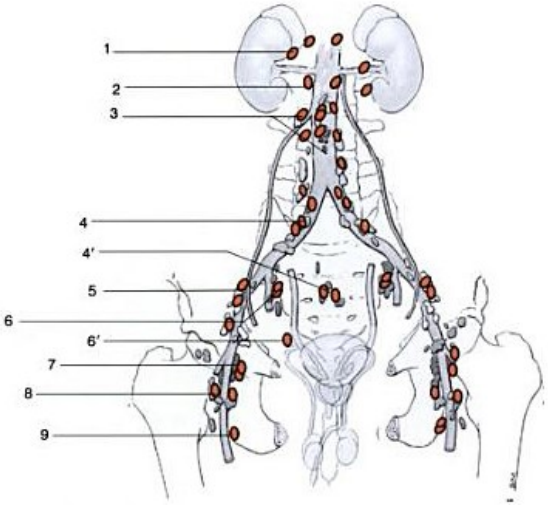

N0 Cancer has not spread to any lymph nodes.
N1 Cancer has spread to a single regional lymph node (inside the pelvis) and is not larger than 2 centimeters
N2 Cancer has spread to one or more regional lymph nodes and is larger than 2 centimeters (¾ inch), but not larger than 5 centimeters
N3: Cancer has spread to a lymph node and is larger than 5 centimeters

M0: The cancer has not metastasized (spread) beyond the regional lymph nodes
M1: The cancer has metastasized to distant lymph nodes (outside of the pelvis), bones, or other distant organs such as lungs, liver, or brain

Note: Regional pelvic lymph nodes

Illustrated left - regional defined as (4') presacral, (5) external iliac, (6') obturator, (6) internal iliac. Other sites are considered as metastatic nodes.

Note: M Staging

Illustrated right — Sub classification of metastatic disease stage. M1a – non-regional nodal involvement; M1b — metastatic bone disease and M1c — other organ involvement

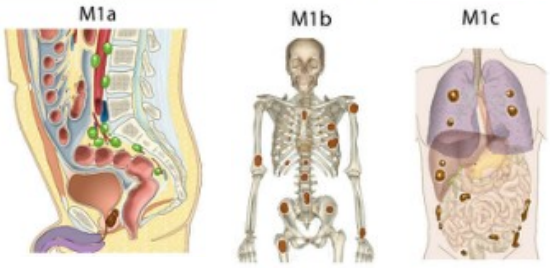

PROSTATE CANCER UK

UCL

LOCATE **Trial Number** L O C – _ _ _ **Patient Initials** _ _ _

Site _____

WB-MRI Imaging- Diffusion and T1 sequences 1/3

Total time to report diffusion and T1 weighted images- Minutes _____

Diffusion weighted image sequences quality– Please tick Good ☐ Adequate ☐ Poor ☐

T1 sequence quality– Please tick Good ☐ Adequate ☐ Poor ☐

Local Tumour						
Location	APICAL RIGHT	APICAL LEFT	BASAL RIGHT	BASAL LEFT	NOT VISIBLE	
Max Dimension (cm)						
T Stage (Circle)	T1	T2a T2b T2c	T3a T3b T3c	T4a T4b		Confidence (Circle) 1- low 2- adequate 3- equivocal 4- good 5- excellent
N Stage (Circle)	NX	N0	N1	N2	N3	Confidence (Circle) 1- low 2- adequate 3- equivocal 4- good 5- excellent

Nodal Sites						
	Negative 1- definitely not present 2- probably not present		**Equivocal** 3- possibility not present 4- possibly present		**Positive** 5- probably present 6- definitely present	
	Negative		**Equivocal**		**Positive**	
Confidence within main classification as negative, equivocal or positive	1	2	3	4	5	6
Regional Nodes						
Presacral						
External iliac						
Internal iliac						
Obturator						
Metastatic Nodes						
Inguinal						
Common iliac						
Para-aortic						
Other abdominal						
Nodes above diaphragm to neck						
Neck nodes						

PROSTATE CANCER UK

UCL

LOCATE Trial Number L O C – Patient Initials

Site

WB-MRI Imaging- Diffusion and T1 sequences 2/3

M Stage										
	Negative 1- definitely not present 2- probably not present		**Equivocal** 3- possibility not present 4- possibly present		**Positive** 5- probably present 6- definitely present					
	Negative		**Equivocal**		**Positive**					
Confidence within main classification as negative, equivocal or positive	1	2	3	4	5	6				
1. All sites (tick diagnostic confidence)										
2. Non-skeletal– all sites (tick diagnostic confidence)										
3. Skeletal– all sites (tick diagnostic confidence)										
Non Skeletal individual disease sites (tick confidence diagnostic							Size of largest organ deposit	Size of second largest organ deposit	Number of **additional** deposits ≥6mm (if ≤10, state number. If >10 state, >10)	Number of **additional** deposits <6mm (if ≤10, state number. If >10 state, >10)
Brain										
Lung (L)										
Lung (R)										
Pleura (L)										
Pleura (R)										
Liver (left lobe)										
Liver (right lobe)										
Spleen										
Adrenal (L)										
Adrenal (R)										
Kidney (L)										
Kidney (R)										
Pancreas										
Mesentery/peritoneum										
Bowel										
Soft tissue neck/chest										
Soft tissue abdomen/ pelvis										
Soft tissue limbs										
Nodal– State_____										
Other– State_____										

PROSTATE CANCER UK

UCL

LOCATE **Trial Number** L O C – _ _ _ **Patient Initials** _ _ _

Site _____

WB-MRI Imaging- Diffusion and T1 sequences 3/3

M Stage continued										
	Negative 1- definitely not present 2- probably not present		**Equivocal** 3- possibility not present 4- possibly present		**Positive** 5- probably present 6- definitely present		Size of largest organ deposit	Size of second largest organ deposit	Number of **additional** deposits ≥6mm (if ≤10, state number. If >10 state, >10)	Number of **additional** deposits <6mm (if ≤10, state number. If >10 state, >10)
	Negative		**Equivocal**		**Positive**					
Confidence within main classification as negative, equivocal or positive	1	2	3	4	5	6				
Skeletal individual disease sites										
Skull										
Cervical spine										
Thoracic spine										
Lumber spine										
Pelvis										
Sternum										
Clavicle/Scapula (L)										
Clavicle/Scapula (R)										
Ribs (L)										
Ribs (R)										
Upper limb (L)										
Upper limb (R)										
Lower limb (L)										
Lower limb (R)										

Completed by: _____

Signature: _____

CRFs should only be completed by appropriately qualified personnel detailed on the site delegation log

Date completed: D D M M Y Y Y Y

Please return to: **LOCATE Co-ordinator**, Centre for Medical Imaging, Level 3 East, 250 Euston Road, London, NW1 2PG

For Office use only

Date form received: _____ Date form entered: _____ Initials: _____

PROSTATE CANCER UK

UCL

LOCATE **Trial Number** L O C – _ _ _ **Patient Initials** _ _ _

Site _____

WB-MRI Imaging- Diffusion, T1 and T2 sequences 1/3

Additional time to report T2 images (in addition to diffusion and T1)- Minutes _____

T2 sequence quality– Please tick Good ☐ Adequate ☐ Poor ☐

Local Tumour						
Location	APICAL RIGHT	APICAL LEFT	BASAL RIGHT	BASAL LEFT	NOT VISIBLE	
Max Dimension (cm)						
T Stage (Circle)	T1	T2a T2b T2c	T3a T3b T3c	T4a T4b		Confidence (Circle) 1- low 2- adequate 3- equivocal 4- good 5- excellent
N Stage (Circle)	NX	N0	N1	N2	N3	Confidence (Circle) 1- low 2- adequate 3- equivocal 4- good 5- excellent

Nodal Sites						
	Negative 1- definitely not present 2- probably not present		**Equivocal** 3- possibility not present 4- possibly present		**Positive** 5- probably present 6- definitely present	
	Negative		**Equivocal**		**Positive**	
Confidence within main classification as negative, equivocal or positive	1	2	3	4	5	6
Regional Nodes						
Presacral						
External iliac						
Internal iliac						
Obturator						
Metastatic Nodes						
Inguinal						
Common iliac						
Para-aortic						
Other abdominal						
Nodes above diaphragm to neck						
Neck nodes						

For Office use only
Date form received: _____ Date form entered: _____ Initials: _____

PROSTATE CANCER UK

UCL

LOCATE **Trial Number** L O C – _ _ _ **Patient Initials** _ _ _

Site _____

WB-MRI Imaging- Diffusion, T1 and T2 sequences 2/3

M Stage										
	Negative 1- definitely not present 2- probably not present		**Equivocal** 3- possibility not present 4- possibly present		**Positive** 5- probably present 6- definitely present					
	Negative		**Equivocal**		**Positive**					
Confidence within main classification as negative, equivocal or positive	1	2	3	4	5	6				
1. All sites (tick diagnostic confidence)										
2. Non-skeletal– all sites (tick diagnostic confidence)										
3. Skeletal– all sites (tick diagnostic confidence)										
Non Skeletal individual disease sites (tick confidence diagnostic							Size of largest organ deposit	Size of second largest organ deposit	Number of **additional** deposits ≥6mm (if ≤10, state number. If >10 state, >10)	Number of **additional** deposits <6mm (if ≤10, state number. If >10 state, >10)
Brain										
Lung (L)										
Lung (R)										
Pleura (L)										
Pleura (R)										
Liver (left lobe)										
Liver (right lobe)										
Spleen										
Adrenal (L)										
Adrenal (R)										
Kidney (L)										
Kidney (R)										
Pancreas										
Mesentery/peritoneum										
Bowel										
Soft tissue neck/chest										
Soft tissue abdomen/ pelvis										
Soft tissue limbs										
Nodal– State_____										
Other– State_____										

For Office use only
Date form received: _____ Date form entered: _____ Initials: _____

PROSTATE CANCER UK

UCL

LOCATE Trial Number L O C – | | | Patient Initials | | |

Site |

WB-MRI Imaging- Diffusion, T1 and T2 sequences 3/3

M Stage continued											
	Negative 1- definitely not present 2- probably not present		**Equivocal** 3- possibility not present 4- possibly present		**Positive** 5- probably present 6- definitely present		Size of largest organ deposit	Size of second largest organ deposit	Number of **additional** deposits ≥6mm (if ≤10, state number. If >10 state, >10)	Number of **additional** deposits <6mm (if ≤10, state number. If >10 state, >10)
	Negative		**Equivocal**		**Positive**					
Confidence within main classification as negative, equivocal or positive	1	2	3	4	5	6				
Skeletal individual disease sites										
Skull										
Cervical spine										
Thoracic spine										
Lumber spine										
Pelvis										
Sternum										
Clavicle/Scapula (L)										
Clavicle/Scapula (R)										
Ribs (L)										
Ribs (R)										
Upper limb (L)										
Upper limb (R)										
Lower limb (L)										
Lower limb (R)										

Completed by:

Signature:

CRFs should only be completed by appropriately qualified personnel detailed on the site delegation log

Date completed: D D M M Y Y Y Y

Please return to: **LOCATE Co-ordinator**, Centre for Medical Imaging, Level 3 East, 250 Euston Road, London, NW1 2PG

For Office use only

Date form received: _____ Date form entered: _____ Initials: _____

LOCATE Trial Number L O C – Patient Initials

Site

WB-MRI Imaging– Final report– All sequences-Diffusion T1 and T2 and contrast enhanced 2/3

M Stage										
	Negative 1- definitely not present 2- probably not present		**Equivocal** 3- possibility not present 4- possibly present		**Positive** 5- probably present 6- definitely present					
	Negative		**Equivocal**		**Positive**					
Confidence within main classification as negative, equivocal or positive	1	2	3	4	5	6				
1. All sites (tick diagnostic confidence)										
2. Non-skeletal– all sites (tick diagnostic confidence)										
3. Skeletal– all sites (tick diagnostic confidence)										
Non Skeletal individual disease sites (tick confidence diagnostic							Size of largest organ deposit	Size of second largest organ deposit	Number of **additional** deposits ≥6mm (if ≤10, state number. If >10 state, >10)	Number of **additional** deposits <6mm (if ≤10, state number. If >10 state, >10)
Brain										
Lung (L)										
Lung (R)										
Pleura (L)										
Pleura (R)										
Liver (left lobe)										
Liver (right lobe)										
Spleen										
Adrenal (L)										
Adrenal (R)										
Kidney (L)										
Kidney (R)										
Pancreas										
Mesentery/peritoneum										
Bowel										
Soft tissue neck/chest										
Soft tissue abdomen/ pelvis										
Soft tissue limbs										
Nodal– State_____										
Other– State_____										

For Office use only
Date form received: _____ Date form entered: _____ Initials: _____

PROSTATE CANCER UK

UCL

LOCATE **Trial Number** L O C – ☐☐☐ **Patient Initials** ☐☐☐

Site ☐

WB-MRI Imaging– Final report– All sequences- Diffusion T1 and T2 and contrast enhanced 3/3

M Stage continued										
	Negative 1- definitely not present 2- probably not present		**Equivocal** 3- possibility not present 4- possibly present		**Positive** 5- probably present 6- definitely present		Size of largest organ deposit	Size of second largest organ deposit	Number of **additional** deposits ≥6mm (if ≤10, state number. If >10 state, >10)	Number of **additional** deposits <6mm (if ≤10, state number. If >10 state, >10)
	Negative		**Equivocal**		**Positive**					
Confidence within main classification as negative, equivocal or positive	1	2	3	4	5	6				
Skeletal individual disease sites										
Skull										
Cervical spine										
Thoracic spine										
Lumber spine										
Pelvis										
Sternum										
Clavicle/Scapula (L)										
Clavicle/Scapula (R)										
Ribs (L)										
Ribs (R)										
Upper limb (L)										
Upper limb (R)										
Lower limb (L)										
Lower limb (R)										

Completed by: ☐

Signature: ☐

CRFs should only be completed by appropriately qualified personnel detailed on the site delegation log

Date completed: D D M M Y Y Y Y ☐☐☐☐☐☐☐☐

Please return to: **LOCATE Co-ordinator**, Centre for Medical Imaging, Level 3 East, 250 Euston Road, London, NW1 2PG

For Office use only

Date form received: _____ Date form entered: _____ Initials: _____

Appendix 2

School of Biosciences and Medicine

Leggett Building

Daphne Jackson Road

Manor Park

Guildford, Surrey GU2 7WG UK

SUN Study Protocol

Title:

Discovering new cancer biomarkers from patients' blood, urine and DNA. A tissue banking project

Objective:

The purpose of this project is: To set up a tissue bank for serum, plasma and DNA as well as tumour tissue of patients with suspected and confirmed diagnosis of cancer and control samples from healthy volunteers.

Start date:

August 2008

Background

The diagnosis and treatment of cancer continues to be a challenge of the 21st century despite an enormous scientific progress. Many cancers are detected too late and curative treatment is impossible. Cancer prevention is the ultimate goal however one of the main tasks of cancer research continues to be early cancer detection. A vast majority of cancers could potentially be cured if detected early. Only very few tumour types can be detected with the help of biomarkers and most of them are not specific

for cancer. Good examples of clinically useful biomarkers are germ cell tumours markers. The levels of alpha-fetoprotein and beta-HCG are often diagnostic and provide important clinical information about the severity of illness, help clinicians to decide the best course of treatment and can indicate recurrence very early on. Unfortunately very few cancers have such tumour markers and intensive research is needed to facilitate progress in this area.

Most biomarkers are made of peptides and proteins. These are usually secreted and found in miniscule amounts in blood, urine, ascites and other body fluids. Current scientific techniques have progressed significantly and it is possible to generate a lot of important ground-breaking scientific data from very small amounts (approximately 50µl) of protein containing fluid. The complexity of such techniques such as proteomics analysis continuous to be a challenge and intensive research is needed to move science and biomarkers studies forward. Proteomics is a large-scale study of proteins, their structure and functions. Similarly other “omics” technologies include immunomic approaches-studying of antibodies and immuno-genomics-analysis of gene polymorphisms associated with immune response genes and cytokines. Analysis of results requires application of computer programmes such as Artificial Neural Network, a form of machine learning capable of accurately modelling biological systems and identifying biomarkers. Published data on purely proteomic approaches have so far identified a panel of biomarkers that have low sensitivity and/or low specificity [1-5]. The data is promising, but the application in clinical practice still very limited as the novel biomarkers are not superior to currently used markers.

A clinically useful biomarker needs to be highly specific for a given cancer and highly sensitive, it should help to diagnose cancer but also give prognostic information regarding the severity of illness, likelihood for recurrence and help detecting early recurrence. To characterise novel biomarkers and their use to predict and characterise the course of malignant disease one needs to analyse the markers throughout the length of illness, from the time of diagnosis, through treatment, progression, development of metastases and resistance to treatment. This requires a long follow up as well as repeated collection and analysis of samples such as blood, urine, ascites and other tissues containing potentially useful biomarkers. The pattern of biomarkers

expression will then subsequently require correlation with clinical data and parameters such as response to treatment, progression free survival and overall survival.

Development of novel biomarkers for a variety of uses including diagnosis and treatment monitoring is on the Cancer Reform Strategy agenda and actively encouraged by the National Cancer Research Institute and MRC.

We propose to set up a tissue bank to collect serum, plasma and DNA specimens from patients referred for investigations of cancer as well as patients with a known diagnosis of cancer. We will also approach healthy volunteers to collect "control" samples. Patients will be requested to offer a blood sample when first presented and if they continue to be followed up in the outpatients setting to donate a blood sample at 6-monthly intervals. A one of DNA sample will be stored at the initial presentation. Patients who undergo an operation to remove the tumour will also be asked to donate a small sample of the tumour tissue. Healthy volunteers will offer one sample only and will not be asked for tissue. At the same time we will ask both: patients with cancer as well as healthy volunteers to offer a nail clipping to exclude an exposure to heavy metals which can have a significant influence on proteins in the samples and a urine specimen.

A minimal set of clinical data will be collected at the same time and stored on a secure password-protected database. All samples will be anonymised immediately and stored at a secure facility.

Use of the samples or data in research

The existence of the bank will be advertised on the University of Surrey Website under the Postgraduate Medical School (PGMS) research section. The samples stored as a tissue bank will be made available to other researchers providing their research is scientifically sound. The samples will be donated to established academic research groups following a structured application process. Each research group will have to

submit a research proposal to the head of Oncology Department at PGMS, Professor Hardev Pandha. Each proposal will then be considered taking into account the quality of the proposed research, the available expertise of the researchers and available research facilities and funding. Samples will be supplied for free except for the transport costs. The results of the research and data gained form the samples will be made available to the public through peer reviewed publications. All patients will be covered under the NHS indemnity scheme as well as University of Surrey Indemnity scheme, pending the circumstances of the event. We will require a regular report on research progress from the team that will request access to the tissue bank samples. The initial report will be requested a year from the time the tissue is released followed by subsequent six-monthly reports.

Selection of participants

Potential participants will be identified in the Royal Surrey County Hospital, Frimley Park Hospital and Ashford and St Peter's NHS Trust and St George's Hospital. We intend to store approximately 400 initial samples. Patients who have been selected will be approached by their consultants in context of a normal medical appointment that requires medical consultation. Patients will be offered an information sheet and will be asked to sign a written consent form. A blood sample will be collected at the time of the clinic appointment. The sample will be anonymised immediately and processed in the Postgraduate Medical School (PGMS) at the University of Surrey. The samples will be stored at a secure -80° freezer and only the principal investigator and the research team will have access to the samples. Tissue samples obtained in theatres during routine and planned operation will either be snap-frozen in liquid nitrogen or placed in a container with RNA-later solution to preserve the tissue. Clinical data of the patients donating the samples will be stored securely on the password- protected database on the University of Surrey Computer and only the Principal Investigator and the data manager will have access to the data. There will be a separate database linking the names of the patients with their assigned tissue bank numbers. The database will be password-protected and the access will be restricted to the Principal

Investigator and the data manager.

Study Protocol

1. Identify patients through diagnostic cancer clinics and cancer treatment clinics in consultation with consultant colleagues based at the Royal Surrey County Hospital and St Luke's Cancer Centre, Ashford and St Peter's Hospital and Frimley Park Hospitals.

   Inclusion:

   - Patients with suspected cancer referred for investigations of cancer for example: patients referred for prostate biopsy due to elevated PSA, patients referred for bronchoscopy due to abnormal imaging

   - Patients with established diagnosis of cancer attending follow up clinics at the Royal Surrey County Hospital and St Luke's Cancer Centre Patients will be given information sheet at the time of the consultation Obtain written informed consent

2. Healthy volunteers will be approached through the poster campaign, given information sheet and following a discussion an informed consent will be obtained.

2. Obtain a blood sample, at presentation request 30ml of blood, at follow up 20ml of blood, request nail clippings. (a one-of request only) and a urine sample.

3. The samples will be anonymised and transferred to secure facility at the PGMS and processed-the initial blood sample will be processed to obtain a sample of DNA and from the remaining blood serum and plasma will be isolated and frozen. The nail clippings and urine specimens will be banked and stored in secure facility for further analysis.

4. For patients at the time of diagnosis correlation with cancer/non-cancer diagnosis will be made when results of histology are available

5. Clinical data will be collected and stored at a secure password-protected database

6. The samples will be stored indefinitely and released to other researchers following a full research application submitted in writing to the Head of the Department Prof. Hardev Pandha

7. Regular reports form applicants will be required, the initial report at one year interval followed by 6-monthly intervals.

8. Samples obtained in theatres during routine operations will be placed in a suitable container and either snap-frozen in liquid nitrogen or placed in RNA-later solution.

References

[1] Banez LL, Prasanna P, Sun L, Ali A, Zou Z, Adam BL, et al. Diagnostic potential of serum proteomic patterns in prostate cancer. The Journal of urology. 2003 Aug; 170(2 Pt 1):442-6. [2] Adam BL, Qu Y, Davis JW, Ward MD, Clements MA, Cazares LH, et al. Serum protein fingerprinting coupled with a pattern-matching algorithm distinguishes prostate cancer from benign prostate hyperplasia and healthy men. Cancer research. 2002 Jul 1;62(13):3609-14. [3] Petricoin EF, 3rd, Ornstein DK, Paweletz CP, Ardekani A, Hackett PS, Hitt BA, et al. Serum proteomic patterns for detection of prostate cancer. Journal of the National Cancer Institute. 2002 Oct 16;94(20):1576-8.

[4] Li J, White N, Zhang Z, Rosenzweig J, Mangold LA, Partin AW, et al. Detection of prostate cancer using serum proteomics pattern in a histologically confirmed population. The Journal of urology. 2004 May;171(5):1782-7. [5] Ornstein DK, Rayford W, Fusaro VA, Conrads TP, Ross SJ, Hitt BA, et al. Serum proteomic profiling can discriminate prostate cancer from benign prostates in men with total prostate specific antigen levels between 2.5 and 15.0 ng/ml. The Journal of urology. 2004 Oct;172(4 Pt 1):1302-5.